



TECHNISCHE UNIVERSITÄT MÜNCHEN

Ingenieurfacultät Bau Geo Umwelt

Lehrstuhl für Siedlungswasserwirtschaft

Development and validation of a novel treatment concept for planned potable reuse based on sequential managed aquifer recharge technology for more sustainable water management

Sema Karakurt-Fischer

Vollständiger Abdruck der von der Ingenieurfacultät Bau Geo Umwelt der Technischen Universität München zur Erlangung des akademischen Grades eines

Doktor-Ingenieurs (Dr.-Ing.)

genehmigten Dissertation.

Vorsitzende: TUM Junior Fellow Dr. Christian Wurzbacher

Prüfer der Dissertation: 1. Prof. Dr. Ing. Jörg E. Drewes
2. Prof. Dr. Christian Griebler
3. Assoc. Prof. Dr. Sung Kyu Andrew Maeng

Die Dissertation wurde am 13.07.2020 bei der Technischen Universität München eingereicht und durch die Ingenieurfacultät Bau Geo Umwelt am 26.10.2020 angenommen.

Abstract

Globally, many municipalities withdraw drinking water either directly or through bank filtration from surface waters. These streams might be impaired and can contain spatially varying amounts of wastewater effluent discharge. The presence of upstream wastewater effluent in a stream subsequently used for drinking water abstraction is sometimes referred to as *de facto* reuse. Which degree of *de facto* reuse may impact drinking water production, in particular via bank filtration, has not been determined yet. Such an assessment is complex given site-specific hydro-geochemical conditions in the subsurface as well as operational variability of water treatment processes. Therefore, under the framework of this PhD project, the degree of potential *de facto* reuse situations in Germany and the resulting consequences on bank filtration were quantified. With the help of an automated ArcGIS assessment, wastewater effluent contributions under minimum and mean average stream run-off in river basins were calculated considering more than 7,500 wastewater facilities across Germany. In rivers with low natural base discharge, wastewater effluent contributions greater than 30-50% were determined under minimum mean annual stream discharge, which are often prevalent from May to September. A conceptual model for estimating the critical bank filtrate shares resulting in the exceedance of toxicologically derived monitoring trigger levels for select indicator chemicals was established and validated using data from field monitoring campaigns. The findings of this study underline the importance of potential limitations of current water management practices. Where conventional freshwater resources are impaired or declining in quantity, alternative water sources (e.g., reclaimed water) might be suitable options. Therefore, another aim of this study was to develop an alternative advanced nature-based water treatment concept without employing high-pressure membranes, which could be utilized for potable water reuse in regions with high water stress.

Subsurface infiltration of water through porous media takes advantage of naturally-occurring treatment mechanisms. Previous studies have demonstrated the efficiency of different removal mechanisms in managed aquifer recharge (MAR) systems (i.e., filtration, biotransformation, adsorption, ion exchange) for enhanced inactivation of pathogens (e.g., protozoa, bacteria and viruses) and removal of many trace organic chemicals (TOrcs) from treated wastewater and highly impacted surface waters. Prior work based on employing high-throughput Amplicon 16S-RNA sequencing has revealed a tremendous potential to select for certain bacteria which are capable of removing TOrcs. However, strictly controlling certain conditions is key to establish a selecting pressure for the microbial community. By applying favorable oxic and oligotrophic conditions through intermediate aeration and a second infiltration step, sequential managed aquifer recharge technology (SMART) could enhance the removal of TOrcs in comparison to conventional MAR systems. Although the SMART concept has successfully been applied at field-scale in Germany and the USA, its widespread application has been hindered by properly maintaining favorable subsurface conditions and its high physical footprint. In addition, in both MAR and SMART applications, a high degree of

heterogeneity can adversely affect the establishment of homogeneous and controlled redox zonation and prevent plug-flow conditions, which are beneficial for improved TOrC and pathogen, in particular virus, attenuation. To minimize the physical footprint, pumping costs, and hydraulic retention times, as well as to overcome the limitations of such heterogeneities, within this PhD project the novel SMART*plus* concept was developed, integrating two main engineered processes, such as high-rate infiltration trenches and *in-situ* oxygen delivery, into a SMART*plus* bioreactor.

The SMART*plus* bioreactor was constructed at pilot-scale using a stainless-steel 3D-flume (6 m x 0.9 m x 1.4 m LxWxH) in trapezoidal form. A rectangular shaft (0.35 m x 0.9 m x 1.5 m), placed at the inflow side of the flume, mimicked a high-rate infiltration trench. While the SMART*plus* bioreactor was filled with technical sand ($d_{10} = 0.75$ mm) providing high homogeneity for plug-flow conditions, the infiltration trench and the outflow compartments were filled with fine gravel ($d_{10} = 3.4$ mm) for rapid vertical infiltration. The bioreactor was constantly fed with WWTP effluent, subject to additional on-site tertiary treatment for enhanced suspended solid removal as well as mitigation of elevated peaks of dissolved organic carbon and ammonium. The flow field within the SMART*plus* bioreactor was confirmed by conservative tracer tests and 3D groundwater flow modelling. Based on the discrepancy between the experimental and modeled breakthrough curves, heterogeneities in the SMART*plus* bioreactor were eliminated, resulting in the successful establishment of plug-flow conditions. The required redox conditions in the bioreactor were achieved by *in-situ* oxygen delivery, to maintain homogenous flow conditions and eliminate typical pumping costs associated with SMART. For this purpose, the feasibility of PDMS gas-liquid membrane contactors for bubble-free and reliable delivery of oxygen was studied first at bench-scale at similar contact times and Reynold numbers (0.2-2), as later applied *in-situ* in the bioreactor. Based on the mass transfer coefficients determined, self-designed PDMS gas-liquid membrane contactors were constructed and deployed into the bioreactor. After commissioning of the membrane contactors homogenous and bubble-free oxygen delivery could be successfully demonstrated at pilot-scale under laminar flow conditions and short contact times. Oxygen concentrations downstream of the membrane contactors met the design specification (>1 mg/L) as long as the required feed water quality was provided.

The results of the three-year investigation demonstrated that the two key features of the SMART*plus* bioreactor, the high-rate infiltration trench and the *in-situ* oxygen delivery device, were capable of providing the required hydraulic and environmental conditions for enhanced TOrC and virus removal at retention times of less than 12 hours. Already during operation without *in-situ* oxygen delivery, well controlled hydraulic conditions resulted in better virus and similar or improved TOrC removal in comparison to slow sand filtration and conventional MAR systems. Even with the conservative LRV estimates from monitoring of ambient concentrations, the SMART*plus* based advanced treatment train (employing GAC filtration and UV disinfection) including a subsequent

environmental buffer could comply with the pathogen performance target of WHO for potable water reuse. *In-situ* oxygen delivery could supply enhanced removal of some TOxCs but the full potential of sequential operation could not be achieved due to high oxygen demand caused by operational disturbances in the WWTP. A preliminary assessment on the costs, carbon and physical footprint demonstrated that SMART*plus* based advanced treatment train could have significantly lower costs than a full-advanced treatment train employing microfiltration/reverse osmosis/UV-AOP. A more detailed cost-benefit analysis and a comparison with other non-high-pressure-membrane based IPR treatment schemes can better underline pros and cons as well as technology transfer suitability of the proposed treatment scheme.

Zusammenfassung

Weltweit entnehmen viele Wasserwerke das für die Trinkwasserversorgung genutzte Rohwasser direkt oder nach einer Uferfiltration aus Oberflächengewässern, die aufgrund der Bevölkerungsdichte und des Klimawandels unterschiedliche Mengen an gereinigtem Abwasser (Klarwasser) enthalten können. Das Vorhandensein von Klarwasser in Oberflächengewässern, die anschließend zur Trinkwassergewinnung genutzt werden, wird als ungeplante Wasserwiederverwendung bezeichnet. Bisher konnte der Grad des Einflusses einer ungeplanten Wasserwiederverwendung auf die Trinkwassergewinnung nur unvollständig beurteilt werden. Insbesondere bei Nutzung einer Uferfiltration ist eine Beurteilung zudem stark abhängig von standortspezifischen hydrogeochemischen Eigenschaften des Untergrunds und der genutzten Betriebsweise. Im Rahmen dieser Doktorarbeit wurden daher die ungeplante Wasserwiederverwendung in Deutschland und die daraus resultierenden Auswirkungen auf das Rohwasser quantifiziert. Mit Hilfe von Python-Skripten in Verbindung mit einem geografischen Informationssystem (ArcGIS), wurden die Klarwasseranteile in Oberflächengewässern unter Berücksichtigung von mehr als 7.500 Kläranlagen und den mittleren Abflüssen sowie mittleren Niedrigwasserabflüssen für die Flusseinzugsgebiete berechnet. In abflussschwachen Gewässern wurden unter mittleren Niedrigwasserabflussbedingungen Klarwasseranteile von mehr als 30-50% ermittelt, die häufig von Mai bis September auftreten. Ein konzeptionelles Modell zur Einschätzung der kritischen Uferfiltratanteile, die zu Überschreitungen von gesundheitlichen Orientierungswerten (GOW) für Indikatorchemikalien führen, wurde erstellt und anhand der Messdaten validiert. Die Ergebnisse dieser Studie unterstreichen, wie wichtig es ist, den *status quo* aber auch mögliche Limitierungen der gegenwärtigen Wassergewinnung aufzuzeigen. Dort, wo Oberflächengewässer qualitativ beeinträchtigt sind oder eine eingeschränkte Wasserverfügbarkeit besteht, könnten auch alternative Wasserressourcen (z.B. die Wiederverwendung von weitergehend gereinigtem Abwasser) als eine Alternative in Frage kommen. Ein weiteres Ziel dieser Studie bestand in der Entwicklung alternativer Wasserwiederverwendungskonzepte ohne den Einsatz von Hochdruckmembranen, basierend auf natürlichen Behandlungstechnologien, die in Regionen mit hoher Wasserknappheit eingesetzt werden können.

Frühere Studien konnten die Effizienz verschiedener Entfernungsmechanismen bei der Grundwasseranreicherung (GWA) und Uferfiltration (d.h. Filtration, Biotransformation, Adsorption, Ionenaustausch) hinsichtlich einer verbesserten Inaktivierung von Krankheitserregern und der Entfernung vieler organischer Spurenstoffe aus Klarwasser und stark belasteten Oberflächenwässern nachweisen. Durch die Etablierung günstiger oxidischer und oligotrophen Bedingungen durch eine Zwischenbelüftung konnte die sequentielle GWA (engl. SMART) die Entfernung von Spurenstoffen im Vergleich zur konventionellen GWA verbessern. Sowohl bei der GWA als auch bei SMART-Anwendungen kann ein hohes Maß an Heterogenität in der Untergrundpassage die Etablierung einer

kontrollierten Redox-Zonierung erschweren und eine Pfropfenströmung verhindern, die für eine verbesserte Entfernung von Spurenstoffe und Pathogenen wie Viren unerlässlich sind. Obwohl das SMART-Konzept in Deutschland und in den USA erfolgreich im Feldmaßstab angewendet wurde, wirkt sich die Voraussetzung geeigneter Untergrundbedingungen und der hohe Flächenbedarf nachteilig auf eine breite Anwendung aus. Zur Minimierung des Flächenbedarfs, der Pumpkosten und der hydraulischen Verweilzeiten sowie zur Überwindung standortspezifischer Limitierungen wurde im Rahmen dieser Doktorarbeit das neuartige SMART*plus*-Konzept entwickelt, bei dem zwei wesentliche Prozesse zum Einsatz kommen: die Sickerschlitzzgraben-Technologie und ein *in-situ*-Verfahren zum Sauerstoffeintrag.

Für die Konstruktion des SMART*plus*-Bioreaktors im Pilotmaßstab wurde eine 3D-Rinne aus Edelstahl (6 m lang x 0,9 m breit x 1,4 m hoch) in Trapezform verwendet. Als Sickerschlitzzgraben diente ein rechteckiger Schacht (0,35 m x 0,9 m x 1,5 m), der an der Zulaufseite der Rinne platziert wurde. Während der horizontal durchströmte SMART*plus*-Bioreaktor mit technischem Sand ($d_{10} = 0.75$ mm) mit hoher Homogenität zur Realisierung von Pfropfenströmungsbedingungen befüllt wurde, wurden der Sickerschlitzzgraben und das Ablaufkompartiment für eine schnelle vertikale Infiltration mit feinem Kies ($d_{10} = 3.4$ mm) befüllt. Der Bioreaktor wurde kontinuierlich mit gereinigtem Abwasser aus Kläranlage Garching gespeist, welches vor Ort einer Tertiärbehandlung unterzogen wurde, um die Entfernung von suspendierten Feststoffen zu verbessern und Spitzen von hohen Konzentrationen an gelöstem organischen Kohlenstoff und Ammonium abzufedern. Die vorgeschlagenen weitergehenden Behandlungsschritte für SMART*plus*-basierte Prozesskombination für eine geplante, indirekte Wasserwiederverwendung, bestehend aus GAK-Filtration, UV-Desinfektion und GWA, wurden nicht im Pilotmaßstab getestet. Die Strömungsverhältnisse innerhalb des SMART*plus* Bioreaktors wurden durch Untersuchungen mit konservativen Tracern und dreidimensionale numerische Grundwassermodellierungen charakterisiert. Anhand der Diskrepanz zwischen den experimentell bestimmten und den modellierten Durchbruchkurven wurden heterogene Kurzschlussströmungen im SMART*plus* Bioreaktor identifiziert und eliminiert, was zur erfolgreichen Etablierung von Pfropfenströmungsbedingungen führte. Die erforderlichen Redox-Bedingungen im Bioreaktor wurden durch *in-situ*-Sauerstoffeintrag erreicht, um homogene Strömungsbedingungen aufrechtzuerhalten und zusätzliche Pumpkosten im Zusammenhang mit SMART zu vermeiden. Zu diesem Zweck wurde eine Machbarkeitsstudie im Labormaßstab für PDMS-Gas-Flüssigkeits-Membrankontaktoren bei ähnlichen Kontaktzeiten und Reynoldszahlen (0,2-2), wie für den Bioreaktor geplant, durchgeführt. Aufgrund der ermittelten Stoffübergangskoeffizienten wurden selbst entwickelte PDMS-Gas-Flüssig-Membran-Kontaktoren konstruiert und in den Bioreaktor eingesetzt. Nach der Inbetriebnahme der Membrankontaktoren konnte der homogene und blasenfreie Sauerstoffeintrag im Pilotmaßstab unter laminaren Strömungsbedingungen und kurzen Kontaktzeiten erfolgreich demonstriert werden. Die Sauerstoffkonzentrationen stromabwärts der

Membrankontaktoren entsprachen dem Auslegungswert von mehr als 1 mg/L, solange die erforderliche Zulaufwasserqualität gewährleistet war.

Die Ergebnisse dieser dreijährigen Untersuchung zeigten, dass die beiden Hauptmerkmale des SMART*plus* Bioreaktors, Sickerschlitzen-Technologie und *in-situ*-Sauerstoffeintrag, in der Lage waren, die erforderlichen hydraulischen und betrieblichen Bedingungen für eine verbesserte Entfernung von Spurenstoffen und Viren zu etablieren. Bereits während des Betriebs ohne den *in-situ*-Sauerstoffeintrag führte die kontrollierte Hydraulik im Vergleich zu Langsandsfiltern und konventioneller GWA zu einer besseren Entfernung von Viren und einer ähnlichen bzw. verbesserten Entfernung von Spurenstoffen. Selbst mit den konservativen log Entfernungswerten ermittelt aus den Routine-Überwachung könnte eine SMART*plus* basierte weitergehende Abwasserbehandlung die mikrobiologischen Leistungsziele der WHO für eine geplante Wasserwiederverwendung erfüllen. Der *in-situ*-Sauerstoffeintrag könnte zu einer verbesserten Entfernung bestimmter Spurenstoffe beitragen. Das vollständige Potential des sequentiellen Betriebs konnte aufgrund des hohen Sauerstoffbedarfs, der infolge außergewöhnlich hoher Ammoniumkonzentrationen im für die Infiltration genutzten Klarwasser wurde, nicht erreicht werden. Eine vorläufige Bewertung der Kosten, der CO₂-Bilanz- und des Flächenbedarfs zeigte, dass eine SMART*plus*-basierte weitergehende Abwasserbehandlung geringere Kosten verursacht als ein MF/RO/UV-AOP-basierter weitergehender Wasserbehandlungskonzept. Eine detailliertere Kosten-Nutzen-Analyse und ein Vergleich mit anderen nicht-RO-basierten weitergehenden Wasserbehandlungskonzepten sind notwendig, um die Vor- und Nachteile sowie die Eignung des vorgeschlagenen Behandlungssystems noch besser herauszustellen.

Danksagung

Die Doktorarbeitsphase war eine der spannendsten, schönsten und intensivsten Zeiten meines Lebens. In den letzten 3,5 Jahren am Lehrstuhl, haben viele Menschen direkt oder indirekt mich, meine Doktorarbeit und diese Phase geprägt. Hiermit möchte ich mich bei all diesen Menschen ganz herzlich bedanken und zum Ausdruck bringen, wie sehr ich Eure/Ihre Unterstützung schätze.

An erster Stelle möchte ich mich bei meinem Doktorvater Prof. Dr.-Ing. Jörg E. DREWES für die Vielzahl an Möglichkeiten aus Ihren Erfahrungen und Ihrer fachlichen Kompetenz zu lernen, das gute Arbeitsklima zwischen uns und die großartige Unterstützung während der Doktorarbeit sowie für meine berufliche Entwicklung herzlich bedanken. Trotz Ihres sehr arbeitsreichen Tagesablaufs hatten Sie immer Zeit für meine Fragen und standen mir mit Ihrem Rat bei. Die intensive Zusammenarbeit hat mich in dieser Zeit sehr geprägt. Dank Ihres Vertrauens und den sich daraus ergebenden Möglichkeiten, von der Mitarbeit in zwei sehr spannenden Projekten, der Entwicklung eines Kurses, über die Teilnahme an der IWA Konferenz in Kalifornien, bis hin zur Mitarbeit im Organisationskomitee der folgenden IWA Konferenz in Berlin, habe ich mich in den letzten 3,5 Jahren weit über eine Promotion hinaus entwickeln können.

Eine absolut riesige Chance war es, Dr.-Ing. Uwe HÜBNER, fortwährend auf meiner Seite stehend, als meinen Betreuer am Lehrstuhl während der gesamten Zeit (tagsüber bis spät abends oder an den Wochenenden) zu haben. Ich habe mich immer sehr wohl gefühlt und bin sehr glücklich, ein Teil Deiner Arbeitsgruppe gewesen zu sein. Du hast die hervorragende Eigenschaft, genau die richtigen Tipps und Kritik zu geben und Deine Unterstützung anzubieten, was mir an den entscheidenden Stellen unheimlich weitergeholfen hat. Darüber hinaus haben mir die lebhaften und spannenden Diskussionen viel Input und wertvolle Anregungen gegeben. Letztendlich haben Deine großartige Unterstützung sowie positive Einstellung bei der Überbrückung der schwierigen Phasen meiner Doktorarbeit und bei der Entstehung dieser Dissertation einen sehr großen Anteil, weshalb ich Dir sehr dankbar bin.

I would also like to thank my committee members Prof. Dr. Christian GRIEBLER and Dr. Sung Kyu Andrew MAENG for agreeing to act as reviewers of this dissertation. Likewise, I would like to thank Dr. Christian WURZBACHER for being the committee chair and for his support.

Auch ein sehr großer Dank geht an die Projektträger BMBF und UBA für die Förderung, in dessen Rahmen diese Untersuchungen durchgeführt wurden. Außerdem möchte ich mich bei meinem Mentor Dr. Alexander SPERLICH für seine große Unterstützung in den letzten Jahren, bei unserem Projektpartner und Ko-Autoren bei den Publikationen, Prof. Dr. Martin JEKEL, Dr. Alicia SANZ-PRAT, Prof. Dr. Gudrun MASSMANN, Dr. Janek GRESKOWIAK, Martin ERGH, Dr. Heiko GERDES, Dr. Regine SZEWZYK, Christian RIEN und zu guter Letzt bei Dr. Hans-Christoph

SELINKA, für die gute und enge Zusammenarbeit sowie die vielen spannenden Gespräche bei den Projekttreffen bedanken.

Außerdem möchte ich mich bei den MitarbeiterInnen unseres Lehrstuhls, Myriam REIF, Wolfgang SCHRÖDER, Dr. Oliver KNOOP, Heidrun MAYRHOFER, Ursula WALLENTITS und Ramona SCHÜTT ganz herzlich für die Unterstützung im Labor und die gute Zusammenarbeit bedanken. Ohne eure Unterstützung wären die Versuche und Laboranalysen nicht möglich gewesen. Hubert MOOSRAINER, Dir gilt ein riesiger, lieber Dank für Deine intensive Unterstützung beim Aufbau und Umbau der Anlage. Ich konnte Dich bei jeglichen Problemen zu jeder Zeit nach deinem Rat und Deiner Hilfe fragen und Du hattest im wahrsten Sinne immer gute Ideen, worauf ich aufbauen konnte.

Im Rahmen von Master- und Bachelorarbeiten, Study Projekts sowie HiWi Stellen habe ich auch in den letzten Jahren von meinen tatkräftigen, engagierten StudentInnen Daniela SCHWEIGER, Emil BEIN, Joshua GALLEGOS, Ludwig SCHMID, Sofia GANTHALER, Marian BACHMAIER, Anastasia RUF, Amr SOUF, Mario GRAMM, Jinjuta CHAROENSIRI, Jad ARBASH, Eric ZIEMENDORF, Katharina SENDLHOFER, Daniel NIESS, Lisa PÖLL, Dennis GÖSSL, Georg SCHÜCKING, Geronimo ETCHECHURY GOMEZ, Alexandra SCHMUCK, Gloria TESSARO und Sarah STANOYEVIC eine unersetzliche Unterstützung bekommen. Herzlichen Dank an Euch alle für die gute Zusammenarbeit.

Außerdem möchte ich mich bei all meinen KollegInnen für die tolle gemeinsame Zeit bedanken. Insbesondere möchte ich mich bei Veronika ZHITENEVA für Deine enge Freundschaft, Deine immerwährende Unterstützung sowie Dein Dasein als liebste Bürokollegin bedanken, bei Johann MÜLLER für Deine durchgängige Hilfsbereitschaft und Deine liebenswerte Art, bei Jürgen EDERER für Deine große Mitwirkung in der Anlage und Unterstützung bei der Anfangsphase der Arbeit, bei David MIKLOS für die witzigsten Pausen, bei Dietmar STRÜBING für die schönsten Klettersessions, bei der Königin und dem König des Schlamms Meriam MUNTAU & Thomas LIPPERT als beste Nachbarn, bei Karin HELLAUER für Dein Vertrauen, bei Susanne WIESSLER für deine Unterstützung und menschliche, tolle Art, bei meinen neuen KollegInnen Emil BEIN & Carolina FEICKERT-FENSKE & Jonas ANIOL für die schönen letzten Monate am Lehrstuhl sowie bei Julia REGNERY für die großartige Unterstützung bei der Anfahphase der Anlage. Mit Euch war es einfach eine Hammerzeit am Lehrstuhl!

Ein besonders großes Dankeschön möchte ich all meinen engen Freunden für die seelisch, moralische Unterstützung, den wichtigen Ausgleich sowie die wunderschönen Urlaube und Freizeiten in den letzten 3,5 Jahre und davor aussprechen. Ohne Euch in meinem Leben hätte ich diese Arbeit nicht schreiben können! Anschließend möchte ich mich ausdrücklich bei Claudia STAUDINGER und Johann MÜLLER für den letzten Schliff der Zusammenfassung und Danksagung Kapitel, und natürlich bei Veronika ZHITENEVA für die sprachliche Korrektur der Arbeit bedanken.

Ebenfalls möchte ich mich ganz herzlich bei Amadeus HEMPEL, Renate und Norbert REICH für die geistreichen, inspirierenden gemeinsamen Abendessen, Euer Vertrauen in mich und Eure wegweisende Unterstützung in Deutschland bedanken. Es ist mir immer eine große Freude nach Hamburg zu kommen und Euch zu treffen!

Liebe Christine FISCHER, danke, dass Du seit dem ersten Tag meines Aufenthalts in Deutschland mich unterstützt, bei jedem wichtigen Moment dabei bist und diese Momente bereicherst.

Bu vesileyle ayrıca hayatımın her evresinde, yaşadığım tüm zorlukları benimle birlikte göğüsleyen, bana sonsuz sevgilerini her an gösteren ve destek olan sevgili aileme; babam Sami KARAKURT, annem Sakine KARAKURT, ablam Seda ŞANLI ve abim Levent ŞANLI' ya sonsuz teşekkürlerimi sunuyorum. Siz ve Mavi birtanesiniz ve benim için çok değerlisiniz!

Als letztes möchte ich mich unendlich bei meinem Mann und besten Freund Boncuk FISCHER bedanken, für die Liebe, die Ermutigung, und die seelische Unterstützung meinen Weg zu gehen!

Table of contents

Abstract	III
Zusammenfassung.....	VII
Danksagung.....	XI
Table of contents	XV
List of figures	XXI
List of tables.....	XXVII
List of abbreviations.....	XXXI
1. General Introduction	1
2. State-of-the-art	3
2.1. Current water management – de facto reuse.....	3
2.2. Fate of emerging contaminants during conventional wastewater treatment and in receiving river streams	4
2.2.1. Level of treatment in conventional wastewater treatment.....	4
2.2.2. Waterborne pathogenic organisms	4
2.2.3. Chemical constituents.....	5
2.3. Planned potable reuse applications	6
2.3.1. Indirect potable reuse	7
2.3.2. Direct potable reuse.....	8
2.3.1. Multiple-barrier concept.....	8
2.4. Requirements and monitoring strategies for potable reuse	9
2.4.1. National and international regulations and guidelines	9
2.4.2. Treatment goals for potable reuse	10
2.5. Water reuse technologies and treatment trains	16
2.5.1. Membrane based full advanced treatment trains	17

2.5.2.	Non-RO based treatment trains	18
2.6.	Advancing natural treatment systems	20
2.6.1.	Managed aquifer recharge systems.....	20
2.6.2.	Sequential managed aquifer recharge technology	22
2.6.3.	Further enhancement of natural treatment systems for IPR applications	23
3.	Research significance and hypotheses.....	25
3.1.	Objective #1: Assessment of municipal wastewater contributions in German surface waters and associated impacts on the drinking water supply	27
3.1.1.	Hypothesis #1: The exceedance of MTLs in bank filtered raw water supplies occurs in several river basins in Germany due to high wastewater effluent contributions during extended time periods.	27
3.2.	Objective #2: Development, construction and operation of a novel hybrid biofilter, SMARTplus, based on sequential managed aquifer recharge technology (SMART) for indirect potable reuse.....	28
3.2.1.	Hypothesis #2: Integration of infiltration trench technology into hybrid biofilter SMARTplus establishes a horizontal flow regime providing rapid infiltration and homogenous plug-flow conditions.....	28
3.2.2.	Hypothesis #3: Establishing homogenous plug-flow conditions within the SMARTplus bioreactor results in enhanced attenuation of viruses in comparison to conventional slow sand filters, despite shorter hydraulic retention times and coarser grain size.....	28
3.2.3.	Hypothesis #4: Bubble-free delivery of oxygen into SMARTplus biofilter can be achieved in-situ under laminar flow conditions and short contact times by diffusive transport through gas-liquid membrane contactors.	29
3.2.4.	Hypothesis #5: Plug-flow conditions, defined and controllable redox zonation in SMARTplus biofilter lead to enhanced TOrCs removal.	29
4.	Dynamics of wastewater effluent contributions in streams and impacts on drinking water supply via riverbank filtration in Germany – A national reconnaissance	31
4.1.	Introduction.....	32
4.2.	Materials and methods	34

4.2.1.	Data acquisition and calculation of treated effluent contribution in rivers - Modeling approach.....	34
4.2.2.	Determination of the degree of impact on drinking water abstraction	36
4.3.	Results and discussion	37
4.3.1.	Dynamic of wastewater effluent contributions to rivers during different discharge conditions	37
4.3.2.	Relevance of elevated wastewater effluent contributions in streams used for drinking water supply	41
4.4.	Acknowledgements.....	43
5.	Developing a novel biofiltration treatment system by coupling high-rate infiltration trench technology with a plug-flow porous-media bioreactor	45
5.1.	Introduction.....	46
5.2.	Materials and methods	48
5.2.1.	Establishment of SMARTplus at pilot scale.....	48
5.2.2.	Laboratory analysis	51
5.2.3.	Numerical simulations of groundwater flow and conservative transport processes...	51
5.3.	Results and discussion	53
5.3.1.	Hydraulic characterization of the SMARTplus bioreactor	53
5.3.2.	Feed water and system characterization during baseline operation.....	57
5.4.	Conclusions.....	61
5.5.	Acknowledgements.....	61
6.	Fate and transport of viruses within a high rate plug-flow biofilter designed for non-membrane based indirect potable reuse applications	63
6.1.	Introduction.....	64
6.2.	Materials and methods	66
6.2.1.	Experimental setup of the SMARTplus based advanced water treatment train	66

6.2.2.	Routine monitoring of SMARTplus bioreactor	68
6.2.3.	Monitoring of virus concentrations indigenous to wastewater	68
6.2.4.	Spiking tests.....	69
6.2.5.	Sample analysis	71
6.3.	Results and discussion	72
6.3.1.	Feed water and system characterization	72
6.3.2.	Effects of hydraulic conditions and water quality on the fate & transport of viruses	73
6.3.3.	Compliance of the SMARTplus based advanced water treatment train with virus performance targets	79
6.4.	Conclusion	80
6.5.	Acknowledgements.....	81
7.	Characterizing a novel <i>in-situ</i> oxygen delivery device for establishing controlled redox zonation within a high infiltration rate sequential biofilter.....	83
7.1.	Introduction.....	84
7.2.	Materials and methods	87
7.2.1.	Description of the SMARTplus pilot plant.....	87
7.2.2.	Performance characterization of the gas-liquid membrane contactor.....	89
7.2.3.	Design of the electron-acceptor compartment equipped with gas-liquid membrane contactors	92
7.2.4.	Sampling and analytical methods	93
7.3.	Results and discussion	93
7.3.1.	Investigating the feasibility of gas-liquid membrane contactors for <i>in-situ</i> oxygen delivery into the SMARTplus bioreactor	93
7.3.2.	Development and implementation of pilot-scale gas-liquid membrane contactors....	95
7.3.3.	Validation of pilot scale gas-liquid membrane contactors for the establishment of redox zonation under varying feed water quality	96

7.3.4.	Effects of the in-situ oxygen delivery and varying feed water quality on the attenuation of TOxCs.....	100
7.4.	Conclusion.....	103
7.5.	Acknowledgements.....	104
8.	Overall discussion and outlook.....	105
8.1.	Assessment of municipal wastewater contributions in German surface waters and associated impacts on drinking water supply.....	105
8.1.1.	Testing Hypothesis #1.....	106
8.1.2.	Relevance of the research findings and future research needs.....	108
8.2.	Development, construction and operation of a novel hybrid biofilter, SMARTplus, based on sequential managed aquifer recharge technology (SMART) for indirect potable reuse.....	111
8.2.1.	Testing Hypotheses #2-#5.....	111
8.2.2.	Recommendations for the establishment of the optimal hydraulic and operational conditions for future pilot- to field-scale applications.....	114
8.2.3.	Future research needs.....	120
9.	Supplementary Information.....	125
9.1.	Peer-reviewed journal articles and author contributions.....	125
9.1.1.	Published and submitted manuscripts.....	125
9.1.2.	Manuscript in preparation.....	126
9.2.	Conference papers, reports and German article.....	126
9.2.1.	Conference papers.....	126
9.2.2.	Reports.....	127
9.2.3.	German article.....	127
9.3.	First author contributions to national and international conferences.....	127
9.3.1.	Presentations.....	127
9.3.2.	Poster.....	127

9.4.	Supplementary information for Chapter 4	129
9.5.	Supplementary information for Chapter 5	133
9.6.	Supplementary information for Chapter 6	138
9.7.	Supplementary information for Chapter 7	140
9.8.	Conference paper related to Objective #1	142
9.9.	Conference paper related to Objective #2.....	146
	References	151

List of figures

Figure 2-1: Conventional drinking water augmentation via induced riverbank filtration (© Berlin Water Company / Technical University of Munich, 2017).....	3
Figure 2-2: A schematic illustration of indirect potable reuse via groundwater augmentation (modified from © Berlin Water Company / Technical University of Munich, 2017).	7
Figure 2-3: A schematic illustration of direct potable reuse (modified from © Berlin Water Company / Technical University of Munich, 2017).	8
Figure 2-4: Schematic examples of managed aquifer recharge systems, GWA indicates groundwater augmentation.	20
Figure 2-5: Concept of SMART based on the availability of biodegradable organic carbon compounds and optimized redox conditions for enhanced removal of trace organic chemicals.	23
Figure 3-1: Development of the SMARTplus bioreactor based on MAR and SMART.	25
Figure 3-2: Structure of the dissertation (Illustrations on the top are modified from © Berlin Water Company / Technical University of Munich, 2017).....	26
Figure 4-1: Comparison of MMAD and MAD hydrological characteristic values with daily average discharges during dry (2003) and average (2005) representative years for three gauging stations of the Rhine (at R), Main (at M) and Neckar (at N) rivers(GRDC, 2017).	38
Figure 4-2: Comparison of wastewater effluent contribution (secondary axis) from GIS model under MMAD (black dots with dashed line) and MAD conditions (black dots with solid line) with dilution calculation using carbamazepine concentrations (grey dots with dashed line). Carbamazepine point samples were measured in wastewater effluents (2010)(Klasmeier et al., 2011) and the Main river (2016)(Fleig et al., 2016).....	39
Figure 4-3: Map of nationwide wastewater effluent contributions under MMAD conditions (a) and share of gauging stations with relative wastewater effluent contributions for river basins under MMAD (b) and MAD (c) conditions.	40
Figure 4-4: Projected benchmark of MTL exceedances for indicator chemicals OXY (MTL: 300 ng/L), VSA (MTL: 300 ng/L) and CBZ (MTL: 300 ng/L) under different percent contributions of wastewater effluent in rivers and bank filtrate in raw water scenarios (left). WWTP effluent concentrations (CBZ 832 ng/L (Loos et al., 2013), VSA 1,310 ng/L (Nödler et al., 2013) and OXY 9,830 ng/L (Funke et al., 2015)) are representing mean values, taken from literature. Guidance for water utilities and regulators in case of indicator chemical MTL exceedance (right).	42

Figure 5-1: Front, side, and top views of the SMARTplus bioreactor indicating the characteristic media of each compartment, and the locations of the monitoring wells (MW) placed into the bioreactor. All dimensions in mm. 49

Figure 5-2: Observed and simulated hydraulic heads at 6 monitoring wells by CTD sensors (see location in Figure 5-1), CTD1, CTD2, CTD3, CTD4, CTD5 and CTD6 in x (i.e. flow) direction, and the outlet compartment, C5, at a flowrate of 300 L/h. 53

Figure 5-3: Normalized BTCs of the observed (black dots) and simulated (black solid lines) KBr concentrations at the observation points during the pulse injection tracer test. The measured and simulated transient inflow KBr concentration is depicted at the top left panel (red solid line), while the observed and simulated concentration at the outflow is shown at the lower right panel. CTD1-CTD6 represent the conductivity sensors located in the middle of the bioreactor at 10 cm from the bottom. The x, y and z coordinates of the sampling ports, CTD sensors and the outflow are expressed in cm. 54

Figure 5-4: Spatial distribution of the normalized tracer plume concentration at four times after pulse injection started from the inlet boundary (top right side) to the outlet boundary (bottom left side). The red area corresponds to the 1 g/L bromide concentration and the white area to the background concentration (0 g/L). 55

Figure 5-5: Hydraulic head measurements at CTD 1 and CTD 2 (200 and 450 mm at x direction) between April 5th and December 30th 2018 at 300 L/h. The thin red lines indicate the exchange of a thin sand layer on the top of the C1 compartment. The thick blue and red lines denote the reduction of the flowrate to 100 L/h and the removal and cleaning of the clogged media from the C1 and C2 compartments, respectively. Data gaps were caused by online measurement failures. 56

Figure 5-6: DO (n=15,512) and NO₃⁻-N (n=10 - 12) concentrations in feed water and at the end of the infiltration trench, prior to EA compartment as well as the entire SMARTplus bioreactor. Percentage removal of DOC concentrations and UVA₂₅₄ (n = 10 - 12), which are calculated by the DOC and UVA₂₅₄ values of infiltration trench, prior to the EA compartment and bioreactor effluent normalized to the corresponding feed water values (Table 5-1). 58

Figure 5-7: Cumulative TOrCs biotransformation, calculated by the TOrC concentrations of the samples taken from the infiltration trench, prior to the EA compartment, and bioreactor effluent normalized to corresponding feed water concentrations (C₀). Mean C₀ [ng/L]: trimethoprim 48±24, 4-FAA 479±176, gabapentin 1397±414, climbazole 166±70, citalopram 180±43, sulfamethoxazole 260±190, metoprolol 286±35, diclofenac 1052±97, benzotriazole 5921±1485, tramadol 198±19, venlafaxine 409±36, carbamazepine 459±60, n=8-9. 60

Figure 6-1: Schematic flow diagram of the SMARTplus based advanced water treatment train for IPR (adapted from Karakurt-Fischer et al., 2020a). The post treatments, GAC filtration and UV disinfection, were not tested at pilot-scale. 67

Figure 6-2: The front and side views of the SMARTplus bioreactor, the utilized porous media , gravel ($d_{10}=2.1$ mm or 3.4 mm) or sand ($d_{10}=0.75$ mm), as well as the locations of the monitoring wells (MWs) and the utilized sampling ports (adapted from Karakurt-Fischer et al. (2020b)). The scale is given in meters. 68

Figure 6-3: Transport of virus surrogates and the conservative tracer primidone in the SMARTplus bioreactor during the spiking test in 2017. The x, y and z coordinates of the sampling ports and the effluent are expressed in meters. 2nd y-axis is given in logarithmic scale..... 75

Figure 6-4: Transport of virus surrogates and conservative tracer primidone in the SMARTplus bioreactor during the spiking test in 2018. The x, y and z coordinates of the sampling ports and the effluent on top of the graphs are expressed in meters. 2nd y-axis is given in logarithmic scale. The concentrations of bacteriophages and MNV-1 are given in pfu/L and genome copies/L, respectively. 76

Figure 6-5: Cumulative log reduction values with the HRTs of the sampling locations (left) and log reduction rates [\log_{10}/m] (right) of MS2, ϕ X174 and MNV-1 surrogate viruses along the SMARTplus bioreactor flow path during the spiking test in 2018. The exact locations of the sampling ports in x, y and z directions can be found in Figure 6-4. The spike concentrations of bacteriophages and MNV-1 are given in pfu/L and genome copies/L, respectively..... 77

Figure 6-6: Compliance of a SMARTplus based advanced water treatment train considering the WHO (9.5 LRVs) virus performance target. Log removal of the surrogate viruses (MS2, ϕ X174 and MNV-1) within the SMARTplus bioreactor were measured during the spiking test in 2018, while log removal of surrogate phages (F^+ phages and somatic coliphages) and indicator viruses (adenovirus and human norovirus) within the WWTP, RDMF and SMARTplus were measured during routine monitoring. While mean LRVs were used for the surrogate viruses, conservative lower LRVs were chosen for the indicator viruses. LRVs assigned to WWTP and RDMF for spiked MS2, ϕ X174 and MNV-1 viruses were taken from the routine monitoring data for F^+ phages, somatic coliphages and human noroviruses, respectively. 80

Figure 7-1: A schematic flow diagram of the SMARTplus pilot plant. WWTPe indicates secondary effluent of the WWTP. 88

Figure 7-2: A schematic flow diagram of the self-made lab-scale gas-liquid membrane contactor, where the contactor design was adapted from (Grassi et al., 2007). The manometer is denoted by ‘M,’ and ‘DO’ indicates the dissolved oxygen measurement sensors..... 89

Figure 7-3: Axonometric front view of the contactor assembly of 17 infiltration wells within the EA compartment. All dimensions in [mm] [left]. A schematic illustration of a self-designed pilot-scale gas liquid membrane conductor submerged in one of the infiltration wells and the O₂ pressure regulation gauge [right]...... 92

Figure 7-4: Modelled and experimentally determined average oxygen mass transfer coefficients for varying Reynolds numbers (left). Share of oxygen mass transfer resistances for varying Reynolds numbers (right)...... 94

Figure 7-5: DO concentrations along sampling locations of SMARTplus bioreactor experiment without (2018, n=15,836) and with (2019, n=3,525) the in-situ oxygen delivery. The red dashed line indicates the threshold DO concentration of 1 mg/L for oxic redox conditions based on the definition by Regnery et al. (2015b). 99

Figure 7-6: Cumulative TOrCs removal calculated by normalizing the TOrC concentrations before the EA compartment and in bioreactor effluent to their corresponding feed water concentrations (C₀) during operation without (left) and with (right) the in-situ oxygen delivery. Mean C₀ [ng/L] 2018 (n=8-9): gabapentin 1397 ± 414, trimethoprim 48 ± 24, 4-FAA 479 ± 176, climbazole 166 ± 70, citalopram 180 ± 43, sulfamethoxazole 260 ± 190, metoprolol 286 ± 35, diclofenac 1052 ± 97, benzotriazole 5921 ± 1485, tramadol 198 ± 19, venlafaxine 409 ± 36, carbamazepine 459 ± 60. Mean C₀ [ng/L] 2019 (n=5-6): atenolol 59 ± 17, trimethoprim 200 ± 52, 4-FAA 1441 ± 327, antipyrine 110 ± 26, climbazole 117 ± 26, citalopram 175 ± 39, sulfamethoxazole 308 ± 29, metoprolol 327 ± 54, diclofenac 1167 ± 119, benzotriazole 5458 ± 497, tramadol 264 ± 93, venlafaxine 400 ± 39, carbamazepine 329 ± 119. The error bars indicate standard deviation of percent removal at different sampling dates..... 100

Figure 8-1: DOC and ΔDOC concentrations during baseline (n=32) and sequential (n=5) operation in the WWTP effluent and along the SMARTplus bioreactor. The abbreviations 1st prior to the EA and 2nd after the EA indicate the compartments prior to and after the in-situ oxygen delivery device. 116

Figure 8-2: Transport of the KBr tracer with a dosing concentration of 8 mg/L along the SMARTplus bioreactor during pulse injections of 30 min., conducted at 0.45 and 0.6 m³/h. The distances are expressed in x direction. 119

Figure 8-3: The water levels along the SMARTplus bioreactor between April 2018 and October 2019 at 300 L/h. The grey backgrounds show the time periods with the occurrence of colmation in the infiltration trench (left) and after the EA compartment (right). The data gaps were caused by online measurement errors. CTD3 and CTD6 displayed less and no change due to colmation, respectively. 120

SI-Figure 9-1: Discharge values and wastewater effluent contributions at the gauging stations along the river Danube under MMAD and MAD conditions.	131
SI-Figure 9-2: Discharge values and wastewater effluent contributions at the gauging stations along the river Rhine under MMAD and MAD conditions.	131
SI-Figure 9-3: Discharge values and wastewater effluent contributions at the gauging stations along the river Neckar under MMAD and MAD conditions.	132
SI-Figure 9-4: Side and top view of the SMARTplus bioreactor together with the locations of the respective compartments, sampling ports and monitoring wells (MWs i.e. CTDs) at x, y and z coordinates in mm. Utilized sampling ports for the tracer tests and system monitoring are indicated in bold.....	136
SI-Figure 9-5: Effective porosities in the bioreactor, derived by monitoring the partial changes in the fluid volume within the bioreactor at different times during the unsteady flow tests. Mean porosity of 0.35 was used as initial value in the numerical model.....	137
SI-Figure 9-6: Numerical scheme of the true three-dimensional finite-element grid: top view of the volume elements and nodes at each layer, inflow (blue area) and outflow (red dot) boundaries. .	137
SI-Figure 9-7: Initial (a, b and c) and optimized (opt.) configuration of MWs #1-6 with the packers and CTDs #1-6 (d).	139
SI-Figure 9-8: The configuration of the contactor assembly with location of the infiltration wells (top view). The length of the infiltration wells are 1.1: 1190 mm; 1.2: 1288 mm; 1.3: 1386 mm; 1.4: 1390 mm; 1.5: 1390 mm; 1.6: 1390 mm; 1.7: 1386 mm; 1.8: 1288 mm; 1.9: 1190 mm; 2.1: 1239 mm; 2.2: 1337 mm; 2.3: 1390 mm; 2.4: 1390 mm; 2.5: 1390 mm; 2.6: 1390 mm; 2.7: 1337 mm; 2.8: 1239 mm.	141
SI-Figure 9-9: Breakthrough curves of conservative tracer primidone along the SMARTplus bioreactor following a pulse tracer test. The influent concentrations indicate the tracer concentrations in the feed water. The effluent BTC is the ensemble response at the bottom of the bioreactor. The coordinates of the sampling ports of the SMARTplus bioreactor are given at x (length), y (penetration depth) and z (height) coordinates in mm as follows: Port 2 (400, 450, 450); Port 8 (1640, 450 450); Port 12 (2640, 450, 450); Port 18 (4140, 450, 450); Port 24 (5600, 450, 450); Effluent (5850, 450, 0).	141
SI-Figure 9-10: Schematic of the SMARTplus bioreactor tested at pilot-scale.	148

SI-Figure 9-11: Spatial distribution of the tracer plume at three different times after pulse injection started. The red area corresponds with the high concentration of bromide, and the blue area with the background concentration. 149

List of tables

Table 2-1: Indicative log reduction values of indicator and surrogate microorganisms (<i>italic</i>) and enteric pathogens during various stages of wastewater treatment, adapted from Asano et al. (2007) and USEPA (2012). n.a. indicates not available.	12
Table 2-2: Proposed monitoring list for the process and health-based indicator chemicals, surrogates and bioassays for IPR, adapted from Drewes et al. (2018). Following acronyms are used to describe gemfibrozil (GFZ), sulfamethoxazole (SMX), iohexol (IOX), sucrose (SUC), total fluorescence (TF), electrical conductivity (EC) and method reporting limit (MRL), the latter is given in ng/L..	16
Table 2-3: Unit operations and advanced water treatment processes, than can be applied for the removal of waste water origin constituents for reuse treatment trains, adapted from Asano et al. (2007), USEPA (2017) and Drewes and Khan (2011). The check mark indicates the suitability of a unit.	17
Table 2-4: Some examples of established potable reuse schemes based on full advanced treatment, adapted from WHO (2017) and USEPA (2017).	18
Table 2-5: Some examples of established potable reuse schemes applying non-RO based treatment, adapted from WHO (2017) and Hooper et al. (2020).	19
Table 4-1: Validation of conceptual approach for case study areas Rhine, Havel and Main by indicator chemicals measurement data both in surface waters and in bank filtration.	43
Table 5-1: Average feed water DOC concentration, UVA ₂₅₄ , specific ultraviolet absorbance (SUVA), NO ₃ -N (n=10-12), and DO concentrations (n=15,512) during baseline operation of the SMARTplus bioreactor.....	57
Table 6-1: Water quality parameters influencing virus removal: mean DOC (n=3-5), NO ₃ -N (n=3-5), DO concentrations (n=1872-2871) and UVA ₂₅₄ (n=3-5), turbidity (n=5-9), pH (n=9) and temperature (n=430) values. The measurements values represent water quality at sampling locations from late August to mid-September 2017 and mid-April to beginning of May 2018. The distances are given in x direction.....	73
Table 7-1: Theoretical and investigated liquid velocities and Reynold numbers for the corresponding SMARTplus bioreactor flow rates. The theoretical velocity corresponds to the effective velocity for the SMARTplus bioreactor and to the flow velocity for the lab scale setup, as the latter contains no porous media. Re is calculated with the outer diameter of the membrane (d _o) as reference length.	90

Table 7-2: Input and calculated parameters for estimating the membrane area and the design of membrane contactors required to ensure 3.0 mg/L DO after the EA compartment.	96
Table 7-3: Mean DOC, DO (n=3,525), NH ₄ ⁺ -N, NO ₃ ⁻ -N concentrations, UVA ₂₅₄ and pH (n=16) values in sampling locations during operation with the in-situ oxygen delivery, 2019 (for the rest of the parameters n=4-5). Locations of the sampling ports in the x direction are given in mm. The locations of the DO sensors are given in Figure 7-5.	97
Table 8-1: The required and measured DOC concentrations (n=32 baseline, n=5 sequential), turbidity values (n=55 baseline, n= sequential) and NH ₄ ⁺ -N (n=3 baseline, n=5 sequential) concentrations for WWTP effluent (WWTPe) and SMARTplus feed water (SMARTplus) during baseline and sequential operation. The measured values are given as mean ± standard deviation.	117
SI-Table 9.4-1: Description and source of WWTP data for each federal states.	130
SI-Table 9.5-1: Specifications of the dual-media filter (d=44 cm). Effective flow velocity (v _e) and hydraulic retention time (HRT) were characterized based on an influent flowrate of 300 L/h.	134
SI-Table 9.5-2: Feed water concentrations of all quantified TO _r Cs during the baseline operation. Mean values are given with standard deviation; TO _r Cs oncentrations < 4*LOQ were excluded..	134
SI-Table 9.5-3: Empirically estimated and calibrated hydraulic conductivities in the SMARTplus bioreactor.	134
SI-Table 9.5-4: Principal hydraulic, transport and numerical model parameters.	135
SI-Table 9.5-5: Estimation of the hydraulic residence times (HRT) at each observation point derived from truncated temporal moment of the simulated breakthrough curves based on a steady input concentration in the SMARTplus bioreactor (Luo et al., 2006).	135
SI-Table 9.6-1: Attenuation of naturally occurring surrogate (F+ phages and somatic coliphages, n=3) and indicator viruses (HuAdV and HuNV, n=2) in the WWTP, RDMF and SMARTplus pilot bioreactor. While the LRVs for the indicator viruses are mean values, the LRVs for surrogate viruses were given as two individual values.	139
SI-Table 9.8-1: Distribution of the WWTP effluent contributions for the selected river basins under MMAD and MAD discharge for all gauging stations (data shown as % gauging stations exceeding specific contributions).	145
SI-Table 9.9-1: Average DO (n=15,512), DOC, and NO ₃ ⁻ -N (n=10-12) concentrations in feed water, at the end of the infiltration trench, 1 st infiltration step and in the effluent between April-September 2018 during baseline operation of the SMARTplus bioreactor. The percent removals of TO _r Cs	

(n=10-12) are calculated by the TOrC concentrations at the infiltration trench, 1st infiltration step and bioreactor effluent normalized to corresponding feed water concentrations. 150

List of abbreviations

Adv	Adenovirus
AhR	Aryl hydrocarbon receptor
AOP	Advanced oxidation processes
AR	Aquifer recharge
ARB	Antibiotic resistant bacteria
ARG	Antibiotic resistant gene
ASR	Aquifer Storage and Recovery
ASTR	Aquifer Storage, Transfer and Recovery
AWT	Advanced water treatment
BDOC	Biodegradable organic carbon
BTC	Breakthrough curve
CBZ	Carbamazepine
CT	Contact time
CTD	Conductivity-temperature-depth
DALYs	Disability adjusted life years
DBPs	Disinfection by products
DO	Dissolved oxygen
DOC	Dissolved organic carbon
DPR	Direct potable reuse
DWTP	Drinking water treatment plant
EA	Electron acceptor
EC	Electrical conductivity
ER-α	Estrogen receptor alpha
EU	European Union
FAT	Full advanced treatment
FTC	Flow through cytometry
GDWQ	Guidelines for Drinking-water Quality
GEA	German Environment Agency
GFZ	Gemfibrozil
GIS	Geo information system
GWR	Groundwater recharge
GWRS	Groundwater replenishment system
HAdV	Human adenovirus
HNv	Human norovirus
HRT	Hydraulic retention time
IBF	Induced bank filtration
IOX	Iohexol
IPR	Indirect potable reuse

LA-qPCR	Long amplification quantitative polymer chain reaction
LC-MS/MS	Liquid chromatography coupled with tandem mass spectrometry
LOQ	Limits of quantification
LRV	Log reduction values
MAD	Mean annual discharge
MAR	Managed aquifer recharge
MABR	Membrane aerated bioreactor
MEC	Monitored environmental concentration
MMAD	Minimum mean annual discharge
MNv	Murine norovirus-1
MRL	Method reporting limit
MTL	Monitoring trigger level
MW	Monitoring well
ORC	Oxygen releasing compounds
OXY	Oxypurinol
PDFs	Probability density functions
PDMS	Polydimethylsiloxane
PE	Population equivalent
PFU	Plaque forming unit
PNEC	Predicted no effect concentration
QMRA	Quantitative microbial risk assessment
qPCR	Quantitative polymer chain reaction
RDMF	Rapid dual-media filter
RO	Reverse osmosis
RT-qPCR	Reverse transcription quantitative polymer chain reaction
RSF	Rapid sand filter
SAT	Soil aquifer treatment
SMART	Sequential managed aquifer recharge technology
SMX	Sulfamethoxazole
SUC	Sucralose
SWRCB	Californian State Water Resources Control Board
TOrCs	Trace organic chemicals
TF	Total fluorescence
TP	Transformation products
UWWTD	Urban wastewater treatment directive
UVA₂₅₄	Ultraviolet absorbance at 254 nm
VSA	Valsartanic acid
WWTP	Wastewater treatment plant
3D	Three-dimensional

1. General Introduction

The availability and quality of conventional drinking water resources, i.e. ground and surface water, is declining due to population growth, climate change, as well as rising water demand in agriculture and industry in many regions worldwide. While approaching the limits of conventional water supplies *water reuse* becomes the utmost holistic and sustainable approach to overcome today's challenges and to meet future needs by (i) supplying an alternative water source at a fit-for-purpose quality, (ii) decreasing the loads of wastewater born constituents by reduced discharge of secondary effluent to the aquatic environment, (iii) reducing the dependence of communities with regard to water supply (iv) providing a well monitored and safe water quality due to risk based management strategies in comparison to current water management praxis (Asano et al., 2007).

Planned potable water reuse was born out of a necessity, as water supply was overburdened, and was then followed by regulatory developments. In the regions, where there is tangible evidence for water scarcity, declining quantity of conventional fresh water sources or increased demand due to rapid population growth, water reuse became attractive to decision makers and utilities. Accordingly, successful water reuse schemes have been applied in densely populated and arid regions, such as the USA, Australia, Singapore and Belgium, mostly based on high-pressure membrane technologies, with concentrated waste streams and high energy demand (USEPA, 2017; WHO, 2017).

Drinking water supply in many countries, in particular in central and western Europe heavily relies on indirect use of surface water via induced bank filtration (IBF) and aquifer recharge (AR) (Hannapel et al., 2014; Sharma and Amy, 2011). Exemplarily, in Germany, a country with comparatively high water availability in most areas, production from IBF and AR accounts for more than 15% of the drinking water supplied nationwide, but at the individual utility level this contribution can be in excess of 70% (Senate Department for Urban Development and Housing Berlin, 2017). In highly populated areas and where substantial natural base discharge is lacking, the quality of surface water can be highly affected by point sources (e.g. effluents of wastewater treatment plants), as well as contributions from various non-point sources (e.g., drainage from agricultural areas, storm water runoff, urban seepage) with not well-characterized effects on the IBF and AR. However, in such regions, where the effects of current water management practices on the drinking water supply is not as clear, planned water reuse faced and still faces obstacles in stakeholder's acceptance, demonstrating the importance of a clear perception on the status quo versus sustainable water resources management. These observations led to the two main objectives of this dissertation: "*Assessment of municipal wastewater contributions in German surface waters and associated impacts on the drinking water supply*" and the "*Development, construction and operation of a novel hybrid biofilter, SMARTplus, based on sequential managed aquifer recharge technology (SMART) for indirect potable reuse*".

2. State-of-the-art

2.1. Current water management – *de facto* reuse

Worldwide many municipalities withdraw drinking water either directly from surface waters, e.g. USA, or through IBF and AR, e.g. central and western European countries (Hannapel et al., 2014; Sharma and Amy, 2011). Beside pristine waters, river segments containing varying amounts of upstream wastewater effluents are being used as a source of drinking water depending on the location of the drinking water treatment plant (DWTP) (Figure 2-1).

Discharging wastewater effluents to a stream that is subsequently used for drinking water abstraction is referred to as unintended or *de facto* water reuse (National Research Council, 2012; Rice and Westerhoff, 2015). There have been a few studies in the USA, Switzerland, China and Spain, which have investigated nationwide or for some river catchment areas, the occurrence of wastewater effluents in the rivers (Mujeriego et al., 2017; Rice and Westerhoff, 2015; Wang et al., 2017; Wiener et al., 2016). Significant shares of 10 to 50% wastewater effluent in the rivers point the need to understand the relevance of discharging wastewater effluents on drinking water supplies and to quantify what degree of *de facto* reuse actually constitutes a potential threat to human health.

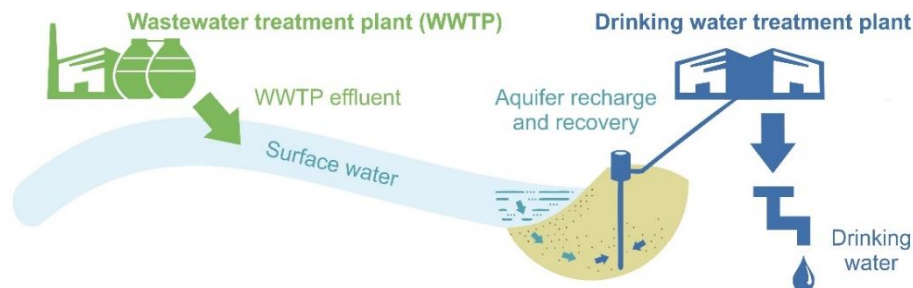


Figure 2-1: Conventional drinking water augmentation via induced riverbank filtration (© Berlin Water Company / Technical University of Munich, 2017).

Where surface waters are directly used for the drinking water supply, subsequent treatment steps are employed in some DWTPs (e.g., disinfection steps or barriers for chemical constituents), which aim to compensate the poor surface water quality. Due to the frequent occurrence of low water levels, the discharges from wastewater treatment plants (WWTPs) are less diluted, which might become a challenge and cause high costs due to required upgrades of DWTPs. In case of indirect use, the chemical and microbial quality of bank filtrate depends not only on surface water quality, the extent of wastewater effluent contributions, and the level of wastewater treatment, but also on a large number of site-specific factors. These include the location and type of wells, flow paths between the surface water and abstraction wells, relative contributions from landside groundwater, and hydro-biogeochemical factors such as hydraulic permeability, sediment conductivity, and prevailing redox conditions (Regnery et al., 2017; Storck et al., 2012). Drinking water facilities are required in many European countries to comply with a 50-day hydraulic retention time (HRT) in the subsurface to

assure proper inactivation of pathogens, i.e. the microbial safety of raw water. However, in regions with karstic subsurface or wells at an immediate proximity to the surface waters, microbial safety of the bank filtrate also might not be guaranteed.

2.2. Fate of emerging contaminants during conventional wastewater treatment and in receiving river streams

2.2.1. Level of treatment in conventional wastewater treatment

Conventional WWTPs mainly composes of primary (e.g. sedimentation) and secondary treatment steps (e.g. activated sludge), aiming the removal of suspended solids, biodegradable organic matter and nutrients (phosphorus and nitrogen). Some WWTPs contain also tertiary treatment, including additional suspended solid removal (e.g. depth filtration) and are partially followed by disinfection (chlorination or UV treatment). Accordingly, unit operations applied in the conventional WWTPs are not designed to remove all of the known constituents from raw sewage, e.g. pathogens, dissolved organic and inorganic chemicals of anthropogenic origin, antibiotic resistant bacteria (ARBs) and resistant genes (ARGs).

2.2.2. Waterborne pathogenic organisms

Waterborne diseases origin from enteric pathogens, including intestinal bacteria (e.g. *Escherichia coli*, *Salmonella*, *Campylobacter*), protozoa (e.g., *Giardia lamblia*, *Cryptosporidium parvum*) viruses (e.g. adenovirus, norovirus, rotavirus) and helminths (e.g. *Ascaris lumbricoides*) (WHO, 2017). Those pathogens occur in raw sewage at relatively high concentrations (e.g. *Escherichia coli* 10^5 - 10^{10} No./100 mL, *Giardia* $<10^0$ - 10^5 No./100 mL, adenovirus 10^0 - 10^6 pfu/100 mL, *Ascaris lumbricoides* 10^0 - 10^3 No./100 mL) (USEPA, 2012; WHO, 2017). Due to their high concentrations in raw sewage and very low infectious dose numbers, their reduction is expressed as log reduction values (LRVs);

$$\log reduction = -\log\left(\frac{C_{eff}}{C_{feed}}\right) \quad [2.1]$$

with feed water concentration of C_{feed} and effluent concentration of C_{eff} . While some protozoa, bacteria (< 1 LRV) and helminth ova (0.3-1.7 LRV) are readily removed during primary clarification, overall pathogens survive primary treatment (Asano et al., 2007). Secondary treatment achieves between 1 to 2 LRVs for wide range of pathogens, whereas a complete elimination cannot be expected, even after final disinfection (Asano et al., 2007).

Protozoa are larger than bacteria or viruses in size and, if depth filtration is applied as tertiary treatment, can be attenuated up to 3 LRVs (Asano et al., 2007; USEPA, 2012). However if disinfection via chlorine is considered as tertiary treatment instead, they may survive (< 1 LRV)

under short contact time and chlorine low doses (USEPA, 2012). Alternatively, UV can be applied as tertiary treatment to reduce the concentrations for protozoa and bacteria up to 3 to >6 LRVs depending on the UV fluence. Due to their relatively small size, viruses are barely removed during primary and secondary treatment. Comparatively higher doses of UV (235 mJ/cm²) can inactivate viruses up to >6 LRV, and therefore are often chosen as a tertiary treatment step (USEPA, 2012; WHO, 2017). Once discharged into surface waters, further concentration elimination may take place due to dilution and die-off, depending on oxygen concentrations, salinity, turbidity, UV light exposure and mainly temperature in the receiving waters (Asano et al., 2007; Gerba, 2007). Surviving pathogens can pose risk to human health, in case of ingestion or contact with water sources containing significant shares of secondary effluent.

2.2.3. *Chemical constituents*

The inorganic (e.g. heavy metals, salts, nutrients) and organic chemical constituents (e.g. natural organic matter, fecal matter, industrial and household organic chemicals) in raw sewage occur naturally and or due to anthropogenic contributions. Many known and unknown synthetic organic chemicals used by industry and households end up in the raw sewage at varying concentrations. During primary and secondary treatment, metal, nutrient and total organic compound concentrations are reduced, however recalcitrant polar organic chemicals remain unchanged or undergo transformations and can be found in the secondary effluent in µg/L to ng/L range due to their hydrophilic properties at typical pH values of 7 to 8 in wastewater (Loos et al., 2013; Ternes, 1998; USEPA, 2017).

The presence of such chemicals at trace levels, referred to as trace organic chemicals (TOrcs), have been subject of research since developments of sensitive instruments for analytical chemistry (Kolpin et al., 2002; Ternes, 1998). TOrcs cover a broad group of compounds; such as pesticides, preservatives, flame retardants, perfluorochemicals, pharmaceutical residues, personal care products, antibiotics, surfactants, steroidal hormones, transformation products (TPs), and disinfection by-products (DBPs). TOrcs can not only be found in secondary effluent but also in the receiving waters, and might make their way into ground water and even drinking water (Ebele et al., 2017; Glassmeyer et al., 2005; Hass et al., 2012; Loos et al., 2009; Reemtsma et al., 2006; 2016; USEPA, 2017).

To date, comprehensive nationwide and international monitoring studies investigated the occurrence of TOrcs, varying in numbers between only a few up to more than 150 substances, in wastewater effluents and river streams (Bernot et al., 2016; Glassmeyer et al., 2005; Loos et al., 2009; 2013; Reemtsma et al., 2010). In a European wide study on the occurrence of TOrcs in wastewater effluents, 125 chemicals (80% of the targeted compounds) could be detected in wastewater effluents ng/L up to µg/L concentration range, 41 compounds of which were present with concentrations of more than 1 µg/L (Loos et al., 2013). In the receiving streams 23 out of 35 selected TOrcs could be detected in

more than 50% of the samples, where benzotriazole, tolytriazole, nonylphenoxy acetic acid, caffeine, carbamazepine, nonylphenol, ibuprofen, diuron, sulfamethoxazole were measured at highest concentrations varying between 1,225 to 100 ng/L (90th percentile) (Loos et al., 2009). Bernot et al. (2016) detected 33 different TOrCs with a frequency of 93% across United States river streams, the most common substances of which were caffeine, carbamazepine, cotinine, sucralose, sulfamethoxazole, triclosan and venlafaxine. Therefore, some of these compounds, such as carbamazepine, acesulfame and oxypurinol, have been proposed and used as wastewater indicators, as they persist in WWTPs, surface waters and subsurface passage (Clara et al., 2004; Funke et al., 2015; Jekel et al., 2015). This widespread dissemination is owed to their complex structures with multiple functional groups, their polar characteristics, as they are tailored to persist during applications in hospitals, households, agriculture, livestock farming, environment and industry.

Some of the TOrCs (e.g., carbamazepine, diclofenac) are known for their ecotoxicological effects and attributed risks due to their high concentrations and detection of frequency (Ebele et al., 2017; Ferrari et al., 2003). Numerous compounds (e.g., carbamazepine, caffeine, ibuprofen and metformin) are known to bio-accumulate due to their lipophilic characteristics (Ebele et al., 2017). While a few chemicals are already recognized as carcinogenic (e.g., perfluorochemicals, 1,4-dioxane, NDMA and bromate), others are presumed to interfere with the endocrine system (Asano et al., 2007; Pal et al., 2014). For the protection of human health, predicted no effect concentrations (PNEC) have been developed based on exposure and toxicity information (Drewes et al., 2018). In Germany, in addition to drinking water threshold values, precautionary values such as health orientation values (in German *gesundheitliche Orientierungswerte*, GOW) have been also used for the compounds with limited toxicological information but occurrence at high concentrations in raw water sources (German Environment Agency, 2018b). However, it is important to consider that for some mixture of compounds, acute toxicity has been reported at lower concentrations than for the compounds individually suggesting synergistic effects (Petrie et al., 2015).

2.3. Planned potable reuse applications

Unequal distribution of water, dynamics in the water quantity due to climate change, deteriorations in the quality of fresh water sources and high demands are the reason for the rising interest in water reuse in different fields worldwide, ranging from potable to non-potable applications. Worldwide, the largest groundwater or surface water withdrawals are due to agricultural irrigation, while industrialized countries and metropolitan areas have comparatively higher water demand for potable purposes and industrial applications (Zimmerman et al., 2008). Given the focus of this dissertation, only potable reuse applications will be addressed in the following chapters.

Potable reuse comprises indirect and direct reuse of advanced treated wastewater to augment drinking water sources. Key components of potable reuse schemes are the employment of advanced water

treatment steps subsequent to conventional wastewater treatment and an overarching monitoring program for performance control. Besides, a source control program is recommended to minimize the discharge of chemicals (e.g. heat stabilizers, biocides, epoxy resins, bleaching chemicals and by-products, solvents, degreasers, dyes, chelating agents, polymers, poly aromatic hydrocarbons, polychlorinated biphenyls, and phthalates), resulting in lower concentrations of chemical constituents in the raw sewage, which not only improves the quality of secondary effluent, thus the final water, but also decreases the cost of subsequent advanced water treatment (Drewes and Khan, 2011).

2.3.1. Indirect potable reuse

Augmentation of drinking water supplies with advanced treated wastewater via an environmental buffer is called indirect potable reuse (IPR) (Figure 2-2), which reduces the dependency and burden on seasonally and climatically changing conventional water sources by shortening the natural hydrological replenishment cycle (Drewes and Khan, 2011). The key element of an IPR design is employment of an environmental buffer either through groundwater augmentation, applying a managed aquifer recharge (MAR) technique, or surface water augmentation into a stream or a reservoir (Drewes and Khan, 2011; National Research Council, 2012).

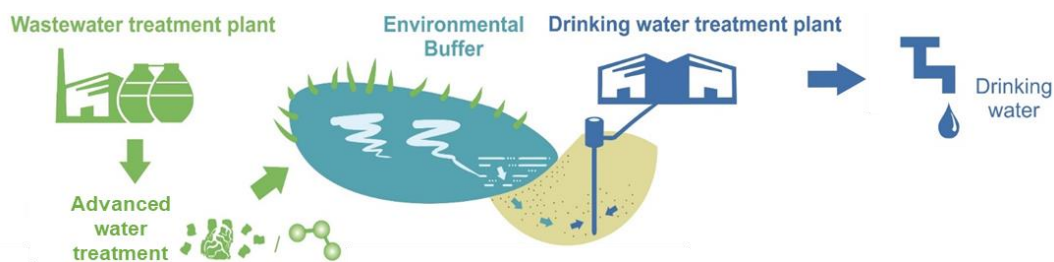


Figure 2-2: A schematic illustration of indirect potable reuse via groundwater augmentation (modified from © Berlin Water Company / Technical University of Munich, 2017).

Environmental buffers might remove constituents of concern, damp varying concentrations, and in many cases result in dilution with other water sources (Dillon, 2005; Drewes and Khan, 2011; Kuehn and Mueller, 2000; Sharma and Amy, 2011). In addition, environmental buffers are used as storage, if the production exceeds the water demand. However, the microbiological or chemical state of surface waters (e.g., pathogen and pesticide content) or ground water (e.g., arsenic and nitrate content) might degrade the advanced treated wastewater quality and therefore, the quality of considered environmental buffer should be analyzed prior to the design phase of a treatment plant. Despite all the benefits of IPR schemes, for the locations with poor surface or groundwater quality, little space and confined aquifer, direct transport of advanced treated wastewater to a DWTP or distribution in the potable water pipeline might be a better alternative (WHO, 2017).

2.3.2. Direct potable reuse

During direct potable reuse (DPR), the use of an environmental buffer is either completely eliminated or exchanged by an engineered storage unit. However, an engineered storage unit might provide only a few hours to days and lack benefits of response time and attenuation processes (Figure 2-3). Therefore, additional and more complex treatment barriers (mainly high energy demand treatment steps, such as reverse osmosis) and higher level of monitoring are applied for DPR schemes. Complex advanced water treatment schemes, residuals management and high degree of automation are associated with additional costs (more information can be found in chapter 2.5).



Figure 2-3: A schematic illustration of direct potable reuse (modified from © Berlin Water Company / Technical University of Munich, 2017).

Overall, when planning potable reuse projects, selection of either IPR or DPR applications should be based on the source water and site specific characteristics, water quality requirements, costs and policies for this region.

2.3.1. Multiple-barrier concept

Given the origin of the source water, potable reuse projects should be carefully designed to provide safe drinking water quality. Therefore, the practices are characterized by the employment of multiple treatment options, so-called *multiple-barrier concept*, providing redundancy and overall robustness (Drewes and Khan, 2011). The overall aim of the multiple-barrier concept is to ensure steady water quality despite of temporary and potential failures in individual treatment steps with diverse removal mechanisms and operation modes. The recommendation of multiple-barrier concept for potable reuse by the WHO dates back to 1975, where at least two to three but preferably more treatment processes were foreseen for each group of pollutants (WHO, 2017).

One barrier of a treatment train can perform in a wide range, depending on the operational conditions and lifetime of the treatment step. A certain degree of redundancy in the treatment steps and auxiliary equipment increases the likelihood of meeting the performance targets. Consequently, WHO recommended that a potable reuse treatment train should include at least seven treatment barriers, tailored to eliminate; (i) pathogens (three of the barriers), (ii) physical and organoleptic (e.g. color, taste, smell) parameters (two of the barriers), (iii) TOxCs (four of the barriers) and (iv) critical parameters without public health risk (e.g. stabilization of water by pH correction, restoration of alkalinity and mineral hardness) (one barrier) (WHO, 2017). Apart from that, online monitoring tools

and management protocols for hazardous events, standby power supplies, emergency storage or disposal options increase the resilience of a treatment train (Drewes and Khan, 2011).

2.4. Requirements and monitoring strategies for potable reuse

2.4.1. National and international regulations and guidelines

To date, there have been several regulations or guidelines passed for potable reuse especially in water scarce areas in the world. In general, the water quality of a potable reuse scheme has to comply with existing drinking water quality standards of the region.

Australia developed their Guidelines for Drinking Water Augmentation to conform to the Guidelines for Drinking-water Quality (GDWQ) published by WHO (2006) with a strong focus on risk management (i.e. Water Safety Plans) and microbial performance targets already in 2008 (NRMMC-EPHC-NHMRC, 2008). Based on the site-specific conditions, the microbial quality targets should be met at the point of compliance, which are defined to be just prior to aquifer recharge for IPR schemes. For chemicals of concern, the guidelines used interim thresholds or screening levels based on the available toxicological information at the time (NRMMC-EPHC-NHMRC, 2008).

In the United States, the guidelines and regulations for drinking water, surface water and wastewater quality date back to the middle of the 20th century (Asano et al., 2007). The reuse guidelines and regulations contributed to the rapid development of water reuse, by ensuring higher quality of wastewater effluents prior to discharge, turning treated effluents readily available sources for water reuse, which include the Water Pollution Control Act (1948); the State Water Code (1960); the Clean Water Act (1972); the Safe Drinking Water Act (1974); the State of California's Wastewater Reclamation Criteria (1978); California's Water Recycling 2030 Plan (2003); and finally the EPA Guidelines for Water Reuse (1992, 2004, 2012, 2017) (Asano et al., 2007; Bieber et al., 2018; USEPA, 2012, 2017; WHO, 2017). In 2014, the State of California set pathogen reduction targets for IPR applications going from conventional WWTP to DWTP, requiring at least three treatment processes for each pathogen, incorporation of reverse osmosis (RO) and advanced oxidation processes (AOPs) for the removal of chemicals, at least two months of HRT for soil aquifer treatment (SAT), and monitoring and operation plans in case of failures (USEPA, 2017; WHO, 2017). Thereby, the California regulations give credits for aquifer recharge techniques (e.g. SAT or surface spreading), whereas the Australian guidelines do not (USEPA, 2017). Other states, such as Texas, also developed guidelines for DPR with targets less stringent than those set by regulators in California (USEPA, 2017; WHO, 2017).

In the European Union, the EU Water Framework Directives promote the reuse of treated wastewater back in 2000. Under the frame of Circular Economy, European Union aimed to develop legislatives to further promote water reuse in Europe (EU Commission, 2015). As a first effort, minimum

requirements for water reuse in agricultural irrigation and aquifer recharge was proposed by Joint Research Committee of the European Union (Alcalde-Sanz and Gawlik, 2017). However, the technical report focused more on agricultural reuse and recommended no EU-wide requirements for aquifer recharge due to site specific boundary conditions and possible health or environmental risk concerns from the member states (Alcalde-Sanz and Gawlik, 2017). As an outcome, very recently, in May 2020, a regulation on the minimum quality requirement for agricultural reuse have been published by the European Parliament, which will be valid in the EU member states within the next three years (EU, 2020). However, as there was no European wide regulations until May 2020 on water reuse, several member states applied their own legislative frameworks, regulations or guidelines (Alcalde-Sanz and Gawlik, 2014). The arid European countries (Spain, Cyprus, Italy, Portugal, Greece and France) possess the most comprehensive standards on reuse for landscape and agricultural irrigation purposes, while Cyprus, Spain and Greece also cover aquifer recharge for non-drinking water aquifers (Alcalde-Sanz and Gawlik, 2014; Drewes et al., 2017). Especially potable reuse is not widely applied in Europe and there are only three IPR projects in operation, located in England, Sweden and Belgium (WHO, 2017). The later was developed based on specific regional standards, without general water reuse guidelines or regulations for Belgium, to augment drinking water and to elevate groundwater table against seawater intrusion (Alcalde-Sanz and Gawlik, 2014; van Houtte and Verbauwheide, 2008).

2.4.2. Treatment goals for potable reuse

Potential transmission of diseases, caused by waterborne pathogens or chemical constituents present in treated wastewater, is the biggest concern for potable reuse. Therefore, in this chapter, pathogens and trace organic compounds will be addressed specifically. While the health risks of waterborne pathogens are well known, the long-term health effects and the environmental impact of emerging chemicals, such as trace organic chemicals or ARBs and ARGs are still subject to further research.

2.4.2.1. Microbial parameters and performance targets

Regulatory agencies require routine monitoring of treatment processes to ensure hygienically safe drinking water quality after water reuse. However, high number of different pathogenic organisms, their varying concentrations and elaborate analytical methods, make it impossible to measure each individual pathogen concentrations after each treatment step, regularly. Therefore, so-called indicator and surrogate microorganisms and surrogate performance parameters are chosen for the assessment of fecal contamination, treatment efficiencies and overall performance of a water reuse treatment train, which are in comparison more abundant and resistant.

For bacterial fecal contamination, fecal coliforms, total coliforms, or a subset of total coliforms (e.g. *Escherichia coli*) are chosen as indicators. Overall, the waterborne bacteria can be easily eliminated

by disinfection and therefore do not cause concern for potable reuse schemes. Due to their high susceptibility to chlorination or UV treatment, the bacterial indicators are not considered suitable indicators for protozoa and viruses (Bonadonna et al., 2002; Brookes et al., 2005; Rose et al., 1988). In water, the protozoa form very persistent cysts or oocysts and can survive easily chlorine disinfection or low doses of UV irradiation (Drewes and Khan, 2011). Therefore, *Giardia* and *Cryptosporidium* are required to be monitored additionally as indicator pathogens, exemplarily by the States of Florida, California and Arizona for potable reuse projects (USEPA, 2012). As an alternative, *Clostridium* can be used as an indicator, spores of which are more resistant to treatment steps similar to these protozoan (USEPA, 2017). Viruses are perceived as the most significant risk for the public health in potable reuse projects due to their small size, high concentrations, low infectious dose – high infectivity and monitoring difficulties (Drewes and Khan, 2011). To achieve a high log reduction for viruses during disinfection, higher chemical concentrations or UV light intensity might be required in comparison to other pathogens. Overall, the bacteriophages (e.g., MS2 – F⁺ phage - RNA, φX174 – somatic coliphage- DNA) were found to be well suited as surrogate for viruses (Asano et al., 2007).

As pathogenic organisms, indicators and surrogates occur at varying concentrations, performance assessment of a technology is often made by challenge tests. Spiking high influent concentrations of surrogates during challenge tests allows the prediction of maximum log reduction capability of a technology at exceptionally high loads (USEPA, 2012). The LRVs of indicator and surrogate organisms during secondary treatment and advanced water treatment can vary to a great extent, due to their design parameters (e.g., pore size, filter depths) and operational conditions (e.g., retention times, concentrations of the chemical additives, treated wastewater and pretreatment) (Table 2-1). Therefore, LRVs should be considered as relative reduction and performance of a unit operation should be validated at pilot scale prior to commissioning.

Once the treatment efficiencies for the indicator and surrogate organisms are assessed during the start-up phase, the indicator and surrogate specific LRVs should be correlated with parameters, such as, turbidity for protozoa during filtration, disinfectant residuals versus contact time (CT) for bacteria and viruses during chemical disinfection, pressure decay tests, sulfate or fluorescent dyes for bacteria, protozoa and viruses during RO treatment (NRMMC-EPHC-NHMRC, 2008; USEPA, 2017; WHO, 2017). The LRVs achieved by the treatment schemes should be also reproducible by the reductions in the measurement values of surrogate parameters. Therefore, instead of turbidity, TOC or EC with only 1 to 2 LRV range, sulfate, phosphate, pressure decay tests and dyes were found to be better surrogates for the performance assessment of ROs regarding their 3 to 5 LRVs (USEPA, 2017). Overall, weekly measurement of indicator and surrogate microorganisms and continuous real-time monitoring of surrogates were recommended by the Australian guidelines (NRMMC-EPHC-NHMRC, 2008).

Table 2-1: Indicative log reduction values of indicator and surrogate microorganisms (*italic*) and enteric pathogens during various stages of wastewater treatment, adapted from Asano et al. (2007) and USEPA (2012). *n.a.* indicates not available.

Treatment technologies	Indicators & Surrogates				Pathogenic microorganisms			
	<i>E. coli</i>	<i>Clostridium</i>	<i>Phage</i>	<i>Campylob.</i>	Viruses	Giardia	Crypt.	Helminth
Second. Treat.	1-2	0.5-1	0.5-2.5	1-3	0.5-2	0.5-1.5	0.5-1	0-2
Filtr. & Coag.	0-1	0-1	1-4	0-1	0.5-2	1-3	1.5-2.5	0-3
UF, NF&RO	4->6	>6	2->6	4->6	2->6	>6	4->6	>6
Storage	1-5	<i>n. a.</i>	1-4	1-5	1-4	3-4	1-3.5	1.5->3
Ozonation	2-6	0-0.5	2-6	2-6	3-6	2-4	1-2	<i>n. a.</i>
UV	2->6	<i>n. a.</i>	3->6	2->6	1->6	3->6	3->6	<i>n. a.</i>
AOP	>6	<i>n. a.</i>	>6	>6	>6	>6	>6	<i>n. a.</i>
Chlorination	2->6	1-2	0-2.5	2->6	1-3	0.5-1.5	0-0.5	0-1

Despite the choice of the right indicators and surrogates for the source water, the measurement methods for monitoring represent another challenge, while assessing the aforementioned treatment efficiencies and overall performance of a potable reuse project. Time intensive cell culture methods might fail in measuring low concentrations of pathogens, which might be still high enough to be infectious (Girones et al., 2010). Due to the lack of culture methods for some pathogenic strains, but also as pathogens might be at a viable but non-culturable stage or embedded into biofilms, the cell culture methods are not capable of measuring all available pathogens, resulting in underestimation of their concentrations (Girones et al., 2010; Hewitt et al., 2011). Development of molecular methods based on nucleic acid amplification (mostly applied as quantitative polymerase chain reaction, qPCR), increase the sensitivity and decrease the time required for detecting specific pathogens (Girones et al., 2010). However, these measurement methods do not distinguish between viable / non-viable cells, and therefore might overestimate their concentrations. Gerba et al. (2017) argued in their review the advantages of qPCR over the cell culture methods in virus detection, as the viruses detected by qPCR were mostly infectious, detected to infectious rate being in the range of 25:1 to 794:1 as reported by Hewitt et al. (2011). Overall, long amplification qPCR (LA-qPCR) measurement might overcome the issues on the differentiation upon viable/non-viable pathogens in the near future for at least UV disinfection treatment steps (Ho et al., 2016), but currently the molecular methods are still accompanied by culture methods. Supplementary, a promising particle detection method, called flow through cytometry (FTC) can be applied, which can provide information within minutes to hours and has been recently applied as a real-time monitoring method for pathogens (Safford and Bischel, 2019). Yet, there are no standardized FTC viability assessments for all pathogens and real-time-FTC monitoring has not been applied for viruses. Prior to the wide-range application of FTC, more research on protocols for specific pathogen detection, standardization and computational tools for data analysis and interpretation are needed (Safford and Bischel, 2019).

For potable reuse, WHO (2017) recommends LRV targets of 9.5 for enteric viruses (norovirus), 8.5 for both enteric bacteria (*Campylobacter*) and enteric protozoa (*Cryptosporidium*), based on a health risk approach with an upper burden limit of 10^{-6} disability adjusted life years (DALYs) per person per year (pppy). DALY is employed to quantify health effects of a disease (i.e., severity, duration) and number of people infected by that pathogen and the upper limit of a burden can be identified higher or lower than 10^{-6} by the policy makers, regarding the site-specific circumstances (WHO, 2011). Pathogen concentrations equivalent to 10^{-6} DALYs were determined as $1.1 \cdot 10^{-5}$ norovirus/L, $2 \cdot 10^{-5}$ *Campylobacter*/L and $1.2 \cdot 10^{-5}$ oocysts/L (WHO, 2017), and eventually the LRV targets were calculated by equation 2.1. While setting these LRV targets, default raw sewage concentrations of $2 \cdot 10^4$ noroviruses/L, $7 \cdot 10^3$ *Campylobacter*/L and $2.7 \cdot 10^3$ infective *Cryptosporidium* oocysts/L were assumed as point values by WHO (2017). This approach was adopted by Australian NRMCC-EPHC-NHMRC (2008) and led to similar LRVs of 9.5 for enteric viruses, 8.1 for enteric bacteria and 8 for enteric protozoa. For IPR projects, the State of California followed a “12/10/10” approach, where enteric viruses should be attenuated by 12, and enteric protozoa (*Giardia* and *Cryptosporidium*) by 10 logs (USEPA, 2017). This approach considers the highest daily concentration of $1 \cdot 10^5$, $1 \cdot 10^5$ and $1 \cdot 10^4$ infectious units/L for norovirus, *Giardia* and *Cryptosporidium* measured in raw sewage, determined by cell culture methods, and aims to achieve a maximum annual infection risk of 10^{-4} pppy (max. 1 infection per 10,000 people), resulting in more conservative target LRVs in comparison to the WHO Guidelines (USEPA, 2017). Accordingly, the LRVs achieved by individual unit operations can be added and a potable reuse treatment train can be developed combining unit operations to meet these health-based LRV targets.

Compliance of pathogenic organisms to health based targets in certain treatment trains/schemes can be estimated by quantitative microbial risk assessment (QMRA), which is composed of 4 steps: hazard identification, dose-response analysis, exposure assessment, and risk characterization (Medema, 2013). The first three steps identify the concentrations of pathogens of concern, their attenuation in treatment steps, how humans can encounter them and these can be described using probability density functions (PDFs) instead of point values. When summing these PDFs and sampling them numerous times using a Monte Carlo analysis during risk characterization, the resulting final risk PDF can be evaluated for average and worst-case values (USEPA, 2012). QMRA not only provides disease burden target levels, but can also be used to identify the most important barriers in a treatment train and the possible impacts of hazardous events on treatment efficiency (Medema, 2013). Based on the outcome of the QMRA, an annual risk of infection can be identified, which can eventually be compared to the WHO guidelines and/or the national regulations.

Recent QMRA based studies, employing updated pathogen density estimates and dose response relationships, recommended to consider higher LRVs to achieve the 10^{-4} pppy annual infection risk benchmark especially for viruses and protozoa (Gerba, 2007; Gerba et al., 2017; Messner and Berger,

2016; Soller et al., 2018; van Abel et al., 2017). Gerba et al. (2017) pointed out the new developments on the virus detection due to molecular methods (qPCR) resulting in increased maximum daily concentrations from $1 \cdot 10^5$ to $1 \cdot 10^7$ or even 10^9 per liter, and thus proposed additional 2 to 3 LRVs to manage peak loads of viruses. Soller et al. (2018) suggested at least 14 LRVs for norovirus and 11 LRVs for *Cryptosporidium*, to meet the aforementioned 10^{-4} benchmark, especially within DPR projects.

Last but not least, the spread of ARBs and ARGs has been identified by the [WHO](#) as one of the greatest risks to global public health, which could cause about 10 million deaths annually by 2050 if measures are not taken (O'Neill, 2016). Their occurrence in drinking water sources might pose a risk to human health. Advanced water treatment technologies applied in potable reuse might achieve similar or better water quality than in the conventional drinking water supplies practicing *de facto* reuse, especially regarding ARBs (WHO, 2017). However, there is still a huge demand for research regarding the selection of ARB and ARG indicators of human influence, characterization methods for ARGs, risk assessment models, mitigation practices and treatment efficiencies (Vikesland et al., 2017). Target removal efficiencies for indicator ARGs can be defined initially based on a qualitative risk approaches (comparison of effluent quality to pristine sources), until quantitative risk assessment methods for ARGs are developed, which is very challenging due to horizontal gene transfer (Hiller et al., 2019). Overall, for the future water management, the extension of the targeted removal parameters to emerging ARBs and ARGs should be considered based on the focused investigations on the aforementioned research gaps.

2.4.2.2. Chemical water quality targets

With regard to more than 10,000 compounds being under regular use, we need to accept that a large portion of compounds, TOxCs and their transformation products are not known and might end up in wastewater (Bieber et al., 2018), which raises concerns about unknown individual but also mixture of chemicals triggering toxicological effects for human health in case of *de facto* and planned reuse and the environment (Escher et al., 2020). Given the wide-range of physiochemical properties of these compounds, there is no single advanced treatment barrier to remove all chemicals from secondary effluent. Therefore, redundant combinations of advanced treatment steps; such as chemical oxidation (e.g., O_3 , AOP/ H_2O_2), adsorption (e.g., GAC, PAC), physical separation (e.g., RO, NF), natural and engineered biological systems (e.g., SAT, IBF, advanced biofiltration) are foreseen for the overall attenuation of known and unknown compounds (USEPA, 2012).

Chemicals with readily available thresholds are addressed in drinking water quality regulations, involving traditional fresh water contaminants, such as heavy metals, pesticides or industrial chemicals, but do not represent all municipal wastewater associated compounds (Drewes and Khan, 2011). Wastewater effluents being one of the major dissemination ways for TOxCs, given the origin

of the source water drinking water target goals should be adopted for potable reuse applications. However traditional approaches, e.g. identification of thresholds for all individual compounds are not seen as expedient given the high number of known and unknown chemicals for potable reuse projects (Escher et al., 2020). Instead, a recent report by the California State Water Resources Control Board (SWRCB), edited by their Science Advisory Panel, recommended a short monitoring list with (i) process-based indicator chemicals exhibiting different physicochemical properties and removal capabilities and (ii) health-based indicator chemicals with toxicological relevance (Drewes et al., 2018). The panel has proposed regular up-dates of monitoring trigger levels for chemicals (MTLs), which are derived from PNECs based on exposure and toxicity assumptions, and prioritization of those substances regarding their monitored environmental concentrations (90th percentile) (MEC/MTL>1) for individual IPR projects (Drewes et al., 2018). Similarly, the process-based indicators are site-specific in their selection, as they should not only have low limits of quantification and well defined moderate to high removal capacities for the applied advanced treatment steps, but also should occur in the source water at high frequency and concentrations (Jekel et al., 2015). In the short monitoring list proposed by SWRCB (Table 2-2), health-based indicators were selected based on the most recent MEC/MTL ratios of chemicals, reported by Californian utilities for secondary or tertiary effluent, which need to be updated in case of changes in MTLs, MECs, as well as identification of new chemicals (Drewes et al., 2018). Considering chemicals with MECs measured outside of California, benzotriazole, gabapentin, oxypurinol, valsartanic acid and metformin have exhibited MEC/MTL>1, which are frequently measured at high concentrations in German and European wastewater effluents (Funke et al., 2015; Loos et al., 2013; Nödler et al., 2013).

Furthermore, to manage high number of unknown constituents and better characterize the chemical state of the water, the monitoring effort can be expanded by bioanalytical monitoring tools, i.e. bioassays (*in-vivo*: whole animal, *in-vitro*: cell or protein based tests) (Drewes et al., 2018; Escher et al., 2020; WHO, 2017). These tests can provide valuable information to the operators and regulators about the bioactivity, acute and chronic toxicity, estrogenic effects, and carcinogenicity in the finished water, by screening a wide range of chemicals, including unknown compounds. In the monitoring list, two *in-vitro* bioassays, *estrogen receptor alpha* (ER- α) and *aryl hydrocarbon receptor* (AhR), were involved to screen for known and unknown endocrine disrupting and dioxin-like carcinogenic chemicals, respectively (Table 2-2).

Quarterly analyses of indicator chemicals were recommended for the assessment of the overall treatment efficacy of a water reclamation facility prior to groundwater recharge, during the start-up phase, which would be reduced to twice a year after one year of operation (Drewes et al., 2018). To assess the efficiency of individual treatment steps, indicator chemicals should be also measured prior to and after each unit operation, employed as chemical barrier, with the same measurement frequency.

Table 2-2: Proposed monitoring list for the process and health-based indicator chemicals, surrogates and bioassays for IPR, adapted from Drewes et al. (2018). Following acronyms are used to describe gemfibrozil (GFZ), sulfamethoxazole (SMX), iohexol (IOX), sucrolose (SUC), total fluorescence (TF), electrical conductivity (EC) and method reporting limit (MRL), the latter is given in ng/L.

IPR Type	Bioassays		Health-based indicator		Performance indicator			Surrogate	
	Tool	MRL	Compound	MRL	Comp.	MRL	%Rem. ⁶	Para.	%Rem. ⁶
Surface spreading	ER- α	0.5	NDMA ¹	2	GFZ ³	10	>90	NH ₄	>90
	AhR	0.5	NMOR ²	2	SMX ⁴	10	>30	NO ₃	>30
			1,4-Dioxane ²	100	IOX ³	50	>90	DOC	>30
						SUC ⁵	100	<25	UVA
							TF	>30	
Direct injection & surface water augmentation	ER- α	0.5	NDMA ¹	2	SMX ⁴	10	>90	EC	>90
	AhR	0.5	NMOR ²	2	SUC ⁵	100	>90	DOC	>30
			1,4-Dioxane ²	100	NDMA ¹	2	25-50		

¹DBP, ²Industrial chemical, ³Pharmaceutical residue, ⁴Antibiotic, ⁵Food additive, ⁶Travel time in subsurface for two weeks and no dilution.

As the secondary effluent quantity and quality might change within hours, diurnally or seasonally, water quality and the system performance needs to be monitored in real time. For this purpose, the laboratory measurements for indicator chemicals should be accompanied by the online measurements of surrogates, e.g. ammonium, nitrate and DOC concentrations, turbidity, electrical conductivity, and UVA₂₅₄ measurements (Drewes and Khan, 2011) (Table 2-2). In case of threshold exceedances for the indicator chemicals and surrogates, the monitoring interval should be increased for the source identification.

2.5. Water reuse technologies and treatment trains

Full-scale potable reuse schemes combines a large variety of processes, employing physical, chemical and biological removal mechanisms, ranging from highly engineered membrane technologies to natural treatment systems to reduce leftover constituents from conventional WWTPs, such as viruses and trace organic chemicals (Table 2-3).

Worldwide, there are approximately 25 successful potable reuse projects, applying multi-barrier membrane and non-membrane based advanced treatment trains with online monitoring and delivering safe water quality (Marron et al., 2019; WHO, 2017).

Table 2-3: Unit operations and advanced water treatment processes, than can be applied for the removal of waste water origin constituents for reuse treatment trains, adapted from Asano et al. (2007), USEPA (2017) and Drewes and Khan (2011). The check mark indicates the suitability of a unit.

Unit operations and processes	Suspended solids	Particulate org. matt.	Dissolved org. matt.	Nitrogen	Phosphorus	TOrCs	Tot. dissolved solids	Bacteria	Protozoa	Viruses	Stabilization
Secondary treatment	√		√	√	√						
Diss. air flotation	√	√							√	√	
Depth filtration	√							√	√		
Surface filtration	√	√						√	√		
Biological filtration	√	√	√	√		√		√	√	√	
Microfiltration	√	√						√	√		
Ultrafiltration	√	√						√	√	√	
Nanofiltration		√	√	(√)		√	√	√	√	√	
Reverse osmosis			√	√	√	√	√	√	√	√	√
Carbon adsorption			√			√					
Electrodialysis			√				√				
Ion exchange			√	√		√	√				
Advanced oxidation		√	√			√		√	√	√	
Disinfection			√			√		√	√	√	√
Decarbonization											√
pH adjustment											√
MAR	√	√	√	√	√	√	√	√	√	√	√

2.5.1. Membrane based full advanced treatment trains

The Orange County Groundwater Replenishment System (GWRS) was the first potable reuse project applying a RO based treatment train as early as 1976 (WHO, 2017). After the detection of NDMA and 1,4-dioxane in final water at concentrations higher than the MTLs, the treatment train was upgraded with AOP (UV/H₂O₂) to provide an additional dual barrier for chemicals and pathogens via physical and chemical treatment processes (Marron et al., 2019). RO membranes are capable of rejecting chemicals with molecular weights more than 200 Da, while lower molecular weight uncharged compounds, like DBPs and organic solvents, can pass through. Therefore, the UV/AOP step is designed to remove low-molecular weight organic chemicals. Regulation in California require 1.2 and 0.5 log reductions for NDMA and 1,4-dioxane, respectively (USEPA, 2017). Since GWRS, the use of full advanced treatment trains (FAT), employing UF/MF→RO→UV/AOP, is considered as the industry standard for IPR with direct injection into a potable aquifer (Drewes and Khan, 2011) (Table 2-4).

Table 2-4: Some examples of established potable reuse schemes based on full advanced treatment, adapted from WHO (2017) and USEPA (2017).

Location	Type	Enviro. buffer	Advanced water treatment train
Cloudcroft, New Mexico, USA	DPR	-	Enhanced secondary treat. (MBR), Cl ₂ , RO , UV/H ₂ O ₂ , blending, UF, UV, GAC, Cl ₂
Big Spring, Texas, USA	DPR	-	MF, RO , UV/H ₂ O ₂ , blending, media filtration, Cl ₂
Beaufort West, South Africa	DPR	-	Media filtration, UF, RO , UV/H ₂ O ₂ , Cl ₂
GWRS, Orange County, California, USA	IPR	Groundwater	Cl ₂ , MF, RO , UV/H ₂ O ₂
West Basin Water Recycling Plant, California, USA	IPR	Groundwater	MF, RO , UV/H ₂ O ₂ , NH ₂ Cl
Arapahoe County/Cottonwood, Colorado, USA	IPR	Groundwater	Media filtration, RO , UV/H ₂ O ₂ , Cl ₂
Scottsdale Water Campus, Arizona, USA	IPR	Groundwater	Media filtration, MF, RO , Cl ₂
Beenyup Groundwater Replenishment Scheme, Perth, Australia	IPR	Groundwater	UF, RO , UV
Torrelee, Wulpen, Belgium	IPR	Groundwater	UF, RO , UV
Los Alimitos, Water Replenishment District of Southern California, USA	IPR	Groundwater	MF, RO , UV
Dominguez Gap Barrier, Los Angeles, California, USA	IPR	Groundwater	MF, RO
Permian Basin, Colorado River Municipal Water District, Texas, USA	IPR	Surface water	UF, RO , AOP, Cl ₂
NEWater, Singapore	IPR	Surface water	UF, RO , UV

FAT schemes are mostly located in coastal areas, where the concentrated waste streams, at least 15% of the treated water, can be discharged directly to the ocean (Pérez-González et al., 2012). The high energy requirements of FAT trains and issues associated with the concentrate disposal, such as environmental concerns and the need to employ costly zero-liquid discharge, motivate utilities to explore non-membrane based treatment processes, in particular in land-locked locations with no option for inexpensive RO brine disposal.

2.5.2. Non-RO based treatment trains

The worldwide oldest DPR project in Windhoek, Namibia dates back to 1968 and is the only full-scale DPR application relying on a treatment train that is not employing high-pressure membranes (Table 2-5). The city of Windhoek is located in an arid region in the center of the country.

Establishing an IPR project either with surface or groundwater augmentation were not suitable, which *ab initio* resulted in the design of a DPR project without a RO based treatment train (Asano et al., 2007). Instead the treatment scheme highly relies on adsorption / oxidation processes for TOC removal and dissolved air flotation, low-pressure membrane filtration and disinfection for pathogen attenuation.

Table 2-5: Some examples of established potable reuse schemes applying non-RO based treatment, adapted from WHO (2017) and Hooper et al. (2020).

Location	Type	Enviro. buffer	Advanced water treatment train
New Goreangab plant, Windhoek, Namibia	DPR	-	O ₃ , dissolved air flotation, RSF, O ₃ , BAC, GAC, UF, Cl ₂
Gwinnett Count, Georgia, USA (<i>pilot-scale</i>)	DPR	-	Two stage (O ₃ , Flocculation, BAC), Cl ₂
Prairie Waters Project, Aurora, Colorado, USA	IPR	Groundwater	IBF , UV/H ₂ O ₂ , BAC, GAC, Cl ₂
Hueco Bolson recharge project, El Paso water utilities, Texas, USA	IPR	Groundwater	PAC, lime clarification, media filtration, O ₃ , GAC, O ₃ , Cl ₂
Montebello Forebay, Los Angeles County, California, USA	IPR	Groundwater	Media filtration, SAT , Cl ₂
Chino Basin groundwater recharge project, California, USA	IPR	Groundwater	Media filtration, SAT , Cl ₂
Gwinnett County, Georgia, USA	IPR	Surface water	Chemical phosphorus removal, UF, O ₃ , GAC
Upper Occoquan service authority, Fairfax County, Virginia, USA	IPR	Surface water	Lime clarification, media filtration, GAC, Cl ₂ , chloramination
Clayton County water authority, Georgia, USA	IPR	Surface water	Land application, UV, Cl ₂
George, South Africa	IPR	Surface water	UF, Cl ₂
Essex and Suffolk, Langford, UK	IPR	Surface water	Biological filtration, UV

To date, in the USA non-RO based IPR schemes are preferably designed for surface water augmentation (Table 2-5). Due to site-specific characteristics, there are a few exceptions of IPR projects with groundwater augmentation (Prairie Waters project, Hueco Bolson recharge project, the Montebello Forebay and Chino Basin groundwater replenishment projects), which do not apply FAT trains (Table 2-5). Hooper et al. (2020) could achieve potable water quality at pilot-scale in a less costly scenario using ozone and GAC in Gwinnett County, Georgia for DPR. These barriers are also strongly emphasized in two applications, the Prairie Water Project and the Hueco Bolson recharge project.

Most of the aforementioned non-RO based IPR applications with groundwater augmentation (Prairie Waters Project, in Colorado and the Montebello Forebay and Chino Basin groundwater recharge projects in California), strongly rely on natural treatment systems, e.g. IBF and SAT. Overall, more research and successfully established pilot- to full-scale applications are needed to increase the credibility of non-RO based treatment trains, especially for groundwater augmentation, which count on cost effective, natural and engineered biological treatment systems. Such developments would reveal a great potential for increasing the number of IPR projects with groundwater augmentation and for growing planned potable reuse schemes from a small number of projects to more wide-spread applications.

2.6. Advancing natural treatment systems

2.6.1. Managed aquifer recharge systems

MAR systems are used to treat or store water for subsequent use and to elevate or maintain groundwater tables as a barrier against sea water intrusion or contaminant dissemination, and are characterized by low carbon footprint and residual-free operation (Dillon, 2005; Regnery et al., 2017; Sharma and Amy, 2011) (Figure 2-4). Different infiltration methods can be employed based on the purpose of application, source water characteristics, the confined or unconfined nature of the aquifer and the integration of the saturated and unsaturated zones employed for the infiltration of the source water. In case of confined aquifers, Aquifer Storage and Recovery (ASR) with direct injection into the aquifer and withdrawal from the same well can be utilized, which benefits rather from the storage capacity of the aquifer and dilution, instead of the water treatment in the subsurface. In comparison, Aquifer Storage, Transfer and Recovery (ASTR) technique incorporates additional water treatment in the aquifer by extending the HRT within the aquifer. As direct injection skips the subsurface treatment, the water quality should mostly meet drinking water standards in order to avoid deterioration of the groundwater quality (Sharma and Amy, 2011).

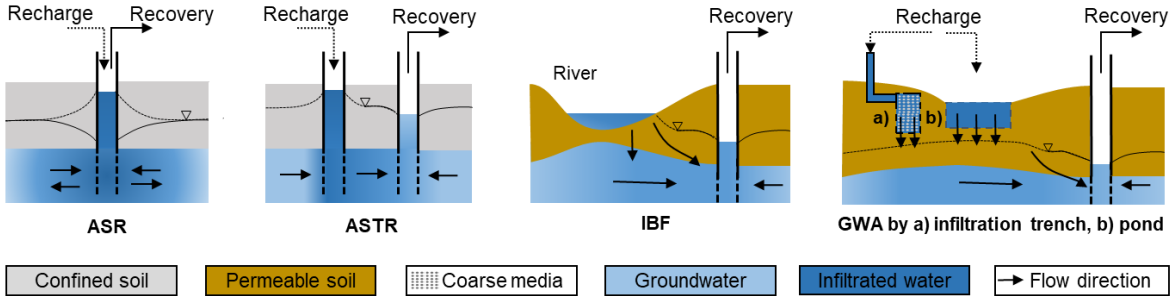


Figure 2-4: Schematic examples of managed aquifer recharge systems, GWA indicates groundwater augmentation.

Groundwater augmentation via subsurface (e.g. infiltration trenches and shallow wells) and surface spreading via infiltration ponds requires on the contrary availability of an unconfined aquifer, permeable soil but can provide additional water treatment, while water infiltrates through unsaturated

and saturated zones. Infiltration ponds are also widely used for infiltrating secondary and tertiary effluent, which is then called soil aquifer treatment (SAT). Moreover, groundwater can be withdrawn by wells with an immediate proximity to pristine to highly impacted surface water sources, e.g. rivers, which induces surface water infiltration through the saturated zone, referred as IBF.

Clogging is one of the main problems occurring during the infiltration techniques employed by MAR systems. Clogging issues take place mainly due to the source water characteristics (i.e., nutrient, suspended solid and mineral content) and environmental conditions (e.g. sun exposure, temperature, algae and plant growth) and might reduce the infiltration rates. While source water characteristics affect the filtration capacity of both subsurface, i.e. vadose zone, and aboveground infiltration techniques, secondary contamination caused by environmental conditions declines substantially the water quality and infiltration rates of the latter method. The hydraulic cycle of an infiltration pond is characterized by four different stages; being (i) vertical infiltration of the source water at a maximum infiltration rate, (ii) establishment of saturated condition in the subsurface and clogging layer leading to lower infiltration rates, (iii) development of an unsaturated zone due to high hydraulic resistance of the clogging layer underneath infiltration pond, and (iv) increase of the water level within the infiltration pond due to the impermeable layer. In case of the fourth stage, the uppermost congested layer of infiltration ponds can be peeled or dried and consequently cracked, and the hydraulic cycle of the pond starts again from the first stage (Greskowiak et al., 2005). Compared to the infiltration ponds, trenches facilitate fast infiltration through a highly porous, internal filter media, and then the surrounding vadose zone, i.e. large subsurface infiltration areas depending on length and depth of trenches (Mikat, 2009). Although the hydraulic cycles (i) and (ii) apply also to the infiltration trenches, as the coarse filter material provide barely any filtration effects, the clogging occurs within the interface, between the filter material and surrounding soil, which is than more difficult to restore due to the subsurface construction characteristics and therefore should be avoided. Beside the selection of the right filter material size, the biological and chemical stability, as well as low suspended solid content of the source water are essential parameters to provide long-term operation without any interruption. Moreover, frequent occurrence of clogging due to suspended solids can be avoided by the placement of a thin sand layer on the top of the course filter media. Infiltration trenches are commonly used for the infiltration of treated surface waters and so far, to the best of our knowledge have not been utilized for SAT applications or within the advanced treatment schemes. Overall, despite the numerous advantages, such as minimization of cross contamination and algae growth, high rate infiltration, and smaller footprint, infiltration trenches are not as widely employed as infiltration ponds, probably due to their high source water quality requirements and complex construction.

Combinations of different biological, chemical and physical removal mechanisms in the subsurface have been found to result in efficient inactivation of pathogens, and attenuation of a wide range of

TOrCs depending on the HRT in the subsurface (Regnery et al., 2017; Sharma and Amy, 2011). Among pathogens, protozoa and viruses are specified as the pathogens of concern for water reuse practices, viruses poses the greatest challenge for MAR systems due to their smaller size (Dullemont et al., 2006; Regnery et al., 2017). Oxidic redox conditions in the aquifer, higher temperatures, homogeneity, mineral content and finer size of the porous media were correlated to the enhanced die-off and the physical removal of viruses (Gerba et al., 1991; Regnery et al., 2017). Oxygen availability was defined as one of the key parameters related to virus survival, since under oxidic conditions the microbial proteins, i.e. the nucleocapside of the viruses, could be damaged (Frohnert et al., 2014; Klitzke et al., 2015; Schijven et al., 2017). For TOrCs, biotransformation and sorption were found to be the most important removal mechanisms in the subsurface (Regnery et al., 2017). While sorption primarily depends on physiochemical characteristics of the soil (e.g., pH, mineral surface characteristics, cation exchange capacity, and the presence of clay minerals), environmental conditions (e.g., availability of the primary substrate, redox conditions, temperature) were related to the activity of the microbial community responsible for the biological degradation. With proper design and operation of MAR systems, the favorable conditions could be established to achieve sustainable and robust water treatment for IPR applications.

2.6.2. *Sequential managed aquifer recharge technology*

Enhanced biotransformation of some TOrCs was found to be dependent on the composition and the concentration range of the primary substrate due to metabolic and co-metabolic removal mechanisms in the soil (Li et al., 2012; Li et al., 2013; Li et al., 2014; Rauch-Williams et al., 2010). While higher BDOC concentrations were related to higher total viable biomass and less diverse microbial community, higher diversity of the prevailing microbial communities were correlated with the refractory characteristics of carbon (Li et al., 2014). Although, a small subset of TOrCs (e.g. carbamazepine, iopromide) were found to better transform under anaerobic conditions (Ghattas et al., 2017; König et al., 2016), the prevalence of stable oxidic conditions (dissolved oxygen concentrations > 1 mg/L) was identified as the key factor for an enhanced and rapid biotransformation of many TOrCs (e.g., diclofenac, 4-FAA, acesulfame, benzotriazole, gabapentin) (Greskowiak et al., 2006; Hellauer et al., 2018a; Massmann et al., 2006; Massmann et al., 2008; Regnery et al., 2015b; Schmidt et al., 2017).

To take advantage of these favorable conditions within natural treatment systems, sequential managed aquifer recharge technology (SMART) was established (Regnery et al., 2016). In this concept, a first infiltration step (e.g. bank filtration) with short residence times is used to remove the readily degradable organic carbon, followed by water recovery, an *ex-situ* aeration and a second infiltration step, where oxidic and carbon-limited conditions can prevail (Figure 2-5). Consequently, various combinations of BDOC and oxygen availability could be configured for the removal of TOrCs, possessing a wide-range of physicochemical properties. Significantly enhanced removal of

several TOrCs by the SMART concept was successfully demonstrated at MAR facilities in Aurora, Colorado, USA and Berlin, Germany for the production of drinking water from surface waters impaired by wastewater effluents (Hellauer et al., 2017; Hellauer et al., 2018a; Regnery et al., 2015b; Regnery et al., 2016).

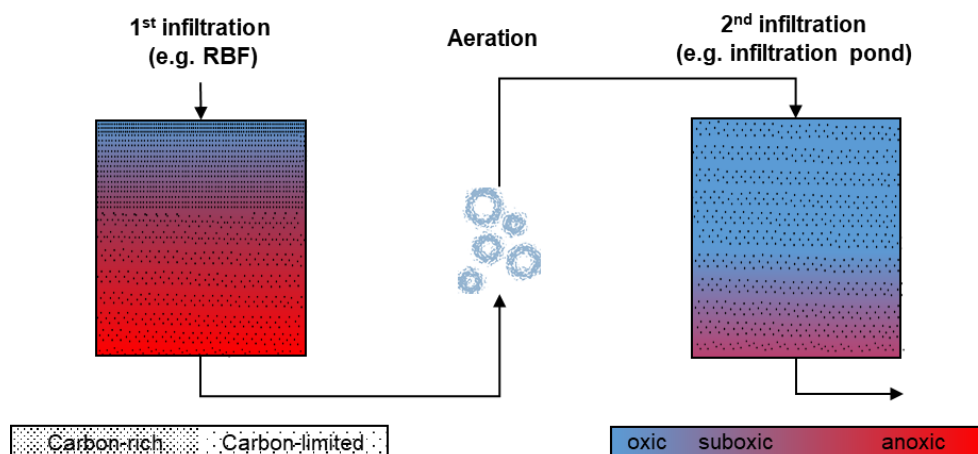


Figure 2-5: Concept of SMART based on the availability of biodegradable organic carbon compounds and optimized redox conditions for enhanced removal of trace organic chemicals.

2.6.3. Further enhancement of natural treatment systems for IPR applications

Conventional SAT applications and the SMART concept commonly employ open recharge basins (i.e. infiltration ponds) to facilitate infiltration of water through the vadose zone. These approaches require large physical areas and suitable subsurface conditions (USEPA, 2012). Incorporation of rapid infiltration techniques might decrease the physical footprint of these applications and prevent secondary contaminations caused by open infiltration. In case of SMART, in order to establish a sequence of controlled redox conditions during subsequent travel through the saturated zone, homogeneous flow conditions are required. Whereas native subsurface environments are usually characterized by a high degree of site-specific heterogeneity, which not only affects the establishment of the redox zonation for the TOrC attenuation, but also the virus attenuation. Further limitations, e.g. clogging problems, increased costs caused by additional pumping, and unpredictable effluent water quality due to subsurface heterogeneities, made in general, the technology and performance transfer of SMART systems difficult. Homogenous flow conditions can be achieved by employing standardized sand or gravel instead of natural soil. Uncontrolled flow and mixing with native groundwater can be furthermore eliminated, if the MAR systems are hydraulically decoupled from the native groundwater by adequate groundwater pumping regimes.

3. Research significance and hypotheses

Separation of drinking water and wastewater comes to an end by their perception as *one water*, which has been as anticipated always recycled by the natural water cycle. Increasing impacts of wastewater effluents on the streams used for drinking water production need to be quantified as a first milestone in the direction of sustainable water management to maintain the balance set in nature. Emerging from this notion, the first main objective of this dissertation has been formulated as the “*Assessment of municipal wastewater contributions in German surface waters and associated impacts on the drinking water supply*”. The high burdens on the conventional water supplies due to the population growth, climate change and concentrated waste stream discharges in highly populated areas, can be eliminated by shortening required time for the natural hydrological replenishment cycle by employing advanced water treatment technologies. Instead of highly energy and cost-intensive treatment steps, e.g. high-pressure membranes, engineered natural treatment systems might be utilized after the conventional WWTPs or within an IPR scheme in regions with high water stress. With this motivation, the second objective of this study was identified as the “*Development, construction and operation of a novel hybrid biofilter, SMARTplus, based on sequential managed aquifer recharge technology (SMART) for indirect potable reuse*” (Figure 3-1).

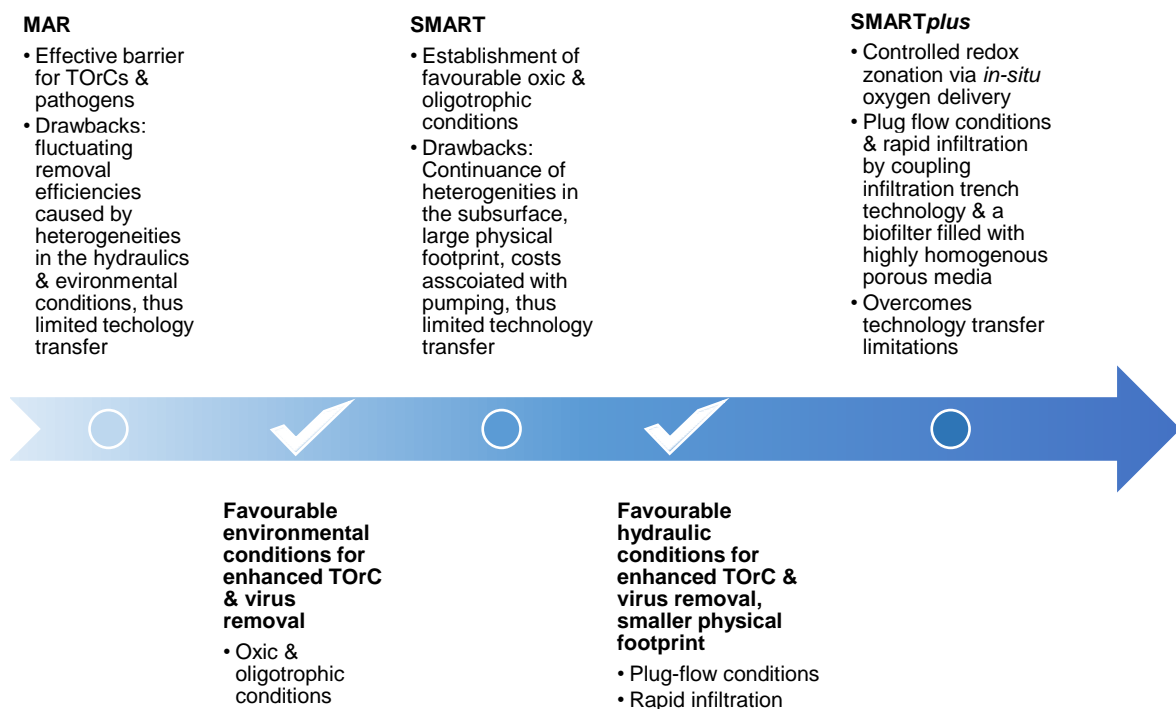


Figure 3-1: Development of the SMARTplus bioreactor based on MAR and SMART.

In the following, the objectives and inherent hypotheses are explained in more detail. An overview on the structure of the dissertation, including the objectives, hypothesis and paper-based chapters can be found in Figure 3-2.

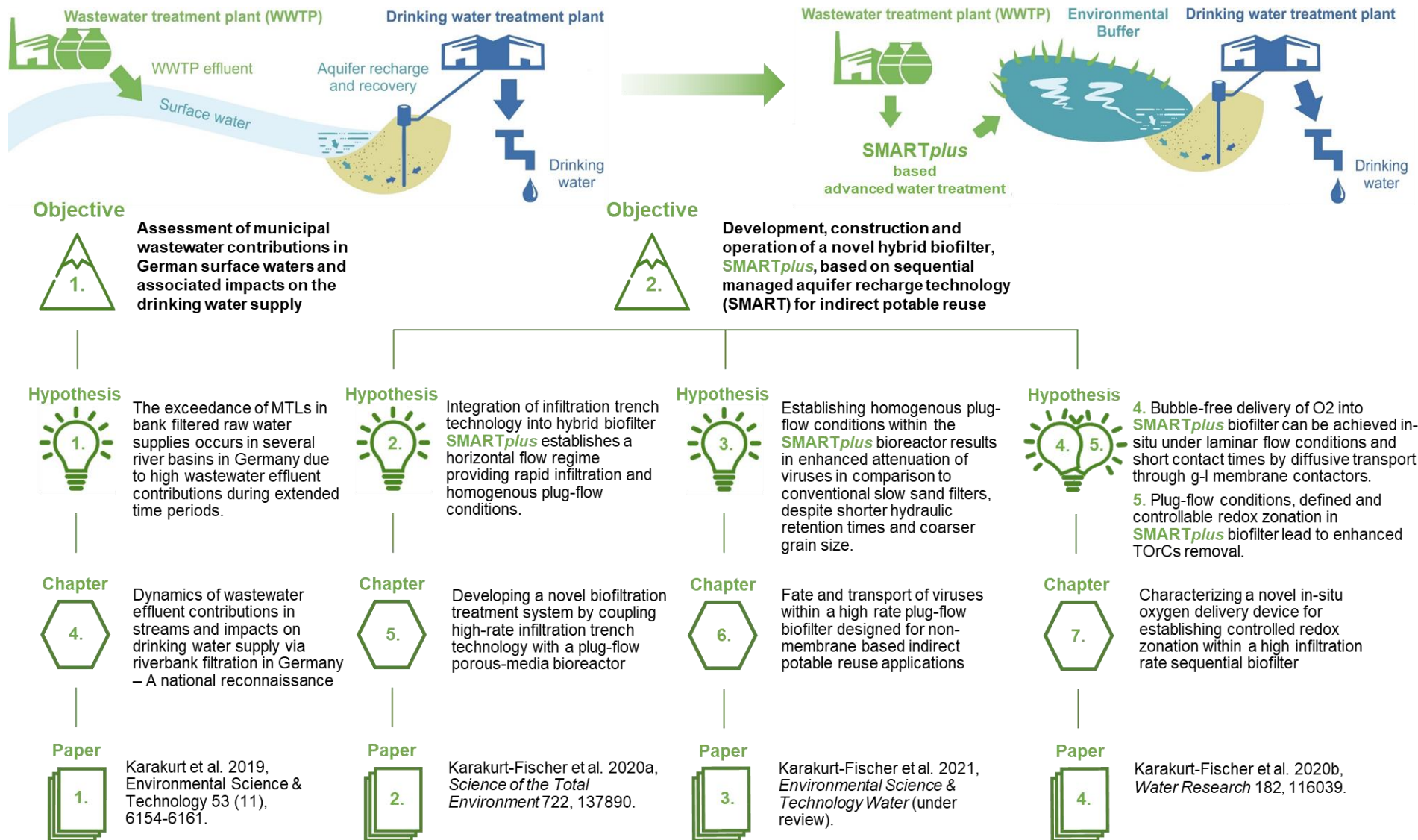


Figure 3-2: Structure of the dissertation (Illustrations on the top are modified from © Berlin Water Company / Technical University of Munich, 2017).

To date, there have been a few studies in the USA, Switzerland, China and Spain, which have quantified nationwide or for some river catchment areas, the relative contribution of wastewater effluents in rivers (Mujeriego et al., 2017; Rice and Westerhoff, 2015; Wang et al., 2017; Wiener et al., 2016). While these studies point to the importance of understanding the relevance of discharge of municipal wastewater effluents on streams used for drinking water supply, quantifying which degree of *de facto* reuse constitutes a threat to human health protection is lacking. In addition, these studies did not consider the efficacy of water treatment processes employed at a water utility or attenuation processes occurring during IBF or groundwater augmentation via infiltration ponds, where surface water is used indirectly. This trend needs to be quantified to be able to address the necessity for a more sustainable water management and use of alternative water resources, such as reclaimed water, also in Germany. With the aim of filling this gap, the first objective of this research is:

3.1. Objective #1: Assessment of municipal wastewater contributions in German surface waters and associated impacts on the drinking water supply

Assessing the impact of wastewater effluents on streams that are subsequently used indirectly via IBF or AR is not straightforward, as it requires an understanding of stream discharge dynamics, relative contributions of augmented groundwater in a production well, and a quantitative assessment of attenuation processes in the subsurface. Given these challenges, water utilities and health officials are looking for guidance on how indirect drinking water abstraction from impaired surface waters via IBF or AR can be adequately managed under shifting climate and discharge conditions. *De facto* potable reuse might become relevant if potentially health relevant chemicals exceed their toxicologically relevant values, defined as monitoring trigger levels (MTLs), in bank filtrate where subsequent drinking water treatment only utilizes conventional treatment processes (i.e. aeration, filtration). We hypothesize that:

3.1.1. Hypothesis #1: The exceedance of MTLs in bank filtered raw water supplies occurs in several river basins in Germany due to high wastewater effluent contributions during extended time periods.

For some regions, the conventional water management might require already risk-mitigating countermeasures and supplementary drinking water sources due to high extent of wastewater contributions in surface water and trends of decreasing stream run-off in numerous river basins. This might also apply to broader regions of Germany. Augmentation of drinking water supplies with reclaimed water via an environmental buffer, known as IPR, reduces the dependency and burden on seasonally and climatically changing conventional water sources by shortening the natural hydrological replenishment cycle (Drewes and Khan, 2011). Optimized nature-based treatment technologies can be developed and employed after conventional WWTPs to mitigate the increasing

number of contaminants in highly populated regions or in watersheds with low base discharge. Instead of highly energy and cost-intensive treatment technologies, e.g. RO, such natural treatment technologies might be also utilized as a key component of an IPR scheme in regions with high water stress. A purposeful addition of reclaimed water meeting high quality standards would diminish negative effects on ground- or surface water, which turns IPR into a sustainable solution. Building upon the positive experiences employing SMART, the second objective of this research is to modify the overall design and improve removal performance of the SMART concept by an engineered approach (*SMARTplus*) that can be deployed independent of local hydrogeological conditions with a significantly reduced physical footprint.

3.2. Objective #2: Development, construction and operation of a novel hybrid biofilter, SMARTplus, based on sequential managed aquifer recharge technology (SMART) for indirect potable reuse

Infiltration trenches can be employed to decrease the physical footprint requirements of conventional MAR and SMART systems, which is characterized by the use of highly porous media enabling rapid infiltration of the source water. To avoid clogging after the infiltration trench technology an adequate pre-treatment step is required for residual suspended solid removal (e.g. rapid sand filtration). Coupling the infiltration trench technology with a horizontal biofilter filled with high uniformity porous material, might overcome the problems associated with the preferential flow paths caused by subsurface heterogeneity and filtration capacity. Based on these assumptions, we hypothesize that:

3.2.1. Hypothesis #2: Integration of infiltration trench technology into hybrid biofilter SMARTplus establishes a horizontal flow regime providing rapid infiltration and homogenous plug-flow conditions.

Furthermore, efficient virus removal within a subsurface suffers from short-circuiting flow patterns caused by the heterogeneous character of the porous media. Establishment of controlled hydraulic conditions can provide high log reductions in comparison to conventional biofilters (e.g. slow sand filtration). As a consequence of planned optimizations in hydraulics, we hypothesize that:

3.2.2. Hypothesis #3: Establishing homogenous plug-flow conditions within the SMARTplus bioreactor results in enhanced attenuation of viruses in comparison to conventional slow sand filters, despite shorter hydraulic retention times and coarser grain size.

The previously tested SMART concept resulted in improved removal performance of conventional MAR techniques by extracting infiltrated water for *ex-situ* aeration and subsequent re-infiltration. Whereas *SMARTplus* concept combines all three steps in one bioreactor to decrease the physical

footprint, operational costs and avoid disturbances of the subsurface flow conditions. Infiltration trench technology of the SMART*plus* bioreactor will be followed by a biofiltration system, characterized by highly controlled redox zonation as well as an appropriate online monitoring and control system. Oxygen introduction into horizontal flow saturated porous media will occur *in-situ*. For this purpose, we will build upon previous experiences from groundwater bioremediation or membrane aerated bioreactors (MABR), where biodegradation is the main mechanism and either active or passive oxygen delivery methods facilitate microbial communities degradation of organic contaminants in water (Barcelona and Xie, 2001; Casey et al., 1999; Haugen et al., 2002). Since flow characteristics, the reactor configuration and high requirements regarding bubble-less oxygen transfer differ in the SMART*plus* bioreactor compared to soil passage in groundwater remediation and MABR, further research was needed on feasibility of different oxygen delivery devices. Moreover, given the fact that the SMART*plus* bioreactor is continuously fed with secondary effluent exhibiting fluctuations in quality, an active controllable redox zonation is essential to maintain steady-state removal of TOrCs. Hollow fiber gas/liquid membrane contactors were considered to be more suitable for reliable and uniform delivery of electron acceptors under laminar flow conditions and short HRTs of SMART*plus* bioreactor. We hypothesize that:

3.2.3. Hypothesis #4: Bubble-free delivery of oxygen into SMARTplus biofilter can be achieved in-situ under laminar flow conditions and short contact times by diffusive transport through gas-liquid membrane contactors.

Regnery et al. (2015b) showed the redox sensitivity of biological TOrC removal in lab-scale soil column experiments simulating MAR systems, where the TOrC removal decreased significantly during anoxic to suboxic in comparison to oxic conditions. Especially the prevalence of stable oxic conditions (DO concentrations > 1 mg/L) improved the removal of TOrCs (Hellauer et al., 2018a), which can be attuned as a function of oxygen demand in a technical system. As a consequence of controlled and well defined redox zonation along the SMART*plus* bioreactor, we hypothesize that:

3.2.4. Hypothesis #5: Plug-flow conditions, defined and controllable redox zonation in SMARTplus biofilter lead to enhanced TOrCs removal.

4. Dynamics of wastewater effluent contributions in streams and impacts on drinking water supply via riverbank filtration in Germany – A national reconnaissance

The following chapter presents investigations related to Hypothesis #1: *The exceedance of MTLs in bank filtered raw water supplies occurs in several river basins in Germany due to high wastewater effluent contributions during extended time periods.*

The chapter has been published with editorial changes as follows:

Karakurt, S.; Schmid, L; Hübner, U.; Drewes, J.E., 2019. Dynamics of wastewater effluent contributions in streams and impacts on drinking water supply via riverbank filtration in Germany – A national reconnaissance. *Environmental Science & Technology* 53 (11), 6154-6161.

Author contributions: Sema Karakurt-Fischer and Jörg E. Drewes conceptualized the research objective and designed the methodology. Sema Karakurt-Fischer and Ludwig Schmid collected and analyzed the data. Sema Karakurt-Fischer applied and validated the models and wrote the paper. Jörg E. Drewes and Uwe Hübner critically reviewed the manuscript. All authors approved the final version of the manuscript.

Abstract

The discharge of wastewater effluents to a stream that is subsequently used for drinking water abstraction has been previously referred to as *de facto* water reuse. Where the abstraction of surface water for drinking water production occurs via induced bank filtration or aquifer additional site-specific factors should be considered to assess the impact of wastewater effluents on bank-filtered water. This study represents the first national reconnaissance to quantify wastewater effluent contributions in streams across Germany and consequences for indirect drinking water abstraction from these streams. An automated assessment using ArcGIS was conducted for river basins considering minimum and mean average discharge conditions of streams as well as discharge from more than 7,500 wastewater facilities. In urban areas, where the natural base discharge is low, wastewater effluent contributions greater than 30-50% were determined under mean minimum discharge conditions, which commonly prevail from May to September. A conceptual model was proposed to estimate critical bank filtrate shares resulting in exceedances of monitoring trigger levels for health-relevant chemicals as a universal qualitative assessment regarding the relevance of *de facto* reuse conditions in surface waters used for drinking water abstraction. This approach was validated using chemical monitoring data for three case study locations.

4.1. Introduction

Drinking water supply in many countries in central and western Europe heavily relies on indirect use of surface water via induced bank filtration (IBF) and aquifer recharge (AR) (Hannapel et al., 2014; Sharma and Amy, 2011). In Germany, production from IBF and AR accounts on average for 15% of the drinking water supplied nationwide (German Environment Agency, 2018a), but at the individual utility level this contribution can be in excess of 70% (Senate Department for Urban Development and Housing Berlin, 2017). While relying on natural treatment processes during IBF and AR, microbial and chemical contaminants in surface water can be effectively attenuated during travel through the subsurface (Sharma and Amy, 2011). In highly populated areas and where substantial natural base discharge is lacking, the quality of surface water can be highly affected by discharge of effluents of municipal wastewater treatment plants (WWTPs), industrial dischargers, as well as contributions from various non-point sources (e.g., drainage from agricultural areas, stormwater runoff, urban seepage). Increasing contributions of wastewater effluents to stream discharge will also result in an increase of the relative portion of wastewater-derived contaminants, such as pathogens and trace organic chemicals (TOrcs) in the water cycle (Bradley et al., 2016; Glassmeyer et al., 2005; Hass et al., 2012; Reemtsma et al., 2016; Schimmelpfennig et al., 2012). This is particularly relevant regarding persistent pathogens but also for poorly degradable and polar wastewater-derived chemicals, which could potentially make their way into drinking water wells (Hass et al., 2012; Reemtsma et al., 2016). This situation will likely become more prevalent considering impacts from climate change resulting in more frequent or long-lasting low-discharge conditions in streams.

Climate change not only adversely affects stream discharge and the relative contribution of wastewater effluents, but also impacts IBF performance as travel times and redox conditions in the subsurface can change with varying discharge conditions and temperatures (Massmann et al., 2006; Massmann et al., 2008; Sprenger et al., 2011).

The discharge of wastewater effluents to a stream that is subsequently used for drinking water abstraction has been previously referred to as unintended or *de facto* water reuse (National Research Council, 2012; Rice and Westerhoff, 2015). In a US-wide study, Rice and Westerhoff (2015) revealed wastewater effluent impact on half of 1,210 targeted drinking water treatment plants (DWTP) practicing surface water treatment and serving more than 10,000 inhabitants under mean annual discharge (MAD) conditions. The effects of mean minimum annual discharge (MMAD) conditions were investigated for an additional 80 DWTPs, where 40% of the utilities were characterized by more than 50% wastewater effluent in their raw water supply (Rice and Westerhoff, 2015). Switzerland engaged in a nationwide study to assess the presence of wastewater-derived chemicals in receiving streams, and revealed wastewater effluent contributions of more than 10-50% under low discharge conditions, particularly in small and medium-sized rivers (Abegglen and Siegrist, 2012). In order to minimize impacts on aquatic life and downstream drinking water abstraction, this situation recently triggered upgrades with either activated carbon filtration or ozone for 100 out of 700 conventional WWTPs across Switzerland (Abegglen and Siegrist, 2012; Eggen et al., 2014). A regional study in Catalonia, Spain, analyzed wastewater effluent contributions to the River Llobregat, a source of drinking water supply for the metropolitan area of Barcelona, and reported between 12 to 25 % wastewater effluent contributions in raw water supplies for three different years with varying annual discharges (Mujeriego et al., 2017). Wang et al. (2017) conducted the first assessment on wastewater effluent discharges at 11 gauging stations within the Yangtze River watershed, China, supporting more than 1/15th of the world's population. The wastewater effluent contributions under low discharge conditions increased from 8% to 14% nearby Shanghai between 1998 and 2014 due to an increase in wastewater discharges and decrease in streamflow (Wang et al., 2017). A similar study at regional scale have been reported, which commonly quantify the degree of impact from wastewater effluent discharge on stream water quality by simple flow balances (Wiener et al., 2016). While these studies point to the need to understanding the relevance of discharge of municipal wastewater effluents on drinking water supplies, quantifying what degree of *de facto* reuse actually constitutes a potential threat to human health is lacking. In addition, these studies did not consider the efficacy of water treatment processes employed at a drinking water utility or attenuation processes occurring during IBF or AR, where surface water is used indirectly. Quantifying the impact of wastewater effluents on streams that are subsequently used indirectly via IBF or AR may become complex as it requires a site-specific assessment of stream discharge dynamics, relative contributions of augmented groundwater in a production well, and a quantitative assessment of attenuation processes in the subsurface. Given these challenges, water utilities and health officials are looking

for guidance on how indirect drinking water abstraction from impaired surface waters via IBF or AR can be adequately managed under shifting climate and discharge conditions.

De facto potable reuse becomes relevant when health relevant chemicals exceed their toxicologically relevant values, defined as monitoring trigger levels (MTLs), in bank filtrate where subsequent drinking water treatment only utilizes conventional treatment processes (i.e., aeration, filtration, disinfection). We hypothesize that the exceedance of MTLs in bank filtered raw water supplies occurs in several river basins in Germany due to high wastewater effluent contributions during extended time periods. This nation-wide, comprehensive study is the first to quantify the relative contribution of wastewater effluents to streams across Germany under varying discharge conditions. It also provides a conceptual impact assessment for downstream drinking water abstraction via IBF or AR, validated by three case studies. The developed approach can guide water utilities and regulators in assessing the relevance of *de facto* reuse and identifying sites where comprehensive follow-up monitoring programs as well as potential mitigation actions are warranted.

4.2. Materials and methods

4.2.1. Data acquisition and calculation of treated effluent contribution in rivers - Modeling approach

Within the framework of the European Directive 91/271/EEC, the federal states of Germany are required to report operational and spatial data of WWTPs with a population equivalent (PE) capacity of more than 2,000 to the German Environment Agency (Thru.de), which subsequently reports this information to the European Commission's data base 'Waterbase – Urban wastewater treatment directive (UWWTD)' (European Environment Agency, 2015; German Environment Agency, 2017). In addition, discharge volumes of WWTPs with a capacity of 50-2,000 PE were provided by individual federal states including the states of Baden-Württemberg, Berlin, Brandenburg, Hesse, North Rhine-Westphalia, Rhineland-Palatinate, and Saxony. Year and source of WWTPs discharge data as well as the capacity of WWTPs included for different federal states can be found in SI-Table 9.4-1. For the federal state of Bavaria, instead of direct discharge volumes of WWTPs with capacities of 50-2,000 PE, discharge volumes derived from reported design capacities were considered in this study. For rivers with cross-boundary catchments (i.e., Danube, Rhine, Maas, Issel, Elbe and Oder rivers), data from WWTPs >2,000 PE of neighboring countries were considered in the model using the Waterbase – UWWTD database (European Environment Agency, 2015). Through this extensive data collection, a comprehensive database considering wastewater contributions from 7,550 WWTPs across Germany was compiled for this study.

Long-term MAD and MMAD from gauging stations over multiple decades were gathered to assess the dynamics of WWTP effluent contributions under MAD and MMAD conditions (GRDC, 2017;

LUBW, 2018; WSV, 2017). Discharge data from two years (2003 and 2005) were chosen to illustrate representative dry and average years.

An ArcGIS model (Esri, Kranzberg, Germany) using spatial and operational WWTP data (i.e., location of the WWTP, point and amount of discharge, capacity and level of treatment) and stream gauging station runoff data was generated to perform automated assessments of relative contributions from treated wastewater effluents to rivers. The locations of WWTP discharge and gauging station (i.e. nodes) were spatially linked to hydrological data of the German river network at a scale of 1:250,000, DLM250 (DLZ, 2017). Flow direction estimation and network analysis for the streams were performed using a geometric network. The wastewater effluents upstream of a river segment were cumulatively calculated and assigned to a specific gauging station. The percentage of wastewater effluent contributions ($WW_{effluent}$ [%]) at each individual gauging station was subsequently determined by calculating the ratio of the total discharge rate of upstream WWTPs ($\sum Q_{WW_{effluent}}$) to the MAD and MMAD data at the respective gauging station ($Q_{gauging\ station}$) using equation 4.1, which was coded into GIS using Python scripts. For rivers of stream order 1-5 (indicating level of branching in a river stream) with more than two gauging stations, the MAD or MMAD along a river were first determined by linear interpolation, and the relative wastewater effluent contributions were subsequently calculated for these fictitious gauging stations with varying discharge conditions in an automated assessment using equation 4.1.

$$WW_{effluent} [\%] = \frac{Q_{WW\ effluent}}{Q_{gauging\ station}} \cdot 100\% \quad [4.1]$$

This nationwide study was limited to the arithmetic mean of annual discharges from municipal WWTPs and did not include other anthropogenic sources of contamination, such as direct discharge of industrial WWTPs, agricultural drainage, and combined sewer and stormwater overflows. However, it has to be noted that the vast majority of industrial complexes in Germany is included into our study, since they discharge their wastewater after partial treatment onsite into a public sewer (indirect industrial discharge), which then is subject to municipal wastewater treatment prior to discharge to a stream. An assessment on the relevance of direct industrial discharges can be found in the supplementary information. To enable the consideration of the chemical loads (i.e. herbicides) from agricultural drainages, more spatio-temporal water quality data as well as models for accurate predictions are needed (Moser et al., 2018). In addition, complete mixing at the point of discharge of the treated wastewater into the receiving river was assumed.

The relative wastewater effluent contributions of the ArcGIS model determined for a given gauging station were validated using water quality monitoring data of the wastewater-derived conservative indicator chemical for select sites at the river Main (equation 4.2). Where the $C_{river\ indicator}$ and the $C_{WW\ effluent\ indicator}$ are the indicator chemical concentrations at the gauging stations and the

wastewater effluent, respectively. These sites and indicator chemical carbamazepine were chosen for this assessment due to data availability provided by local water utilities and regulatory agencies (Fleig et al., 2016).

$$WW_{effluent} [\%] = \frac{C_{river\ indicator}}{C_{WW\ effluent\ indicator}} \cdot 100\% \quad [4.2]$$

If the secondary effluent is subject to advanced wastewater treatment prior to discharge (i.e., activated carbon or ozone treatment), indicator chemicals may no longer be present at levels enabling them to serve as wastewater tracers (Scheurer et al., 2011). For this reason, WWTPs employing advanced wastewater treatment processes were indicated in the model, to avoid any bias while examining the feasibility of our method. As only 24 WWTPs out of 7,550 facilities across Germany are currently employing advanced wastewater treatment processes, their discharge did not result in a substantial effect on validation of the predicted wastewater contributions.

Between 2014 and 2016, carbamazepine exhibited consistent average (70-80 ng/L) and maximum concentrations (110-140 ng/L) across the entire stretch of the river Main (ARW, 2016). Monitoring data of the indicator chemicals, however, represent grab samples from river streams at different times of the year. Thus, samples did not hydraulically correspond with wastewater effluent samples taken.

4.2.2. Determination of the degree of impact on drinking water abstraction

A nationwide assessment of the impact of wastewater derived compounds on drinking water supply is hindered by the fact that national or federal state DWTP databases on the origin and quality of the raw water in Germany are lacking. Thus, a conceptual approach to estimate the relevance of elevated wastewater effluent contributions in rivers, coupled with the percent bank filtrate in raw water was developed. Conservative wastewater-derived chemicals, present at elevated concentrations in European wastewater effluents, characterized by a relatively high subsurface mobility and exhibiting persistent behavior under aerobic-anoxic conditions, were selected as indicator chemicals for this assessment (Dickenson et al., 2011; Funke et al., 2015). Among the conservative wastewater indicator chemicals, potentially health relevant compounds were chosen if their measured environmental concentrations (MEC) in wastewater effluent was greater than their MTL (German Environment Agency, 2018b), i.e. $MEC/MTL > 1$, (carbamazepine, valsartanic acid and oxypurinol) referring to the concept adopted by the State of California for monitoring purpose (Drewes et al., 2018). For wastewater effluent contribution scenarios ranging from 0-100%, critical bank filtrate contributions ($\% BF_{critical}$) in drinking water wells (i.e. raw water) were determined where MTLs of indicator chemicals ($MTL_{indicator\ chemical}$) in raw water could be exceeded using equation 4.3. The critical bank filtrate contribution is assuming that the subsequent DWTP is relying only on conventional treatment processes (i.e., subsurface passage followed by aeration and granular media filtration). At locations where advanced treatment processes are employed at a DWTP (e.g.,

ozonation, activated carbon filtration), these processes might provide additional barriers to health-relevant chemicals and therefore additional margins of safety.

$$\text{Min. \% } BF_{critical} = \frac{MTL_{indicator\ chemical}}{\% WW_{effluent} \cdot C_{WW\ effluent\ indicator}} \cdot 100\% \quad [4.3]$$

To validate the proposed approach in order to qualify *de facto* reuse conditions, this concept was applied at three case study locations practicing IBF for drinking water abstraction. The selected watersheds of the Havel, Rhine and Main rivers are substantially affected by wastewater effluent contributions.

4.3. Results and discussion

4.3.1. Dynamic of wastewater effluent contributions to rivers during different discharge conditions

A potential impairment of river stream and bank filtrate quality may occur especially during low discharge regimes over a longer period, where the relative contribution from wastewater effluents in surface waters increases (Rice et al., 2015; Wang et al., 2017). Thus, long-term MMAD and MAD recordings were chosen after considering 2,344 gauging stations across Germany to illustrate the effect of wastewater effluent contributions during changing discharge conditions on river streams. The prevalence of MMAD and MAD scenarios for the Rhine, Main and Neckar rivers were compared with daily discharges of years (2003 and 2005) representing typical low and average annual rainfall conditions, respectively. These results are depicted in Figure 4-1 for one representative gauging station for each river.

These results reveal that daily discharges were 63-83% lower than MAD values during both dry and average years (2003 and 2005) and reflect MMAD conditions for each of the three gauging stations. This comparison illustrates that low discharge conditions prevail for almost six months from spring into the summer and fall when water demand is the highest, a situation that may become more prevalent in the future considering projected climate change impacts.

The ArcGIS model deriving wastewater effluent contributions in the Main river was validated by concentrations of the wastewater indicator chemical carbamazepine, determined both in the wastewater effluent and along the river. Grab samples were taken at nine gauging stations along the Main river during March 2016 (Fleig et al., 2016). Wastewater effluent contributions calculated by carbamazepine concentrations more closely follow the distribution of MMAD conditions (average CBZ-MMAD = 4%±4%) than MAD conditions (average CBZ-MAD = 15%±5%) (Figure 4-2).

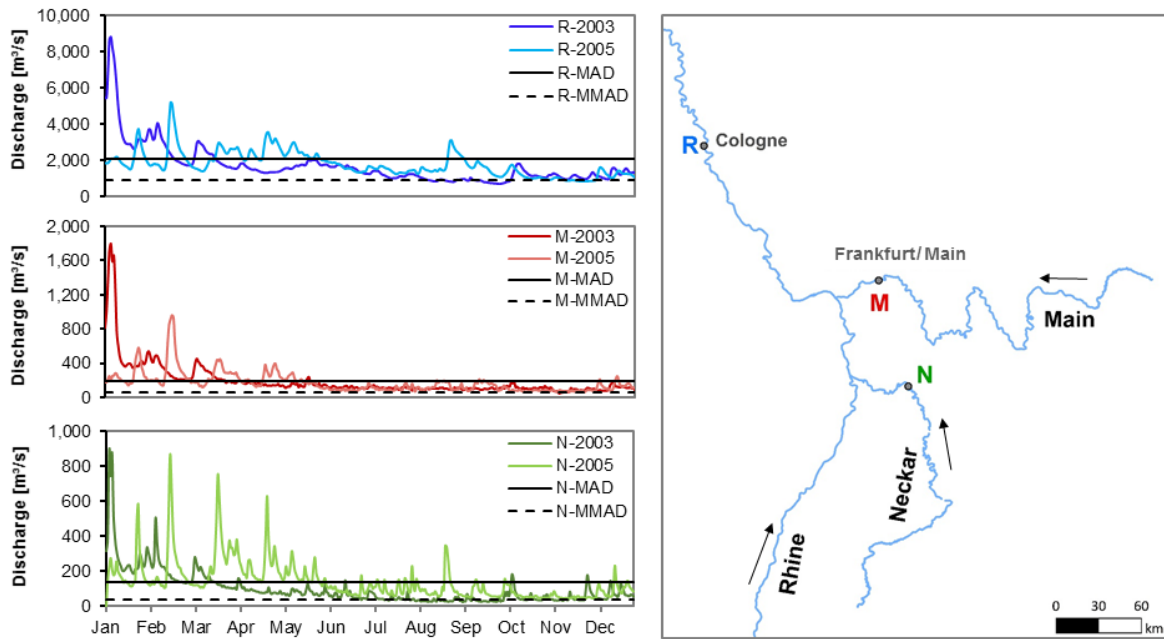


Figure 4-1: Comparison of MMAD and MAD hydrological characteristic values with daily average discharges during dry (2003) and average (2005) representative years for three gauging stations of the Rhine (at R), Main (at M) and Neckar (at N) rivers (GRDC, 2017).

Given the prevalence of low discharge conditions, wastewater effluent contributions during MMAD conditions were determined and depicted for all rivers across Germany (Figure 4-3a). Based on the results of this study, wastewater effluent contributions of more than 10-20% during MMAD conditions dominate in a large number of river basins (Figure 4-3b). For more than 40% of their gauging stations, the rivers Neckar, Ems, Main, and tributaries of the lower and middle Rhine exhibit wastewater effluent contributions of more than 20-30%. During MAD conditions, however, the contributions from wastewater effluents vary only between 0 and 5% for more than 50% of the gauging stations nationwide, except for the Neckar river basin (Figure 4-3c).

The impact of wastewater effluent contributions can be considerably less for locations where the natural discharge is high. As an example, the tributaries of the Danube river originating from the alpine foreland (i.e., Iller: 8-54 m³/s, Lech: 49-113 m³/s, and Isar: 95-174 m³/s under MMAD-MAD conditions) dominate the natural discharge of the Danube river and are characterized by wastewater effluent contributions of less than 10-20% under MMAD conditions. Thus, the confluence of the Iller river results in the dilution of wastewater effluent contributions from 30-50% (at gauging station Kirchen-Hausen) to 10-20% (Neu-Ulm) in the river Danube (SI-Figure 9-1). Another example is the watershed of the middle and lower Rhine river, whose tributaries are dominated by wastewater effluent contributions of more than 50% under MMAD conditions. However, wastewater effluent contributions in the receiving middle and lower Rhine river vary only between 10-20% and in the upper Rhine river of less than 5-10% due to a high natural discharge (for both MMAD and MAD conditions (SI-Figure 9-2)). On the other hand, rivers originating in the central uplands and the north German plain (such as Ems, Ruhr, Havel, Neckar and Main rivers) are characterized by lower

discharges of typically less than 20 to 90 m³/s for MMAD conditions and 80 to 240 m³/s for MAD conditions, respectively. Furthermore, these rivers flow through highly urbanized areas, resulting in more than 30 % and for some in more than 50% wastewater effluent contributions during MMAD conditions (SI-Figure 9-3, Figure 4-2 and Figure 4-3a).

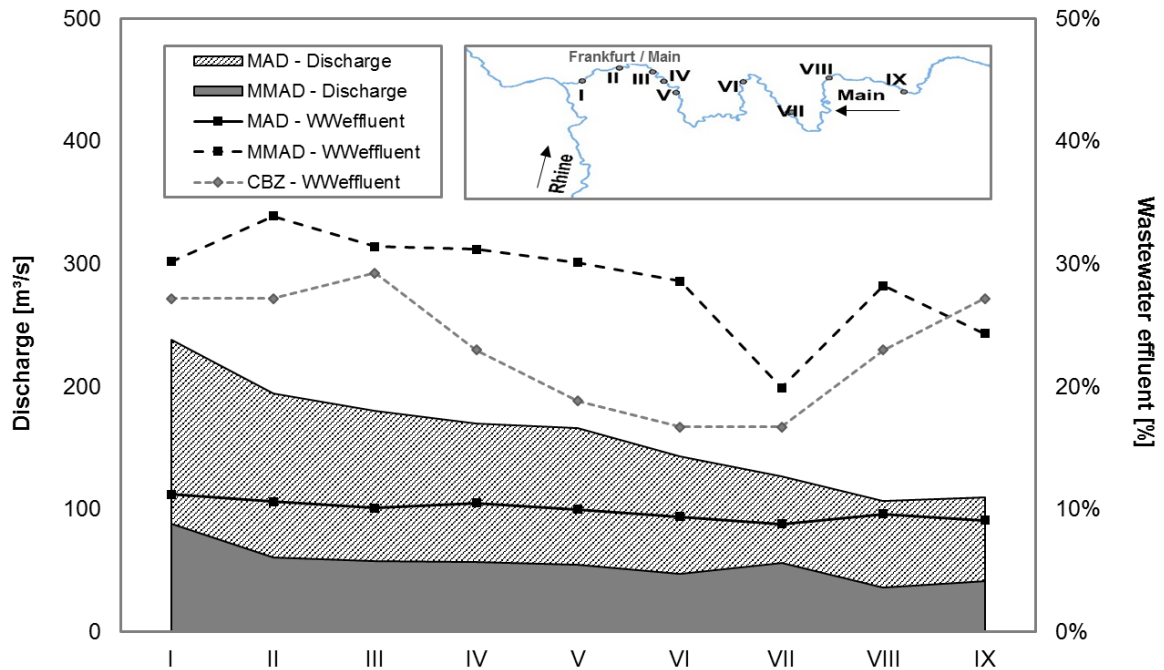


Figure 4-2: Comparison of wastewater effluent contribution (secondary axis) from GIS model under MMAD (black dots with dashed line) and MAD conditions (black dots with solid line) with dilution calculation using carbamazepine concentrations (grey dots with dashed line). Carbamazepine point samples were measured in wastewater effluents (2010)(Klasmeier et al., 2011) and the Main river (2016)(Fleig et al., 2016).

The findings of this study reveal a high degree of wastewater impact on streams, which also serve as an important source water for drinking water abstraction, industrial usage or irrigation purposes, particularly in many urbanized areas across Germany. Moreover, high wastewater effluent contributions can impair the ecological and chemical state of surface water due to oxygen consumption, discharge of hazardous substances, and elevated amounts of nutrients, which might pose a higher risk to aquatic life.

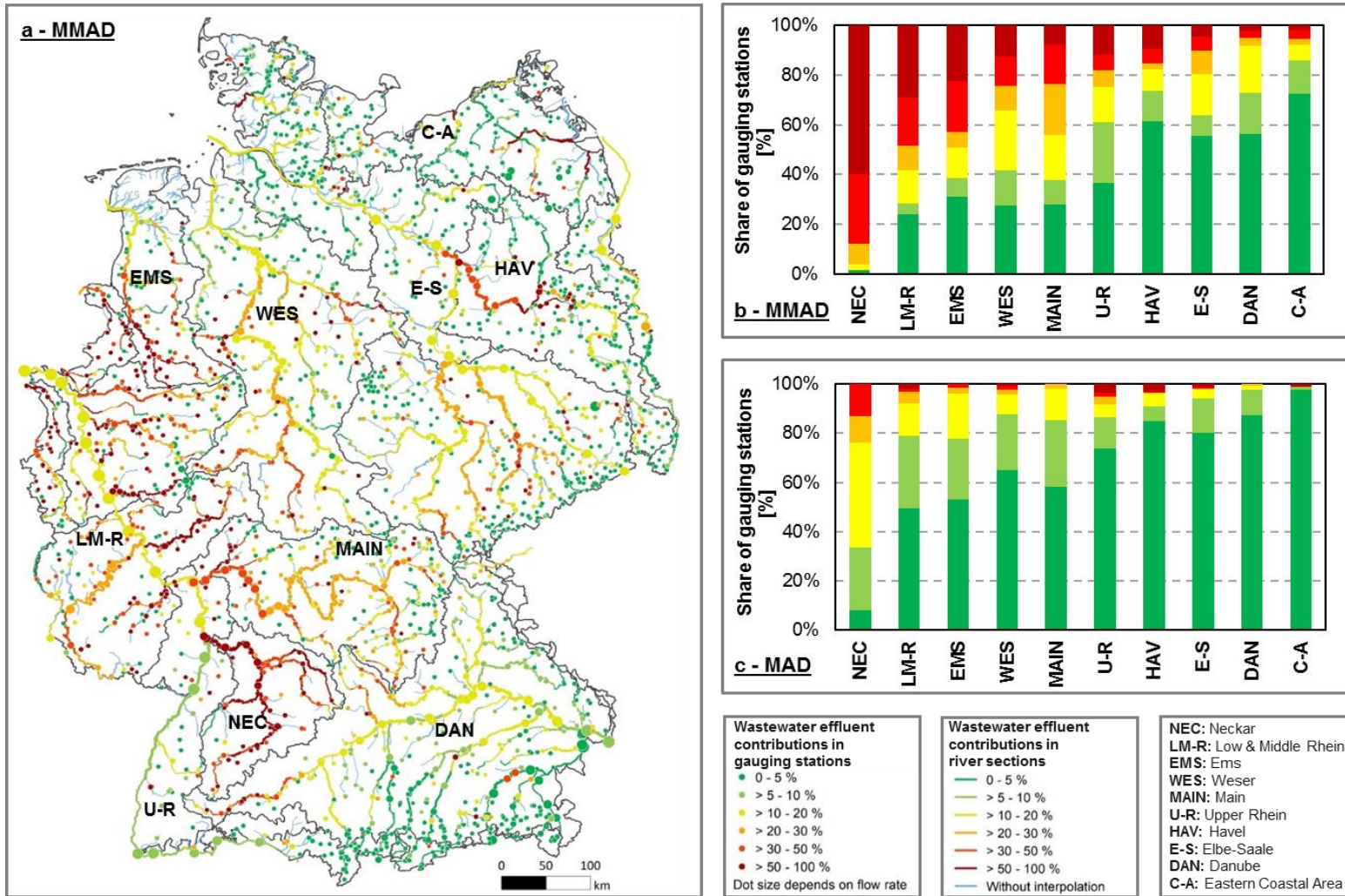


Figure 4-3: Map of nationwide wastewater effluent contributions under MMAD conditions (a) and share of gauging stations with relative wastewater effluent contributions for river basins under MMAD (b) and MAD (c) conditions.

4.3.2. *Relevance of elevated wastewater effluent contributions in streams used for drinking water supply*

The quality of bank filtrate at a given location depends not only on surface water quality, the extent of wastewater effluent contributions, and the level of wastewater treatment, but also on a large number of site-specific factors. These include location and type of wells, distance between the surface water and abstraction wells, relative contributions from landside groundwater, and hydrobiogeochemical factors such as hydraulic permeability, sediment conductivity, and prevailing redox conditions (Regnery et al., 2017; Storck et al., 2012). Due to these multiple factors, generating a nationwide cumulative estimate of bank filtrate shares (i.e. contributions of bank filtrate to drinking water supply) and expected water qualities in drinking water abstraction wells without detailed information on the aforementioned factors or local water quality data, was not possible within the scope of this study. Further research is essential to generate relevant water quality data per catchment area, including the locations of DWTPs and site-specific hydrogeological factors. Instead, the conceptual approach to determine critical bank filtrate contributions developed in this study (see Section 4.2.2) was applied for three selected indicator chemicals: oxypurinol (OXY), valsartanic acid (VSA), and carbamazepine (CBZ). These compounds are highly persistent in the aqueous environment, originate from wastewater effluent, and occur at high concentrations in German and European rivers (Dickenson et al., 2011; Funke et al., 2015; Loos et al., 2009; Loos et al., 2013; Nödler et al., 2013). An assessment of their toxicological relevance regarding human health protection (MTLs) has been provided by German Environment Agency (2018b). Critical bank filtrate shares in wells, in which the MTL values for each of the three indicator chemicals would be exceeded, were calculated for different wastewater effluent contributions ranging from 0-100% (Figure 4-4, left). Based on this conceptual approach, the MTL of oxypurinol exhibiting high average wastewater effluent concentrations would be exceeded in a scenario with only 5% bank filtrate and 60% wastewater effluent contribution in the stream (Figure 4-4, left). For carbamazepine, which exhibited lower wastewater effluent concentrations, MTL exceedances would occur when both the effluent contribution to the stream and the bank filtrate share were about 60% (Figure 4-4, left).

This assessment using suitable indicator chemicals, known toxicological information, and the calculation of critical bank filtrate contributions in drinking water wells provides a universal qualitative approach for any location worldwide to qualify possible *de facto* reuse situations. With the assistance of this conceptual approach, possible hot spots of *de facto* reuse can be identified, if the site-specific data on indicator chemical concentrations in wastewater effluent and the percent wastewater effluent contribution in a river are known. A proposed workflow building upon the results of the ArcGIS model developed during this study (Figure 4-4, right) can be used by water utilities and regulators to identify sites where MTL exceedances could potentially occur, reducing the need

for comprehensive monitoring campaigns for a large number of drinking water facilities and to engage in site-specific actions to reduce a potential impact on drinking water quality.

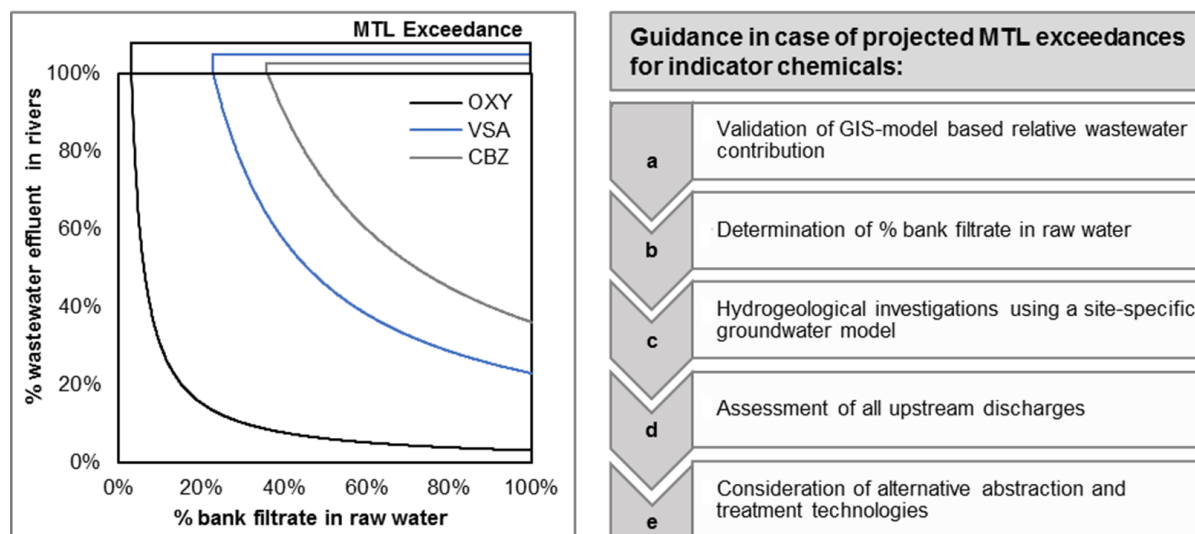


Figure 4-4: Projected benchmark of MTL exceedances for indicator chemicals OXY (MTL: 300 ng/L), VSA (MTL: 300 ng/L) and CBZ (MTL: 300 ng/L) under different percent contributions of wastewater effluent in rivers and bank filtrate in raw water scenarios (left). WWTP effluent concentrations (CBZ 832 ng/L (Loos et al., 2013), VSA 1,310 ng/L (Nödler et al., 2013) and OXY 9,830 ng/L (Funke et al., 2015)) are representing mean values, taken from literature. Guidance for water utilities and regulators in case of indicator chemical MTL exceedance (right).

The conceptual approach was validated by site-specific indicator chemical measurements (i.e., oxypurinol and carbamazepine) for three different case studies located along the rivers Rhine, Havel and Main, which are affected by wastewater effluent contributions of 7 and 17% under MAD and 42% MMAD conditions according to the ArcGIS model, respectively (Table 4-1). Wastewater effluent contributions were determined to be 10% based on locally measured chemical data in the river Rhine close to the DWTP-A Düsseldorf, where bank filtered water subsequently undergoes ozonation and activated carbon filtration. Contributions of surface water in the bank filtrate were determined to be 79% on average and did not result in MTL exceedance of carbamazepine. Furthermore, due to subsequent advanced treatment at the DWTP, MTL exceedances for indicators even with high wastewater effluent concentrations are not expected in the finished drinking water. At case study DWTP-B drinking water is abstracted at Lake Tegel, Berlin via IBF, which serves drinking water with approximately 80% bank filtrate shares to 0.8 million inhabitants (Rehfeld-Klein, 2017; Schimmelpfennig et al., 2016; Senate Department for Urban Development and Housing Berlin, 2017). MTL exceedances in their lake-impacted drinking water production wells were projected for both carbamazepine (0.3 µg/L) and oxypurinol (1.8 µg/L) according to site-specific measurements (Table 4-1). Supporting the findings of our conceptual approach, in finished drinking water approximately 13-14% wastewater-derived sources were determined by the Berlin Water Company for DWTP-B in 2016. Subsequently, the finished drinking water, composed of bank filtrate and landside groundwater, from DWTP-B contained mean valsartanic acid (1 µg/L) and oxypurinol

(0.4 µg/L) concentrations, which were above their MTLs (0.3 µg/L) (Rehfeld-Klein, 2017). This situation has triggered actions taken by Berlin Water Company to mitigate the impacts of elevated wastewater contributions in streams in Berlin. The case study area DWTP-C validates a scenario characterized by high wastewater effluent contributions (42% MMAD) but low bank filtrate shares (11%), resulting in MTL exceedance of oxypurinol in bank filtrate by 500 ng/L as projected by the conceptual approach (Figure 4-4).

Table 4-1: Validation of conceptual approach for case study areas Rhine, Havel and Main by indicator chemicals measurement data both in surface waters and in bank filtration.

River & DWTP	Indicator	Mean $C_{WW\ effluent}$ [$\frac{ng}{L}$]	WW effluent contribution in		IBF shares in wells* [%]	C_{BF} [$\frac{ng}{L}$]
			River (GIS)	River*		
Rhine DWTP-A	CBZ	478 (Klasmeier et al., 2011)	7.4 (MAD)	9.8	78.7	37
Havel DWTP-B	CBZ	1,800 (Altmann et al., 2014)	17 (MAD)	32.8	100	300 ⁺
	OXY	9,830 (Funke et al., 2015)		17.3	100	1,800 ⁺
Main DWTP-C	OXY	9,830 (Funke et al., 2015)	42 (MMAD)	45.8	11	500

*Calculations of the bank filtrate shares in wells and bank filtrate concentrations in Rhine-Düsseldorf and Main DWTP-C are based on locally measured confidential data from municipal utility of Düsseldorf and Bavarian Environmental Agency, 2018. Carbamazepine and oxypurinol concentrations from Lake Tegel are taken as 590 ng/L (Schimmelpfennig et al., 2016) and 1,700 ng/L (Hellauer et al., 2018a), respectively. +Mean carbamazepine and oxypurinol concentrations in bank filtrate of DWTP-B, Havel, are based on the data from Hellauer et al. (2018a)

The findings of this study might also suggest a potential impact by microbial contaminants (e.g. viruses) on the quality of bank filtered water under the influence of wastewater effluent discharges. Due to lack of monitoring data and in particular information on travel time in the subsurface, no conclusions on occurrence of the microbial contaminants during *de facto* reuse can be drawn. However, drinking water facilities in Germany are required to comply with a 50-day hydraulic retention time in the subsurface to assure proper inactivation of pathogens, i.e. the microbial safety of raw water. However, where *de facto* reuse conditions (i.e. exceedance of MTL's) have been identified, follow-up studies should also include a comprehensive microbial risk assessment.

4.4. Acknowledgements

We would like to thank the German Environment Agency for funding this study (grant number: 91 182) and the German Ministry of Education and Research (grant number: 02WAV1404A).

Furthermore, we would like to thank Rolf Timmermann, Simone McCurdy and Peter Schätzl (DHI-WASY) and Marian Bachmaier (TUM) for their support during the ArcGIS model implementation.

5. Developing a novel biofiltration treatment system by coupling high-rate infiltration trench technology with a plug-flow porous-media bioreactor

The following chapter presents investigations related to Hypothesis #2: *Integration of infiltration trench technology into hybrid biofilter SMARTplus establishes a horizontal flow regime providing rapid infiltration and homogenous plug-flow conditions.*

The chapter has been published with editorial changes as follows:

Karakurt-Fischer, S.; Sanz-Prat, A.; Greskowiak, J.; Ergh, M.; Gerdes, H.; Massmann, G.; Ederer, J.; Regnery, J.; Hübner, U.; Drewes, J.E., 2020. Developing a novel biofiltration treatment system by coupling high-rate infiltration trench technology with a plug-flow porous-media bioreactor. *Science of the Total Environment* 722, 137890.

Author contributions: Sema Karakurt-Fischer, Uwe Hübner and Jörg E. Drewes conceptualized the research objective. Sema Karakurt-Fischer and Jürgen Ederer constructed the experimental setup. Sema Karakurt-Fischer designed and conducted the experiments and the analyses. Alicia Sanz-Prat and Martin Ergh simulated the tracer transport. Heiko Gerdes, Gudrun Massmann and Julia Regnery supervised the study. Sema Karakurt-Fischer and Alicia Sanz-Prat wrote the paper. Jörg E. Drewes, Uwe Hübner and Janek Greskowiak critically reviewed the paper. All authors approved the final version of the manuscript.

Abstract

The sequence of two infiltration steps combined with an intermediate aeration named ‘sequential managed aquifer recharge technology (SMART)’ proved to be a promising approach to replenish groundwater using treated wastewater effluents or impaired surface waters due to efficient inactivation of pathogens and improved removal of many trace organic chemicals. To minimize the physical footprint of such systems and overcome limitations through site-specific heterogeneity at conventional MAR sites, an engineered approach was taken to further advance the SMART concept. This study investigated the establishment of plug-flow conditions in a pilot scale subsurface bioreactor by providing highly controlled hydraulic conditions. Such a system, with a substantially reduced physical footprint in comparison to conventional MAR systems, could be applied independent of local hydrogeological conditions. The desired redox conditions in the bioreactor are achieved by *in-situ* oxygen delivery, to maintain the homogenous flow conditions and eliminate typical pumping costs. For the time being, this study investigated hydraulic conditions and the initial performance regarding the removal of chemical constituents during baseline operation of the SMART*plus* bioreactor. The fit of the observed and simulated breakthrough curves from the pulse injection tracer test indicated successful establishment of plug-flow conditions throughout the bioreactor. The performance data obtained during baseline operation confirmed similar trace organic chemical biotransformation as previously observed in lab- and field-scale MAR systems during travel times of less than 13 hours.

5.1. Introduction

The rising water demands of cities, agriculture, and industry in many regions worldwide are resulting in an increasing pressure on quality and quantity of surface and groundwater and have motivated the exploitation of alternative freshwater resources. Augmentation of drinking water supplies with reclaimed water via an environmental buffer, defined as indirect potable reuse (IPR), reduces the dependency and burden on seasonally and climatically changing conventional water resources by shortening the natural hydrological replenishment cycle (Drewes and Khan, 2011).

Given the origin of the source water used in IPR schemes, removal of contaminants of concern (e.g. pathogenic microorganisms, trace organic chemicals (TOrcs), or antibiotic resistant bacteria and resistance genes) by reliable and redundant treatment processes is mandatory to ensure a safe water quality. For this reason, IPR design is characterized by a multi-barrier approach applying combinations of advanced water treatment processes (e.g., membrane filtration, adsorption, advanced chemical oxidation and biological treatment) followed by an environmental buffer providing additional retention time and storage capacity prior to use (Drewes and Khan, 2011; National Research Council, 2012). Low-energy managed aquifer recharge (MAR) systems such as soil-aquifer treatment (SAT) take advantage of natural attenuation processes for chemical and

microbial contaminants during the soil passage, generate no residuals and do not require the addition of chemicals (Regnery et al., 2017). Moreover, these technologies can dampen varying input concentrations of these contaminants in reclaimed water by way of dilution with other water sources.

Previous studies have demonstrated that the combination of different removal mechanisms in MAR systems (i.e., filtration, biotransformation, adsorption, ion exchange) results in an efficient inactivation of pathogens, especially viruses or protozoa, and provides an effective removal of many TOrCs from treated wastewater and highly anthropogenically impacted surface water (Regnery et al., 2017). Recent research showed that biotransformation of some TOrCs is enhanced under oxic and carbon limited conditions (Alidina et al., 2014; Hellauer et al., 2017; Hoppe-Jones et al., 2012; Li et al., 2012). To take advantage of these favorable conditions, a new engineering concept called sequential managed aquifer recharge technology (SMART) was established (Regnery et al., 2016). In this process, an initial infiltration step (e.g. bank filtration) with short travel times of a few days is used to remove the readily degradable organic carbon, followed by water recovery, an intermediate aeration, and a second infiltration step, where oxic and carbon-limited conditions can prevail in the subsurface. Enhanced removal of several TOrCs by the SMART concept was successfully demonstrated at MAR facilities in the United States and Germany for the production of drinking water from surface waters impaired by wastewater effluents (Hellauer et al., 2017; Hellauer et al., 2018a; Regnery et al., 2016).

Building upon these experiences, the aim of this study was to further advance the design and performance of the SMART concept by developing an engineered approach that can be deployed independent of local hydrogeological conditions with a significantly reduced physical footprint, highly controlled hydraulic conditions, and a similar or better performance. We hypothesize that this novel SMART_{plus} concept can establish homogenous plug-flow conditions by utilizing high-rate infiltration trench technology, which facilitates rapid infiltration through a highly porous vadose zone, thereby requiring only a very small physical footprint, followed by a sequence of well-defined reaction zones in the subsurface. In addition, the sequence of well-defined redox conditions can be adjusted through the integration of an *in-situ* electron acceptor (EA) delivery system that is closely coupled to an appropriate online monitoring and control system to accommodate variable feed water qualities. In this paper, we investigated the performance of the key elements of this innovative sequential biofiltration treatment system at pilot scale and tested the hypothesis that subsurface hydraulic conditions can be tightly controlled and adjusted during continuous baseline operation over a period of 650 days. Performance data during baseline operation prior to the commissioning of an EA delivery system are presented.

5.2. Materials and methods

5.2.1. Establishment of SMARTplus at pilot scale

Conventional SAT systems commonly employ open recharge basins to facilitate infiltration of water through the vadose zone (Regnery et al., 2013). This approach requires large physical areas and suitable subsurface conditions. In the SMARTplus approach, we are employing high-rate trench infiltration technology which facilitates rapid infiltration through a highly porous vadose zone requiring only a very small physical footprint (Mikat, 2009). In order to establish a sequence of controlled redox conditions during subsequent travel through the saturated zone, homogeneous flow conditions are required. Native subsurface environments are usually characterized by a high degree of hydraulic and/or chemical heterogeneity. Thus, we proposed to replace the natural substratum by granular filter media with a high uniformity coefficient ($U=1.3$) and an effective grain size (d_{10}) of 0.75 mm to establish homogenous horizontal flow conditions. These flow conditions could be induced by a groundwater pumping regime at field scale that also minimizes uncontrolled mixing of infiltrated water with native groundwater.

The SMARTplus bioreactor pilot system was fed continuously with real-time tertiary effluent after dual-media filtration (named here as rapid sand filtration (RSF), see specifications in SI-Table 9.5-1) to remove suspended solids followed by three coupled buffer tanks with an overall storage capacity of 2,700 L. In order to establish the SMARTplus bioreactor at pilot scale, a stainless steel flume, with dimensions of 6 m length, 0.85 m width, and 1.4 m height, was constructed. The SMARTplus bioreactor is composed of five internal compartments (C1-5), each divided by stainless steel mesh sheets with an opening of 3 mm (Figure 5-1). A rectangular shaft (0.35 x 0.85 x 1.5 m) was placed on top of the bioreactor at the inflow side (C1) mimicking the infiltration trench. Water is distributed at the top of the shaft through a horizontally oriented, screened PVC pipe ($d=50$ mm), which allows uniform distribution of feed water across the length of the trench. A PVC plate (2.5 cm thick) covers the first 300 cm of the horizontal infiltration to seal the reactor as a confined saturated artificial aquifer, where three removable caps (at x direction 1,000 mm, 1,400 mm and 2,600 mm from the infiltration trench) for sampling of filter media and air siphons are installed. Along the entire length of the reactor, in total 24 sampling ports were installed at heights of 45 cm and 105 cm below surface and at two different penetration depths of 20 cm and 45 cm into the bioreactor (SI-Figure 9-4).

To enable rapid vertical infiltration and establish horizontal plug flow along the bioreactor, the first compartment (C1, infiltration trench) is filled with gravel ($d_{10}=3.4$ mm), which is covered with a thin (10 cm) sand layer (Quarzwerke GmbH, Germany, $d_{10}=0.75$ mm) on top for the retention of any residual suspended solids. The compartments in front of (C2) and after the EA compartment (C4) are filled with technical sand ($d_{10}=0.75$ mm). Prior to the installation of the EA (oxygen) delivery device, the EA compartment (C3) was filled with gravel ($d_{10}=2.1$ mm) from a tertiary sand filter of the

wastewater treatment plant (WWTP) Munich Gut Marienhof to facilitate biofilm growth in the system. The outlet compartment (C5) is filled with gravel ($d_{10}=3.4$ mm) to allow high drainage rates. In order to maintain fully saturated conditions, the water level of the outlet compartment is controlled by a constant head device as a function of the flowrate in the bioreactor.

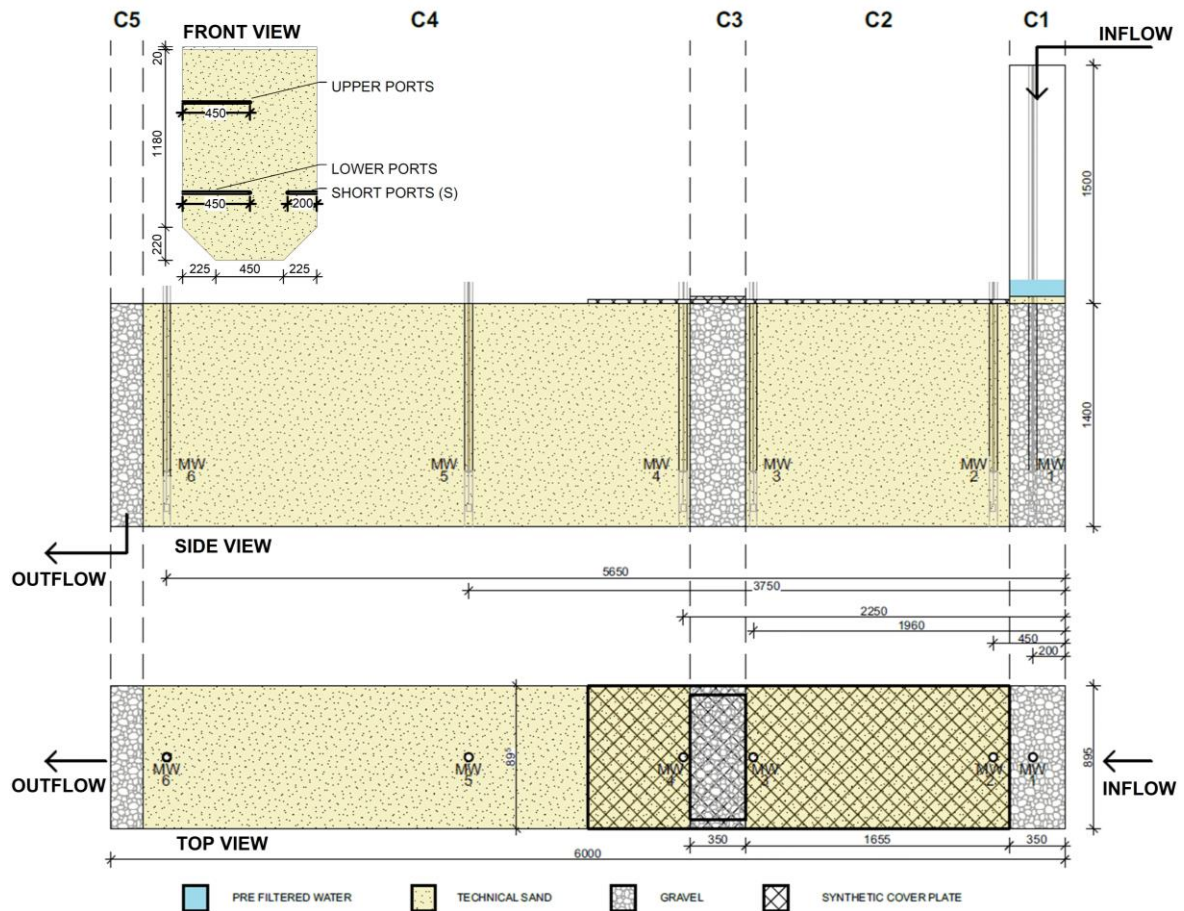


Figure 5-1: Front, side, and top views of the SMARTplus bioreactor indicating the characteristic media of each compartment, and the locations of the monitoring wells (MW) placed into the bioreactor. All dimensions in mm.

At the inflow and the outflow of the SMARTplus bioreactor, a 254 nm ultraviolet absorbance (UVA_{254}) sensor AF45 (optek-Danulat GmbH, Germany) and a magnetic-inductive flow meter SM8100 (ifm GmbH, Germany) were installed. In addition, conductivity, temperature and depth (CTD) sensors (CTD10 3 in 1, Decagon Devices, USA), and dissolved oxygen sensors (DO, DP-PSt6, PreSens GmbH, Germany) were deployed in 6 PVC monitoring wells along the bioreactor and were continuously logging data every 10 minutes. The wells were positioned 10 cm above the bottom of the flume and perforated only at the lowest 30 cm. In order to avoid dead volumes, packers were installed into the MWs at a height of 35 cm.

5.2.1.1. *System operation and performance characterization*

The SMART*plus* pilot bioreactor was continuously fed with tertiary effluent from the Garching WWTP over a period of more than 1.5 years (January 2017 – September 2018) at an inflow rate of 300 L/h. Between the months of April to September, tertiary effluent received from the Garching WWTP was also UV disinfected. Synoptic water samples were collected weekly at the influent and effluent (5,850 mm in x direction) based on estimated hydraulic retention times of RSF and the SMART*plus* pilot bioreactor, as well as at sampling ports 2 (400 mm), 8 (1,640 mm) and 12 (2,640 mm) for ammonia, nitrate, dissolved organic carbon (DOC), UVA₂₅₄, and selected TOxCs. Turbidity and pH measurements were carried out daily at the inflow and outflow of the RSF and the bioreactor with a hand-held 2100Qis turbidimeter (HACH, USA) and a hand-held 202710 pH/ORP meter (JUMO, Sensors, Germany).

5.2.1.2. *Head loss determination*

The hydraulic gradients in the bioreactor were determined by monitoring the hydraulic heads at the 6 CTD sensors and at the outlet compartment C5 after establishing four different steady-state flow rates varying from 150 L/h to 600 L/h. For each flow rate tested, the constant head device located at the outlet boundary of the bioreactor was positioned manually to achieve fully saturated conditions from the inflow to monitoring well #4, as well as to avoid an overflow at the end of the confined part of the bioreactor.

5.2.1.3. *Porosity test*

A total of three unsteady flow tests were performed to determine the effective porosity in the bioreactor according to the following procedure under steady-state conditions: the outflow rate was significantly increased by lowering the constant head device at the outflow side of the bioreactor, while the inflow rate was kept constant. This resulted in a sudden decrease of the water levels in the bioreactor. The system was operated until the water levels were stable again. Then, a second adjustment of the constant head device at the outflow back to the original water level was performed. The effective porosity of the media was derived by monitoring the partial changes in the fluid volume within the bioreactor at different times during the unsteady flow tests. The outcomes for 10 measurements at each CTD sensor, ranging from porosities of 0.28 to 0.39, are depicted in SI-Figure 9-5.

5.2.1.4. *Tracer experiments*

A tracer experiment was conducted in order to characterize the hydraulic retention time and the mass-solute transport processes at higher resolution within the bioreactor at an inflow of 300 L/h. A pulse injection of a KBr solution (mean concentration 1 g/L) was performed over 12 hours. During the

tracer test, EC data were recorded using the CTD sensors located in the monitoring wells, and the outflow was augmented by additional manual measurements conducted at selected ports (1, 2, s1, s3, s4, 7, 8, 11, 12, 18 and 24). The sampling frequency was chosen according to pre-tracer tests, whereby shorter measurement intervals were chosen for the expected peak arrival time.

5.2.2. *Laboratory analysis*

Water samples for ammonia, nitrate, organic bulk parameters, and TO_{RC} analyses were taken in pre-rinsed amber glass bottles and filtered immediately with 0.45 µm cellulose acetate membrane filters (VWR International, USA). Samples for DOC analysis were acidified to a pH of 2 using hydrochloric acid and stored at 4 °C prior to analysis on a vario TOC cube analyzer (Elementar, Germany). The UVA₂₅₄ of the water samples was measured on a DR 6000™ UV-VIS spectrophotometer (Hach Lange, Germany). Nitrate and ammonia concentrations were determined using cuvette tests LCK 339 and 304 (Hach Lange, Germany) on a DR 6000™ UV-VIS spectrophotometer. TO_{RC} samples were processed according to the method described by Müller et al. (2017) and were measured using liquid chromatography coupled with tandem mass spectrometry (LC-MS/MS) with direct injection. More detailed information on mean and median TO_{RC} concentrations in feed water and their respective limits of quantification (LOQ) can be found in

SI-Table 9.5-2.

5.2.3. *Numerical simulations of groundwater flow and conservative transport processes*

A three-dimensional (3D) numerical model mimicking the unsaturated/saturated flow within the tank was developed to support the design of the SMART_{plus} bioreactor and characterize the hydraulic head loss, hydraulic retention times, as well as flow and subsequently mass-solute transport processes. The deterministic approach utilizes the modelling software SPRING, based on the finite element method (König et al., 2015). The numerical outcome of the tracer experiment was used to identify potential deviations from an ideal flow and transport behavior within the tank that might arise from preferential flow and non-equilibrium mass-transfer processes due to physical heterogeneities of the porous media. SI-Figure 9-6 illustrates the numerical set-up of the SMART_{plus} bioreactor showing the geometry and the conceptualization of the inlet and outlet boundary. The model grid is 3D with parallel layers of 0.02 m thickness. The media was considered isotropic and the flow regime steady state and fully saturated, except for the last meter of the tank where lowered hydraulic heads cause unsaturated conditions. The inflow boundary at the infiltration trench was prescribed as a constant hydraulic head of 1.4 m (Dirichlet boundary condition); the infiltrating water enters the system through an area limited to the center of the thin sand layer (see blue area in SI-Figure 9-6). The outflow boundary (see red dot in SI-Figure 9-6) corresponds to a prescribed flow rate through the bottom of the tank of 300 L/h (Neumann boundary condition). The mean values of the hydraulic

heads registered at the 6 monitoring wells equipped with CTD sensors during the tracer tests were used as reference for the manual calibration of the hydraulic conductivities, K_h [m/s]. For each compartment (C1-C5), the initial values for K_h used were derived from the empirical Hazen equation (Hazen, 1911): $K_h = c(d_{10})^2$, where c is an empirical constant, and d_{10} [mm] represents the effective grain size of the media. This approach assumes a relatively uniform grain size distribution within the respective media. The initial and calibrated values of K_h for C1 – C5 are shown in SI-Table 9.5-3.

At a flowrate of 300 L/h, the dominating transport process is advection. Therefore, the effective porosity is a highly sensitive parameter for calibration. The initial value of the effective porosity, ϵ , was set to 0.35 [-], which is within the range of values confirmed by the unsteady flow tests (0.28 – 0.39). It was adjusted to 0.5 for the whole tank during the process of calibration. Regarding dispersion, the horizontal transverse dispersivity, α_{ht} , was set to one tenth of the longitudinal dispersivity, α_l , and the vertical transverse dispersivity, α_{vt} , to one hundredth of α_l . The principal hydraulic, transport and numerical model parameters are summarized in the SI-Table 9.5-4. For the conservative transport simulation, an observed time-variant concentration of 1 g/L KBr at the inflow boundary was set during the tracer injection over 12 hours. The varying concentration at the inflow was presumably due to incomplete dissolution of KBr into the stock solutions, which had to be separately prepared as four individual solutions due to the high water volume required for the tracer test. The total simulation time was 28.6 hours. The electrical conductivities (EC) generated by the bromide solution and the mean background electrical conductivity ($EC_{\text{background}} = 1,150 \mu\text{S/cm}$), were measured at the CTD sensors at the selected ports and normalized with respect to the maximum injected EC ($EC_{\text{injected}}^{\text{max}} = 2,265 \mu\text{S/cm}$, by the expression: $(EC - EC_{\text{background}})/(EC_{\text{injected}}^{\text{max}} - EC_{\text{background}})$). The maximum injected EC was estimated by conversion of the injected bromide concentration (Weast and Lide, 1989; Wolf, 1966). Thus, the numerical outcome is directly comparable with experimental data, since the model set a maximum injected bromide concentration of 1 g/L and null initial concentration. Observed and simulated normalized breakthrough curves (BTCs) of the tracer signal at each monitoring well and the effluent were compared to obtain the best fit in the process of calibration. Further, the quantitative analysis of the numerical BTC was performed by using the temporal moment equation (Luo et al., 2006), which estimates the statistics of the normalized BTCs and provides their mean travel times, i.e. hydraulic retention times. The approach is only valid for an idealized box-shaped, i.e. steady, input concentration. Thus, in order to allow the calculation of the hydraulic retention times, a box-shaped input concentration curve was simulated in addition to the real observed tracer input curve.

5.3. Results and discussion

5.3.1. Hydraulic characterization of the SMARTplus bioreactor

A fundamental benefit of the SMARTplus bioreactor is the establishment of highly controlled hydraulic conditions providing the prerequisite for a sequence of controlled redox zones. Thus, a detailed hydraulic characterization regarding the high hydraulic load, the flow field and transport features for dissolved compounds of the reactor was performed.

5.3.1.1. Hydraulic flow field in the SMARTplus bioreactor

The observed and simulated hydraulic heads at the CTD sensors and the outlet boundary of the SMARTplus tank, with a head difference of approximately 10 cm between CTD1 and the end of the tank, are depicted in Figure 5-2. Such low hydraulic gradient suggests that the hydraulic flow field runs quasi-parallel to the bottom of the tank, with exception of the inlet boundary. The discrepancy between the observed and simulated hydraulic heads at the outlet compartment (C5) of the SMARTplus bioreactor is caused by the pressure losses at the sensor assembly piping located at the outflow of the bioreactor. Due to its dimensions at pilot scale, the bioreactor can be operated at a maximum flow rate of 1,200 L/h. However, future applications of such a bioreactor design should explicitly consider not only the desired and maximum operational flowrate, but also the flow field along the bioreactor at the desired flowrate, to assess whether or not homogenous flow conditions can be provided in order to achieve the desired treatment efficiency. In general, an excellent fit between observed and simulated hydraulic head was achieved after calibration of hydraulic parameters.

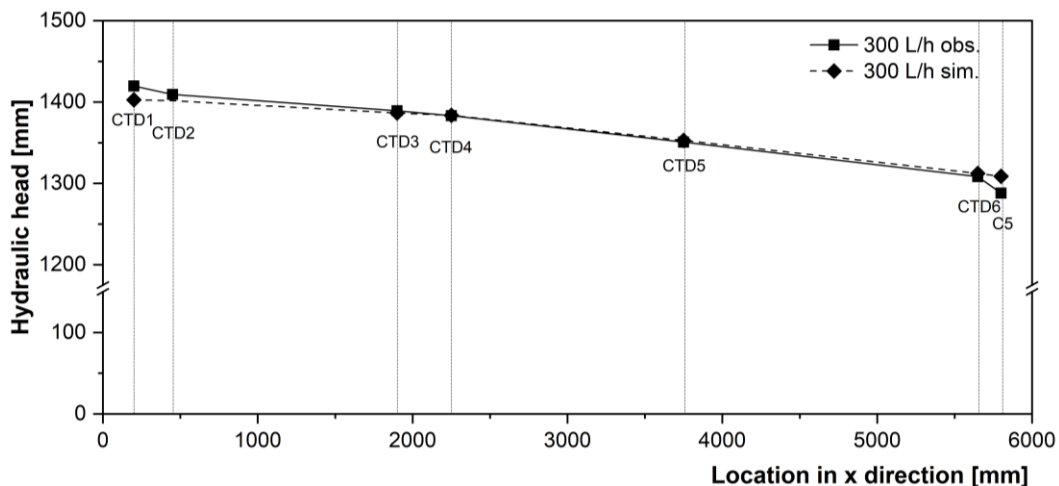


Figure 5-2: Observed and simulated hydraulic heads at 6 monitoring wells by CTD sensors (see location in Figure 5-1), CTD1, CTD2, CTD3, CTD4, CTD5 and CTD6 in x (i.e. flow) direction, and the outlet compartment, C5, at a flowrate of 300 L/h.

5.3.1.2. Tracer test analysis

Figure 5-3 depicts the normalized breakthrough curves (BTCs) of the tracer concentration during 28 hours after the pulse injection started (black dots). The breakthrough of tracer at the sampling ports was distinguished by a distinct double peak pattern due to the transient tracer concentration at the inflow (Figure 5-3). The varying concentration at the inflow was presumably caused by incomplete dissolution of KBr into the stock solutions, which had to be separately prepared as four individual batches (0.9 m³ each) due to the high water volume required for the tracer test (3.6 m³ in total). It can be seen that the shape of the input concentration curve propagated to all of the downstream sampling ports, including the outflow. While the sampling ports reflected the characteristics of the input curve, the observed signal at the CTD sensors were considerably distorted. This might be attributed to the fact that the CTD sensors were installed in screened PVC monitoring wells containing a dead volume of 196 cm³. Therefore, the data from the CTD sensors were not as reliable as the data from the sampling ports and thus should not be used to evaluate the flow and transport behavior inside the tank. The so-called global BTC at the outflow represents the integrated response of the whole tank to the tracer pulse injection, and therefore it is more relevant than the local BTCs at the CTD sensors. The fit of the observed and simulated global BTCs at the outflow of the tank and no tailing in the observed BTC revealed that the preferential flow paths and related non-equilibrium effects were of minor importance for the overall transport behavior within the tank.

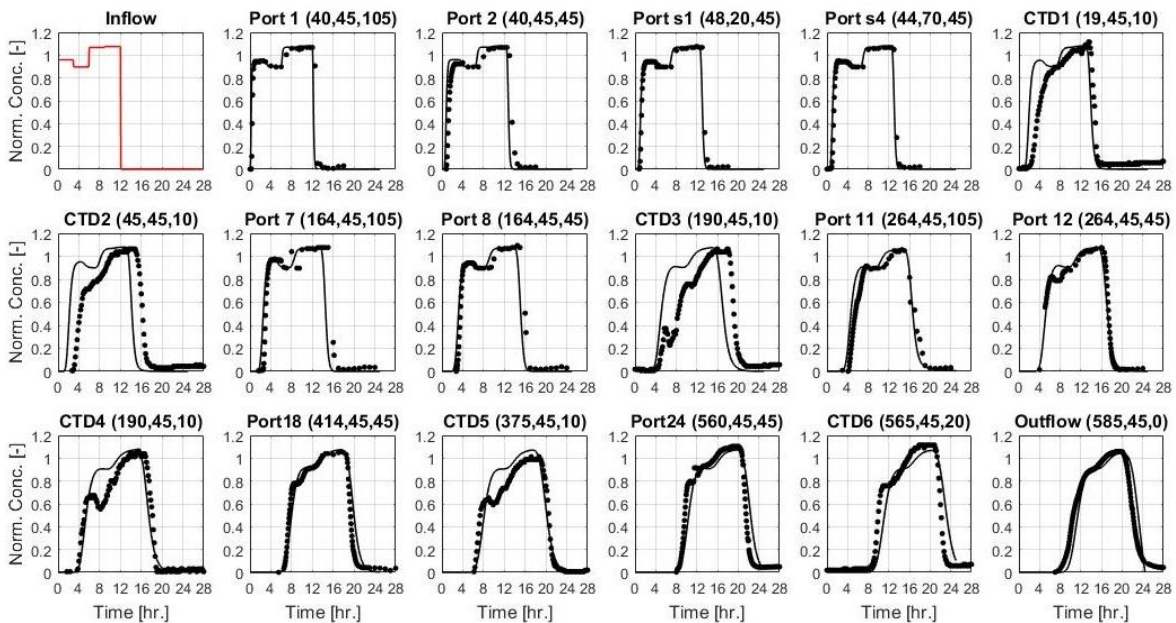


Figure 5-3: Normalized BTCs of the observed (black dots) and simulated (black solid lines) KBr concentrations at the observation points during the pulse injection tracer test. The measured and simulated transient inflow KBr concentration is depicted at the top left panel (red solid line), while the observed and simulated concentration at the outflow is shown at the lower right panel. CTD1-CTD6 represent the conductivity sensors located in the middle of the bioreactor at 10 cm from the bottom. The x, y and z coordinates of the sampling ports, CTD sensors and the outflow are expressed in cm.

For visualization purposes, Figure 5-4 represents the spatial distribution of the tracer plume across the porous media at different times after the injection. 30 minutes after injection, a sharp front plume entered the tank from the top-left side, and after 2 hours, the solute plume covered the entire y- z-direction plane. Notice that the tracer plume became more perpendicular to the bottom of the tank whilst increasing distance from the inflow, and the plume front widened due to longitudinal dispersion. After 8 hours of continuous tracer injection, the plume occupied more than half of the bioreactor, and at 20 hours, the plume almost passed through the whole tank. The hydraulic retention time values (overall HRT 12.6 h) derived from the temporal moments method corresponded to the numerical BTC results (see SI-Table 9.5-5). Transverse and vertical dispersivity had negligible influence in mixing and spreading of the plume. Based on these results, it can be concluded that the advection process dominated the transport of the tracer. The results of the flow and transport modelling confirm that hydraulic conditions are close to plug-flow conditions required to establish a sequence of controlled redox conditions inside the bioreactor.

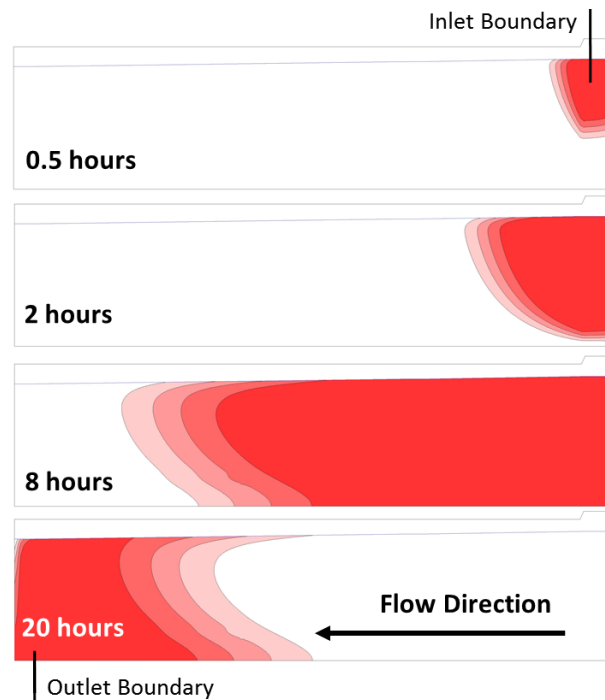


Figure 5-4: Spatial distribution of the normalized tracer plume concentration at four times after pulse injection started from the inlet boundary (top right side) to the outlet boundary (bottom left side). The red area corresponds to the 1 g/L bromide concentration and the white area to the background concentration (0 g/L).

5.3.1.3. Media aging

The intrusion of residual suspended solids despite pretreatment by the RSF and the development of a biofilm may alter the available void volume of such a system at pilot or field scale during continuous operation while feeding nutrient rich water. To avoid operational disturbances, incidences of media aging should be well monitored, and followed by improvement of the pretreatment if

necessary. Thus, hydraulic heads along the bioreactor were continuously monitored after the commissioning of the reactor.

The continuous hydraulic head measurements at CTD1 and CTD2 sensors located at the inflow side of the SMART $plus$ bioreactor acquired over a period of 9 months are depicted in Figure 5-5. While the flow rate throughout the bioreactor was held constant at about 300 L/h, a gradual increase of the water level at CTD1 with respect to CTD2 took place over the entire period. The reduction of the flow-effective cross-section, i.e. aging of the system, might be caused by remaining suspended solids after the pretreatment clogging the grain interspace and/or the gradual establishment of a biofilm on the grains. Aging phenomena are primarily expected at locations with high flow velocities, which occur particularly in the transition from areas of coarser to finer material, e.g. the transition from the infiltration trench (C1) to the C2 compartment of the bioreactor. Since the sensor CTD1 is located in the C1 and CTD2 in the C2 compartment of the bioreactor, it can be assumed that the observed aging is a consequence of a clogging layer gradually forming in the transition area between the two sensors.

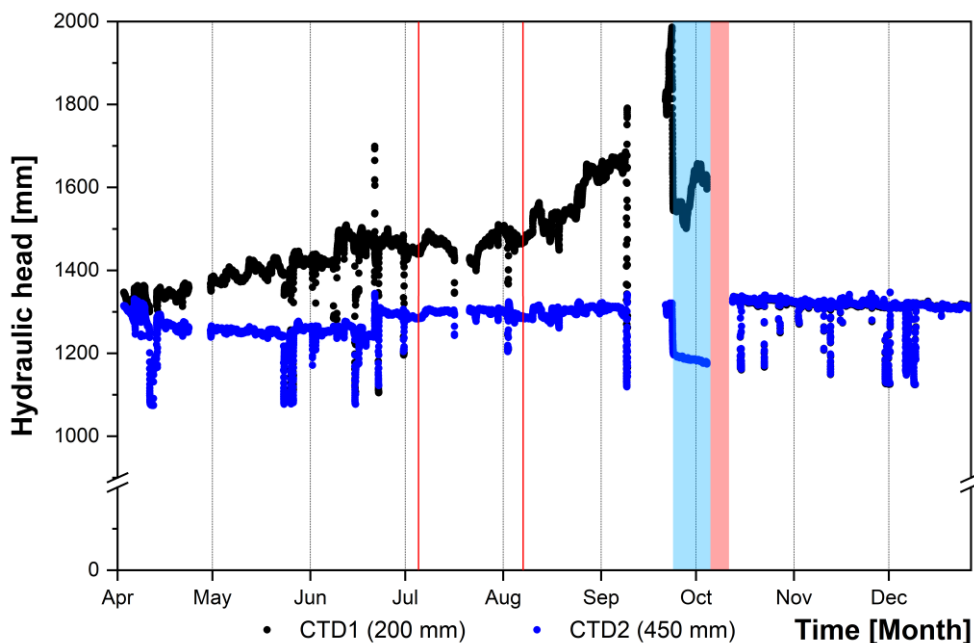


Figure 5-5: Hydraulic head measurements at CTD 1 and CTD 2 (200 and 450 mm at x direction) between April 5th and December 30th 2018 at 300 L/h. The thin red lines indicate the exchange of a thin sand layer on the top of the C1 compartment. The thick blue and red lines denote the reduction of the flowrate to 100 L/h and the removal and cleaning of the clogged media from the C1 and C2 compartments, respectively. Data gaps were caused by online measurement failures.

To decelerate the increase of the water level at the C1 compartment, the thin sand layer on the top of the gravel was changed twice, after 76 and 82 weeks of operation, resulting in a slight improvement. By the end of September 2018, after 20 months of operation, the increase of head loss finally led to an overflow of the infiltration trench. Therefore, the flowrate of the bioreactor was decreased to 100 L/h and the hydraulic conductivity was restored by removing and cleaning the media in the inflow compartment C1 and approximately the first 40 cm of the C2 compartment after 90 weeks of

operation. In addition, as a long-term solution, the RSF was equipped with in-line coagulation to enhance removal of suspended solids prior to feeding the SMARTplus bioreactor.

5.3.2. Feed water and system characterization during baseline operation

Feed water quality, removal of bulk organic carbon, redox zonation, and attenuation of TOrCs along the SMARTplus bioreactor were characterized prior to the envisaged sequential operation and compared with conventional MAR studies as well as sequential biofiltration systems.

5.3.2.1. Feed water quality and variability

The average feed water quality and DO concentrations of the SMARTplus bioreactor during steady-state operation (April to September 2018) prior to the commissioning of the EA delivery device are displayed in Table 5-1. All parameters strongly fluctuated due to the continuous feeding of the pilot-scale SMARTplus bioreactor with tertiary effluent from the adjacent WWTP Garching, representing operational conditions of a field-scale system.

Table 5-1: Average feed water DOC concentration, UVA₂₅₄, specific ultraviolet absorbance (SUVA), NO₃-N (n=10-12), and DO concentrations (n=15,512) during baseline operation of the SMARTplus bioreactor.

DOC [mg/L]	UVA ₂₅₄ [1/m]	SUVA [L/m*mg]	DO [mg/L]	NO ₃ -N [mg/L]
10.2 ± 2.4	± 0.6	1.4 ± 0.3	5.1 ± 1.8	12.6 ± 2.3

5.3.2.2. Redox zonation and fate of bulk organic carbon

The fluctuations in the feed water quality resulted in varying DO consumption and removal percentages of DOC and UVA₂₅₄ throughout the entire bioreactor during baseline operation. Within the infiltration trench, rapid consumption of feed water DO was observed, resulting in a mean DO concentration of 1.0 ± 0.9 mg/L at the beginning of the C2 compartment, thus a shift from oxic to suboxic redox conditions (Figure 5-6). During the sampling period, denitrification was not observed along the flow path of the bioreactor, with mean nitrate concentrations in the feed water and effluent of 12.6 ± 2.3 mg N/L and 12.7 ± 2.4 mg N/L, respectively (Figure 5-6). No nitrate reduction (<0.5 mg N/L) and low DO concentrations (<1 mg/L DO) confirmed suboxic conditions along the rest of the bioreactor, based on the classification of redox conditions by Regnery et al. (2015b).

According to the theoretical DO consumption required for the complete mineralization of DOC based on a simple mass balance (2.7 mg DO / mg DOC), a mean reduction of 17 ± 9% in DOC (ΔDOC removal of 1.7 ± 1.0 mg/L) coincided with the observed DO consumption of 4.3 ± 1.4 mg/L within the first horizontal 45 cm of the bioreactor. Under steady-state baseline operation, mean reductions of UVA₂₅₄ by 1.0 ± 0.4 1/m in the infiltration trench and 1.2 ± 0.4 1/m in the entire bioreactor were observed. The feed water SUVA value increased slightly from 1.4 ± 0.3 L/m*mg to 1.8 ± 0.4 L/m*mg in the effluent as expected, indicating a preferred removal of easily degradable

aliphatic structures compared to more aromatic, refractory DOC. Removal of remaining DO and a corresponding increase in the mean DOC removal of $26 \pm 12\%$ occurred within the C2 compartment. In a pilot-scale sequential biofiltration system, receiving the same WWTP effluent ($\text{DOC} = 6.9 \pm 1.8$ mg/L) as SMARTplus but operated with an intermediate aeration step, the DOC concentration remaining in the effluent was 4.0 ± 0.5 mg/L in comparison to 7.5 ± 2.0 mg/L in the SMARTplus effluent (Müller et al., 2017). Given the fact that SMARTplus was characterized during baseline operation without the sequential approach, i.e. *in-situ* DO delivery in the C3 compartment, the total DOC removal remained steady after the C3 compartment. Based on the results from Müller et al. (2017), it can be assumed that the addition of oxygen in the EA compartment will result in an enhanced removal of BDOC after the C3 compartment of the SMARTplus bioreactor.

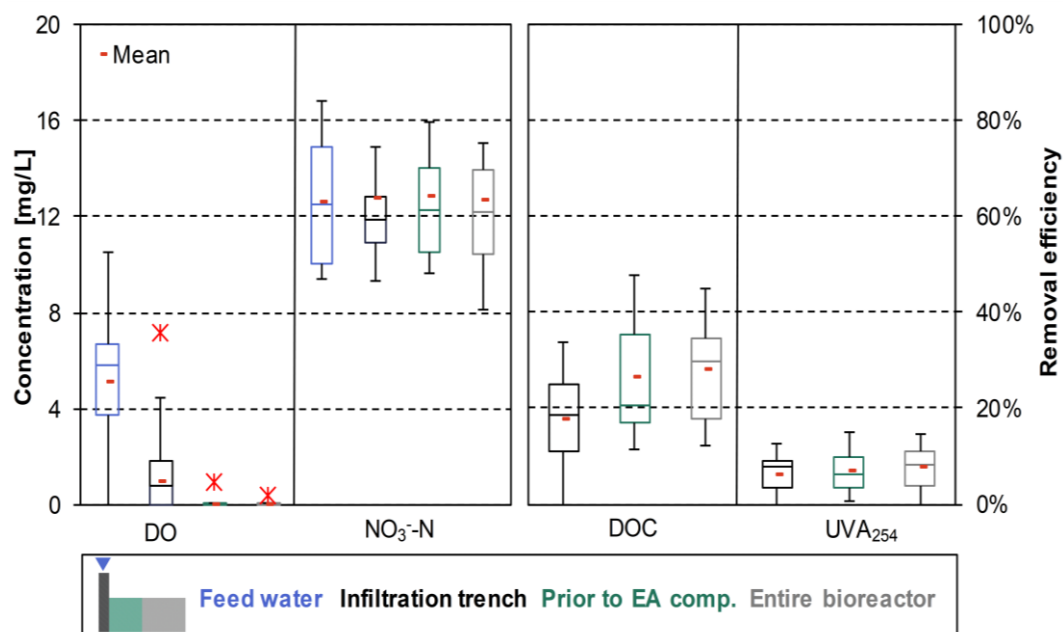


Figure 5-6: DO ($n=15,512$) and NO_3^- -N ($n=10 - 12$) concentrations in feed water and at the end of the infiltration trench, prior to EA compartment as well as the entire SMARTplus bioreactor. Percentage removal of DOC concentrations and UVA_{254} ($n = 10 - 12$), which are calculated by the DOC and UVA_{254} values of infiltration trench, prior to the EA compartment and bioreactor effluent normalized to the corresponding feed water values (Table 5-1).

5.3.2.3. Attenuation of trace organic chemicals

The transformation of TOrcs in the bioreactor was observed to be compound specific, similar to results of previous conventional MAR studies without *in-situ* EA delivery (Figure 5-7) (Burke et al., 2018; Clara et al., 2004; Hellauer et al., 2018a; Maeng et al., 2011; Massmann et al., 2006; Wiese et al., 2011). As the SMARTplus bioreactor is filled with quartz sand, biodegradation was considered to be the main attenuation mechanism for TOrc transformation, as reported in previous studies (Alidina et al., 2014; Hellauer et al., 2018b).

Among the 12 compounds measured, carbamazepine, venlafaxine and tramadol exhibited persistent behavior along the bioreactor. High persistence of carbamazepine is well known, and it has been proposed as a wastewater indicator due to its limited biological removal and poor sorption in the aquatic environment, mostly independent of the prevailing redox and hydraulic conditions (Burke et al., 2018; Clara et al., 2004; Müller et al., 2017; Rauch-Williams et al., 2010; Regnery et al., 2016). For such persistent compounds, a reliable removal must be ensured by additional barriers, e.g. in-situ ozonation, other reactive barriers within the bioreactor, and/or a suitable post-treatment, to provide a high product water quality based on the SMART*plus* bioreactor. Under conditions similar to the C1 and C2 compartments of SMART*plus*, Hellauer et al. (2018b) also did not observe removal of the structurally similar substances venlafaxine and tramadol under suboxic to anoxic conditions within the 1st infiltration step (HRT= 4.2 days) of a lab-scale SMART column system fed with WWTP effluent. However, under oligotrophic and oxic conditions, a steady transformation of tramadol (70%) and venlafaxine (<LOQ) was observed (Hellauer et al., 2018b). An improved attenuation of these substances might also be expected during sequential operation in the SMART*plus* bioreactor. At an infiltration basin fed by WWTP effluent intermittently, 50 to 63% of tramadol and 86 to 90% of venlafaxine were retained under rather dynamic redox conditions (Muntau et al., 2017). Ghattas et al. (2017) suggest that strictly anaerobic conditions might also enhance the removal of venlafaxine, carbamazepine and sulfamethoxazole. Moreover, the transformation products of venlafaxine formed under anaerobic conditions found to be subsequently degraded under aerobic conditions Ghattas et al. (2017), pointing the efficiency of sequential applications for the biodegradation of TOrCs.

Good removal of gabapentin ($67\% \pm 7\%$), 4-FAA ($78\% \pm 11\%$), and trimethoprim ($85\% \pm 7\%$) was observed in the SMART*plus* bioreactor, with relevant removal occurring in the infiltration trench under oxic-suboxic, carbon rich conditions. While rapid biodegradation is known for trimethoprim and 4-FAA, especially under oxic conditions, higher recalcitrance in MAR systems has been reported for gabapentin (Hellauer et al., 2017; Hellauer et al., 2018a; Onesios and Bouwer, 2012). A significant enhancement of gabapentin attenuation at a field-scale SMART system in comparison to conventional MAR was also reported by Hellauer et al. (2018a).

Benzotriazole, diclofenac, metoprolol, sulfamethoxazole, citalopram, and climbazole were poorly to moderately transformed during baseline operation. These compounds are known to be moderately to well biodegradable under steady-state oxic conditions with long hydraulic retention times (Burke et al., 2018; Hellauer et al., 2018a; Hellauer et al., 2018b; Müller et al., 2017; Reemtsma et al., 2010). The major attenuation of those compounds occurred in the infiltration trench during a hydraulic retention time of 30 minutes, where partially oxic conditions prevailed. The compounds benzotriazole and diclofenac have been reported to be very redox sensitive compounds favoring oxic conditions for improved biotransformation, which might have eventually terminated after oxygen

was consumed in the infiltration trench (Hellauer et al., 2018a; Hellauer et al., 2018b; Müller et al., 2017). After commissioning of the *in-situ* oxygen delivery device, a significant improvement of removal of these redox sensitive compounds (including gabapentin) can be expected (Müller et al., 2017).

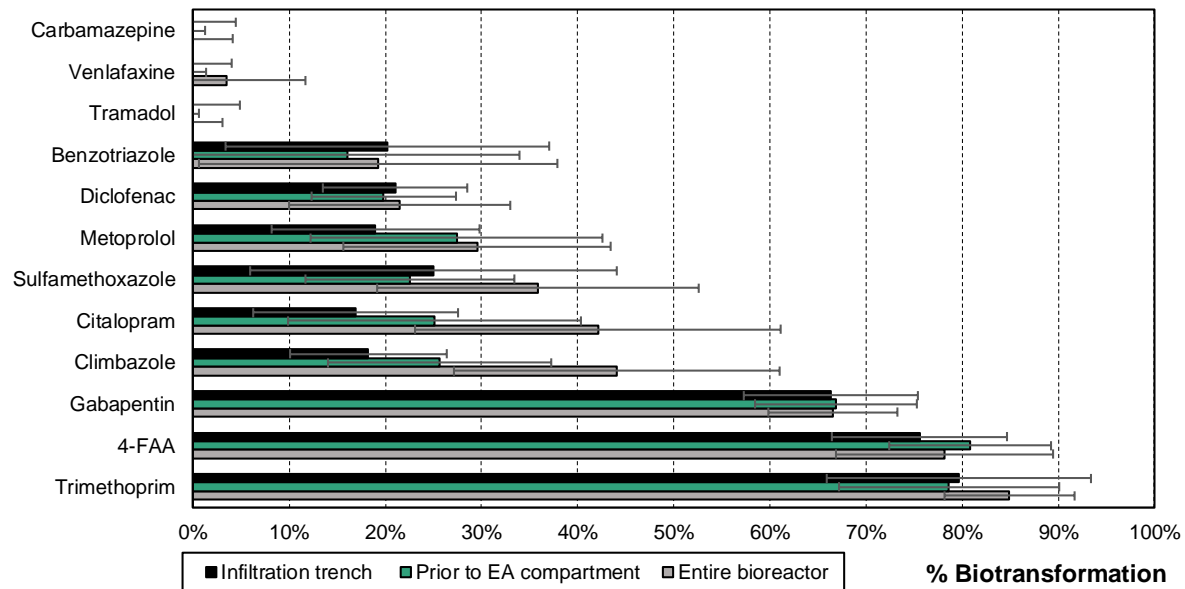


Figure 5-7: Cumulative TOrCs biotransformation, calculated by the TOrC concentrations of the samples taken from the infiltration trench, prior to the EA compartment, and bioreactor effluent normalized to corresponding feed water concentrations (C_0). Mean C_0 [ng/L]: trimethoprim 48 ± 24 , 4-FAA 479 ± 176 , gabapentin 1397 ± 414 , climbazole 166 ± 70 , citalopram 180 ± 43 , sulfamethoxazole 260 ± 190 , metoprolol 286 ± 35 , diclofenac 1052 ± 97 , benzotriazole 5921 ± 1485 , tramadol 198 ± 19 , venlafaxine 409 ± 36 , carbamazepine 459 ± 60 , $n=8-9$.

Metoprolol, sulfamethoxazole, citalopram, and climbazole were further degraded after the infiltration trench under suboxic/anoxic conditions. Citalopram was better biodegraded in sequentially operated biofilters with prolonged HRTs up to more than 70 % during the longest HRT of 2,000 minutes despite of depleted DO (Hermes et al., 2019). Suarez et al. (2010) also observed moderate, non-redox-specific removal of citalopram under aerobic and anoxic conditions in two lab-scale conventional activated sludge reactors. Climbazole and metoprolol were transformed in lab-scale column systems operated by Hellauer et al. (2018b) within the first infiltration step even under anoxic conditions but at long HRTs of 4.2 days. At the full-scale SAT system investigated by Muntau et al. (2017), a similar removal of more than 75% for climbazole has been noted after 1 day of HRT. For the sequential biofilters operated by Müller et al. (2017) climbazole was better attenuated under oxic conditions and transformation improved similar to citalopram under longer HRTs (Hermes et al., 2019). For sulfamethoxazole, various removal performances of poor to moderate removal during MAR were reported (Grünheid et al., 2005). Sulfamethoxazole and trimethoprim biotransformation in a slow sand filter fed with WWTP effluent was found to be even independent of oxygen and easily degradable acetate concentration (Zhang et al., 2019). However, other studies demonstrated that removals of sulfamethoxazole and trimethoprim are still enhanced under oxic conditions compared

to suboxic or anoxic environments (Regnery et al., 2015b; Regnery et al., 2016; Wiese et al., 2011). After the commissioning of the *in-situ* oxygen delivery device, steady-state oxic redox conditions will be provided behind the EA compartment. This will presumably result in more reliable removal compared to rather slow anoxic degradation of poorly or moderately transformed TOrCs.

5.4. Conclusions

The feasibility of the SMART*plus* bioreactor concept coupled with high-rate infiltration trench was tested at pilot scale as a proof of concept. The results from the tracer and head loss determination tests and the validated 3D-groundwater modeling characterized the hydraulics of the SMART*plus* bioreactor during the initial commissioning confirmed successful establishment of plug-flow conditions. Nevertheless, increasing head loss during continuous operation demonstrates that an efficient pretreatment to remove turbidity is necessary to preserve demonstrated plug-flow conditions and minimize the effects of aging due to the varying suspended solids load in the WWTP effluent.

Similar removal of TOrCs as seen in conventional MAR schemes was observed during operation prior to installation of the *in-situ* oxygen delivery system. After commissioning of the EA-compartment, further removal of BDOC and an improved attenuation of TOrCs can be expected, based on results from previous studies. Further investigations on the optimization of oxygen dosing to attune the impacts of varying influent wastewater qualities on the attenuation of chemical and microbial contaminants are underway. This study demonstrated that highly controlled subsurface conditions can be established for enhanced removal of key constituents while simultaneously substantially lowering the physical footprint. These findings suggests that through proper design, construction, performance and maintenance of a system like SMART*plus*, the benefits of MAR systems can be significantly improved.

5.5. Acknowledgements

The project on which this paper is based was funded by the Federal Ministry of Education and Research (BMBF) under funding agreement 02WAV1404A. We thank our collaborators, Veronika Zhiteneva, Hubert Moosrainer, Daniela Schweiger, Joshua Gallegos, Dennis Goessl, Johann Müller, and Anastasia Ruf, for their support regarding soil and hydraulic characterization, bioreactor design, construction, and sampling.

6. Fate and transport of viruses within a high rate plug-flow biofilter designed for non-membrane based indirect potable reuse applications

The following chapter presents investigations related to Hypothesis #3: *Establishing homogenous plug-flow conditions within the SMARTplus bioreactor results in enhanced attenuation of viruses in comparison to conventional slow sand filters, despite shorter hydraulic retention times and coarser grain size.*

The chapter is submitted to Environmental Science & Technology Water:

Karakurt-Fischer, S.; Rien, C.; Sanz-Prat, A.; Szewzyk, R.; Hübner, U.; Drewes, J.E; Selinka, H.C., 2021. Fate and transport of viruses within a high rate plug-flow biofilter designed for non-membrane based indirect potable reuse applications. *Environmental Science & Technology Water* (under review).

Author contributions: Sema Karakurt-Fischer, Hans-Christoph Selinka, Uwe Hübner and Jörg E. Drewes conceptualized the research objective. Sema Karakurt-Fisher designed the experiment and constructed the experimental set-up. Sema Karakurt-Fisher, Christian Rien and Hans-Christoph Selinka conducted the experiments and the analyses. Sema Karakurt-Fisher wrote the paper. Alicia Sanz-Prat simulated the conservative tracer transport. Hans-Christoph Selinka, Uwe Hübner, Jörg E. Drewes, Christian Rien, Alicia Sanz-Prat, and Regine Szewzyk critically reviewed the manuscript. All authors approved the final version of the manuscript.

Abstract

Numerous chronic health effects might be caused by the presence of chemical constituents in reclaimed water, however, an acute risk for water-borne diseases is mostly associated with pathogens. For potable reuse applications, the greatest risk among pathogens is posed by viruses due to their small size and low infectious dose. An advanced water treatment train not utilizing high-pressure membranes, but employing the novel SMART*plus* biofilter with highly controlled plug-flow and redox conditions, was proposed and tested during a 3D-pilot-scale study as a barrier against viruses. Spiking tests with bacteriophages (MS2 and ϕ X174) and murine norovirus-1, accompanied by the conservative tracer, primidone, were conducted to study their transport and maximal reduction under controlled hydraulic conditions. While maintaining plug-flow conditions, mean log reduction values (LRVs) of 5.1, 5.0 and 3.5 were achieved for MS2, ϕ X174, and murine norovirus-1, respectively. Given the short hydraulic retention time of 12.6 hours and a travel distance of 6 m, the demonstrated LRVs in the pilot-scale SMART*plus* bioreactor were significantly higher than conventional slow sand filters. This SMART*plus* based advanced water treatment train, employing post UV-disinfection followed by subsequent groundwater recharge as environmental buffer, would comply with the performance targets for potable water reuse defined by WHO.

6.1. Introduction

Planned water reuse schemes operated following risk based management principles can provide a potable water supply from alternative and impaired sources by decreasing wastewater-borne microbial and chemical constituents present to safe levels (Asano et al., 2007; Karakurt et al., 2019; Rice and Westerhoff, 2015; Zimmerman et al., 2008). Enteric pathogens, like viruses (e.g., adenoviruses, noroviruses), protozoa (e.g., Giardia, Cryptosporidium), bacteria (e.g. Campylobacter), and helminths (e.g., Ascaris) are one of the main concerns of potable reuse, since major water borne diseases originate mostly from pathogens rather than from chemical constituents (WHO, 2017). Of these pathogens, human viruses represent the highest risk for public health due to their small size, low infectious dose – high infectivity, and monitoring challenges (Drewes and Khan, 2011; Symonds et al., 2009). While various regulations and guidelines require 9.5 to 12 LRVs for enteric viruses over the span of raw sewage to safe drinking water, secondary treatment might only provide 0.5-2 LRVs (Asano et al., 2007; NRMCC-EPHC-NHMRC, 2008; USEPA, 2017; WHO, 2017). These treatment goals for potable reuse schemes can be achieved by combining reliable and redundant treatment processes (e.g., disinfection, membrane filtration and biofiltration), referred to as multi-barrier approach (Drewes and Khan, 2011). The LRVs achieved by individual unit operations are cumulated to assess compliance of a potable reuse scheme with health-based treatment targets.

While direct potable reuse (DPR) applications directly feed advanced treated water into a drinking water treatment plant or distribution system, in indirect potable reuse (IPR), the effluent is introduced

into an environmental buffer through either managed aquifer recharge (MAR) or surface water augmentation into a stream or a reservoir for subsequent treatment and storage (Drewes and Khan, 2011; National Research Council, 2012). A great benefit of MAR systems is the combination of biological, chemical and physical removal mechanisms occurring in the subsurface, resulting in the adsorption and/or die-off of pathogens and attenuation of a wide range of trace organic chemicals (TOrcs) (Regnery et al., 2017; Sharma and Amy, 2011). Since the treatment efficiency of MAR systems is controlled by the synergy of site-specific soil characteristics and operational parameters (Regnery et al., 2017; Schijven et al., 2017), their removal capacity to date has not been as specifically defined as for above ground water treatment processes.

Building upon the experiences from MAR systems, sequential managed aquifer recharge technology (SMART) was developed as an advanced treatment process, to enhance TOrc removal in particular, but also foster pathogen attenuation from impaired water sources. Key elements responsible for enhanced TOrc biodegradation during SMART are the prevalence of stable oxic and oligotrophic conditions, achieved by employing induced bank filtration followed by surface spreading with an intermediate aeration step (Regnery et al., 2016). Although this technology has successfully been applied at field-scale in the USA and Germany (Hellauer et al., 2018a; Regnery et al., 2016), its application might be hindered by the need of favorable subsurface conditions as well as space requirements. A high degree of heterogeneity can adversely affect the establishment of homogenous and controlled redox zonation in the subsurface as well as diminish plug-flow conditions, which are essential for improved TOrc and especially virus removal.

As an alternative to the SMART system, the SMART $plus$ technology can be deployed independently of local hydrogeological conditions with a significantly reduced physical footprint (Karakurt-Fischer et al., 2020b). In the SMART $plus$ bioreactor, the high-rate infiltration trench technology is combined with a horizontal biofilter filled with highly uniform porous media with a larger effective size ($d_{10} = 0.75$ mm) than typical slow sand filters ($d_{10} = 0.15-0.45$ mm), which results in rapid deep-bed filtration (effective flow velocity of 0.58 m/h) under controlled plug-flow conditions (Karakurt-Fischer et al., 2020b). To adjust redox conditions, oxygen can be delivered *in-situ* into the saturated porous media by gas-liquid membrane contactors, avoiding additional pumping and maintaining controlled hydraulics without any flow disturbances (Karakurt-Fischer et al., 2020a). While the desired flow and redox conditions as well as high biological activity have been successfully established and their effects on the TOrc attenuation was studied, to date virus log reduction performance of the novel pilot-scale SMART $plus$ bioreactor has not been assessed.

The large number of different viruses present, their varying abundances, and the need for sensitive analytical methods make it impossible to assess LRVs for each individual virus (USEPA, 2017; WHO, 2017). Therefore, so-called surrogate viruses have been chosen, which are more abundant and resistant to treatment in comparison to indicator viruses (Nieminski et al., 2000). F+ specific

bacteriophages (F+ phages, e.g. MS2) and somatic coliphages (e.g. ϕ X174 bacteriophages) are found to be well-suited surrogates to study the fate of viruses in natural or technical filtration systems (Asano et al., 2007; Nieminski et al., 2000; Regnery et al., 2017). Bacteriophages MS2 and ϕ X174 possess similar shape, charge and size properties as enteric viruses, and can be found at higher abundances in raw sewage than enteric viral pathogens (Frohnert et al., 2014). Due to its genetic similarity and environmental persistency, murine norovirus-1 (MNV-1) is also a suitable surrogate for human norovirus (Bae and Schwab, 2008; Betancourt et al., 2019). Performance assessment of a unit treatment process should ideally be evaluated via reduction considering indigenous virus concentrations and spiking tests. Spiking high concentrations of surrogate viruses into the influent of a unit treatment process allows to assess the maximum log reduction capability of the treatment at exceptionally high loads (USEPA, 2012). Moreover, spiking tests with surrogate viruses become more important for risk assessment, since larger log reductions can be demonstrated compared to measurement of commonly low abundances of indigenous viruses. However, operational conditions need to be carefully controlled by online monitoring to ensure the validity of the experimental results from the spiking tests.

Due to the strictly controlled hydraulics, we hypothesize that establishing homogenous plug-flow and prevailing oxic conditions within the SMART*plus* bioreactor results in enhanced attenuation of viruses in comparison to conventional slow sand filters, despite short hydraulic retention times and coarser grain size. In this paper, the efficiency of virus attenuation within the pilot-scale 3D-SMART*plus* bioreactor was tested at baseline operation, without establishing the *in-situ* oxygen delivery yet. The focus was set on presenting results of indigenous virus log reductions as well as transport and attenuation behavior of surrogate viruses MS2, ϕ X174, and MNV-1 via spiking tests, accompanied by a novel conservative chemical tracer, primidone.

6.2. Materials and methods

6.2.1. Experimental setup of the SMARTplus based advanced water treatment train

The treatment steps of the SMART*plus* based advanced water treatment train are depicted in Figure 6-1. Secondary treated municipal wastewater from the wastewater treatment plant (WWTP) Garching (capacity of 31,000 population equivalent) was used as feed water. Tertiary treatment using a rapid dual-media filter (RDMF), composed of sand and anthracite layers, was employed for additional suspended solid removal (for more details see Karakurt-Fischer et al. (2020b)). The tertiary effluent was stored in three buffer tanks with a total volume of 2.7 m³ (0.9 m³ each) and was continuously fed to the SMART*plus* bioreactor at a flow rate of 0.3 m³/h. Further post-treatment steps (i.e., GAC filtration and UV disinfection) were not tested at pilot-scale. The effluent of the advanced water treatment train is intended to augment a groundwater aquifer via vadose zone

infiltration wells for subsequent treatment and storage in excess of 120 days to achieve a minimum of 4 LRVs prior to abstraction (Figure 6-1).

The SMART $plus$ bioreactor was established as a stainless steel 3D-flume in a trapezoidal form with dimensions of 6 m in length, 0.85 m in width, and 1.4 m in height (Figure 6-2). A rectangular shaft (0.35 m long x 0.85 m wide x 1.5 m high) placed on top of the flume at the inflow side mimicked the infiltration trench. Tertiary effluent was fed into the SMART $plus$ bioreactor via the infiltration trench through a horizontal, screened PVC pipe (d=50 mm), providing uniform distribution of the tertiary effluent across the width of the trench. The infiltration trench was filled with very fine gravel for rapid vertical infiltration of feed water. The compartments before and after the electron acceptor (EA), where oxygen can be delivered *in-situ*, were filled with technical sand with a uniformity coefficient of 1.3 to maintain desired plug-flow conditions, essential for enhanced virus attenuation during subsequent travel through the saturated zone. During the spiking tests performed prior to installing the *in-situ* delivery system, the EA compartment was filled with very fine gravel from a tertiary sand filter (WWTP Gut Marienhof, Munich), to facilitate biofilm growth in the system. The outflow compartment was also filled with very fine gravel to allow high drainage rates.

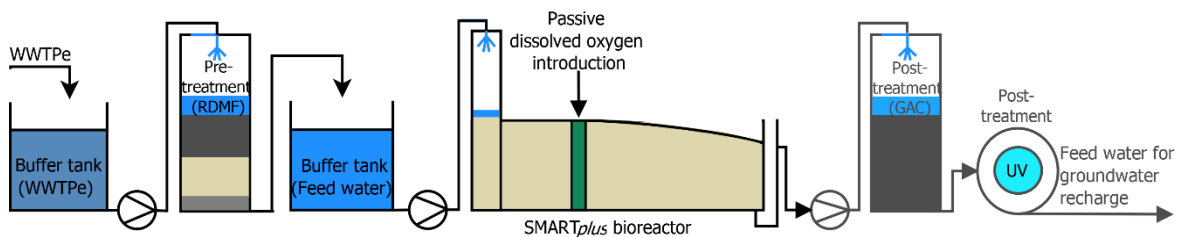


Figure 6-1: Schematic flow diagram of the SMART $plus$ based advanced water treatment train for IPR (adapted from Karakurt-Fischer et al., 2020a). The post treatments, GAC filtration and UV disinfection, were not tested at pilot-scale.

Dissolved oxygen sensors (DO, DP-PSt6, PreSens GmbH, Germany), as well as conductivity, temperature and depth (CTD) sensors (CTD10 3 in 1, Decagon Devices, USA) were deployed in 6 PVC monitoring wells (MWs) along the bioreactor, logging data at an interval of 10 minutes. The sensors were positioned in the MWs 10 cm above the bottom of the flume (SI-Figure 9-7). After the first spiking test, hydraulic optimizations were conducted to eliminate preferential flow path indications, which were mainly attributed to the complete perforation of MW #1 and dead volumes in other MWs (SI-Figure 9-7). Consequently, before the second spiking test, the MW #1 was replaced by a partially perforated well and packers were installed at a height of 35 cm in all MWs as a physical barrier between the perforated section and the rest of the MW (SI-Figure 9-7). With the help of these technical measures, the flow conditions in the SMART $plus$ bioreactor improved significantly. For more detailed information on the design and hydraulic characterization of the SMART $plus$ bioreactor including the information on all online sensors and sampling ports please refer to Karakurt-Fischer et al. (2020b).

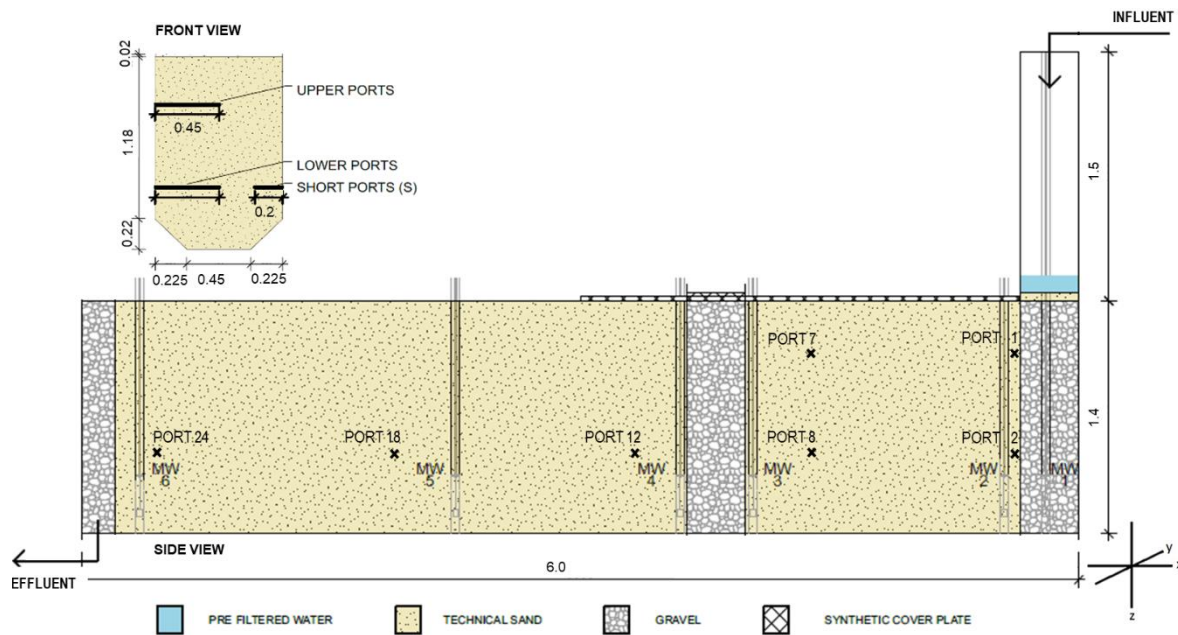


Figure 6-2: The front and side views of the SMARTplus bioreactor, the utilized porous media, gravel ($d_{10}=2.1$ mm or 3.4 mm) or sand ($d_{10}=0.75$ mm), as well as the locations of the monitoring wells (MWs) and the utilized sampling ports (adapted from Karakurt-Fischer et al. (2020b)). The scale is given in meters.

6.2.2. Routine monitoring of SMARTplus bioreactor

To monitor water quality parameters in the SMARTplus bioreactor, 250 mL of water samples for dissolved organic carbon (DOC), nitrate (NO_3^- -N), UV absorbance at 254 nm (UVA_{254}), turbidity and pH measurements were taken weekly or bi-weekly from the feed water (0 m at x direction), the sampling ports in the infiltration trench (0.4 m, port 2), before (1.64 m, port 8) and after (2.64 m, port 12) the EA compartment, and from the effluent (5.85 m) of the bioreactor.

6.2.3. Monitoring of virus concentrations indigenous to wastewater

Three sampling campaigns were conducted in January, April, and September 2018 to investigate the abundances of indigenous viruses, namely human adenoviruses (HuAdV) and human noroviruses (HuNV), as well as stool-associated somatic coliphages and F^+ phages in the raw sewage and secondary effluent of the WWTP and the SMARTplus bioreactor.

HuAdV were selected as indicator viruses as they can be found in sewage all year round, are natural viral pathogens and have been suggested as potential indicator for fecal contamination of waters (Hartmann et al., 2013). HuAdV are double strand DNA viruses with sizes of 70 to 90 nm and characteristic fibers connected to the penton capsomers. As a further indicator virus, HuNV of the genogroup II (GGII) were selected due to their high concentrations in raw sewage and high infectivity as well as high relevance for risk assessments. Monitoring of human viruses was performed with 5 ml samples from WWTP influent to 10 L from the SMARTplus pilot plant.

6.2.4. Spiking tests

Two spiking tests with surrogate viruses and a conservative chemical tracer, were performed in September 2017 and April 2018 to determine the transport and fate of the surrogate viruses in comparison to conservative solute transport within the SMART*plus* bioreactor. The second test was conducted not only to validate the experimental results of the first spiking test, but also to assess the effects of hydraulic optimizations (SI-Figure 9-7) on the transport of surrogate viruses. Moreover, the sampling duration in 2018 was prolonged to assess the tailing effects subsequent to the spiking period.

6.2.4.1. Selection of the conservative tracer and surrogate viruses

Instead of frequently used inorganic tracers (e.g., KBr, KCl, NaCl), the anti-depressant drug primidone was chosen as a novel conservative tracer, since it is known to be persistent and mobile in biological treatment systems (Bertelkamp et al., 2014; Müller et al., 2017; Regnery et al., 2017). It can be analyzed at low concentrations through LC-MS/MS and does not interfere with phage analyses.

The following bacteriophages, with a capsid diameter of about 25 nm, were spiked as surrogates for enteric viruses during both spiking tests: single stranded (ss) RNA(+) phage MS2 from the *Leviviridae* family with an isoelectric point of 3.9 and ssDNA phage ϕ X174 from the *Microviridae* family with spike proteins rising 3 nm from the surface of the capsid and an isoelectric point of 6.6 (Michen and Graule, 2010). During the second spiking test, the MNV-1, with an icosahedral capsid of 28-35 nm and an isoelectric point of 4.7 (Esseili et al., 2015), was additionally spiked as a non-pathogenic surrogate for human noroviruses due to its genetic similarities and persistency.

Due to large amounts required during the spiking tests, both bacteriophages were grown in 1 L liquid cultures. After 4.5 hours, phage lysates were purified and collected until stock solutions (10 mL) with 10^{12} - 10^{13} phages were obtained, allowing permanent spiking of phages into the tertiary effluent over a time span of 24 h. MNV-1 isolate S99 (Müller et al., 2007) was propagated on RAW 264.7 monolayer cells (ATCC TIB-71). After cytopathic effects (CPE; 48h), 0,1 ml of supernatant was transferred to flasks with fresh monolayer cells and culture supernatants were saved after CPE until a stock solution of about 5×10^{12} plaque-forming units (pfu) of these viruses were obtained for the spiking tests. For the spiking tests, high-titered stock solutions were prepared to allow application of small volumes of test viruses to large volumes of wastewater required due to the pilot-scale dimensions of the SMART*plus* bioreactor and the high operational flow rates.

6.2.4.2. Design and implementation of the spiking tests

In both tests, time-variant, pulse injections of spiking solutions occurred over 24 hours, at an inflow rate of $0.3 \text{ m}^3/\text{h}$ composed of a mixture of primidone, ϕ X174 and MS2 (mean concentrations in 2017:

1.0 µg/L, $4.90 \cdot 10^7$ pfu/L and $1.36 \cdot 10^8$ pfu/L, and in 2018: 1.1 µg/L, $9.88 \cdot 10^7$ pfu/L and $6.08 \cdot 10^8$ pfu/L, respectively). The slightly different concentrations at the influent were possibly caused by the variable dissolution of primidone and the phages into the stock solutions, which were separately prepared as 8 individual batches (0.9 m³ each and 7.2 m³ in total) due to the long dosing duration. In 2018, MNV-1 was additionally spiked during the first three hours of the dosing (first batch) at a concentration of $6.50 \cdot 10^8$ genome copies/L, since MNV-1 stock solutions prepared by cell-cultures were more limited than phage stocks.

6.2.4.3. *Monitoring and sample collection*

In 2017, the transport of the spiking solution was monitored for 24 hours as long as the duration of the spiking. In total, 89 samples were taken from the batch solutions (influent), selected sampling ports (#1, 2, 7, 8, 11, 12, 18 and 24, see Figure 6-2), and the bioreactor effluent for primidone (50 mL/sample in pre-rinsed glass bottles each) and phages analyses (200 mL/samples in sterile, pre-rinsed plastic bottles each). In 2018, the phages and primidone were also spiked for 24 hours but were monitored for a duration of 78 hours to observe declining concentrations of phages by washing off effects. MNV-1 was spiked during the first 3 hours of the experiment and sampling was carried out for 30 hours. In total, 158 samples for primidone and bacteriophages, as well as 124 samples for MNV-1 were taken from the sampling locations specified above. The sampling intervals for both spiking tests were determined based on pre-tracer tests and sampling intervals were shortened according to the expected peak arrival times (Karakurt-Fischer et al., 2020b).

6.2.4.4. *Modelling of the conservative tracer primidone*

During both virus spiking tests, the saturated groundwater flow and conservative advective-dispersive transport processes in the SMART_{plus} bioreactor were modeled using a 2D numerical model based on MODFLOW and MT3DMS software package (Harbaugh et al., 2017; Zheng, 2010). The model assumed homogeneous soil properties and stationary hydraulic boundary conditions (BC), constant hydraulic head at the inflow (1st type BC), and constant water flow controlled by a general head device at the outflow (3rd type BC). The background concentration of primidone was set at $C_i = 40$ ng/L, according to the measured values from routine monitoring, and the average values measured in the batch tanks were selected as spiking concentration, C_{spike} , in the model. The calibration of hydraulic and transport parameters relied on the visual fitting between experimental data and numerical outcome of hydraulic heads at the CTD sensors, and the breakthrough curves of normalized tracer concentration, $nC^{obs, sim} = (C^{obs, sim} - C_i)/(C_{spike} - C_i)$, at the observation ports. HRTs were estimated from a conservative tracer test conducted in 2018 based on the temporal moment method described by Luo et al. (2006). Results can be found in Karakurt-Fischer et al. (2020b).

6.2.5. Sample analysis

6.2.5.1. Physicochemical parameters

Water samples for nitrate, DOC, UVA₂₅₄, and primidone analyses were taken in pre-rinsed amber glass bottles, filtered immediately with 0.45 µm cellulose acetate membrane filters (VWR International, USA), and stored at -4 °C pending analysis. Samples for DOC analysis were acidified to pH 2 using hydrochloric acid and analyzed by a vario-TOC cube analyzer (Elementar, Germany). The UVA₂₅₄ of the water samples was measured on a DR 6000™ UV-VIS spectrophotometer (Hach Lange, Germany). Nitrate concentrations were measured by cuvette tests LCK 339 and 304 (Hach Lange, Germany) on a DR 6000™ UV-VIS spectrophotometer. Turbidity and pH values were measured daily by a 2100Qis turbidimeter (HACH, USA) and a 202710 pH/ORP meter (JUMO, Sensors, Germany). Primidone samples were processed based on the preparation and analytical method described in Müller et al. (2017) and were analyzed by liquid chromatography coupled with tandem mass spectrometry (LC-MS/MS) with direct injection.

6.2.5.2. Phages and viruses

MS2 (DSM 13767) and φX174 (DSM 4497) bacteriophages were both cultivated in the laboratory and quantified basically according to DIN ISO 10705-1 and DIN ISO 10705-2 by double layer agar methods using the host bacteria *Salmonella Typhimurium* (WG49; NCTC 12484), *E. coli* CN (WG5; ATCC 700078), and *E. coli* K12 Hfr (NCTC 12486), respectively. Plaque assays were performed as described by Frohnert et al. (2015). Plates were incubated at 36 ± 2 °C for 18 ± 2 h. For MS2, plates with 10 to 300 plaques were counted and used for calculation/quantification. Because of their larger plaque sizes, φX174 phages were counted only in the range of 10 to 150 plaques per plate. Detection limits were 1 pfu/mL for 1 mL sample volume and 0.1 pfu/mL for 10 mL volumes.

Large sample volumes from routine monitoring of the indicator viruses were concentrated by filtration through Rexeed-25A columns (AshaiKasei, Japan). Ten liter samples were passed through an ultrafilter and eluted in 100 mL of PBS/0.05 % Tween 80. Without further concentration steps, the detection limit using Rexeed pre-concentration for both viruses were in the range of 20 genomic copies/L (calculated by spike experiments with known concentrations of phages and viruses).

Nucleic acids from water samples and filtrates were extracted by the NucliSENS® method (bioMérieux), as described by Beyer et al. (2020). As quality controls for extraction efficacies, a sample spiked with a defined concentration of purified HuAdV 2 was included for each set of samples subjected to the nucleic acid extraction procedure. HuAdV were subsequently detected by quantitative PCR (qPCR), HuNV and MNV-1 by one-step reverse transcription qPCR (RT-qPCR). In brief, 5 mL samples were mixed with 2 volumes of lysis buffer. After incubation for 10 min, 50 µL magnetic silica dispersion were added, incubated for another 10 min and magnetic silica particles

were washed, thus separated from the liquid by using a magnetic stand. Finally, the silica particles were eluted in 200 µL buffer (pre-warmed 5 min at 60 °C) to release the nucleic acids. Until further use aliquots were frozen at -80 ± 10 °C.

Quantification of HuAdV was performed using the protocol and primer systems described by Hernroth et al. (2002). HuNV GGII were quantified as stated by Höhne and Schreier (2004). Quantification of MNV-1 was performed according to Müller et al. (2007). In all qPCR and RT-qPCR assays 10 µL of undiluted and 1:10 diluted nucleic acid samples were tested. Dilutions of double stranded gblock fragments, corresponding to the amplified virus sequences, were used to generate standard curves in the range from 10^1 to 10^6 copies per well, each in triplicates. Diethylpyrocarbonate (DEPC)-treated, deionized water served as non-template control, while three parallels of $0.5 \cdot 10^3$ copies of the respective PCR standards were used as positive controls. Reagents were mixed and filled up with DEPC water to achieve a total volume of 25 µL per well. Mastermix and templates were pipetted into MicroAmp® Optical 96-Well Reaction Plates (Applied Biosystems), sealed and analyzed in the Applied Biosystems 7500 Real-Time PCR System (ThermoFisher). Amplification efficiencies were in the range of 90–110 %. Results of the three dilution steps were compared to each other to exclude inhibitory effects. If values of the dilution steps gave comparable results, concentrations in samples were calculated from values of all dilutions. If diluted samples gave higher results, only dilutions without obvious inhibitory effects were used for calculations.

6.3. Results and discussion

6.3.1. Feed water and system characterization

Removal of viruses within MAR and technical biofilters highly depends on prevalent water quality and operational conditions. Therefore, feed water quality (DOC, turbidity, pH), redox zonation, and temperature values in the bioreactor were characterized weekly to biweekly starting from two weeks before the spiking tests in 2017 and 2018 (Table 6-1). Due to the continuous operation with real secondary effluent, all parameters fluctuated, representing operational conditions of a regular field-scale system. Overall, better water quality, including lower DOC and NO_3^- -N concentrations and lower turbidity values were measured in the influent and effluent of the SMART $plus$ bioreactor in 2017 compared to 2018. Predominant redox conditions were characterized as oxic (DO concentrations >1 mg/L) along the entire flow path of the bioreactor with a mean effluent DO concentration of 1.4 mg/L.

During the experiments conducted in 2018, including the second spiking test and monitoring of indigenous virus concentrations, high feed water DOC concentrations caused suboxic conditions after the infiltration trench, characterized by DO concentrations below the detection limit of 0.05 mg/L and limited nitrate reduction (<0.5 mg N/L) (see Table 6-1 and Karakurt-Fischer et al.,

2020a). Observed pH values (7.5-7.8) were stable and representative of secondary effluent qualities during both experimental periods.

Table 6-1: Water quality parameters influencing virus removal: mean DOC (n=3-5), NO₃-N (n=3-5), DO concentrations (n=1872-2871) and UVA₂₅₄ (n=3-5), turbidity (n=5-9), pH (n=9) and temperature (n=430) values. The measurements values represent water quality at sampling locations from late August to mid-September 2017 and mid-April to beginning of May 2018. The distances are given in x direction.

		DOC [mg/L]	UVA ₂₅₄ [1/m]	NO ₃ -N [mg/L]	DO [mg/L]	Turb. [NTU]	pH [-]	T [°C]
2017	0 m, Influent	8.8 ± 0.7	12.5 ± 0.7	11.5 ± 1.1	6.5 ± 0.6	0.9 ± 0.4	7.8 ± 0.1	18.4 ± 0.6
	After 0.4 m	-	-	-	3.9 ± 0.8	-	-	18.4 ± 0.6
	After 1.64 m	-	-	-	2.1 ± 0.5	-	-	18.4 ± 0.6
	After 2.64 m	-	-	-	1.8 ± 0.6	-	-	18.4 ± 0.6
	Eff., 5.85 m	6.2 ± 0.6	11.4 ± 0.7	11.4 ± 1.2	1.4 ± 0.5	0.5 ± 0.4	7.8 ± 0.1	18.4 ± 0.6
2018	0 m, Influent	12.4 ± 1.2	13.5 ± 0.8	15.2 ± 0.9	6.7 ± 1.7	1.9 ± 0.6	7.4 ± 0.1	16.5 ± 1.1
	After 0.4 m	10.6 ± 1.5	14.1 ± 1.1	16.1 ± 0.7	0.5 ± 0.9	-	-	16.5 ± 1.1
	After 1.64 m	9.4 ± 1.7	13.0 ± 1.1	16.0 ± 0.8	<0.015	-	-	16.5 ± 1.1
	After 2.64 m	9.9 ± 1.7	12.9 ± 1.0	16.7 ± 1.3	<0.015	-	-	16.5 ± 1.1
	Eff., 5.85 m	9.9 ± 1.0	12.8 ± 0.8	15.8 ± 0.5	<0.015	0.6 ± 0.2	7.5 ± 0.2	16.5 ± 1.1

6.3.2. Effects of hydraulic conditions and water quality on the fate & transport of viruses

6.3.2.1. Reductions in the indigenous virus concentrations

The LRVs for naturally occurring indicator (HuAdV and HuNV) and surrogate (F⁺ phages and somatic coliphages) virus abundances were estimated for the WWTP Garching, the RDMF and the SMART_{plus} bioreactor (see SI-Table 9.6-1). During treatment at the WWTP Garching, the surrogate viruses were reduced by 1.6-1.9 LRVs, while only 1 log reduction was observed for the indicator viruses. RDMF resulted in further reductions of less than 1 log for all tested surrogate and indicator viruses. Significantly higher LRVs were observed for the SMART_{plus} bioreactor, varying between ≥2.2-3 logs for the surrogate and ≥2.5 – 4 for the indicator viruses, with major log reductions in the first 1.64 meters of the bioreactor. However, noting the relatively low number of samples for naturally occurring surrogate (n=3) and indicator viruses (n=2), increased sampling efforts need to be facilitated for a more robust evaluation. Moreover, since the surrogate and indicator viruses have been removed to below the detection limit, the maximum removal capacity of the SMART_{plus} bioreactor can only be demonstrated by additional spiking tests with higher surrogate virus concentrations (see Chapter 6.3.2.2).

Overall, extrapolation of LRVs from laboratory-scale experiments with limited length and controlled conditions to field-scale is not recommended, as different removal behavior can be expected for natural or field-scale technical systems (Pang, 2009). Although the SMART_{plus} bioreactor was

operated with real-time wastewater at pilot-scale using a 3D-flume, a transfer of these LRVs to other biological treatment applications needs to be taken with caution due to not only the limited number of samples and but also the non-linear reduction of viruses along the travel distance and time in field-scale applications (Pang, 2009; Regnery et al., 2017).

6.3.2.2. *Fate and transport of spiked surrogate viruses*

More information on the transport of viruses along the SMART*plus* bioreactor was gained with the help of two high-resolution spiking tests conducted in 2017 and 2018, using high-titered concentrations of surrogate viruses MS2, ϕ X174 and MNV-1. For both spiking tests, transport behavior of primidone complied very well with the conservative flow and mass transfer model, indicating the suitability of primidone as a conservative tracer (Figure 6-3 and Figure 6-4).

While dissolved compounds would travel through all micro- and macro-pores in heterogeneous soils or filter media, viruses usually behave like colloids and preferably move along the macro pores, following preferential flow paths and cracks due to pore size exclusion (Schijven et al., 2017). Such a transport pattern can result in less dispersion, thus earlier arrival and narrower breakthrough of viruses than of conservative tracers (Schijven et al., 2017). In 2017, primidone concentrations in the effluent increased 1.5 hours prior to the simulated primidone concentrations, indicating the occurrence of preferential flow paths, since the behavior of the effluent breakthrough curve depicts the overall response of the SMART*plus* bioreactor. In addition, slightly earlier arrival of MS2 and ϕ X174 phages in comparison to primidone in ports 2 and 7 was observed (Figure 6-3). Lower MS2 LRVs were measured for the effluent (3.1 ± 0.1) in comparison to port 24 (4.9 ± 0.5), although this sampling point is located only 25 cm after port 24. Moreover, MS2 appeared 4 hours earlier in the effluent than primidone. The ϕ X174 phage could also be measured at slightly higher concentrations in the effluent (5.6 ± 0.2 LRVs) than in port 24 (>5.8 LRVs), whereas the arrival time matched that of primidone. These observations confirmed the occurrence of preferential flow paths in the SMART*plus* bioreactor during the spiking test in 2017. Preferential flows, as observed in the pilot scale plant, are most likely also frequent in natural systems and have to be carefully controlled by measurements.

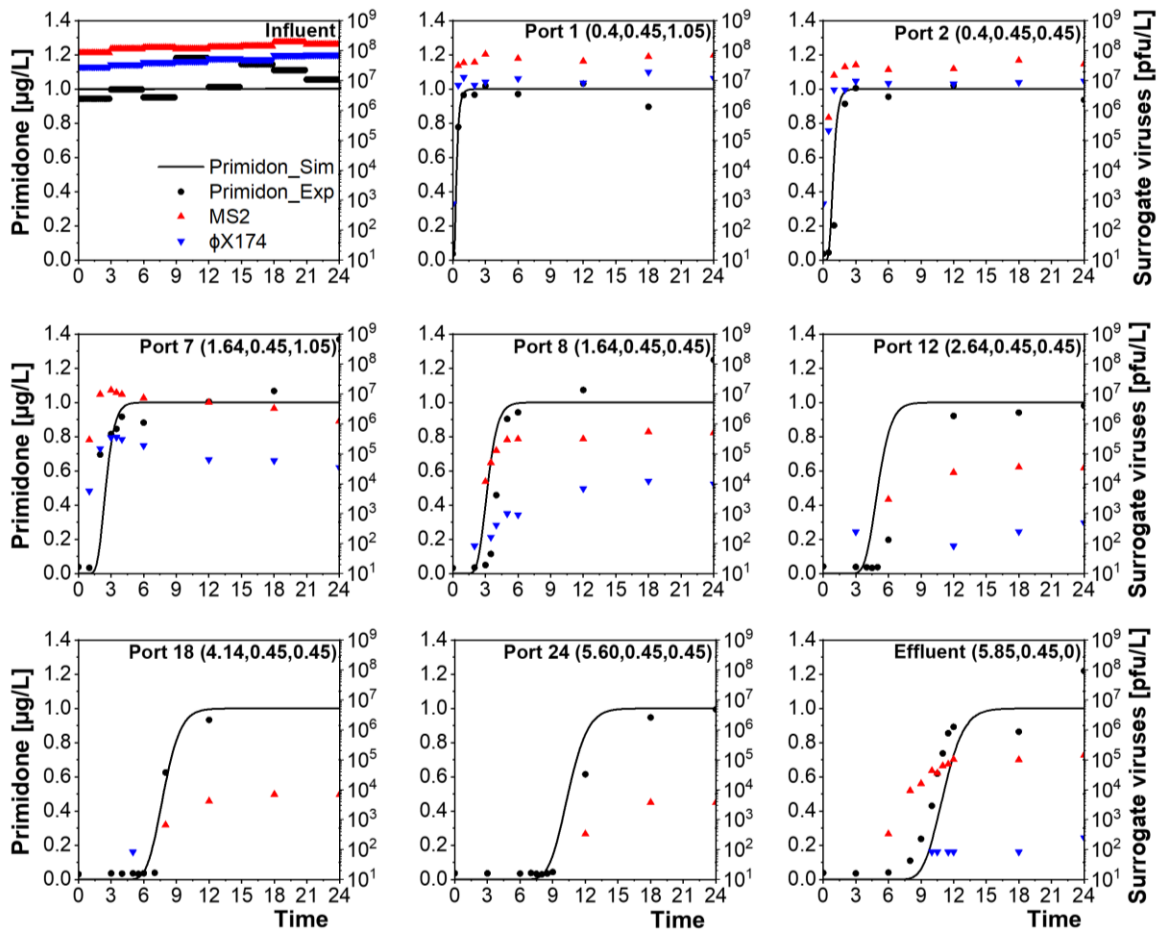


Figure 6-3: Transport of virus surrogates and the conservative tracer primidone in the SMARTplus bioreactor during the spiking test in 2017. The x , y and z coordinates of the sampling ports and the effluent are expressed in meters. 2nd y -axis is given in logarithmic scale.

In 2018, the breakthrough of the conservative tracer at the sampling ports was characterized by a double peak pattern due to the transient influent concentrations (Figure 6-4). The shape of the influent concentration curve could be recognized in all downstream sampling points, with the breakthrough curves of the ports closer to the effluent displaying more dispersion. A mean background concentration of somatic phages (245 pfu/L) was measured in the ϕ X174 phage assay for all sampling ports and effluent during the experiment prior to dosing the spike solution, (see in Figure 6-4, ports 2-24 and effluent). However, these signals were caused by concentrations of ϕ X174-like somatic coliphages indigenous to the wastewater and were not related to an early arrival of the spiked ϕ X174. In 2018, the matching of the experimental and simulated global breakthrough curves for primidone, including the width of the breakthrough curves, the arrival time of the tracer, no pre-peaks, and no pronounced tailing confirmed that the preferential flow paths were of little importance for the overall transport behavior in the SMARTplus bioreactor. In comparison to 2017, the bacteriophages and MNV-1 had a similar transport velocity as primidone without any preliminary breakthrough, underlining the success of the countermeasures to establish conditions very close to plug-flow (Figure 6-4). Consequently, despite favorable operational conditions with higher DOC and

low DO concentrations in 2017, the LRVs from the spiking test in 2018 seem to be more reliable for further assessments for the operation of SMARTplus bioreactor without *in-situ* oxygen delivery.

Longer monitoring during 2018 revealed insights on the virus attenuation after the spike duration for both phages and MNV-1. Prolonged tailing after the spike period indicated that adsorption instead of inactivation dominated the virus retention during the operation without the *in-situ* oxygen delivery, which is also expected due to the high flow velocities, short HRTs and moderate temperatures within the SMARTplus bioreactor. Virus adsorption was also considered to be the most important removal mechanisms in sandy soil passages, while the degree of adsorption was virus type and strain dependent (Goyal and Gerba, 1979). Lower concentrations after the spiking test resulted in changing equilibrium, favoring desorption, which might explain the long tailing effects. Detachment of viruses after changing ambient concentrations was also pointed out by Regnery et al. (2017). Consistent with our results, long tailing effects occurring for more than 5 to 12 days after 48 hours of spiking, were also observed by Hijnen et al. (2004) and Anderson et al. (2009) in spiking tests using pilot-scale slow sand filters.

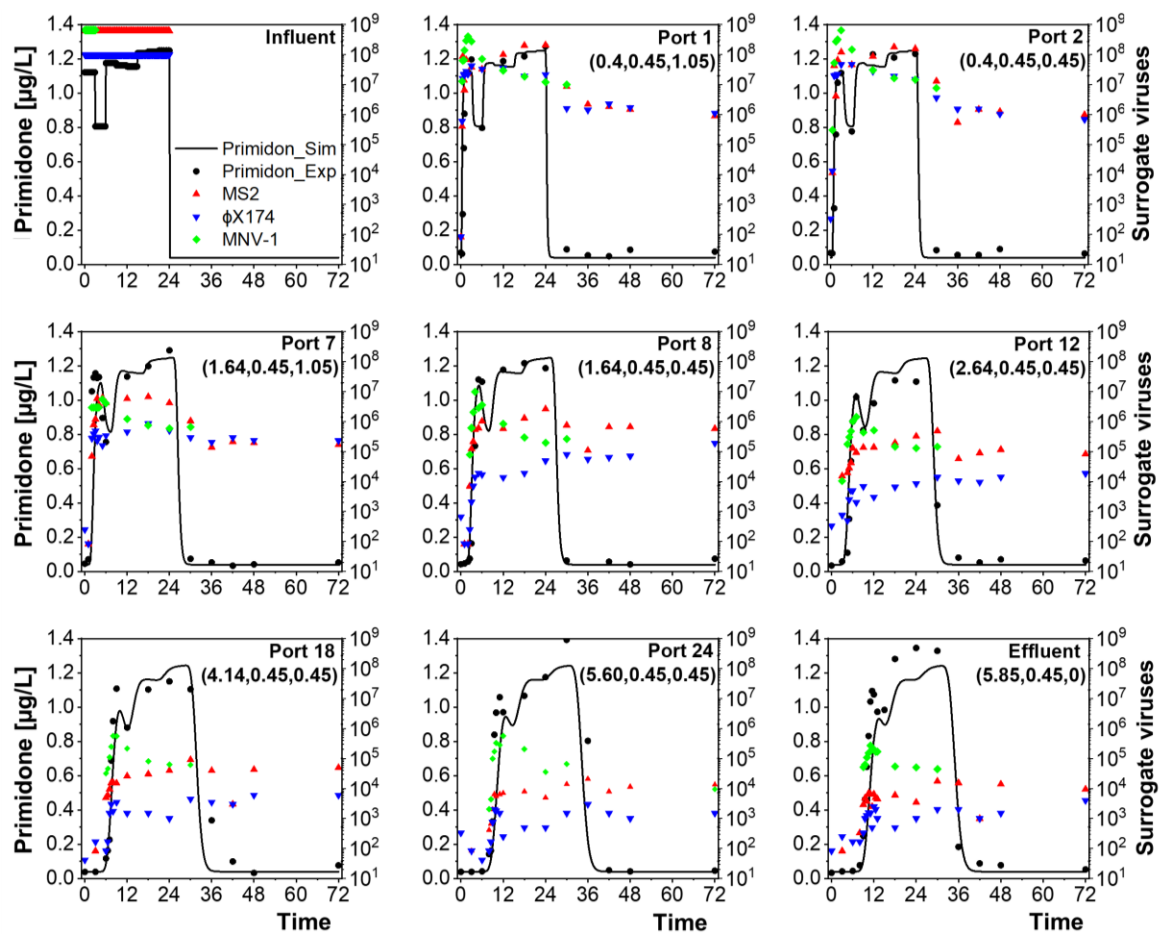


Figure 6-4: Transport of virus surrogates and conservative tracer primidone in the SMARTplus bioreactor during the spiking test in 2018. The x , y and z coordinates of the sampling ports and the effluent on top of the graphs are expressed in meters. 2nd y -axis is given in logarithmic scale. The concentrations of bacteriophages and MNV-1 are given in pfu/L and genome copies/L, respectively.

The LRVs at individual sampling ports during the spiking test in 2018 were calculated from average influent concentrations and concentrations determined at the sampling locations for the time period from estimated mean HRTs of individual sampling locations until the end of dosing. MS2, ϕ X174, and MNV-1 were reduced by 5.1 ± 0.1 , 5.0 ± 0.3 , and 3.5 ± 0.1 LRVs, respectively, within an HRT of less than 13 hours and a travel distance of less than 6 meters under optimized hydraulic conditions in the SMART $plus$ bioreactor (Figure 6-5). Thereby, it should be noted that two different assays were used to detect bacteriophages and MNV-1. While the plaque assays used for bacteriophage monitoring reveal the number of remaining viable surrogate viruses, the real-time RT-PCR used for MNV-1 monitoring reveals remaining genomic gene fragments from both viable and inactivated viruses. Considering that, the MNV-1 removal in porous media is associated with inactivation (Betancourt et al., 2019), the lower LRVs for MNV-1 may be due to additional detection of inactivated viruses by the real-time RT-PCR measurement. In comparison, MS2 and ϕ X174 removal is dominated by adsorption, which likely is the governing removal mechanism in the SMART $plus$ bioreactor. Similar to indigenous indicator and surrogate viruses, the major log reduction occurred within the first 1.64 meters of the bioreactor until port 8 with the highest mean reduction rates of 1.8 ± 0.2 , 2.3 ± 0.1 and 1.4 ± 0.2 \log_{10}/m for MS2, ϕ X174 and MNV-1, respectively (Figure 6-5). In their review, Regnery et al. (2017) also concluded that the removal of microorganisms and viruses was greater within the first meters of the soil passage. The elimination rates for 12.6 hours of HRTs for MS2, ϕ X174 and MNV-1 were calculated as 0.4 ± 0.0 , 0.4 ± 0.0 and 0.3 ± 0.0 \log/h , respectively.

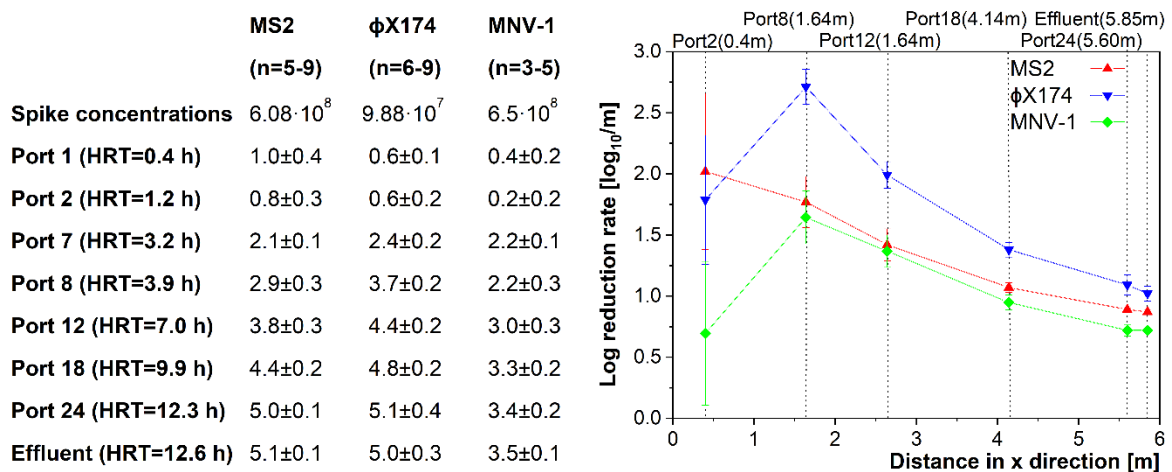


Figure 6-5: Cumulative log reduction values with the HRTs of the sampling locations (left) and log reduction rates [\log_{10}/m] (right) of MS2, ϕ X174 and MNV-1 surrogate viruses along the SMART $plus$ bioreactor flow path during the spiking test in 2018. The exact locations of the sampling ports in x, y and z directions can be found in Figure 6-4. The spike concentrations of bacteriophages and MNV-1 are given in pfu/L and genome copies/L, respectively.

In particular, the LRVs for MS2 in 2018 seem to improve under the prevalence of plug-flow conditions, i.e. due to the elimination of bigger void volumes and partially higher pore water velocities, in comparison to 2017 (Figure 6-3 and Figure 6-4). However, this is not as obvious for the ϕ X174 phages. A significant improvement of MS2 in comparison to ϕ X174 reduction at lower

pore water velocities has also been observed by Syngouna and Chrysikopoulos (2013). Nevertheless, the observed differences in the transport behavior and reduction of the MS2 and ϕ X174 phages in 2017 and 2018 might also be additionally related to other factors influencing the virus-matrix interactions, such as redox conditions as well as dissolved or bound organic matter.

At the experimental pH of 7.5 to 8 (Table 5-1) both bacteriophages are negatively charged and readily repulsed from negatively charged sand surfaces (Schijven and Hassanizadeh, 2000). The lower isoelectric point of MS2 (pI 3.9) in comparison to ϕ X174 (pI 6.6) leads to stronger electrostatic repulsion and less adsorption, which might explain better ϕ X174 removal in 2017. Lower removal of MS2 compared to ϕ X174 has also been observed in field-scale MAR systems with sandy aquifers and column studies (Frohnert et al., 2014; Schijven and Hassanizadeh, 2002; van der Wielen et al., 2008). Other researchers, however, considered hydrophobicity as even more important for the transport behavior of virus (Dika et al., 2015). While the present dissolved organic matter compete for the same adsorption areas as the viruses, bonded organic matter might enhance virus attachment by providing new hydrophobic binding sites (Schijven and Hassanizadeh, 2000). Aging of the bioreactor is expected to increase the content of bounded organic matter in the filter, resulting in a shift from electrostatic to hydrophobic virus-soil interactions (Betancourt et al., 2019; Zhuang and Jin, 2003). This effect would also favor the removal of MS2 phage in 2018 due to its higher hydrophobicity (Dika et al., 2015). In contrast, the competition for adsorption sites by dissolved organic carbon in the feed water, which was higher in 2018, seemed to be of minor importance during our spiking experiments. Similar removal of ϕ X174 in 2017 and 2018 despite the changes in hydraulic conditions and organic matter content indicates that also the prevalence of oxic redox conditions might play a role, although the removal of both phages was mainly attributed to sorption. Eventually, the exact influence and relevance of the discussed factors on the reduction of MS2 and ϕ X174 could not be determined based on the available data from the experiments in 2017 and 2018.

Nevertheless, even the spiking test in 2017 prevails that SMART*plus* bioreactor can achieve high LRVs of 3.1 ± 0.1 and 5.6 LRVs for MS2 and ϕ X174 under suboptimal hydraulic conditions, which might occur also in field-scale applications for a period of time. In comparison, pilot-scale slow sand filters filled with fine sand ($d_{10}=0.21$) operated by Seeger et al. (2016) could achieve a mean LRV of 1 for MS2 under a significantly lower hydraulic loading rate (0.1 m/h). Anderson et al. (2009) observed 0.2 to 2.2 LRVs for MS2 during spiking tests under varying media depth (0.45 to 0.9 meters), hydraulic loading rates (0.1 to 0.4 m/h), water temperatures (3 to 24°C), and a lower grain size ($d_{10}=0.37$ mm) with higher LRVs towards lower loading rates, higher temperatures and media depth. Higher LRVs of 2 and 3 were reported for somatic coliphages compared to MS2 by Seeger et al. (2016) and Bauer et al. (2011), whose experiments were operated under even lower hydraulic loading rates of 0.05 m/h. Consequently, as hypothesized higher mean LRVs were

measured for the SMART*plus* bioreactor in comparison to conventional slow sand filters based on the spiking tests.

Log removal reductions determined by spiking tests demonstrate the robustness of a treatment train to virus peak concentrations in the influent and should be considered as maximal LRVs. The response of treatment steps under high concentrations enables assessments whether the treatment process is capable of mitigating such loads. Determining the dampening capability of a treatment step is essential, since it can also affect the removal capacity and the functionality of the downstream treatment steps substantially, e.g. a UV disinfection step. However, contrary to the naturally occurring viruses in wastewater, viruses used for spiking tests are cultivated under laboratory conditions and are therefore rather uniform in their survival or reduction due to their homogenous charge, size, and shape. Thus, the log reductions from routine monitoring with increased sampling efforts should be included to determine the overall performance of treatment steps. The log reduction performance of the SMART*plus* bioreactor under real-world conditions will likely lay between the reductions observed under ambient conditions and during the spiking test in 2018. If the LRVs will be used for risk assessments (e.g. by QMRA), a probability density function can be generated integrating the LRVs determined from both the routine monitoring and the spiking test.

Since under oxic conditions viral proteins, i.e. the nucleocapside, could be damaged, an increased removal or inactivation of viruses has been observed under oxic conditions (Frohnert et al., 2014; Klitzke et al., 2015; Schijven et al., 2017). However, in particular the spiking test and routine monitoring in 2018 were conducted under rather suboxic conditions. Consequently, during sequential operation with *in-situ* oxygen delivery and under sustained plug-flow conditions, an even more enhanced attenuation and elimination of viruses is expected. Therefore, LRVs from this study can be considered as conservative estimates of SMART*plus* bioreactor performance and *in-situ* decay tests are recommended to assess the full performance under field-scale conditions.

6.3.3. Compliance of the SMARTplus based advanced water treatment train with virus performance targets

Considering an abundance of approximately $2 \cdot 10^4$ noroviruses/L in raw sewage, the WHO Potable Reuse Guidelines recommend that potable reuse treatment trains should achieve 9.5 LRVs, based on a health-based risk approach with an upper burden limit of 10^{-6} disability adjusted life years (DALYs) (WHO, 2017). The compliance of a SMART*plus* bioreactor based IPR treatment train with the aforementioned requirement was assessed for both LRVs, determined by monitoring of reductions in ambient concentrations and the spiking test in 2018 (Figure 6-6). The LRVs were taken from WHO (2017) for the UV disinfection (4 LRVs at 186 mJ/cm²) and from Regnery et al. (2017) for MAR (4 LRVs at 120+ days of HRT). Hereby the MAR, i.e. environmental buffer, can mitigate instationary virus abundances and increases the robustness and the resilience of the SMART*plus*

based IPR treatment scheme. No removal credits were assigned to GAC treatment, as it is not considered a barrier for viruses. Although conservative LRVs for the SMART_{plus} bioreactor were taken due to performance data from the operational period without the *in-situ* oxygen delivery, the observed performance complies with the health-based target defined by WHO.

Such compliance studies should be supported with a quantitative microbial risk assessment approach (QMRA). The outcome of the QMRA is an estimate of relative risk, either a disease burden or an annual risk of infection, which can be compared to the WHO guidelines and/or national regulations. Therefore, a QMRA using Bayesian networks will be conducted to confirm the safety of the effluent water quality of the proposed treatment train.

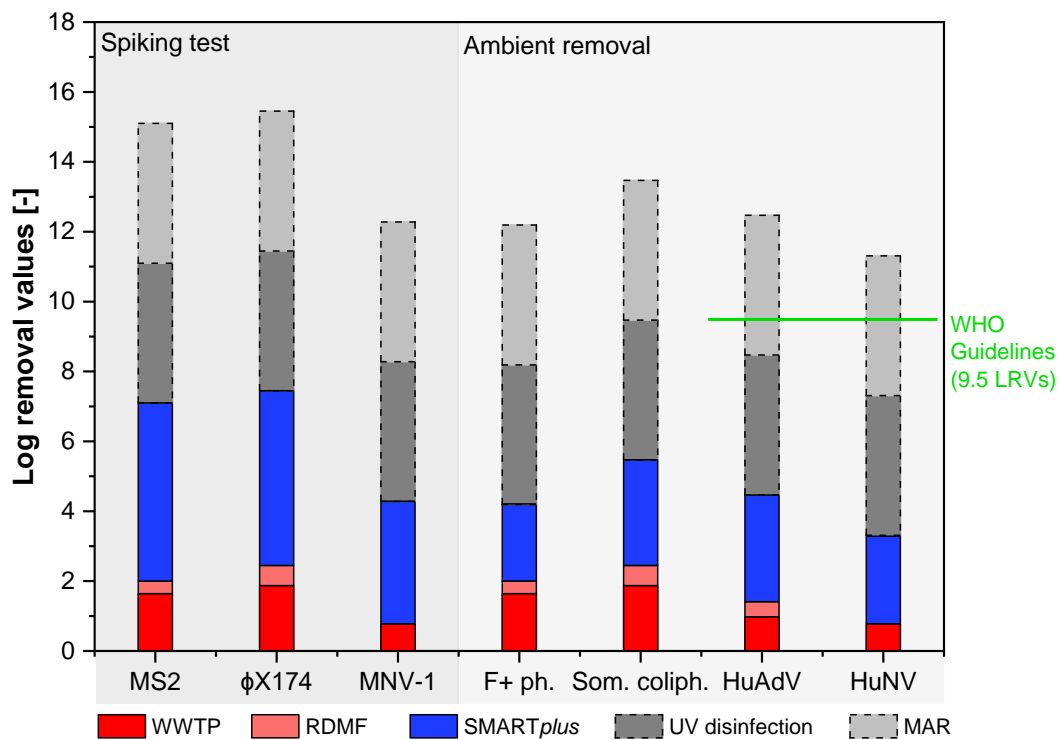


Figure 6-6: Compliance of a SMART_{plus} based advanced water treatment train considering the WHO (9.5 LRVs) virus performance target. Log removal of the surrogate viruses (MS2, φX174 and MNV-1) within the SMART_{plus} bioreactor were measured during the spiking test in 2018, while log removal of surrogate phages (F⁺ phages and somatic coliphages) and indicator viruses (adenovirus and human norovirus) within the WWTP, RDMF and SMART_{plus} were measured during routine monitoring. While mean LRVs were used for the surrogate viruses, conservative lower LRVs were chosen for the indicator viruses. LRVs assigned to WWTP and RDMF for spiked MS2, φX174 and MNV-1 viruses were taken from the routine monitoring data for F⁺ phages, somatic coliphages and human noroviruses, respectively.

6.4. Conclusion

This study investigated the potential of a novel plug-flow bioreactor, SMART_{plus}, for enhanced virus attenuation at pilot-scale during spiking tests using MS2, φX174 and MNV-1 and by monitoring the reduction of naturally occurring concentrations of HuNV, HuAdV, F⁺ phages and somatic coliphages in wastewater. Findings from this pilot-scale application confirmed our hypothesis that

establishing homogenous plug-flow conditions within the SMART*plus* bioreactor can result in significantly enhanced attenuation of viruses in comparison to conventional slow sand filters, despite shorter hydraulic retention times and coarser grain size.

Within a HRT of less than 13 hours and a travel distance of less 6 meters in the SMART*plus* bioreactor, LRVs of 5.1 ± 0.1 , 5.0 ± 0.3 and 3.5 ± 0.1 were determined for MS2, ϕ X174, and MNV-1, respectively during the spiking test in 2018. Moreover, the transport of the surrogate viruses matched the transport of the conservative tracer primidone under optimal hydraulic conditions. An additional reduction in virus concentrations is expected during the operation of an *in-situ* oxygen delivery. Overall, the LRVs for viruses complied with WHO health-based performance targets for an IPR project employing SMART*plus*, UV disinfection, and groundwater recharge with a residence time of 120 days. For field-scale application of the proposed treatment train, the attenuation of protozoa (*Giardia* and *Cryptosporidium*) has also to be surveilled, since their resting stages increase their survival capacity during disinfection processes. However due to their size, they are expected to be attenuated effectively in the SMART*plus* bioreactor and subsequent MAR system. Since the SMART*plus* bioreactor performance highly relies on controlled hydraulics, particular caution should be taken to maintain plug-flow conditions. This requires a feed water quality with no residual suspended solids to minimize their introduction into the filter media.

These findings underscore the microbial safety of non-membrane based treatment trains used for groundwater augmentation, utilizing a cost effective, nature-based, engineered biological-physical treatment system. Such developments reveal a great potential for increasing the number of planned potable reuse schemes.

6.5. Acknowledgements

This study was funded by the Federal Ministry of Education and Research (BMBF) under grant numbers 02WAV1404A and 02WAV1404H. We would like to thank our colleagues and graduate students for their help with the sampling of the SMART*plus* bioreactor and the laboratory analysis: Daniela Schweiger, Anastasia Ruf, Alexandra Kretschmer and Hendrick Treuner. Thank you also to Veronika Zhiteneva for editing supports.

7. Characterizing a novel *in-situ* oxygen delivery device for establishing controlled redox zonation within a high infiltration rate sequential biofilter

The following chapter presents investigations related to Hypothesis #4: *Bubble-free delivery of oxygen into SMARTplus biofilter can be achieved in-situ under laminar flow conditions and short contact times by diffusive transport through gas-liquid membrane contactors* & Hypothesis #5: *Plug-flow conditions, defined and controllable redox zonation in SMARTplus biofilter lead to enhanced TOxCs removal.*

The chapter has been published with editorial changes as follows:

Karakurt-Fischer, S.; Bein, E.; Drewes, J.E; Hübner, U., 2020. Characterizing a novel *in-situ* oxygen introduction device for establishing controlled redox zonation within a high infiltration rate biofilter. *Water Research* 182, 116039.

Author contributions: Sema Karakurt-Fischer, Uwe Hübner and Jörg E. Drewes conceptualized the research objective. Sema Karakurt-Fisher designed the pilot-scale experimental set-up, conducted the experiments and analysis, and wrote the paper. Sema Karakurt-Fisher and Emil Bein constructed the lab-scale experimental setups, conducted the experiments and the data analyses. Uwe Hübner, Jörg E. Drewes and Emil Bein critically reviewed the manuscript. All authors approved the final version of the manuscript.

Abstract

By applying favorable oxic and oligotrophic conditions through subsequent aeration and an additional infiltration step, the sequential managed aquifer recharge technology (SMART) was proven to better remove trace organic chemicals (TOrcs) than conventional MAR systems. To minimize the physical footprint, pumping costs and hydraulic retention times, as well as to overcome limitations of site-specific heterogeneities of such systems, the SMART concept was further upgraded by two main engineered technologies. This SMART*plus* bioreactor is comprised of an infiltration trench and highly homogenous porous media to provide high infiltration rates and plug-flow conditions. Additionally, an *in-situ* oxygen delivery device, in particular a self-designed PDMS gas-liquid membrane contactor, was designed to establish favourable subsurface oxic conditions. This novel SMART*plus* technology was investigated at pilot scale and is designed for advanced water treatment either in the context of water reuse or treatment of impaired surface water. To determine the design specifications and to construct a pilot-scale membrane contactor, the mass transfer coefficients of the PDMS membrane were investigated at lab-scale for varying Reynold numbers (0.2-2). With the help of the customized membrane contactor, homogenous, bubble-free and passive oxygen delivery could be successfully demonstrated at pilot-scale under laminar flow conditions and short contact times. Oxygen concentrations downstream of the membrane contactors met the design specifications (>1 mg/L) as long as the required feed water quality was provided. However, high NH_4^+ concentrations in the secondary effluent resulted in higher and unsteady oxygen demand than the target oxygen transfer rates could meet and suboxic conditions prevailed. Although a 20-50% enhancement in the removal of certain compounds (4-FAA, antipyrine, sulfamethoxazole, and citalopram) was achieved, demonstration of the full potential of enhanced TOrc removal by SMART*plus* was hindered due to unsteady feed water quality.

7.1. Introduction

The United Nations have identified water as “the primary medium through which we will feel the effects of climate change” ([UN-Water, 2020](#)). To increase water availability and improve surface water quality, the importance of innovations in advanced water treatment technologies has risen. Combinations of advanced oxidation, adsorption and membrane filtration processes have proven to effectively remove chemical and microbial contaminants from WWTP effluents (Eggen et al., 2014; Rizzo et al., 2020). However, the potential of low-energy, nature-based attenuation processes that do not produce residues or require the addition of chemicals have not been extensively studied for advanced water treatment. Many studies have focused on the attenuation of trace organic chemicals (TOrcs) in natural treatment systems such as bank filtration or managed aquifer recharge (MAR) applications (Grünheid et al., 2005; Hamann et al., 2016; Hoppe-Jones et al., 2010; Hoppe-Jones et al., 2012; Onesios et al., 2009; Onesios and Bouwer, 2012). Enhanced biotransformation of some TOrcs was found to be dependent on the composition and the concentration range of the primary

substrate due to co-metabolism (Li et al., 2012; Li et al., 2013; Li et al., 2014; Rauch-Williams et al., 2010). The prevalence of stable oxic conditions (dissolved oxygen concentrations > 1 mg/L) was identified as the key factor for the biotransformation of many TOrCs (Hellauer et al., 2018b; Regnery et al., 2015a; Schmidt et al., 2017).

Based on those findings, a sequential managed aquifer recharge technology (SMART) for enhanced TOrC removal from impaired water sources was developed. The SMART concept improved the removal performance of conventional MAR techniques, where water is infiltrated into the subsurface, through three distinct steps. First, infiltrated water is extracted from the subsurface, after which it is aerated *ex-situ*, and then subsequently re-infiltrated under favorable oxic and oligotrophic conditions (Regnery et al., 2016). However, some limitations, such as the unpredictable effluent water quality due to subsurface heterogeneity (Regnery et al., 2017), clogging problems associated with Fe⁻ and Mn⁻ precipitation, high physical footprint due to the usage of two infiltration units, increased costs caused by additional pumping, and secondary contamination in the open infiltration basins have hindered the broad application and the technology transfer of conventional MAR and SMART systems.

Consequently, the SMART*plus* concept, combining all three aforementioned steps into one bioreactor, was developed, which is designed as an advanced water treatment technology for IPR applications. The SMART*plus* bioreactor, in comparison to conventional MAR systems, has a smaller physical footprint, reduced operational costs, and avoids disturbances in the flow conditions. The controlled hydraulic conditions within the SMART*plus* bioreactor was successfully established by combining high rate infiltration trench technology and a horizontal biofiltration system, filled with highly uniform porous media (Karakurt-Fischer et al., 2020b). Compared to conventional bank filtration systems with a minimum HRT requirement of 50 days, SMART*plus* demonstrated similar TOrC removals with an HRT of <13 hours during baseline operation, i.e. without intermediate aeration (Karakurt-Fischer et al., 2020b).

To enhance TOrC biotransformation, SMART*plus* is designed to achieve oxic redox conditions via *in-situ* dissolved oxygen (DO) delivery into the porous media of the bioreactor. Due to fluctuations in the feed water quality of the SMART*plus* bioreactor during continuous operation with tertiary effluent, an adjustable oxygen delivery device is essential to achieve steady-state TOrC transformation. For this purpose, approaches from groundwater bioremediation or membrane aerated bioreactors (MABR) were initially considered. Previous studies have used active or passive oxygen delivery methods to facilitate microbial degradation of organic contaminants in water, as biodegradation is the main removal mechanism for TOrCs (Barcelona and Xie, 2001; Casey et al., 1999; Haugen et al., 2002; Syron and Casey, 2008; Wilson and Mackay, 2002). However, active gas sparging into porous media would result in decreased hydraulic conductivity and air binding, as the gas would be trapped in otherwise saturated media. The other active method, direct injection of liquid

through needles, displaces the contaminated water, resulting in non-uniform oxygen introduction (Fry et al., 1997; Wilson and Mackay, 2002).

Passive delivery of electron acceptors, via different types of gas-liquid membrane contactors or oxygen releasing compounds (ORCs), such as CaO_2 or MgO_2 , may allow uniform distribution and provide bubble-less, steady sources of oxygen over the long term (Ahmed et al., 2004; Barcelona and Xie, 2001; Fang et al., 2002; Li et al., 2010). To avoid immediate dissolution of the compound, ORCs are impregnated with high-pH cement, which also affects the activities of microorganisms due to the pH increase of the water (Obiri-Nyarko et al., 2014). Furthermore, as the dissolution rate of oxygen is not synchronized with the demand, bubble formation can still take place due to the passive nature of ORCs.

A gas-liquid membrane contactor is a system which provides a well-defined and tailored interface for diffusive transfer without direct mixing or dispensing of one phase into another (Gabelman and Hwang, 1999). For this reason, controllable gas-liquid membrane contactors were deemed promising for the SMART*plus* bioreactor. Since the SMART*plus* bioreactor flow characteristics, reactor configuration, packed porous media and bubble-less oxygen transfer requirement are different from soil passages in groundwater remediation and MABR, this study focused on the feasibility of gas-liquid membrane contactors for reliable delivery of electron acceptors into the tertiary effluent under laminar flow conditions and short contact times.

Bubble-less gas delivery can be achieved via dense or microporous gas permeable membranes. The pores of microporous membranes act as the contact area between the gas and liquid phases, whereas in dense membranes the gas is absorbed into the membrane, facilitating diffusive gas transfer from one bulk phase to another through the membrane (Al-saffar et al., 1997; Côté et al., 1988). On one hand, to avoid gas bubble formation on the surface of microporous membranes, the gas pressure should be lower than the bubble point of the membrane, which depends on the pore size, surface tension of the liquid, hydrophobicity and the resulting contact angle of the liquid at the membrane (Bazhenov et al., 2018). Due to non-uniform pore sizes, gas bubbles might still appear under very low gas pressures in the ranges of 0.1.-0.2 bar, although the theoretical bubble point, calculated by nominal pore size, is not reached (Ahmed and Semmens, 1992). A high gas pressure can be only applied if the liquid side is also uniformly pressurized, so that the transmembrane pressure does not exceed the bubble point at any point of the membrane. On the other hand, to avoid membrane pore wetting, the liquid side pressure should be less than the breakthrough pressure (Al-saffar et al., 1997). However, pore wetting may still take place in porous membranes over time during continuous operation regardless of hydrophobicity, which causes high mass transfer resistances and fouling (Al-saffar et al., 1997). Furthermore, in presence of low surfactant concentrations, reduction in surface tension may occur, leading to reduction in liquid breakthrough pressure (Gabelman and Hwang, 1999).

Although microporous membranes may exhibit more favorable mass transfer characteristics, particularly at higher liquid velocities, gas-liquid contactors made from dense membranes provide a better process stability and were considered to be more suitable for the SMART*plus* bioreactor. The total mass transfer coefficient can be expressed by the gas side, the membrane and the liquid side mass transfer coefficients. For both dense and microporous membranes, the gas film resistance can be neglected, if the gas velocity is considered to be much higher than the liquid velocity. In the SMART*plus* bioreactor, the hydraulics are governed by laminar flow conditions, with a liquid velocity of $1.55 \cdot 10^{-4}$ m/s and a rather low Reynolds number (0.5). The liquid film resistance is very sensitive to the hydraulic conditions, decreasing from 78.5% to 45.5% of the total resistance when the Reynolds number increases from 0.6 to 49 (Côté et al., 1989). In addition to liquid film resistance, membrane resistance, which depends on membrane thickness, gas selectivity and diffusivity, and thus permeability, needs to be considered for dense membranes. However, if highly oxygen permeable membranes such as silicone rubber – Polydimethylsiloxane (PDMS) (Charati and Stern, 1998) with a thin membrane wall are applied, the remaining liquid side resistance would still govern the mass transfer under laminar flow conditions (Côté et al., 1989). In addition to their high oxygen permeability, silicone membranes are particularly stable during long-term operation. Another mass transfer resistance to consider is the development of biofilms on the membrane surface, if membranes are delivering oxygen into water in the presence of biodegradable organic substance, such as tertiary effluent (Essila et al., 2000). Although a seemingly negative attribute, the membrane fibers could support biofilm growth and attachment, potentially decreasing bubble formation due to simultaneous oxygen degradation (Essila et al., 2000).

We hypothesize that bubble-free delivery of oxygen into the SMART*plus* bioreactor can be achieved under laminar flow conditions and short contact times by diffusive transport through gas-liquid membrane contactors. This will no longer require an external aeration step and therefore reduce the physical footprint of the SMART concept while improving TO_rC attenuation during continuous operation of the SMART*plus* bioreactor. In this paper, we describe the design and application of a promising passive oxygen delivery system and its effects on the redox zonation and TO_rC attenuation at pilot-scale.

7.2. Materials and methods

7.2.1. Description of the SMARTplus pilot plant

Secondary treated municipal wastewater from the Garching wastewater treatment plant (WWTP, 31,000 PE) was used as feed water for the SMART*plus* pilot plant. Tertiary treatment by a polypropylene filter cartridge (100 µm, 20", Putsch GmbH) and a subsequent rapid sand filter (DynaSand, Nordic Water GmbH) was provided on-site. The DynaSand effluent was stored in a

1,800 L buffer tank and was fed continuously to the SMART*plus* bioreactor at a flow rate of 0.3 m³/h (Figure 7-1).

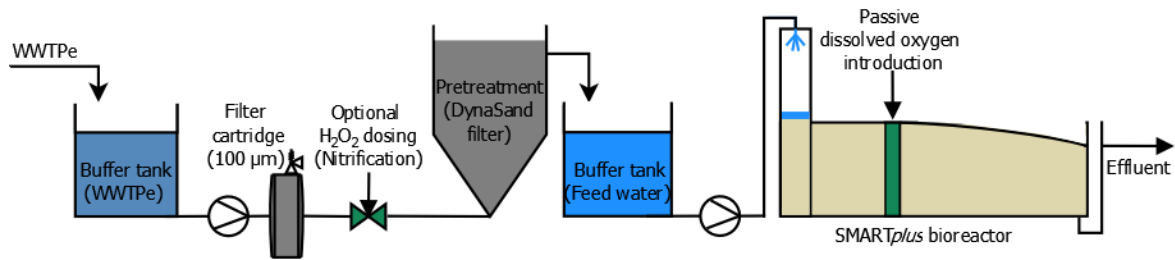


Figure 7-1: A schematic flow diagram of the SMART*plus* pilot plant. WWTPe indicates secondary effluent of the WWTP.

During the experimental period (May–October 2019), operational disturbances in the biological treatment of the WWTP resulted in increased ammonium (NH₄⁺) concentrations in the effluent supplied to the bioreactor. Thus, during elevated NH₄⁺-N concentrations (>1.5 mg/L), the DynaSand filter was operated with inline H₂O₂ dosing as an adjacent nitrification step, designed for a maximum of 3 mg/L NH₄⁺-N removal. During high NH₄⁺-N concentrations in the feed water (>4 mg/L), partial circulation of the bioreactor effluent into fresh incoming tertiary effluent ensured that NH₄⁺-N concentrations remained below 4 mg/L in the feed water supplied to the SMART*plus* bioreactor.

The pilot-scale SMART*plus* bioreactor was composed of a stainless steel flume (6 m long x 0.9 m wide x 1.4 m high), where the first 3 meters were sealed with a lid to mimic a confined saturated aquifer. A rectangular shaft (0.35 m long x 0.9 m wide x 1.5 m high) atop the bioreactor at the inflow side served as an infiltration trench. The infiltration trench was filled with gravel (d₁₀=3.4 mm) for rapid vertical infiltration of feed water, followed by horizontal plug flow conditions in the rest of the bioreactor. The compartments before and after the electron acceptor (EA) compartment were filled with uniform technical sand (uniformity coefficient 1.3, d₁₀=0.75 mm) to maintain the plug flow conditions, which is essential for establishing controlled sequential redox conditions during subsequent travel through the saturated zone. The EA compartment (detailed information in Chapter 7.2.3) and the outflow compartments were filled with gravel (d₁₀=2.1 and 3.4 mm, respectively). Twenty-four water sampling ports at different heights and depths along the length of the bioreactor and three filter media sampling ports for the sealed area were installed. Dissolved oxygen (DO) sensors (DP-PSt6, PreSens GmbH, Germany) were deployed in 6 PVC infiltration wells along the bioreactor and continuously logged data every 10 minutes. More detailed information on the design and operation of the SMART*plus* bioreactor including the hydraulic characterization prior to the commissioning of the *in-situ* oxygen delivery device have been published in Karakurt-Fischer et al. (2020b).

7.2.2. Performance characterization of the gas-liquid membrane contactor

7.2.2.1. Design and operation of a gas-liquid membrane contactor at lab-scale

A lab-scale flow through setup was constructed to investigate bubble formation and determine mass transfer coefficients (Figure 7-2). The initial setup to test bubble formation in tap water and tertiary effluent consisted of a bottom-up flow-through acrylic glass column (30 cm in length, 14 cm in diameter), in which the membrane was fixed approximately 10 cm above the bottom. Experiments to determine mass transfer coefficients corresponding to flow velocities in SMARTplus (Table 7-1) were carried out with tap water in a stainless steel column (30 cm in length, 15 cm in diameter, membrane fixed 18 cm from the bottom). PDMS membranes of 2 m length and an inner/outer diameter of 1.98/3.18 mm (DOW Silastic, Cole-Parmer GmbH) were woven onto a metal grid. The PDMS membrane material is well characterized by Berry et al. (2017) to model oxygen and ozone mass transfer.

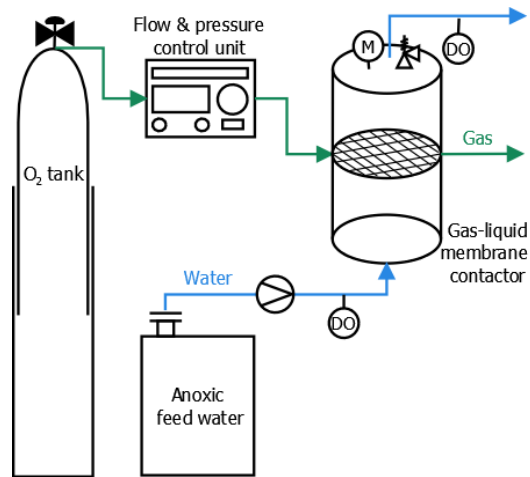


Figure 7-2: A schematic flow diagram of the self-made lab-scale gas-liquid membrane contactor, where the contactor design was adapted from (Grassi et al., 2007). The manometer is denoted by 'M,' and 'DO' indicates the dissolved oxygen measurement sensors.

Technical-grade pressurized oxygen (99.9% O₂, Air Liquide Deutschland GmbH) with a feed pressure of 0-1 bar and a constant gas flow rate at 0.1 L/min was used in all experiments. To mimic the redox conditions at the entrance of the EA compartment of SMARTplus bioreactor, the feed water was sparged with nitrogen gas for 10-15 minutes to adjust DO concentrations to below 1.5 mg/L. The feed water was then pumped through the experimental setup with a rotary pump, except for the lowest velocity ($4.72 \cdot 10^{-5}$ m/s), for which a peristaltic pump was used instead. DO concentrations were continuously monitored using flow through sensors (DP PSt6, PreSens GmbH) in the column influent and effluent until equilibrium was reached, after approximately two hydraulic retention times. The equilibrium concentration was recorded every 10 seconds for additional five minutes and averaged to calculate $C_{l,out}$. The water temperature (17.9-19.6 °C) was measured at the

outlet immediately after each experiment, and was similar to water temperatures observed in the SMARTplus bioreactor during the experimental period (17.2-22.0 °C).

Table 7-1: Theoretical and investigated liquid velocities and Reynold numbers for the corresponding SMARTplus bioreactor flow rates. The theoretical velocity corresponds to the effective velocity for the SMARTplus bioreactor and to the flow velocity for the lab scale setup, as the latter contains no porous media. Re is calculated with the outer diameter of the membrane (d_o) as reference length.

$Q_{SMARTplus}$ [m ³ /h]	$v_{l,theo}$ [m/s]	$v_{l,exp}$ [m/s]	Re_{theo} [-]	Re_{exp} [-]
0.1	$5.37 \cdot 10^{-5}$	$4.72 \cdot 10^{-5}$	0.17	0.15
0.3	$1.61 \cdot 10^{-4}$	$1.55 \cdot 10^{-4}$	0.50	0.48
0.5	$2.68 \cdot 10^{-4}$	$2.64 \cdot 10^{-4}$	0.83	0.82
0.7	$3.76 \cdot 10^{-4}$	$3.70 \cdot 10^{-4}$	1.16	1.14
0.9	$4.83 \cdot 10^{-4}$	$4.79 \cdot 10^{-4}$	1.49	1.48
1.1	$5.90 \cdot 10^{-4}$	$5.83 \cdot 10^{-4}$	1.82	1.80

7.2.2.2. Determination of mass transfer coefficients in cross flow

The flux of gas across a membrane can be described as

$$J = K \cdot \Delta C \quad [7.1]$$

With mass transfer coefficient K and the characteristic concentration difference ΔC , which has been characterized as the difference between saturation concentration at the gas-phase inlet $C_{sat,in}$ and the equilibrium concentration in the bulk liquid C_l (Ahmed and Semmens, 1992; Fang et al., 2002). However, to include the pressure drop along the membrane contact area, ΔC becomes

$$\Delta C = \frac{C_{sat,in} - C_{sat,out}}{\ln\left(\frac{C_{sat,in} - C_{l,av}}{C_{sat,out} - C_{l,av}}\right)} \quad [7.2]$$

where a logarithmic average is built over the total membrane length with $C_{sat,in}$ and the saturation concentration at the gas-phase outlet $C_{sat,out}$ (Côté et al., 1989). Instead of C_l the averaged liquid phase concentration $C_{l,av}$ of liquid-side concentrations at the inlet $C_{l,in}$ and outlet $C_{l,out}$ is taken as the bulk liquid concentration, which has been proposed for slow flow velocities (Fang et al., 2002).

The overall mass transfer coefficient K is typically expressed using the resistance-in-series model

$$\frac{1}{K} = \frac{1}{k_g} + \frac{1}{k_m} + \frac{1}{k_l} \quad [7.3]$$

with local resistances in gas-phase k_g , membrane material k_m and liquid-phase k_l . The resistance at the boundary between a wall and a fluid depends on the fluid velocity and the gas exchange geometry (Wickramasinghe et al., 1992; Yang and Cussler, 1986). The higher the fluid velocity, the thinner the liquid or gaseous boundary layer, and the lower the resistance, respectively. As the gas velocity in the investigated system is much higher than the liquid velocities, k_g was neglected in the resistance term. k_m can be derived from the permeability of oxygen P_m in PDMS, Henry's law constant H and the wall thickness τ (Casey et al., 1999) as

$$k_m = \frac{P_m H}{\tau} \quad [7.4]$$

The liquid-side resistance k_l depends on the flow velocity and can be described by numerous dimensionless correlations containing the Sherwood number ($Sh = \frac{K \cdot d_o}{D}$), the Reynolds number ($Re = \frac{v \cdot d_o}{\nu}$) and the Schmidt number ($Sc = \frac{\nu}{D}$) as

$$Sh = A \cdot Re^b \cdot Sc^c \quad [7.5]$$

with liquid velocity ϑ_l , fiber outer diameter d_o , kinematic viscosity ν , and diffusivity D . The dimensionless correlations were determined with porous membranes, which were assumed to have a minor membrane resistance, thus can be used as approximation for k_l . Examples and further references can be found in Gabelman and Hwang (1999).

For the modelled mass transfer coefficients, equations 4 and 5 were solved for k_m and k_l . All physical parameters such as the kinematic viscosity of water and the diffusion coefficient of oxygen in water were adjusted to the given experimental conditions. The calculated k_m and k_l values were used to obtain the overall K value. In case of k_l , several empirical correlations, which were determined in a cross flow design with porous hollow fibers were tested. The selected correlation that fits best ($Sh = 1.38 \cdot Re^{0.34} \cdot Sc^{0.33}$) was set up by Yang and Cussler (1986) at flow velocities starting approximately from $2.5 \cdot 10^{-3}$ m/s with a densely packed, cross flow contactor containing 750 polypropylene fibers with an outer diameter of 0.4 mm.

Experimental mass transfer coefficients for the PDMS membrane were determined for steady-state conditions ($\frac{dC}{dt} = 0$) with two mass balances of the system, as suggested by Orgill et al. (2019):

$$V_l \cdot \frac{dC}{dt} = Q_l \cdot C_{l,in} - Q_l \cdot C_{l,out} + K \cdot \Delta C \cdot A_{mem} \quad [7.6]$$

$$V_l \cdot \frac{dC}{dt} = Q_g \cdot C_{g,in} - Q_g \cdot C_{g,out} - Q_l \cdot (C_{l,out} - C_{l,in}) \quad [7.7]$$

This includes liquid flow rate Q_l , gas flow rate Q_g , contact chamber volume V_l , liquid- C_l and gas-side C_g concentrations and logarithmic average of the inner and outer surface area A_{mem} . In equation 6 the oxygen transfer rate is calculated by multiplying K and ΔC with A_{mem} . First, the experimentally determined concentrations $C_{l,in}$ and $C_{l,out}$ are used in equation 7 to calculate $C_{g,out}$ with knowledge of $C_{g,in}$ as this depends on the partial gas pressure. Then, ΔC in equation 2 is calculated by applying Henry's Law to solve the equation 6 for K – including a temperature correction (Sander, 2015) – and Ideal Gas Law.

7.2.3. Design of the electron-acceptor compartment equipped with gas-liquid membrane contactors

The EA compartment was initially filled with gravel from a tertiary sand filter of the WWTP Munich Gut Marienhof to facilitate biofilm growth in the system. This gravel was then partially removed to install the contactor assembly for the *in-situ* oxygen delivery. The contactor assembly was composed of perforated PVC infiltration wells (GWE pumpenboese GmbH, inner diameter=50 mm, slot width=0.3 mm), in which the gas-liquid membrane contactors were submerged (Figure 7-3). The perforated wells acted as a physical barrier between the gravel and membrane conductors for easy installation and maintenance.

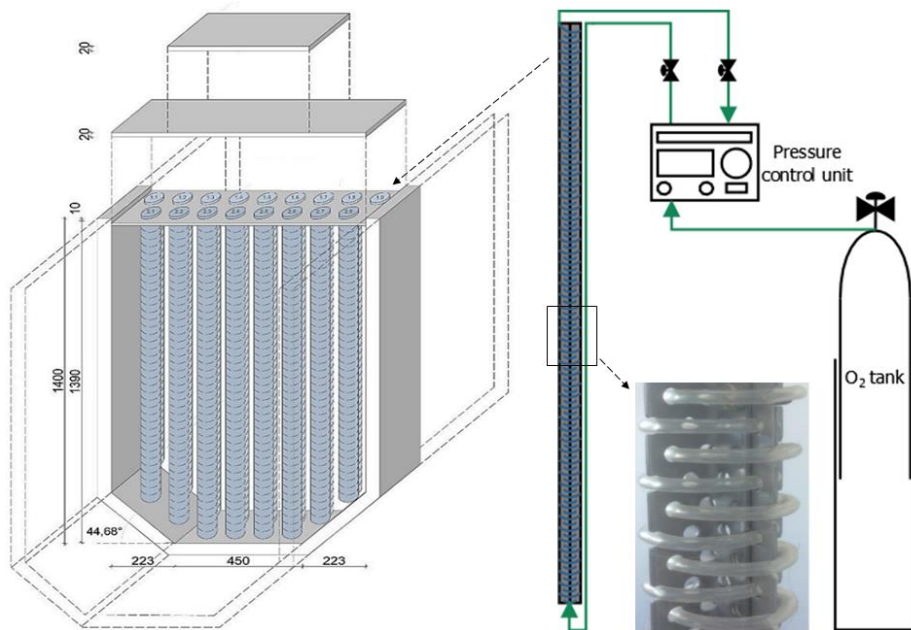


Figure 7-3: Axonometric front view of the contactor assembly of 17 infiltration wells within the EA compartment. All dimensions in [mm] [left]. A schematic illustration of a self-designed pilot-scale gas liquid membrane conductor submerged in one of the infiltration wells and the O₂ pressure regulation gauge [right].

The configuration of the infiltration wells is based on the borehole dilution theory stating that “the natural lateral hydraulic capture width of an unpumped well with an inner diameter of d_i amounts to twice of its diameter ($2 d_i$)” (Wilson et al., 1997). This resulted in the installation of 9 infiltration wells in a row, according to the width of SMART_{plus} bioreactor (895 mm) (Figure 7-3-left). To guarantee the homogenous and sufficient oxygen distribution at the cross section, an additional 8 infiltration wells were placed in a second row in a staggered arrangement. As the SMART_{plus} bioreactor has a trapezoidal bottom, each infiltration well was trimmed, depending on its position within the compartment, to an appropriate length and tightly sealed with a PVC disk. The 17 wells were fixed horizontally by a cover plate on top and vertically by a support plate in the middle via fixing strips. The gravel used to fill the void volume between the infiltration wells additionally

secured the position of the wells after their installation. The exact locations and the length of the infiltration wells can be found in the supporting information (SI-Figure 9-8).

The total membrane areas (A_{mem}) required for 17 membrane contactors were calculated based on the oxygen transfer rate O_r necessary to maintain a stable oxygen concentration downstream of the EA compartment. This assumes mixing over the compartment length in accordance with the borehole dilution theory. O_r is expressed as

$$O_r = K \cdot \Delta C \cdot A_{\text{mem}} \quad [7.8]$$

and is solved for the required membrane area A_{mem} to achieve the desired oxygen concentrations after the EA compartment.

The membrane contactors were composed of a metallic cross structure to hold the membranes in place, tubing for the oxygen distribution (PUN-H-6X1-BL 6x4 mm, Festo AG & Co. KG), two plastic fittings to connect the oxygen distribution tubing to the membrane fiber (reducer 4 mm-1.6 mm, Rotilabo®), and two ball valves to regulate inflow and outflow (QH-QS-6, Festo AG & Co. KG). The metallic cross structures were constructed from two individual metallic sheets (1 mm thickness, Mevaco GmbH) with a width of 30 mm and a length of 1,100-1,250 mm, depending on the length of the infiltration well. The sheets had a porous structure (pore diameter 4 mm) through which the silicon membrane was threaded in a double spiral fashion (Figure 7-3). The tubing for the oxygen distribution was attached to the metallic cross structure but had no contact to the membrane surface, and the contactors were fed with oxygen bottom-up. The oxygen transfer rate can be attuned by a pressure regulation gauge. The outlet gas pressure was monitored with a manometer to detect any gas leakages.

7.2.4. Sampling and analytical methods

In addition to online monitoring of DO, water pressure, temperature and conductivity, samples for ammonia, nitrate, dissolved organic carbon (DOC), UV absorbance at 254 nm (UVA₂₅₄), and TOxCs were taken from the feed water, the infiltration trench (0.4 m at x direction), from the sampling ports before (1.64 m) and after (2.64 m) the EA compartment, and from the effluent (5.85 m) of the SMARTplus bioreactor. Samples were analyzed according to methods described in Karakurt-Fischer et al. (2020b).

7.3. Results and discussion

7.3.1. Investigating the feasibility of gas-liquid membrane contactors for in-situ oxygen delivery into the SMARTplus bioreactor

To design the pilot-scale membrane contactors, the mass transfer coefficients of the PDMS membranes had to be determined. Experimental mass transfer coefficients determined at lab-scale

for the flow conditions specified in Table 7-1 varied between $2.01 \cdot 10^{-6}$ and $6.42 \cdot 10^{-6}$ m/s, and agreed well with the model (Figure 7-4-left). Finding a suitable correlation through experimental verification allows the estimation of the flux across the membranes, in relation to membrane geometry, partial oxygen pressure and flow velocity. Although the membrane geometry used in the lab-scale experiments was different from the wounded modules which would be placed into the pilot-scale SMARTplus bioreactor, the boundary layer in different types of cross flow designs has been shown to be similar (Wickramasinghe et al., 1992).

The dependence on the liquid-side velocity is visible from the positive response of mass transfer coefficients to rising liquid velocities. The K value increases by 131% from $2.01 \cdot 10^{-6}$ to $4.65 \cdot 10^{-6}$ m/s when the flow velocity is increased from $4.72 \cdot 10^{-5}$ to $1.55 \cdot 10^{-4}$ m/s, which corresponds to applying a flow rate of 0.1 to 0.3 m³/h in the SMARTplus bioreactor. By changing the partial pressure of oxygen while other parameters, such as temperature and membrane surface, remain constant, the oxygen transfer can be adjusted to different hydraulic conditions.

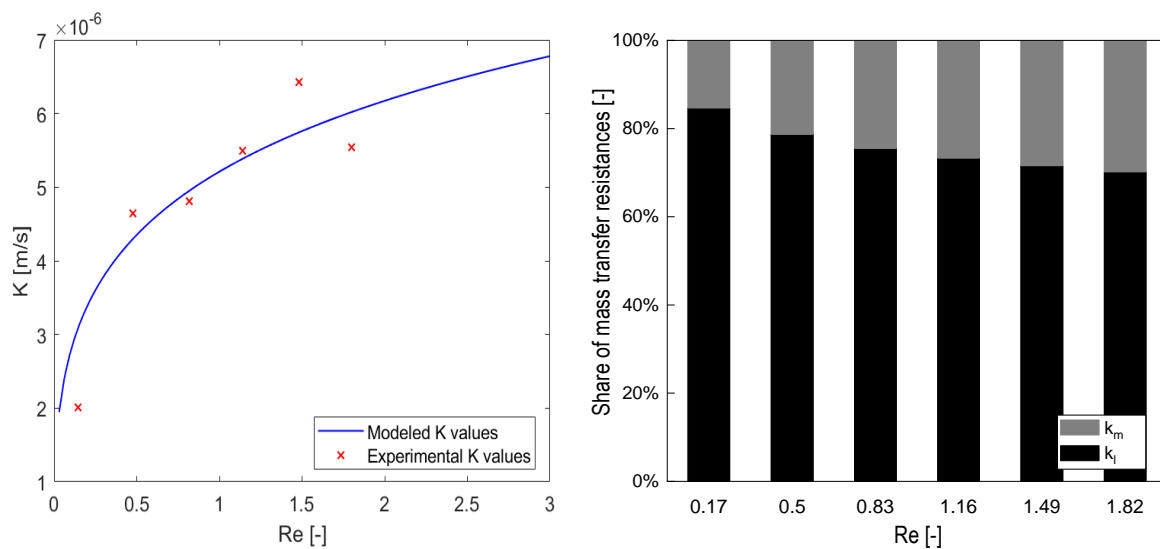


Figure 7-4: Modelled and experimentally determined average oxygen mass transfer coefficients for varying Reynolds numbers (left). Share of oxygen mass transfer resistances for varying Reynolds numbers (right).

To quantify the impact of the membrane wall and the liquid side velocity, the shares of modeled liquid and membrane resistances were compared (Figure 7-4-right). The liquid side resistance held between approximately 85 and 75% of the total resistance, similar to the results of Côté et al. (1989) for laminar flow regimes. The discussed advantage of having a minor membrane resistance if using porous membranes thus is of minor importance for this application. Additionally, the share of the membrane resistance can be decreased by selecting a thinner membrane wall, which is a trade-off between mechanical stability and higher mass transfer coefficients. Moreover, the higher mass transfer resistance in dense membranes due to additional membrane resistance can be compensated by increasing the driving force, therefore the concentration difference by increasing the partial

pressure of oxygen. However, microbubbles on the surface of the fibers can be observed under high oxygen partial pressures, which grow while attached to the membrane surface and detach once a critical size is reached. For this reason, a driving force increase should be matched by a decrease in liquid film resistance to avoid exceeding saturation and to avoid degassing at the membrane wall (Côté et al., 1989).

Due to the high dependence on the liquid-side resistance, bubble formation was observed at $1.55 \cdot 10^{-4}$ m/s flow velocity ($Re_{theo}=0.50$) at pressure ranges between 0.2 to 0.8 bars of O₂ partial pressure during the experiments with tap water. After 4 days of operation with the tertiary effluent, the bubble formation ceased. This was explained by the increased oxygen demand and biofilm formation induced changes to the membrane surface, also shown for MABR applications (Essila et al., 2000). Due to the absence of bubbles and suitable mass transfer coefficients, the gas-liquid PDMS membrane contactor was deemed suitable for the *in-situ* oxygen delivery into the SMART*plus* bioreactor.

7.3.2. Development and implementation of pilot-scale gas-liquid membrane contactors

When assuming fully nitrified and oligotrophic water quality (BDOC < 1 mg/L) before the EA compartment, less than 2.7 mg/L oxygen demand (2.7 mg DO / mg DOC (Rivett et al., 2008)) after the EA compartment was expected. To meet this oxygen demand, maintain oxic conditions (>1 mg/L) in the effluent of SMART*plus* bioreactor and not to consume oxygen excessively, a DO concentration of 3-4 mg/L was targeted for the EA compartment and adjusted according to the fluctuating feed water quality.

Accordingly, a total membrane area of 1.54 m² and a fiber length of 11.39 m for each membrane contactor were calculated using equation 8, based on the modeled mass transfer coefficient of $4.35 \cdot 10^{-6}$ m/s at 0.3 m³/h ($1.55 \cdot 10^{-4}$ m/s). This membrane size would provide a DO concentration of 3.0 mg/L with 0.8 bar O₂ partial pressure after the EA compartment, without considering oxygen depletion by aerobic biotransformation (Table 7-2). If the oxygen pressure would be increased to 1 bar, the DO concentration would increase to 4.1 mg/L.

To minimize the required membrane length for the silicone tubing contactor and/or achieve higher DO concentrations, oxygen partial pressure in the contactor can be increased from 0.8 bar to 2.5 bar. During the experiments, gas leakages were observed at 2.5 bar due to a membrane adaptor disconnection. However, in the pilot-scale application, calculations showed that 100% oxygen saturation (9.3 mg/L at 19 °C and 1 atm) could be achieved downstream of the EA compartment already with 2.3 bar partial pressure in the membrane module, assuming perfect mixing of oxygen in the compartment. Therefore, the adaptors were not replaced for the pilot-scale membrane contactors. For higher pressures, however, a different adaptor for the membrane contactor would be required.

Finally, the membrane contactors were designed and constructed with a membrane length of 11-12 m, depending on the length of the infiltration well in which they were submerged.

Table 7-2: Input and calculated parameters for estimating the membrane area and the design of membrane contactors required to ensure 3.0 mg/L DO after the EA compartment.

Input parameters	Inner diameter, d_{in} [mm]	1.98
	Wall thickness, τ [mm]	0.60
	Permeability, P_M [mol/(m·s·Pa)]	$1.63 \cdot 10^{-13}$
	Diffusivity, D [m ² /s]	$2.03 \cdot 10^{-9}$
	Kinematic viscosity of water, ν [m ² /s]	$1.03 \cdot 10^{-6}$
	O ₂ partial pressure, P [bar]	0.80
	Liquid side temperature [K]	292.15
	Henry constant O ₂ [mol/m ³ ·Pa]	$1.20 \cdot 10^{-5}$
Calculated parameters	Reynolds-number, Re [-]	0.50
	Schmidt-number, Sc [-]	507.26
	Sherwood-number, Sh [-]	8.68
	Liquid side, k_l [m/s]	$5.54 \cdot 10^{-6}$
	Membrane side, k_m [m/s]	$2.02 \cdot 10^{-5}$
	Total, K [m/s]	$4.35 \cdot 10^{-6}$
	Required total membrane area, A_{mem} [m ²]	1.54
	Required average tubing length per module, L_t [m]	11.39

The membrane contactors were then conditioned by submerging them into a transparent container filled with tertiary effluent for five days, to visibly check for any leaks. The goal of the conditioning was to enhance the initial biofilm growth prior to installing the membranes into the EA compartment, therefore inhibiting initial bubble formation during commissioning in the SMARTplus bioreactor. After the commissioning, the modules were operated in closed mode at varying oxygen partial pressures (0.8-1.0 bar) and the modules were flushed once a day to remove nitrogen.

7.3.3. Validation of pilot scale gas-liquid membrane contactors for the establishment of redox zonation under varying feed water quality

To trace the spatial oxygen depletion and determine whether the favorable oxic and oligotrophic conditions could be established with the membrane contactors, the bioreactor water quality was monitored at six locations. Samples for DO, DOC, NH₄⁺-N, NO₃⁻-N concentrations and UVA₂₅₄ values were taken from the secondary effluent, in the feed water, after the infiltration trench, before and after the EA compartment, and in the effluent of the SMARTplus bioreactor (Table 7-3).

The mean secondary effluent DOC concentration during the *operation with in-situ oxygen delivery / September-October 2019* (8.1 ± 0.9 mg/L) was less than the concentration measured during *baseline operation / April-September 2018* (11.5 ± 3.2 mg/L) (Karakurt-Fischer et al., 2020b). The discrepancies and the standard deviations portray seasonal and weekly quality fluctuations of the

secondary effluent of Garching. After the pre-treatment, a DOC concentration of 10.2 ± 2.7 mg/L in the feed water was achieved, which was then further degraded along the bioreactor to 7.5 ± 2.3 mg/L during baseline operation (Karakurt-Fischer et al., 2020b). Mean feed water DO concentration during baseline operation (5.1 ± 2.3 mg/L) was lower than during operation with *in-situ* oxygen delivery (8.3 ± 0.5 mg/L) due to high feed water temperatures up to 27 °C and higher feed water DOC concentrations (Figure 7-5). DO of 5.1 ± 2.3 mg/L in feed water was then rapidly consumed, resulting in a mean DO concentration of 1.0 ± 1.0 mg/L at the end of the infiltration trench, thus shifting from oxic to suboxic redox conditions according to the redox definitions by Regnery et al. (2015b) (Figure 7-5-left). No nitrate reduction (<0.5 mg N/L) and low DO concentrations (<1 mg/L DO) confirmed mostly suboxic conditions along the remainder of the bioreactor (Karakurt-Fischer et al., 2020b).

During operation with the *in-situ* oxygen delivery, a feed water DOC concentration of 7.9 ± 0.8 mg/L was obtained after the pre-treatment with DynaSand filter. Similar mean feed water DOC concentrations (7.3 ± 1.0 mg/L) were observed in a pilot-scale sequential biofiltration system with intermediate aeration (HRT >33 hours), fed in batch mode with the same secondary effluent as SMARTplus (Müller et al., 2017). In the second biofilter, 4.4 mg/L DOC persisted in the effluent, while DO concentrations remained above 2 mg/L (Müller et al., 2017). The prevalence of oxic conditions in the biofilter effluent and the HRT of more than 33 hours indicate the refractory character of the remaining 4.4 mg/L DOC in the Garching secondary effluent (Müller et al., 2017). Eventually, 3.1 ± 1.1 mg/L of DOC was removed in SMARTplus, resulting in 4.8 ± 0.6 mg/L DOC before the EA compartment. The substantial depletion in the UVA₂₅₄ from the feed water after the infiltration trench supports the main removal of BDOC within the first 40 cm of the bioreactor (Table 7-3). Stable DOC concentrations and UVA₂₅₄ values were observed for the remainder of the bioreactor, as the changes were not significant after passage through the EA compartment ($\alpha=0.05$, 2-sided, paired student's t-test).

Table 7-3: Mean DOC, DO ($n=3,525$), $\text{NH}_4^+\text{-N}$, $\text{NO}_3^-\text{-N}$ concentrations, UVA₂₅₄ and pH ($n=16$) values in sampling locations during operation with the *in-situ* oxygen delivery, 2019 (for the rest of the parameters $n=4-5$). Locations of the sampling ports in the x direction are given in mm. The locations of the DO sensors are given in Figure 7-5.

	DOC [mg/L]	UV ₂₅₄ [1/m]	DO [mg/L]	NH ₄ ⁺ -N [mg/L]	NO ₃ ⁻ -N [mg/L]	pH [-]
Secondary effluent	8.1 ± 0.9	-	-	4.4 ± 1.5	12.0 ± 1.8	7.4 ± 0.1
SMARTplus feed water	7.9 ± 0.8	11.8 ± 0.6	8.3 ± 0.5	1.9 ± 0.6	13.0 ± 2.8	7.3 ± 0.1
Infiltration trench (400 mm)	5.0 ± 0.6	9.5 ± 0.4	<0.015	-	12.1 ± 2.4	-
Before the EA (1640 mm)	4.8 ± 0.6	9.8 ± 0.4	<0.015	<0.015	12.3 ± 3.5	-
After the EA (2640 mm)	5.3 ± 0.7	10.5 ± 0.6	2.6 ± 1.9	-	15.6 ± 3.6	-
SMARTplus eff. (5850 mm)	5.1 ± 0.5	10.2 ± 0.8	1.4 ± 1.4	<0.015	15.2 ± 3.0	7.2 ± 0.1

During the baseline operation in 2018 and the experiments conducted by Müller et al. (2017), ammonium was not measured in the Garching tertiary effluent. In 2019, operational disturbances at

the WWTP caused effluent $\text{NH}_4^+\text{-N}$ concentrations to increase up to 5.9 mg/L (90th percentile). Through inline H_2O_2 dosing in the DynaSand filter, which was designed for maximum 3 mg/L N removal, a lower mean $\text{NH}_4^+\text{-N}$ concentration (1.9 ± 0.6 mg/L) was achieved in the SMART $plus$ feed water (Table 7-3). All available oxygen in the feed water (8.3 ± 0.5 mg/L) was depleted in the infiltration trench due to both nitrification and DOC removal (Table 7-3 & Figure 7-5), bringing $\text{NH}_4^+\text{-N}$ concentrations before the EA compartment to <0.015 mg/L. However, due to the synoptic sampling and fluctuating water quality, intermittent occurrences of surplus ammonium before the EA compartment cannot be excluded. Despite the observed nitrification, mean nitrate concentration decreased within the infiltration trench indicating that nitrate was also partially used as an electron acceptor for DOC removal. Furthermore, the increase of the mean nitrate concentration right after the EA compartment ($\Delta\text{NO}_3^-\text{-N}=3.4 \pm 1.4$ mg/L) indicates that the nitrification was partially incomplete and/or some ammonium was still present before the EA compartment. Overall, observed denitrification supported the presence of anoxic conditions before the EA compartment and the oxygen provided by the EA compartment was partially used to complete the nitrification process. This additional demand was not considered during the design of the membrane contactors but was tried to be compensated by higher O_2 pressures. The oxygen demand from nitrification, however, seems to be variable and could not be quantified.

When assuming fully nitrified feed prior to the EA compartment, oxygen demand can be estimated from the remaining BDOC of 0.4 mg/L (based on DOC concentration of 4.8 mg/L before the EA compartment and persistent DOC of 4.4 mg/L in the effluent of sequential biofilters). For this transformation, *in-situ* introduction of >2 mg/L DO would be required to meet the resulting oxygen demand and to establish oxic conditions (>1 mg/L) in the effluent. According to the experimental and modeled mass transfer coefficients, as well as the design parameters of the pilot-scale membrane contactors, O_2 pressure was adjusted to 0.8-1 bar to establish DO concentrations of 3.0-4.1 mg/L, which would meet this theoretical oxygen demand.

During the entire experimental period, however, oxygen demand occasionally exceeded 2 mg/L due to the fluctuating influent water quality. DO concentrations in the reactor directly downstream of the EA compartment (2250 mm) showed that 80% of measurements were >1 mg/L DO (mean = 2.6 mg/L, 90th percentile = 5.3 mg/L) (Figure 7-5). In the effluent of the SMART $plus$ bioreactor, however, half of the measured concentrations were <1 mg/L (mean = 1.4 mg/L, 90th percentile = 4.1 mg/L). The continuous monitoring with online DO measurements (interval 10 min, $n=3,525$) indicated substantially higher water quality fluctuations than the analysis of synoptic DOC, ammonium and nitrate samples. Further depletion of DO downstream of the EA compartment (mean $\Delta\text{DO} = 1.2$ mg/L, 90th percentile = 4.1 mg/L) was therefore not directly comparable with the steady DOC and $\text{NH}_4^+\text{-N}$ attenuation derived from the synoptic samples. Moreover, the disturbances of the hydraulic conditions before and within the EA compartment during the experimental period in 2019

(SI-Figure 2) possibly resulted in poor mixing of DO over the length of the EA compartment, which was assumed for the validity of the borehole dilution theory and homogenous oxygen concentrations downstream of the EA compartment (Chapter 7.2.3). After the EA compartment, the arrival of the tracer at the ports and the outflow of the bioreactor corresponded to their hydraulic retention times (SI-Figure 2). However the poor mixing within the EA compartment might have still resulted in the occurrence of spatial differences downstream, thus higher (up to 5.3 mg/L, 90th percentile) and lower DO concentrations than the targeted 3.0-4.1 mg/L within one cross section. For this reason, even though oxic conditions were provided, DO concentrations were presumably not homogenous and the redox conditions were not at steady state.

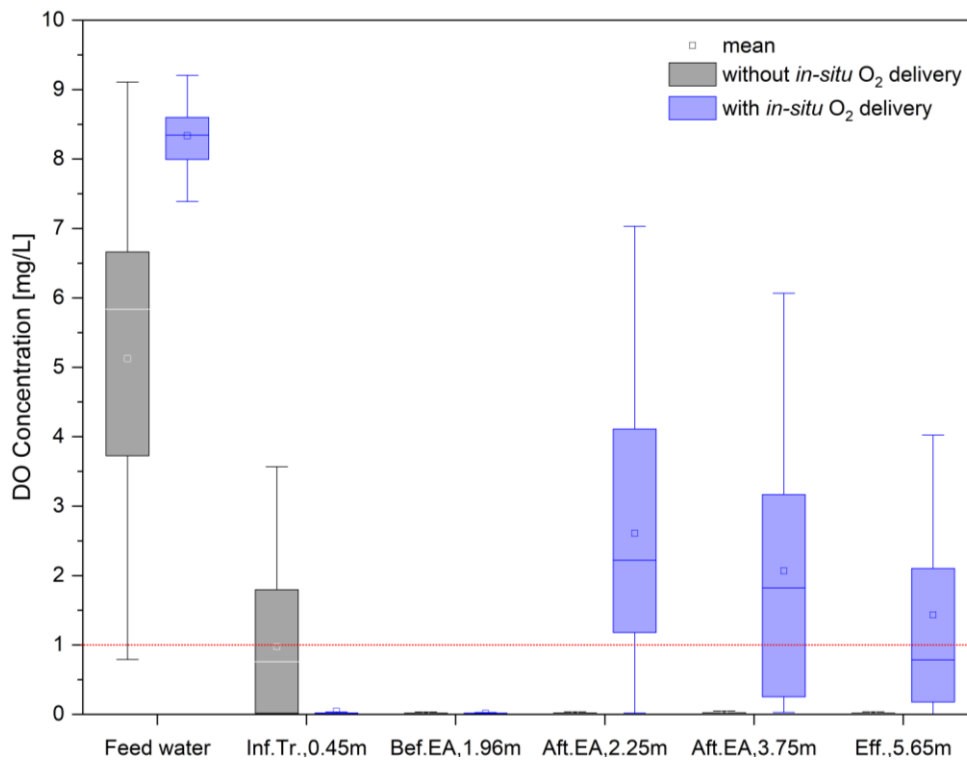


Figure 7-5: DO concentrations along sampling locations of SMARTplus bioreactor experiment without (2018, $n=15,836$) and with (2019, $n=3,525$) the *in-situ* oxygen delivery. The red dashed line indicates the threshold DO concentration of 1 mg/L for oxic redox conditions based on the definition by Regnery *et al.* (2015b).

Overall, the bubble-less *in-situ* oxygen delivery to SMARTplus bioreactor via gas/liquid membrane contactors has been proven to be successful at pilot scale. Although the water quality of the tertiary effluent was improved, the strong feed water fluctuations in ammonia could not be compensated. Smaller changes in oxygen demand could be compensated with an automated process control by using monitoring data from the DO and UVA₂₅₄ sensors to assess quality changes and oxygen demand. Thus, a reliable source water quality is a prerequisite for advanced wastewater treatment technologies in order to achieve and maintain the targeted treatment efficiencies. Likewise, steady oxic conditions after the EA compartment can only be established if the wastewater effluent quality is stable.

7.3.4. Effects of the in-situ oxygen delivery and varying feed water quality on the attenuation of TORCs

Due to the incomplete nitrification in the WWTP and described variabilities in redox conditions, the expected enhanced removal of TORCs in the SMART_{plus} bioreactor could not be observed. However, the prevailing redox conditions within the SMART_{plus} bioreactor (oxic → anoxic → oxic → suboxic) still revealed attenuation of 14 TORCs and demonstrated the complexity of mechanisms involved in their biotransformation (Figure 7-6). The full breakthrough of the sorptive compound benzotriazole in 2019 indicated that biodegradation was the main removal mechanism for TORC transformation within the quartz sand porous media, as reported in previous studies (Alidina et al., 2014; Hellauer et al., 2018b; Müller et al., 2017; Reemtsma et al., 2010).

The transformation of most of the TORCs in the anoxic zone before the EA compartment decreased from 2018 to 2019, possibly due to the competitive oxygen demand caused by high ammonium concentrations and corresponding nitrifying and denitrifying (anoxic) conditions. Nevertheless, additional removal was observed after the *in-situ* oxygen delivery resulting in a similar or improved removal capacity of most of the TORCs in 2019 in comparison to operation in 2018 without the oxygen delivery (Figure 7-6).

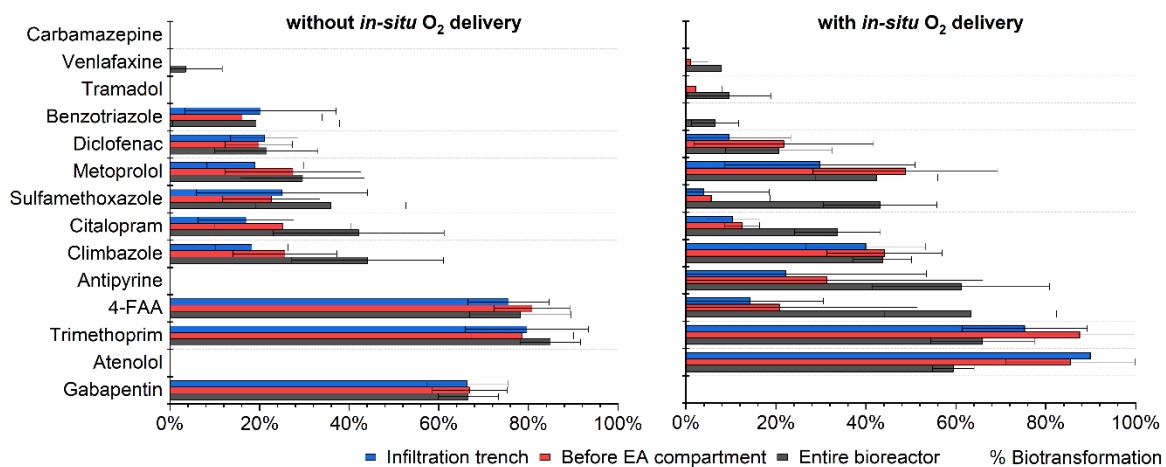


Figure 7-6: Cumulative TORCs removal calculated by normalizing the TORC concentrations before the EA compartment and in bioreactor effluent to their corresponding feed water concentrations (C_0) during operation without (left) and with (right) the *in-situ* oxygen delivery. Mean C_0 [ng/L] 2018 (n=8-9): gabapentin 1397 ± 414 , trimethoprim 48 ± 24 , 4-FAA 479 ± 176 , climbazole 166 ± 70 , citalopram 180 ± 43 , sulfamethoxazole 260 ± 190 , metoprolol 286 ± 35 , diclofenac 1052 ± 97 , benzotriazole 5921 ± 1485 , tramadol 198 ± 19 , venlafaxine 409 ± 36 , carbamazepine 459 ± 60 . Mean C_0 [ng/L] 2019 (n=5-6): atenolol 59 ± 17 , trimethoprim 200 ± 52 , 4-FAA 1441 ± 327 , antipyrine 110 ± 26 , climbazole 117 ± 26 , citalopram 175 ± 39 , sulfamethoxazole 308 ± 29 , metoprolol 327 ± 54 , diclofenac 1167 ± 119 , benzotriazole 5458 ± 497 , tramadol 264 ± 93 , venlafaxine 400 ± 39 , carbamazepine 329 ± 119 . The error bars indicate standard deviation of percent removal at different sampling dates.

Major transformation of gabapentin (66%) occurred in 2018 under the prevalence of both BDOC and oxygen in the infiltration trench of the SMART_{plus} bioreactor, which is the most biologically active

compartment in the system. In 2019, 93% of gabapentin was removed already within the DynaSand filter prior to the SMART*plus* bioreactor, where also both high BDOC and DO concentrations, due to H₂O₂ dosing, prevailed. A similar strong correlation between the biotransformation of gabapentin and DO consumption, BDOC removal and microbial activity was also observed in the sequential biofiltration system operated by Müller et al. (2019). In contrast, higher recalcitrance of gabapentin has been reported in conventional lab- and field-scale MAR applications (Hellauer et al., 2017; Hellauer et al., 2018a; Onesios and Bouwer, 2012), although Hellauer et al. (2018a) observed good oxic transformation of gabapentin at field-scale under rather oligotrophic conditions.

Atenolol and trimethoprim behaved similar to gabapentin and were attenuated up to 90% and 75% within the infiltration trench characterized by high BDOC concentrations and oxic conditions. Rapid biodegradation of trimethoprim and atenolol within the first infiltration step of a SMART system has also been reported by Regnery et al. (2016). While no further removal was observed for atenolol, trimethoprim removal increased from 75% up to 88% before the EA compartment under anoxic conditions. Further removal of trimethoprim under anoxic to anaerobic conditions have also been reported by Ghattas et al. (2017) and Falås et al. (2016). Schmidt et al. (2017) examined the attenuation of atenolol under varying redox conditions at lab-scale incubation experiments. In this study, a complete degradation of atenolol was observed both under oxic and anoxic, denitrifying conditions similar to the findings of Regnery et al. (2015b) at a groundwater recharge site. After the EA compartment, an increase in effluent concentrations reduced the total removal capacity of the SMART*plus* bioreactor for both atenolol (59%) and trimethoprim (66%). This might be explained by soil disturbances and desorbing effects. However, to the best of our knowledge, this effect has not been reported before for these substances.

A moderate climbazole removal (44%) was observed during both experimental periods. In previous studies conducted by Hellauer et al. (2018b), Muntau et al. (2017) and Müller et al. (2017), good removal of climbazole (> 85%) was noted under longer hydraulic retention times (>1 day) in comparison to the SMART*plus* bioreactor (<13 hours), regardless of prevailing redox conditions. Hermes et al. (2019) also confirmed the redox insensitivity of climbazole, as enhanced degradation was observed both under oxic and suboxic conditions during sequential biofiltration. Metoprolol removal (42%) was improved during the operation in 2019 and 20% of this removal was observed under anoxic conditions. Better and faster removal of metoprolol has been noted under oxic in comparison to anoxic-suboxic conditions in previous studies (Bertelkamp et al., 2016; Hellauer et al., 2017; Schmidt et al., 2017). Müller et al. (2019) also reported an improved removal for metoprolol in the sequential biofiltration system when HRTs increased from 10 hours (42%) to 35 hours (95%) under steady oxic conditions. The strict oxic conditions and longer HRTs may be required for further removal of metoprolol after the EA compartment in 2019.

Diclofenac (21%) was poorly removed, and no biotransformation was observed for benzotriazole (<10 %). These compounds were reported to be very redox sensitive, favoring oxic conditions for improved biotransformation with long adaptation periods from 1.5 months to almost a year (Hellauer et al., 2018a; Hellauer et al., 2018b; Müller et al., 2017). Rapid depletion of oxygen within the infiltration trench, unsteady DO concentrations after the EA compartment and shorter experimental period presumably could not provide those conditions.

High persistence of carbamazepine, venlafaxine, and tramadol was observed in 2019, similar to the experimental period before the commissioning of the *in-situ* oxygen delivery in 2018. Carbamazepine is widely known to exhibit persistent behavior and has been proposed and used as a wastewater indicator due to its limited biological removal and poor sorption in the aquatic environment under varying redox and hydraulic conditions (Burke et al., 2018; Hellauer et al., 2018a; Karakurt et al., 2019; Müller et al., 2017; Regnery et al., 2016). Only under strict anaerobic conditions and long HRTs (>14 days), Falås et al. (2016) showed improved removal of carbamazepine. The persistent behaviour of venlafaxine and tramadol supported the previous findings from Müller et al. (2017) and Hermes et al. (2019). A steady transformation of tramadol (70%) and venlafaxine (<LOQ) was observed under oligotrophic and oxic conditions with higher HRTs (>4.6 days) by Hellauer et al. (2018b). Higher HRTs under strict oxic conditions can be applied at field scale for the SMART*plus* bioreactor, possibly improving also tramadol and venlafaxine attenuation.

A positive effect of oxic conditions downstream of the EA compartment was observed for 4-FAA, antipyrine, sulfamethoxazole, and citalopram, resulting in 20-50% increased removal (Figure 7-6). Compared to 76% overall removal in 2018, only 14% of 4-FAA was removed within the infiltration trench in 2019, possibly due to the rapid depletion of oxygen. However, a significant increase in the removal of 4-FAA up to 63% was eventually achieved with DO supply downstream of the EA compartment. Similar rapid biodegradation of 4-FAA under oxic conditions was reported also in previous studies in MAR systems (Hellauer et al., 2017; Hellauer et al., 2018a; Massmann et al., 2006). For sulfamethoxazole, various removals during MAR treatment have been reported, ranging from poor to moderate removal (Grünheid et al., 2005). Sulfamethoxazole biotransformation in a slow sand filter fed with WWTP effluent was found to even be independent of oxygen and easily degradable acetate concentration (Zhang et al., 2019). However, other studies demonstrated that removal of sulfamethoxazole is still enhanced under oxic conditions compared to suboxic or anoxic environments (Regnery et al., 2015b; Regnery et al., 2016; Wiese et al., 2011). Sulfamethoxazole transformation increased to 43% in 2019 and 36% removal first occurred under oxic conditions after the EA compartment. Barbieri et al. (2012) addressed the complex effects of denitrifying conditions on diclofenac and sulfamethoxazole, which resulted in their retransformation towards the end of batch experiments.

7.4. Conclusion

This study investigated the potential of PDMS gas-liquid membrane contactors for *in-situ* oxygen delivery into the SMART*plus* bioreactor and the effects of additional oxygen supply on TOxC biotransformation. Mass transfer coefficients and bubble formation were investigated for the PDMS membrane at lab-scale with tertiary effluent, based on which the self-tailored membrane contactors were constructed and established at pilot-scale. Results from lab- and pilot-scale applications confirm our hypothesis that “bubble-free delivery of oxygen into the SMART*plus* bioreactor can be achieved under laminar flow conditions and short contact times by diffusive transport through gas-liquid membrane contactors”.

The pilot-scale gas-liquid membrane contactors were designed based on the borehole dilution theory in a staggered configuration and were capable of providing the modelled oxygen transfer in the SMART*plus* bioreactor. The DO concentrations were successfully elevated to >1 mg/L downstream of the EA compartment. However, due to the temporarily poor secondary effluent quality of the Garching WWTP (NH₄⁺-N up to 5.9 mg/L) and despite the in-line dosing of H₂O₂ into the pre-treatment to reduce incoming ammonium concentrations (<2 mg/L), steady oxic conditions could not be achieved. High nutrient content in the feed water caused anoxic conditions before the EA compartment, but also resulted in substantial variation of oxygen demand after the membrane contactors. As a result, suboxic conditions prevailed towards the end of the bioreactor. Increased disturbances of hydraulic conditions during *in-situ* oxygen delivery in comparison to the baseline operation (Karakurt-Fischer et al., 2020b) might also have contributed to higher fluctuations of DO concentrations within the EA compartment. These findings underline the importance of reliable upstream wastewater treatment for water reuse applications, in particular regarding full nitrification prior to advanced water treatment with SMART technologies. Furthermore, an appropriate online monitoring and control system for customized oxygen delivery could improve the robustness of the SMART*plus* bioreactor and provide stable oxic conditions (>1 mg/L) without introducing excess oxygen.

The transformation of TOxCs in the bioreactor was compound specific. Removal of some compounds (4-FAA, antipyrine, sulfamethoxazole, and citalopram) was enhanced significantly by *in-situ* oxygen supply, resulting in 20-50% increase in removal capacity. For persistent compounds, like carbamazepine, tramadol, and venlafaxine, a reliable removal requires additional barriers, e.g. *in-situ* ozonation, other reactive barriers within the bioreactor, and/or a suitable post-treatment, to provide a high product water quality. For other compounds, which were effectively degraded in previous experiments under SMART conditions (climbazole, metoprolol, diclofenac, and benzotriazole), no enhanced removal was observed. Further improvement in the removal of 4-FAA, antipyrine, sulfamethoxazole, citalopram, diclofenac, benzotriazole, and metoprolol can be expected, if steady feed water quality can be guaranteed to provide stable oxic and oligotrophic conditions for a longer

period. Additionally, if oxic conditions are maintained, the removal of metoprolol, climbazole, tramadol, and venlafaxine may benefit from higher HRTs (1-5 days) in a field scale application of the SMART*plus* bioreactor.

7.5. Acknowledgements

These experiments were funded by the Federal Ministry of Education and Research BMBF, funding codes 02WAV1404A and 02WIL1523. We would like to thank our colleagues and students for their help with the development and construction of the electron acceptor compartment, the gas-liquid membrane contactors, sampling of the SMART*plus* bioreactor and the laboratory analysis: Hubert Moosrainer, Daniela Schweiger, Amr Souf, Alexandra Schmuck, Mario Gramm, Anastasia Ruf, Geronimo Etchechury, Jad Arbash, Eric Seagren, Jannis Wenk, Johann Müller and Veronika Zhiteneva.

8. Overall discussion and outlook

Within the scope of this dissertation, five research hypotheses related to (i) the impacts of wastewater effluent discharges on drinking water supply and (ii) a new IPR treatment concept designed as a barrier against microbial and chemical contaminants, SMART*plus*, were developed. The hypotheses were investigated through bench- and pilot-scale experiments and modelling approaches. The main findings of these investigations were presented in four chapters (Chapters 4-7) based on peer-reviewed publications.

In Chapter 4, the dynamics of wastewater effluent contributions in streams across Germany were investigated. Furthermore, using a conceptual approach, the impacts of elevated wastewater effluent contributions on drinking water supply related to hypothesis #1 were assessed. Chapters 6 and 7 tested hypotheses #2 to #5, which addressed the development of a plug-flow bioreactor, SMART*plus*, coupled with high-rate infiltration trench technology and a novel *in-situ* oxygen delivery device from lab- to pilot-scale. Results of the experimental and simulated breakthrough of conservative tracers confirmed the establishment of plug-flow conditions and optimized hydraulics within the SMART*plus* bioreactor (Chapter 5). Subsequently, Chapter 6 addressed the attenuation of viruses under such optimized hydraulic conditions with minimized preferential flow paths via spiking tests and routine monitoring of indicator and surrogate viruses. Finally, Chapter 7 focused on characterizing the *in-situ* oxygen delivery device and its impacts on TOrC attenuation by comparing TOrC removal efficiencies prior to and after its commissioning.

The following comprehensive and critical discussion focuses on the underlying fundamental principles of the proposed technologies, and discusses the main findings of this research and their relevance to engineering practice. In addition, recommendations for the re-commissioning of the pilot-scale SMART*plus* bioreactor and field-scale applications are given and factors affecting the applicability of the proposed treatment technology are discussed. Finally, future research needs related to wastewater effluent contributions in streams and the SMART*plus* bioreactor concept are provided.

8.1. Assessment of municipal wastewater contributions in German surface waters and associated impacts on drinking water supply

A clear understanding of the *status quo* of conventional drinking water supply can help stakeholders to define present or emerging challenges regarding the reliability of the existing water abstraction and treatment infrastructure. For this assessment, a quantitative investigation of the impacts of wastewater effluent discharges on streams used for drinking water production is warranted, which leads to the first objective of this study “*Assessment of municipal wastewater contributions in German surface waters and associated impacts on the drinking water supply*”. Within the scope of

this objective, **Hypothesis #1** “*The exceedance of monitoring trigger levels (MTLs) in bank filtered raw water supplies occurs in several river basins in Germany due to high wastewater effluent contributions during extended time periods*” was developed and tested through modelling and conceptual approaches.

8.1.1. Testing Hypothesis #1

Hypothesis #1 aimed to reveal the extent of wastewater effluent contributions in German rivers and streams under varying river discharge conditions, and to determine whether MTLs for wastewater-derived indicator chemicals occurring in bank filtered raw water supplies are exceeded. Accordingly, **Hypothesis #1** was tested in two steps:

- 1) Estimation of wastewater effluent contributions by Python scripts coded into ArcGIS, using operational and spatial WWTP data across Germany and neighboring countries, and stream run-off data from gauging stations for mean annual discharge (MAD) and minimum mean annual discharge (MMAD) conditions, and
- 2) Development of a conceptual model determining indicator chemical MTL exceedances in raw water for different scenarios of wastewater effluent contributions in rivers and bank filtrate.

Operational and spatial data from 7,500 municipal WWTPs (with capacities exceeding either 50 or 2,000 PE) as well as stream run-off data (MAD and MMAD) from 2,344 gauging stations were spatially linked to the German river network (DLM250). A further assessment on the duration of MAD and MMAD conditions was conducted for three river streams (Neckar, Main, Rhine, characterized by low, middle and high average discharges) for two model years representing low and average rain fall patterns. This comparison illustrated the prevalence of MMAD-like flow conditions during almost six continuous months from spring to fall, a period where the water demand is the highest. Notoriously, MMAD conditions will become more frequent due to climate change, underlining the importance of characterizing wastewater effluent contributions under these conditions. The wastewater effluent contributions were subsequently determined by calculating the ratio of the total upstream wastewater effluent discharges to the stream run-off for each individual gauging station automatically using Python scripts, which was then visualized in ArcGIS. For locations with low natural base discharge and urbanized areas, wastewater effluent contributions during MMAD conditions were found to be greater than 30–50%. The estimated effluent contributions were validated exemplarily for the Main river by the conservative wastewater tracer carbamazepine. The effluent contributions estimated by carbamazepine suggested a range typical of MAD and MMAD effluent contributions for this river stretch, validating the ArcGIS model. The findings of this assessment demonstrate a high degree of wastewater impact on streams serving as drinking water sources in many urbanized areas and river basins with low natural discharge.

This assessment was followed by an investigation of wastewater effluent impacts on drinking water sources abstracted by IBF. The focus was on IBF contributing on average approximately 8% of the drinking water supply in Germany (German Environment Agency, 2018a). However, the contribution from river water in abstracted bank filtrate can vary widely given local conditions. Exemplarily, at the waterworks Berlin-Tegel, for which the hydraulic conditions and flow paths for the given abstraction wells are very well characterized by groundwater models, the share of bank filtrated water in the raw water was determined to be up to 70% (Senate Department for Urban Development and Housing Berlin, 2017). These contributions justify a comprehensive assessment on the impacts of wastewater effluents on IBF across Germany. However, such an assessment is not a straightforward task, since considering just surface water sources directly used for drinking water abstraction, which has been performed in the USA (Rice and Westerhoff, 2015), is not representative of the drinking water abstraction practice in Germany, which is rather indirect and relies heavily on subsurface treatment. IBF provides subsequent removal of microbial and chemical constituents in surface water impaired by discharge from wastewater effluents and other non-point sources. The degree of the treatment efficiency during IBF highly depends on site-specific and operational conditions such as location and type of wells, set-back distances from the stream to the abstraction wells, relative contributions from landside groundwater, and hydro-biogeochemical factors such as hydraulic conductivity, temperature, and prevailing redox conditions (Regnery et al., 2017). For these reasons, a conceptual approach for determining indicator chemical MTL exceedances in raw water for different scenarios was chosen. These scenarios represented different wastewater effluent contributions in rivers and bank filtrate shares in raw water, which was then validated using monitoring data for select TOxCs for three case study areas. For this approach the conservative indicator chemicals oxypurinol and carbamazepine were chosen, which are highly persistent and occur at high concentrations in wastewater effluents. Based on this model, oxypurinol exceedance could be observed in a scenario of only 5% bank filtrate and 60% wastewater effluent contributions in the stream. For carbamazepine, MTL exceedances would occur with 60% wastewater effluents in streams and a share of 60% bank filtrate in raw water. Applying these scenarios to case studies revealed the exceedance of MTLs for carbamazepine and oxypurinol at two drinking water treatment plants located at the Havel and Main rivers. Similar wastewater effluent contributions and bank filtrate shares have also been observed for other DWTPs along the Rhine, Main, Elbe, Ruhr, Havel, and Neckar river basins (Funke et al., 2015; Hillenbrand et al., 2014; Reemtsma et al., 2010; Scheurer et al., 2011; Storck et al., 2012). Thus, MTL exceedances have been already shown or might be expected in their raw waters. Based on these findings, **Hypothesis #1** can be **accepted**.

Overall, the validation of the ArcGIS model and the conceptual model assessing the relevance of wastewater effluent contributions in raw water were based on the indicator chemicals (such as carbamazepine) present in secondary treated effluents. If the secondary effluent is subject to advanced wastewater treatment (i.e., activated carbon or ozone treatment) prior to discharge,

indicator chemical concentrations might be too low to serve as wastewater tracers. For this reason, WWTPs employing advanced water treatment (AWT) processes were noted but still considered in the model to avoid any bias while examining the feasibility of the method. As only 24 of the considered 7,550 WWTPs facilities across Germany currently are using AWT processes, their discharge did not result in a substantial quality improvement of the entire stream. With an increasing number of WWTPs employing AWT technologies, the load of chemicals will ultimately decrease, also resulting in less impacts of wastewater effluent on drinking water supply. Upgrading WWTPs with advanced treatment, especially in highly urbanized areas or river streams with low natural discharge, as it is currently pursued in Switzerland (Eggen et al., 2014), would substantially improve the river water quality.

8.1.2. *Relevance of the research findings and future research needs*

The outcome of this study revealed a high degree of wastewater effluent impacts on river streams serving as major water sources for drinking water supply and industrial or irrigation purposes across Germany. In addition, such high wastewater effluent contributions also impair the chemical and ecological state of surface waters due to discharge of potentially still hazardous substances and elevated amounts of nutrients, as well as related oxygen consumptions, which might pose a more direct risk to aquatic life. Therefore, the results of this study can be used not only to assess the impacts on surface waters as a source for further use, but also to evaluate the ecological and chemical state of the surface waters by environmental agencies according to the European Water Framework Directive. Moreover, the conceptual model developed in this study provides a universal qualitative methodology to identify possible *de facto* reuse situations worldwide, if the site-specific data on suitable indicator chemical concentrations in wastewater effluent and the wastewater effluent contributions in a river stretch are known. This approach reduces the need for comprehensive monitoring campaigns for a large number of drinking water facilities. The proposed workflow can be used as a guidance for water utilities and regulators to assess MTL exceedance of indicator or other chemicals as a basis to minimize potential adverse impacts on drinking water quality. It is important to note that an indicator chemical MTL exceedance in raw water does not represent an immediate threat to public health. However, counter measures are recommended to avoid long-term and increasing occurrences of MTL exceedances while maintaining a sustainable and natural treatment based drinking water practice. MTL exceedances might become more frequent with the impacts of climate change, which does not only affect the stream discharge, but also the performance of subsurface treatment due to changing temperatures during extended heat periods, chemical concentrations, water levels and redox conditions (Sprenger et al., 2011).

From some German federal states (i.e., Bremen, Hamburg, Mecklenburg-Vorpommern, Lower Saxony, Saxony-Anhalt, Schleswig Holstein, Thuringia and Saarland) no further data on the WWTPs were provided by the environmental agencies (SI-Table 9.4-1). For this reason, spatial and

operational WWTP data were taken from the [Thru.de](https://www.thru.de) webpage of the German Environmental Agency for the current version of the ArcGIS model, which only considers WWTP capacities of more than 2,000 PE. Based on our investigations in Bavaria (considering also WWTPs with a PE>50), we can conclude that small WWTPs discharging into streams with low base discharge might significantly impair the surface water and the raw water quality for drinking water abstraction. Similar contributions like in the state of Bavaria might be also observed, exemplarily in the state of Thuringia (WWTP with a PE>2,000), once WWTPs within the range 50 to 2,000 PE are also considered in the model. For this reason, greater data density for the aforementioned federal states is required for the ArcGIS model.

In addition, a complete mixing at the point of discharge of the wastewater effluents into the receiving river was assumed for the ArcGIS model. Therefore, high resolution calculation of the wastewater effluent contributions in the cross section of the river streams was not possible. However, the point discharges of the WWTP effluents can behave as plumes with varying mixing characteristics, since complete vertical and horizontal mixing can be assumed after 20 to 100 times the river depth and 100 to 350 times the river width (Vandenberg et al., 2005). Applying these findings to the Rhine River (2.5 m depth and 100 to 500 m width), vertical mixing can be achieved after 50 to 250 meters, while complete transverse mixing, even considering the fastest mixing rate, might take 10 to 50 km (Uehlinger et al., 2009). This estimation underlines the presence of long-lasting wastewater effluent plumes especially in wide river streams, resulting in higher relative wastewater effluent contributions than the model predicted for the nearby downstream DWTPs located on the same side of the river as the WWTP. Mixing characteristics of the plumes within a river based on its width might be incorporated to a smaller scale module of the ArcGIS model for a river basin with a wide river stream (e.g., Rhine, Elbe, Spree, Neckar). Such an assessment is becoming more interesting when the exact locations of the DWTPs along this river stream is known.

The ArcGIS model can be upgraded with operational and spatial data for DWTPs, which can be used to better understand the effects of wastewater effluent contributions on drinking water quality. Moreover, for the validation of the developed ArcGIS model, monitoring is essential to generate relevant water quality data per catchment area. These efforts can be combined with further validation of the conceptual approach for the identified DWTPs. Chemical loads (biocides and pesticides) from agricultural drainages and combined sewer overflows can also be considered during the impact analysis on raw water quality, which, however, requires new models for accurate predictions of their concentrations and spatial-temporal water quality data for the validation of these models (Eggimann et al., 2017; Moser et al., 2018). In addition, chemicals with concentrations lower than their MTLs or LOQ might still lead to mixture toxicity, since compounds with the same mode of action might act according to a simple additive model (Escher et al., 2020). Bioanalytical methods can be used as a quantitative tool to assess the mixture effects for monitoring the toxicity increase correlated to the

relative wastewater effluent contributions (Escher et al., 2020; Völker et al., 2019). Such an assessment combined with new spatial-temporal water quality data can be conducted to further validate the ArcGIS model outcomes and conceptual approach in future studies.

Finally, the ArcGIS model can be expanded to other European countries, which would identify river streams and drinking water abstraction areas with high wastewater effluent contributions, and would specify river stretches with the need for more expensive monitoring requirements, complying with the European Commission's Green Deal Goal of "*protecting natural sources from persistent and mobile chemicals*". Including European countries into the model would increase also the precision of the model outcomes, since the river streams are mostly transnational and the wastewater effluent discharges from upstream countries impact the contributions downstream. A prerequisite for this assessment would be the availability of operational and spatial WWTP data as well as stream run-off data from gauging stations. The validation of the model outcomes and further assessments on the drinking water supply would require close cooperation with the utilities and environmental agencies of the participating European countries.

As an outlook, high wastewater effluent contributions and MTL exceedances might also indicate high exposure to microbial contaminants and a shift in the microbial population along a river stretch under high loads of wastewater effluent discharges (Mansfeldt et al., 2020). If the bank filtration complies with the German requirements of a minimal travel time of 50 days prior to abstraction, proper inactivation of pathogens, in particular bacteria, can be provided. However depending on the pathogen abundance in river streams, the removal performance of the subsurface might deteriorate over a long period of exposure to high pathogen concentrations (Schijven et al., 2017). Moreover, in case of preferential flow paths in the subsurface and non-compliance with the required HRTs, the microbial safety of the raw water cannot be guaranteed in particular for the viruses, as they are the main concern for MAR applications due to their smaller size and high concentrations (Regnery et al., 2017; Schijven et al., 2017). Due to the lack of monitoring data on pathogen abundances and site-specific information, to date no comprehensive conclusion on their prevalence during *de facto* potable reuse in Germany can be drawn. Therefore, future research is also needed to model the fecal contamination in river streams and predict the microbial safety of raw water after the bank filtration. A correlation between the wastewater effluent contributions and indicator (e.g., adenovirus, *Cryptosporidium*) and surrogate (e.g., coliphages) pathogen concentrations in river streams (considering mean WWTP effluent abundances and decay and reduction rates from literature), would assist in further identifying river stretches with potential microbial contamination for drinking water facilities, as well as potentially risky recreational and bathing water locations. Within the model, the key parameters (e.g., sun exposure, turbidity, temperature) affecting decay and reduction rates and thus pathogen survival after discharge into rivers (Gerba, 2007), as well as heavy rainfall, can be evaluated for different scenarios. The bottleneck of this assessment is the absence of monitoring data

for indicator and surrogate microorganisms which impedes validation of the model outcomes and raw water quality. However, the need for more comprehensive monitoring campaigns for a large number of river streams and drinking water facilities could be prevented through the proposed approach, since the most important monitoring locations would be identified with the help of the model. The microbial samples taken from the recommended locations for the validation of the model estimates and to address the shifts in the microbial communities in the rivers with high wastewater effluents can be conducted for instance by online flow through cytometry coupled with qPCR methods (Girones et al., 2010; Mansfeldt et al., 2020; Safford and Bischel, 2019).

8.2. Development, construction and operation of a novel hybrid biofilter, SMARTplus, based on sequential managed aquifer recharge technology (SMART) for indirect potable reuse

Using alternative fresh water sources, such as reclaimed water with reliable and relatively constant quantity and quality, may provide a sustainable and safe solution for the regions with increased water stress or high secondary effluent contributions in their raw water (Asano et al., 2007). The increasing interest in planned water reuse applications brings along the demand for new process combinations in many regions, driven by their site-specific characteristics, such as economic strength of the utility, social acceptance, availability of resources and infrastructure. Increasing the credibility of non-RO based treatment trains would push forward a new era by increasing the number of planned potable reuse schemes. This trend has formed the second main objective of this research - “*Development, construction and operation of a novel hybrid biofilter, SMARTplus, based on sequential managed aquifer recharge technology (SMART) for indirect potable reuse*”.

8.2.1. Testing Hypotheses #2-#5

To minimize the physical footprint, pumping costs and HRTs, as well as to overcome limitations of site-specific heterogeneities of conventional MAR and SMART systems, the SMARTplus bioreactor concept is characterized by two main engineered processes: high-rate infiltration trench technology coupled with a highly homogenous horizontal biofilter and *in-situ* oxygen delivery. First, a stainless steel 3D-flume (6 m in length, 0.85 m in width, 1.4 m in height) of the proposed SMARTplus bioreactor was constructed as a prototype at pilot scale to test **Hypotheses #2 to #5**. A rectangular shaft placed on top of the horizontal flow biofilter mimicked the high-rate infiltration trench (0.35 m in length, 0.85 m in width, 1.5 m in height). The influent water quality of the SMARTplus bioreactor should be equivalent to tertiary treated effluent with low suspended solids content. Therefore, first a rapid dual-media filter (RDMF) serving as on-site tertiary treatment was additionally constructed for the Garching WWTP secondary effluent. The RDMF was later replaced by a DynaSand (Nordic Water) filter with continuous backwash cycles due to easier operation. Post-treatment steps (e.g., GAC filtration, UV disinfection) after the SMARTplus bioreactor were not tested, since these

technologies are well established and literature data is available to assess their removal capabilities. The effluent of the advanced treatment train is envisioned to be released into an aquifer via vadose zone infiltration wells for subsequent treatment. The pilot-scale SMART*plus* system was operated for a total of three years.

Whether combining the infiltration trench technology and a horizontal biofilter filled with highly homogenous porous media could achieve rapid infiltration and plug-flow conditions was tested in **Hypothesis #2** “*Integration of infiltration trench technology into hybrid biofilter SMARTplus establishes a horizontal flow regime providing rapid infiltration and homogenous plug-flow conditions*”. This hypothesis was investigated mainly by the help of conservative tracer tests and 3D groundwater flow modelling approaches (MT3DMS and SPRING). During the first year of operation, four tracer tests with conservative tracers (potassium bromide) as well as one with primidone and bacteriophages were conducted to characterize the flow conditions within the SMART*plus* biofilter operating at a high effective velocity of 0.58 m/h ($Q = 0.3 \text{ m}^3/\text{h}$) in comparison to conventional slow sand filters. The experimental breakthrough curves indicated small hydraulic disturbances resulting in flatter or double peaks, while the modeled breakthrough curves did not show such results. This discrepancy between the experimental and modeled breakthrough curves revealed the first indications of preferential flow paths, since the 3D groundwater model simulates the conservative flow and mass transfer of a tracer. Moreover, the spiking experiments performed with bacteriophages and primidone strongly indicated the prevalence of heterogeneities in the filter media, since bacteriophages can behave like colloids and move along the preferential flow paths, which resulted in an earlier arrival than the conservative tracer. Based on these results, hydraulic optimizations were undertaken to minimize such preferential flow paths at the end of 2017, which were mainly attributed to the complete perforation of MW #1 and dead volumes in other MWs. After the replacement of MW #1 with a partially perforated well and the installation of packers, two additional tracer tests were conducted with KBr, bacteriophages and primidone in 2018 at the same flow velocity, which revealed that controlled hydraulic conditions had finally been established. Based on these investigations **Hypothesis #2** was **accepted**.

In **Hypothesis #3** “*Establishing homogenous plug-flow conditions within the SMARTplus bioreactor results in enhanced attenuation of viruses in comparison to conventional slow sand filters, despite shorter hydraulic retention times and coarser grain size*” the effects of homogenous plug-flow conditions on the attenuation of viruses were investigated within the SMART*plus* bioreactor. The LRVs for surrogate and indicator viruses were determined by monitoring ambient abundances of surrogate (F^+ phages: 2.2 LRVs and somatic coliphages: 3.0 LRVs) and indicator viruses (human norovirus: 2.5 LRV and adenovirus: 3.1 LRV). Moreover, to assess the transport and maximal virus reduction capacity of the SMART*plus* bioreactor under controlled hydraulic conditions, spiking tests with MS2 and ϕ X174 bacteriophages and MNV-1, accompanied by the conservative chemical tracer

primidone, were conducted. The transport of the bacteriophages and MNV-1 complied well with the conservative tracer primidone, which proved the prevalence of plug-flow conditions. Mean LRVs of 5.1, 5.0 and 3.5 attributed to adsorption were determined for MS2, ϕ X174, and MNV-1, respectively, during the spiking test under plug-flow conditions. Under short HRTs of only 12.6 hours within a travel distance of 6 m, and despite coarser grain size, the SMART*plus* demonstrated LRVs higher than conventional slow sand filters reported in the literature (Anderson et al., 2009; Bauer et al., 2011; Seeger et al., 2016). Due to enhanced die-off of viruses under oxic conditions (Frohnert et al., 2014; Klitzke et al., 2015), even higher LRVs for viruses are expected during the operation with the *in-situ* oxygen delivery device. The results of this investigation led to the **acceptance** of **Hypothesis #3**.

To enhance TO_{RC} biotransformation and virus removal, the establishment of oxic redox conditions via an *in-situ* oxygen delivery system into the porous media of the SMART*plus* bioreactor was desired. Therefore, **Hypothesis #4** “*Bubble-free delivery of oxygen into SMARTplus biofilter can be achieved in-situ under laminar flow conditions and short contact times by diffusive transport through gas-liquid membrane contactors*” focused on the development of a bubble-free *in-situ* oxygen delivery device for the SMART*plus* biofilter. A gas-liquid membrane contactor was identified as a promising technology to facilitate the diffusive transport of the oxygen under laminar flow conditions and short contact times after a comprehensive literature review. To date, this technology has been used for groundwater remediation or MABR (Casey et al., 1999; Côté et al., 1988; Gabelman and Hwang, 1999), which have different flow characteristics, reactor configurations, packed porous media types and bubble-less oxygen transfer requirements than what is needed in the SMART*plus* bioreactor. For this reason, the feasibility of gas-liquid membrane contactors for reliable delivery of oxygen into tap water and tertiary effluent was first studied at lab-scale using PDMS membranes at similar contact times and Reynold numbers (0.2-2) as expected for the pilot-scale bioreactor. Based on the mass transfer coefficients gathered during these lab-scale experiments, a custom PDMS gas-liquid membrane contactor was constructed and tested at pilot-scale. With the help of the membrane contactors, homogenous, bubble-free and passive oxygen delivery could be successfully demonstrated at pilot-scale under laminar flow conditions and short contact times. Oxygen concentrations downstream of the membrane contactors met the design specifications (>1 mg/L) as long as the required feed water quality was provided. Accordingly, **Hypothesis #4** was **accepted**.

Finally, **Hypothesis #5** “*Plug-flow conditions, defined and controllable redox zonation in SMARTplus biofilter lead to enhanced TO_{RCs} removal*” dealt with the question whether defined and controllable redox zonation in SMART*plus* biofilter can enhance the TO_{RCs} removal. To date, lab-to field-scale SMART applications were capable of enhancing the removal of a wide-range of moderately and easily degradable TO_{RCs} by establishing oligotrophic and oxic conditions in the second infiltration step (Hellauer et al., 2017; Hellauer et al., 2018a; Müller et al., 2017; Regnery et al., 2016). Due to the improved hydraulics, no blending effects caused by heterogeneities in the filter

media were expected, leading to expected better removals in the SMART*plus* bioreactor. To establish the desired oligotrophic conditions after the EA compartment during the sequential operation, the compartment prior to the EA is expected to remove a substantial part of the BDOC. Despite the removal of residual BDOC after the EA compartment, maintaining high DO concentrations (i.e. >1 mg/L) and thus oxic conditions, should be guaranteed. Although *in-situ* oxygen delivery could be successfully demonstrated at pilot-scale (Figure 7-5), unsteady oxygen demand in the feed water due to elevated ammonium concentrations resulted in suboxic instead of oxic conditions during half of the experimental phase. The high NH₄⁺ concentrations in the WWTP effluent and hydraulic problems resulted in operational disturbances during the sequential operation and finally the decommissioning of the SMART*plus* bioreactor. As noted, the prevalence of stable oxic conditions (DO concentrations >1 mg/L) during long-term experimental periods was correlated with the improved removal of TOrCs, since the adaptation of the microorganisms might take up to three months of steady-state operation (Hellauer et al., 2018a). For this reason, despite a 20 to 50% enhancement in the removal of certain compounds (i.e., 4-FAA, antipyrine, sulfamethoxazole, and citalopram) after the EA compartment, demonstration of the full potential of enhanced TOrC removal by SMART*plus* was hindered due to the operational issues encountered. Therefore, **Hypothesis #5** could be **neither accepted nor rejected**. The characterization of the removal performance during the sequential operation is recommended to be repeated, providing the WWTP Garching operates under steady-state conditions.

8.2.2. Recommendations for the establishment of the optimal hydraulic and operational conditions for future pilot- to field-scale applications

The novel SMART*plus* technology is designed for advanced water treatment either in the context of IPR, for the treatment of the WWTP effluents prior to discharge, or for impaired surface waters for drinking water supply. For field-scale applications, the SMART*plus* bioreactor is envisioned to be constructed below surface but still hydraulically decoupled from the local groundwater. A controlled groundwater pumping regime is therefore recommended to minimize uncontrolled mixing of infiltrated water with native groundwater. In the following sections, recommendations for field-scale applications and the re-commissioning of the pilot-scale SMART*plus* bioreactor will be given based on the experiences during this study period.

8.2.2.1. Requirements for the feed water quality

The SMART*plus* bioreactor has been developed as an advanced water treatment technology, which depends on a reliable WWTP operation with complete nitrification and on-site tertiary treatment, in particular with regard to mitigating DOC peaks and providing low turbidity values or total suspended solid concentrations. The pilot-scale bioreactor was operated for a period of 2.5 years at baseline operation, i.e. without *in-situ* oxygen delivery. During this period, beyond the hydraulic

characterization, the BDOC removal capability based on DO availability and the required feed water DOC and turbidity threshold values could be determined. The following estimation does not consider an additional DO demand due to remaining ammonium concentrations in the WWTP effluent, since complete nitrification in the WWTP ($\text{NH}_4^+\text{-N}$ concentrations of less than 0.5 mg/L in the effluent) is a prerequisite for a reliable operation of the SMART*plus* bioreactor similar to other advanced water treatment technologies (e.g., ozonation).

Although at 19 °C, the solubility of oxygen is approximately 9.3 mg/L, the DO concentrations in the feed water of the SMART*plus* bioreactor varied between 6 and 8 mg/L, likely due to the high BDOC content of the feed water. Assuming a mean DO concentration of 7 mg/L in the feed water, a maximum of approximately 2.5 mg/L BDOC would be removed prior to the EA compartment (2.7 mg DO / mg BDOC (Rivett et al., 2008)). An additional 3 mg/L of BDOC removal could be achieved after the EA compartment under sequential operation, assuming a maximum of 9 mg/L DO enrichment due to the saturation point during the *in-situ* oxygen delivery, noting that the oxygen transfer might be slightly higher due to the quick consumption of DO within the biofilm formed on the surface of the gas-liquid membrane contactors (for more details please refer to Chapter 7). During the operation of a pilot-scale sequential biofiltration system with the same WWTP effluent, Müller et al. (2017) could show approximately 4.5 mg/L of refractory DOC present in WWTP effluent. While still providing oxic conditions after the EA compartment, the maximum favored BDOC concentration in the feed water of the pilot-scale SMART*plus* bioreactor would be approximately 5.5 mg/L, leading thus to 10 mg/L DOC concentration threshold for the wastewater matrix of the WWTP Garching (Table 8-1). Based on the refractory character of the DOC in the source water of future SMART*plus* applications, the aforementioned DOC concentration threshold might vary. At field-scale or larger pilot-scale applications, higher than 2.5 mg/L BDOC concentrations in the feed water prior to the EA compartment might be compensated by extending the anoxic filtration zone, resulting in overall higher threshold DOC concentrations. Due to the differences in the kinetics of BDOC removal between anoxic and oxic conditions, however, prolonged hydraulic retention times would be required for an efficient removal under anoxic conditions (Grünheid et al., 2005).

However, during the 2.5 years of baseline operation higher feed water DOC concentrations, varying between 6.2 to 14.5 mg/L (mean 10.8 ± 2.4 mg/L) were observed in the feed water of the SMART*plus* bioreactor (Figure 8-1). Consequently, more than 60% of the sampling points were above the desired 10 mg/L DOC in the feed water. Hereby, the observed mean DOC concentration in the Garching WWTP effluent (11.9 ± 3.0 mg/L) was in accordance with the DOC concentrations observed in previous studies (Benstoem et al., 2017; Katsoyiannis and Samara, 2007; Zietzschmann et al., 2014). Prior to the EA compartment, i.e. at the end of the suboxic zone, a mean DOC concentration of 8.5 ± 2.2 mg/L could be achieved. Although an efficient BDOC removal of 2.2 ± 2.1 mg/L was provided prior to the EA compartment, the standard deviation demonstrates the fluctuations in the

process performance over a longer period caused by varying DOC concentrations in the WWTP effluent. Such fluctuations indicate that the *in-situ* oxygen delivery should be closely linked to the BDOC concentrations in the WWTP effluent and the feed water of the SMARTplus bioreactor, to be able to maintain oxic conditions after the EA compartment. If even higher feed water DOC concentrations of more than 10 mg/L were observed, they could be compensated by an on-site tertiary treatment step with in-line H₂O₂ dosing, and/or a second EA compartment within the SMARTplus bioreactor, providing additional 3 mg/L of BDOC removal.

During the sequential operation, neither the WWTP effluent nor the feed water DOC concentrations fluctuated as much as during the baseline operation due to a shorter experimental period (Figure 8-1). Due to exceptionally high NH₄⁺-N concentrations in the effluent of the WWTP Garching, caused by operational and construction problems, nitrification and denitrification problems occurred within the SMARTplus bioreactor during the sequential in comparison to the baseline operation. Therefore, the BDOC removal during the sequential operation could not be properly correlated directly to the DO consumption (for more information please refer to Chapter 7).

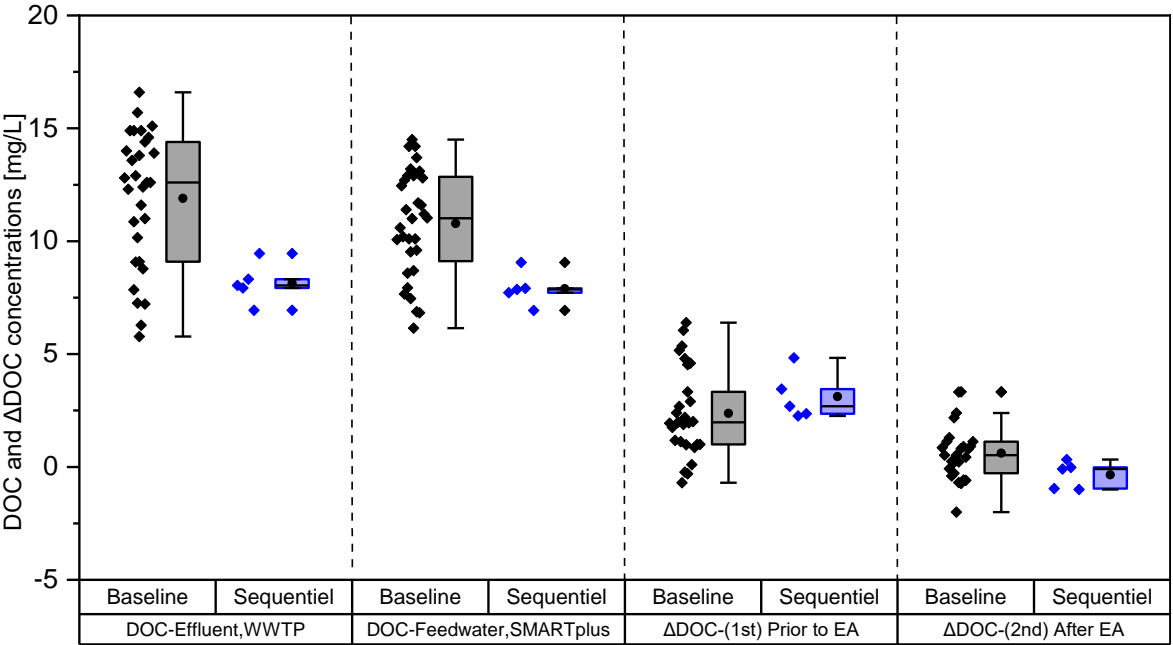


Figure 8-1: DOC and ΔDOC concentrations during baseline (n=32) and sequential (n=5) operation in the WWTP effluent and along the SMARTplus bioreactor. The abbreviations 1st prior to the EA and 2nd after the EA indicate the compartments prior to and after the *in-situ* oxygen delivery device.

Turbidity is an indicator for the content of colloidal substances and residual suspended solids in a water source. Since the SMARTplus bioreactor is not designed for backwashing, feed water with higher turbidity values will likely result in clogging issues, which would lead to hydraulic failure of the SMARTplus bioreactor. Normally, the turbidity values for conventional WWTPs are between 1.5-2.0 NTU (Asano et al. 2007), which is required to be reduced further to below 0.5 NTU through tertiary treatment (e.g., RDMF, DynaSand filter coupled with a filter cartridge, etc.) before feeding

into the SMART $plus$ bioreactor. In order to provide the required 0.5 NTU in the feed water, a RDMF was set up at pilot-scale, which, however, could not always comply with the threshold values during the baseline operation. First, the RDMF was upgraded by an inline flocculation device with FeCl₃ dosing. The combination of the RDMF and the adjacent flocculation reduced the turbidity values to 0.65 NTU on average. FeCl₃ dosing concentrations (2.0-3.5 mg/L) were not further increased to not risk the deposition of iron hydroxides in the sand matrix of the RDMF and possibly adversely affecting the hydraulic regime. Despite low dosing concentrations, measurable iron concentrations were observed in the sand samples taken along the SMART $plus$ bioreactor. Iron present in the bioreactor might have been caused by the remobilization of the iron flocs retained in the RDMF under anoxic conditions, caused by high ammonium concentrations. For this reason, a polypropylene filter cartridge and a subsequent DynaSand filter (backwash phase 10 min. and filter phase 10 to 20 min.) with an inline H₂O₂ dosing device (for DOC peaks mitigation and nitrification if required) were provided for pre-treatment. The mean turbidity values could be reduced to 0.75 NTU. For lower turbidity values, the filter media and the cartridge can be exchanged with a finer sand (e.g, d=0.5-1.0 mm instead of 0.7-1.25 mm) and finer filter mesh of 90 μ m instead of 100 μ m. Since smaller grain sizes will increase the filter resistance, an effective diameter of less than 0.5 mm is not recommended for the operation. Beside the turbidity values, ammonium concentrations remained higher than required despite the inline H₂O₂ dosing during the end of the baseline and during the sequential operation, likely due to the construction works at the Garching WWTP plant (Table 8-1).

Table 8-1: The required and measured DOC concentrations (n=32 baseline, n=5 sequential), turbidity values (n=55 baseline, n= sequential) and NH₄⁺-N (n=3 baseline, n=5 sequential) concentrations for WWTP effluent (WWTPe) and SMART $plus$ feed water (SMART $plus$) during baseline and sequential operation. The measured values are given as mean \pm standard deviation.

Parameter	Required	Baseline Operation		Sequential Operation	
	SMART $plus$	WWTPe	SMART $plus$	WWTPe	SMART $plus$
DOC [mg/L]	<10*	12.0 \pm 3.7	10.8 \pm 2.4	8.1 \pm 0.9	7.9 \pm 0.8
Turbidity [NTU]	<0.5	1.7 \pm 0.9	1.2 \pm 0.6	1.5 \pm 0.6	0.8 \pm 0.3
NH ₄ ⁺ -N [mg/L]	<0.5	<0.015	-	4.4 \pm 1.5	1.9 \pm 0.6

*Required during the operation with one EA compartment and without a tertiary treatment with in-line H₂O₂ dosing. If the DOC concentrations are higher than 10 mg/L an enhanced tertiary treatment and a second line of an EA compartment might be required to mitigate DOC peaks.

Since real-time WWTP effluent was used for the operation of the pilot-scale SMART $plus$ bioreactor, the high fluctuations in the inlet water quality (DOC, turbidity) during the pilot-scale operation might also represent operational conditions at field-scale (Table 8-1). The exceptional ammonium problems were caused by construction and operational problems at the WWTP Garching. Usually, after a reliable biological treatment in a conventional WWTP, complete nitrification is expected.

These measurement results reveal the importance of online UV absorbance (as a surrogate for DOC), NH₄⁺-N, and turbidity measurement devices prior to tertiary treatment (RDMF or DynaSand filter)

as well as the SMART*plus* bioreactor, and well-defined procedures in case of non-compliance with the required feed water quality. To prevent suboxic/anoxic conditions after the EA compartment, it is recommended to establish an automated operation of the inline H₂O₂ dosing device based on especially online UVA but also NH₄⁺-N measurement devices located before the DynaSand filter. Nevertheless, H₂O₂ should be dosed carefully to prevent the inhibition of the biofilm in the tertiary treatment or degassing. In case of high ammonium peaks, immediate nitrification cannot be provided due to the low abundance of nitrifying bacteria in the secondary treated effluent. Therefore, partial circulation of the SMART*plus* bioreactor might be considered for pilot-scale to dampen the ammonium concentrations in the feed water during such periods. For the field-scale application, complete nitrification in the WWTP or within the tertiary treatment must be guaranteed. Such measures, i.e. reliable tertiary treatment and online measurement devices, would ensure compliance with the required feed water quality after the re-commissioning of the pilot-scale SMART*plus* bioreactor as well as for the field-scale applications.

8.2.2.2. *Characterization and monitoring of the hydraulic conditions*

Due to the dimensions of the 3D-flume at pilot-scale, the SMART*plus* bioreactor could be operated at a maximum flow rate of 1.2 m³/h. For higher flow rates, the cross section of the pilot-scale bioreactor as well as the height and/or the cross section of the infiltration trench must increase. To investigate the transferability and maximum hydraulic loads at which the plug-flow conditions can be maintained, tracer tests have been conducted in addition to flows of 0.3 m³/h, 0.45 and 0.6 m³/h (Figure 8-2). Already at a flow of 0.45 m³/h, double-peaks were observed despite the hydraulic optimizations, which were presumably caused by rapid movement of the tracer through the narrow gap between the upper part of the bioreactor and the PVC cover plate on top (Figure 8-2). The plume short-circuiting on the top of the SMART*plus* bioreactor could sink within the EA compartment filled with filter media and result in higher hydraulic conductivities, which were indeed subsequently measured by CTD4 located after the EA compartment and downwards (Figure 8-2).

This effect was not observed during the operation at 0.3 m³/h due to slightly lower water levels. Since the bioreactor cover was utilized to mimic confined saturated aquifer conditions within the pilot-scale prototype, such a factor is not expected to cause any hydraulic problems at field-scale. However, with every new flowrate tested within the desired filtration capacity, the limits of the bioreactor can be identified also for field-scale application. Therefore, future applications of such a bioreactor design should explicitly consider not only the desired and maximum operational flowrates, but also the flow field along the bioreactor at the desired flowrate range in order to guarantee the required treatment efficiency. To assess whether or not homogenous flow conditions can be provided at field, tracer tests should be conducted for the desired flowrate range, and abstraction well operation can be modified to optimize hydraulic conditions accordingly.

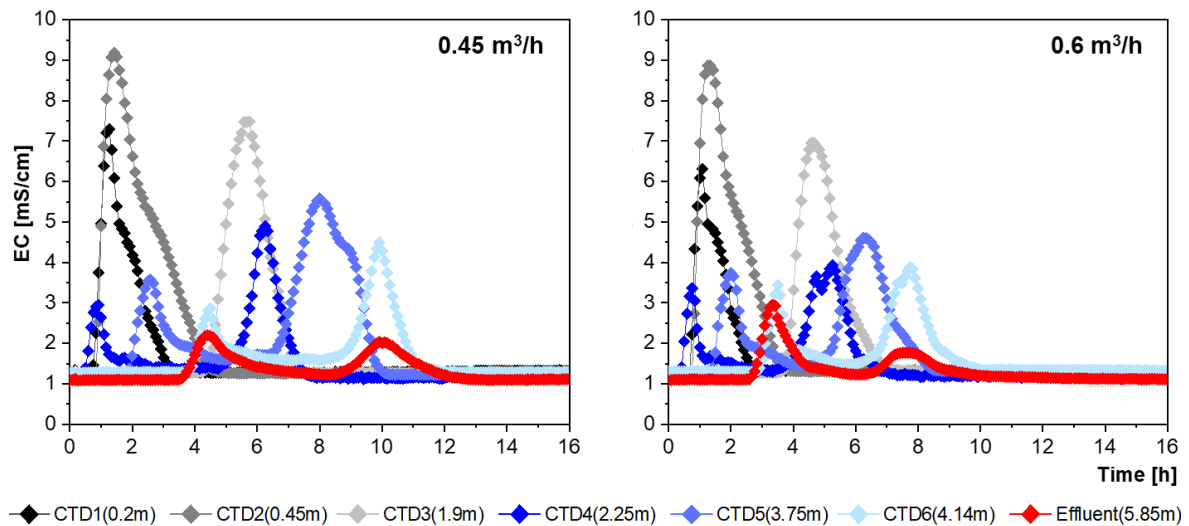


Figure 8-2: Transport of the KBr tracer with a dosing concentration of 8 mg/L along the SMARTplus bioreactor during pulse injections of 30 min., conducted at 0.45 and 0.6 m³/h. The distances are expressed in x direction.

Colmation is one of the main problems in the filtration processes used for water treatment. Strong biofilm growth, caused by inflow water with high nutrient content (e.g., DOC and NH₄⁺), can change the permeability of such a system at pilot- or field-scale during continuous operation (see Chapter 8.2.2.1). The proposed operation of the tertiary treatment with in-line H₂O₂ dosing can also hinder the excessive biofilm growth caused, by frequent DOC peaks. Otherwise as mentioned, colmation can be caused by suspended solids (turbidity >0.5 NTU) in the feed water and iron/manganese precipitates in the sand matrix (>1 % iron/manganese per kg sand, while technical sand contains 0.56% iron), leading to reductions in the permeability of the filter material, areas with fast or slow filter velocities, and thus the deterioration in the homogenous flow conditions. Due to greater sand volumes required at field-scale applications, the usage of natural soil might become more attractive for operators. However, the heterogeneities in the soil matrix would result in preferential flow paths. Moreover, the iron and manganese in the soil matrix might precipitate under changing redox conditions during the commissioning phase of a field-scale SMARTplus application if constructed with natural soil. Besides, operational interruptions at field-scale applications could also cause iron and manganese precipitation, since reduced groundwater might immobilize iron and manganese ions resulting in their intrusion into the flow path during disturbances in the confined saturated conditions and might come into contact with the EA compartment. The experiences gained during the operation of the pilot-scale SMARTplus bioreactor, constructed with technical sand, already demonstrate the difficulties in maintaining controlled hydraulics. Therefore, it is recommended to utilize technical sand with high uniformity instead of natural soil.

The scalability of the SMARTplus bioreactor, i.e. its applicability to the field-scale, depends mainly on successfully maintaining controlled hydraulics. The water levels along the bioreactor should be continuously monitored with CTD sensors to pre-detect and localize any aging phenomena. The

continuous measurements of the water levels recorded by the CTD sensors over a period of 1.5 years are shown in Figure 8-3. Aging phenomena occur at high flow velocities especially at the transition areas from coarser to finer material (e.g., at the transition between the infiltration trench (CTD1) to after the horizontal biofilter (CTD2), and before (CTD4) and after (CTD5) the EA compartment, Figure 8-3). Moreover, the area after the EA compartment might be exposed to strong biofilm growth due to high oxygen concentrations, depending on nutrient availability. These transition areas should therefore be easily accessible for a possible exchange of the filter media in case of clogging, which can be physically separated from the rest of the filter media with the help of a proper stainless steel grate without causing pressure drops.

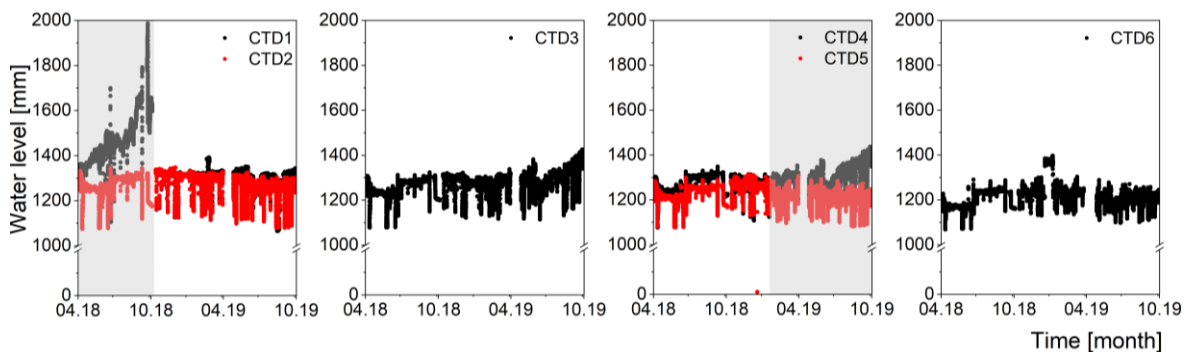


Figure 8-3: The water levels along the SMARTplus bioreactor between April 2018 and October 2019 at 300 L/h. The grey backgrounds show the time periods with the occurrence of colmation in the infiltration trench (left) and after the EA compartment (right). The data gaps were caused by online measurement errors. CTD3 and CTD6 displayed less and no change due to colmation, respectively.

8.2.3. Future research needs

The results from these investigations confirmed the viability of the two key features of the SMARTplus bioreactor. The high-rate infiltration trench technology coupled with horizontal biofilter and the *in-situ* oxygen delivery device were capable of providing hydraulic and environmental conditions required for enhanced TO_rC and virus attenuation. Both technologies can also be used individually to improve the performance of conventional MAR and SMART systems, e.g., for rapid infiltration of treated water into the aquifer, to avoid cross contamination, to decrease the physical footprint and to provide favorable oxic conditions *in-situ*. Already during the baseline operation, better virus removal as well as similar to improved TO_rC biotransformation could be achieved, demonstrating the effects of controlled hydraulics. However, the impact of *in-situ* oxygen delivery device on the attenuation of microbial and chemical constituents was not fully demonstrated, justifying further investigations during a steady-state sequential operation.

A long-term monitoring of the *in-situ* oxygen delivery device and the operational stability was not possible to assess due to the aforementioned operational disturbances. First of all, a detailed analysis is recommended to determine the oxygen delivery rates and characterize the distribution of the oxygen during the operation with tap water. For this assessment, DO can be considered as a plume,

continuously introduced by the EA compartment and the distribution can be simulated by a 3D groundwater model. Additional DO sensors can be placed after the EA compartment at two cross-sections to experimentally evaluate whether the oxygen distribution is homogenous and to validate the model results. For this, a second multi-channel Oxygen Meter (PreSens GmbH, Germany) might be required to be able to continuously log the additional sensors. During the operation with tap water, multiple point values per day can be also logged by hand measurement devices, which can be sufficient to characterize the distribution and the homogeneity of the DO concentrations due to the absence of the water quality fluctuations. Moreover, different designs for the gas-liquid membrane contactors and the contactor assembly (i.e., increased numbers perforations or improved design of the contactor assembly without the MWs) can be further assessed to enhance the oxygen delivery. In addition, different operational modes, such as continuous versus pulse oxygen delivery can be used to minimize the operational costs during the operation with low DOC concentrations. Given the high concentrations of dissolved oxygen right after the EA compartment, clogging issues might occur once the feed water is switched from tap to tertiary effluent due to simultaneous nutrient availability, thus increase biofilm growth. These effects might be negligible if the feed water is fully nitrified and the DOC concentrations are below 8 mg/L. However, concerning the DOC fluctuations in the feed water (Figure 8-1), long-term operation of the EA compartment and its effects on the biofilm development and hydraulics should be characterized in detail during future investigations. For this purpose, the CTD 3 and 4 sensors should be well calibrated and a discrepancy in their measurement values, i.e., a continuous increase in the water levels measured by the CTD 4 sensor, should be used to detect the pressure losses due to the biofilm growth.

Instead of pure oxygen, *in-situ* ozone delivery, containing typically 15% O₃ and 85% O₂, might be used to provide an additional barrier against especially chemicals and as well as for pathogens (Merle et al., 2017; Nimmer et al., 2000). Although ozone has been shown to effectively reduce pathogen concentrations, the contact time in the EA compartment and the difficulties in the 100% homogenous *in-situ* gas introduction would lead to less LRVs in comparison to typical ozone disinfection units. To date, for *in-situ* ozone delivery, porous membranes have been utilized, which can be used only under constant pressure on the liquid side to eliminate bubble formation or pore wetting (Merle et al., 2017). As utilized for the *in-situ* oxygen delivery device, gas permeable dense silicone membranes, e.g., PDMS, can be also used, which might degrade under continuous operation with ozone (Berry et al., 2017). However, the lifetime durability of PDMS membranes during continuous operation has not been determined yet, thus, long-term lab-scale studies focusing on the durability of PDMS material during operation with ozone should be conducted prior to field-scale application. Moreover, high doses of ozone or fluctuating water quality might result in the intrusion of remaining ozone into the biofilter after the EA compartment, which would likely react within the first centimeters of the biofilter. Therefore, an inhibition of the microbial community after the EA compartment is not expected. On the contrary, since the reaction of refractory DOC with ozone

results in the formation of easily degradable carbon sources (Bourgin et al., 2018), even higher biofilm growth might be observed after the EA compartment, which needs to be considered regarding the applicability of *in-situ* ozonation for the SMART*plus* bioreactor. Therefore, the maximum feasible ozone dosing concentration and effects of remaining ozone on the biofilm should be studied with the help of lab-scale column experiments filled with porous media. Due to the fast reaction of ozone, the configuration of the membrane conductors should be adapted to be able to improve the chemical removal but also to benefit from the disinfection capacity of ozone. This might be achieved by reducing the distance between the two membrane modules to less than the recommended distances given by the borehole dilution theory for non-reactive compounds (Wilson et al., 1997). The maximum feasible distance for a successful chemical oxidation and disinfection, as well as the minimum required distance to avoid concentration polarization can be determined with the help of CFD (Kavousi et al., 2016). An additional second row of membrane modules could ensure the effectiveness of the ozonation, which should also be placed closer to the first row in the configuration determined by the CFD model. Finally, comprehensive process evaluation including the formation of TPs and toxicity assessment should be conducted in case of *in-situ* ozone delivery (Bourgin et al., 2018; Völker et al., 2019).

After the proposed long-term investigations on the feasibility of the *in-situ* oxygen delivery, a detailed analysis on its scalability would be required to assess the applicability of the proposed technology at field-scale. Overall, the major benefits of the *in-situ* oxygen delivery via gas-liquid membrane contactors are the following: effective oxygen transfer due to sealed modules resulting in no losses and thus minimum oxygen demand in comparison to gas sparging; tailored oxygen dosing and control options; and maintaining controlled hydraulics. Namely, pumping and re-infiltration of the treated water for *ex-situ* applications would lead to the destruction of the plug-flow conditions. The re-establishment of the controlled hydraulics would not be possible at field-scale in short distances, which would then affect the overall physical footprint of the proposed SMART*plus* technology. To determine whether the benefits of the *in-situ* oxygen delivery would justify the investment and maintenance costs, a comparison with the pumping and investment costs related to place requirements of reference biofilters operated with *ex-situ* aeration can be undertaken.

The growth, metabolism and functionality of microbial communities play a key role in the performance of such systems, as they are based on natural attenuation processes such as biotransformation (Li et al., 2012; Li et al., 2013; Li et al., 2014). Once the required steady-state oxic and oligotrophic conditions are established by *in-situ* oxygen or ozone delivery after the EA compartment, a better understanding of the microbial community composition (taxonomy analysis) and its genetic functions can help to identify the metabolic and/or co-metabolic transformation for a large number of different TOxCs within the SMART*plus* bioreactor operating with real-time tertiary effluent. While metagenome analysis can provide information about available species present in the

samples, more information on the transcriptional activity of genes can be gained by metatranscriptome analyses (Hassa et al., 2018; Simon and Daniel, 2011). In future studies, these investigations can be conducted via batch studies with the sand taken from the SMART*plus* bioreactor.

Dynamic process control options for the on-site tertiary treatment, i.e. an optimized DynaSand filter with smaller grain size, and for the SMART*plus* bioreactor might provide additional flexibility related to the WWTP effluent quality while maintaining the required process performance. The inline H₂O₂ dosing can be attuned to the WWTP effluent by real-time UVA and NH₄⁺-N measurements. For the SMART*plus* bioreactor, the measurement values of both UVA and NH₄⁺-N but also the online DO sensors can be used. The fluctuating influent water quality and DO depletion rates within the infiltration trench can be fed to a machine learning algorithm to determine correlations. For this purpose, additional DO sensors can be placed within and right after the infiltration trench, in thinner self-tailored monitoring wells (d10) composed of fine stainless-steel mesh. Based on the developed correlation, an input parameter (e.g., DO values at the infiltration trench and/or UVA values of feed water) can be selected to maintain the DO concentrations above 1 mg/L (set point) at the effluent by attuning the partial pressure (control factor) of the membrane contactors.

A preliminary assessment of the costs, carbon and physical footprint demonstrated that SMART*plus* based advanced treatment train (SMART*plus* with *in-situ* O₂ or O₃ delivery/GAC/UV/MAR) has lower costs than MF/RO/UV-AOP based full-advanced treatment (Kebinger et al., in review). Although this assessment underlined the low process complexity, lower operational and investment costs of the proposed treatment train than advanced membrane-based treatment trains, a more comprehensive study coupled with life cycle analysis is required for a better evaluation of the SMART*plus* technology. This evaluation should include the benefits but also the bottlenecks of the SMART*plus*, regarding the capital and operational costs, the sensitivity in maintaining the hydraulics and its scalability. Finally, the proposed SMART*plus* based advanced treatment train should be compared with other non-high-pressure-membrane based IPR and DPR schemes, which rely specifically on GAC/BAC filters followed by disinfection with chlorine or ozone (Hooper et al., 2020). Such an assessment would furthermore highlight the pros and cons of the SMART*plus* based advanced treatment train in comparison to other non-membrane based applications.

9. Supplementary Information

9.1. Peer-reviewed journal articles and author contributions

9.1.1. Published and submitted manuscripts

1. **Karakurt-Fischer, S.;** Rien, C.; Sanz-Prat, A.; Szewzyk, R; Hübner, U.; Drewes, J.E; Selinka, H.C., 2021. Fate and transport of viruses within a high rate plug-flow biofilter designed for non-membrane based indirect potable reuse applications. *Environmental Science & Technology Water* (under review).

Author contributions: Sema Karakurt-Fischer, Hans-Christoph Selinka, Uwe Hübner and Jörg E. Drewes conceptualized the research objective. Sema Karakurt-Fisher designed the experiment and constructed the experimental set-up. Sema Karakurt-Fisher, Christian Rien and Hans-Christoph Selinka conducted the experiments and the analyses. Sema Karakurt-Fisher wrote the paper. Alicia Sanz-Prat simulated the conservative tracer transport. Hans-Christoph Selinka, Jörg E. Drewes, Uwe Hübner, Christian Rien, Alicia Sanz-Prat, and Regine Szewzyk critically reviewed the manuscript. All authors approved the final version of the manuscript.

2. **Karakurt-Fischer, S.;** Bein, E.; Drewes, J.E.; Hübner, U., 2020. Characterizing a novel *in-situ* oxygen introduction device for establishing controlled redox zonation within a high infiltration rate biofilter. *Water Research* 182, 116039.

Author contributions: Sema Karakurt-Fischer, Uwe Hübner and Jörg E. Drewes conceptualized the research objective. Sema Karakurt-Fisher designed the pilot-scale experimental set-up, conducted the experiments and analysis, and wrote the paper. Sema Karakurt-Fisher and Emil Bein constructed the lab-scale experimental setups, conducted the experiments and the data analyses. Uwe Hübner, Jörg E. Drewes and Emil Bein critically reviewed the manuscript. All authors approved the final version of the manuscript.

3. **Karakurt-Fischer, S.;** Sanz-Prat, A.; Greskowiak, J.; Ergh, M.; Gerdes, H.; Massmann, G.; Ederer, J.; Regnery, J.; Hübner, U.; Drewes, J.E., 2020. Developing a novel biofiltration treatment system by coupling high-rate infiltration trench technology with a plug-flow porous-media bioreactor. *Science of the Total Environment* 722, 137890.

Author contributions: Sema Karakurt-Fischer, Uwe Hübner and Jörg E. Drewes conceptualized the research objective. Sema Karakurt-Fischer and Jürgen Ederer constructed the experimental setup. Sema Karakurt-Fisher designed and conducted the experiments and the analyses. Alicia Sanz-Prat and Martin Ergh simulated the tracer transport. Heiko Gerdes, Gudrun Massmann and Julia Regnery supervised the study. Sema Karakurt-Fischer and Alicia Sanz-Prat wrote the paper. Jörg E. Drewes,

Uwe Hübner and Janek Greskowiak critically reviewed the paper. All authors approved the final version of the manuscript.

4. **Karakurt, S.**; Schmid, L.; Hübner, U.; Drewes, J.E., 2019. Dynamics of wastewater effluent contributions in streams and impacts on drinking water supply via riverbank filtration in Germany – A national reconnaissance. *Environmental Science & Technology* 53 (11), 6154-6161.

Author contributions: Sema Karakurt-Fischer and Jörg E. Drewes conceptualized the research objective and designed the methodology. Sema Karakurt-Fischer and Ludwig Schmid collected and analyzed the data. Sema Karakurt-Fischer applied and validated the models and wrote the paper. Jörg E. Drewes and Uwe Hübner critically reviewed the manuscript. All authors approved the final version of the manuscript.

9.1.2. Manuscript in preparation

Sanz-Prat, A.; **Karakurt-Fischer, S.**; Greskowiak, J.; Hübner, U.; Drewes, J.E; Massmann, G., *in preparation*. Model assessment of oxygen-dependent degradation of 12 trace organic compounds in a novel biofiltration treatment system. *To be submitted in Environmental Science and Technology*.

Author contributions: Alicia Sanz-Prat, Gudrun Massmann and Janek Greskowiak developed the research objective. Jörg E. Drewes, Uwe Hübner and Sema Karakurt-Fischer designed the experiment set-up. Sema Karakurt-Fischer conducted the SMART*plus* bioreactor pilot-scale experiments. Alicia Sanz-Prat modelled the degradation of trace organic chemicals. Alicia Sanz-Prat wrote the paper. Uwe Hübner, Jörg E. Drewes, Sema Karakurt-Fischer, Janek Greskowiak and Gudrun Massmann critically reviewed the manuscript. All authors approved the final version of the manuscript.

9.2. Conference papers, reports and German article

9.2.1. Conference papers

1. **Karakurt, S.**; Schmid, L.; Hübner, U.; Drewes, J.E., 2019. The status of de facto potable reuse – A national reconnaissance of Germany. 12th IWA International Conference on Water Reclamation and Reuse, Berlin, Germany.
2. **Karakurt, S.**; Sanz-Prat, A.; Ergh, M.; Hübner, U.; Drewes, J.E., 2019. Coupling high-rate infiltration trench technology with a plug-flow bioreactor (SMART*plus*) for indirect potable reuse via groundwater recharge. 12th IWA International Conference on Water Reclamation and Reuse, Berlin, Germany.
3. Drewes, J.E., Zhiteneva, V., **Karakurt, S.**, Schwaller, C., Hübner, U., 2019. Risk management in water reuse – International perspectives and approaches for Germany. *Wasserkreisläufe neu*

denken, 20./21. Februar 2019 in Braunschweig. 14. Niedersächsisches Grundwasserkolloquium, 6. International Symposium RE-WATER Braunschweig. Schweizerbart, Stuttgart.

9.2.2. Reports

1. Drewes, J.E.; **Karakurt, S.**; Schmid, L.; Bachmaier, M. Hübner, U., 2018. Dynamik der Klarwasseranteile in Oberflächengewässern und mögliche Herausforderungen für die Trinkwassergewinnung in Deutschland-UBA Abschlussbericht.
2. Drewes, J.E.; Hübner, U.; Zhiteneva, V.; **Karakurt, S.**, 2017. Characterization of Unplanned Water Reuse in the EU. Technical University of Munich (Prepared for the European Commission DG Environment).

9.2.3. German article

Helmecke, M.; Drewes, J.E.; **Karakurt, S.**; Hübner, U.; Timmermann, R., 2018. Klarwasser in Flüssen: Herausforderung für die Trinkwassergewinnung, DVGW energie | wasser-praxis.

9.3. First author contributions to national and international conferences

9.3.1. Presentations

1. **Karakurt, S.**; Sanz-Prat, A.; Ergh, M.; Rien, C.; Selinka, H.C.; Hübner, U.; Drewes, J.E., 2019. Coupling high-rate infiltration trench technology with a plug-flow bioreactor (SMART $plus$) for indirect potable reuse via groundwater recharge. 12th IWA International Conference on Water Reclamation and Reuse, Germany.
2. **Karakurt, S.**; Schmid, L.; Hübner, U.; Drewes, J.E., 2019. The status of de facto potable reuse – A national reconnaissance of Germany. 12th IWA International Conference on Water Reclamation and Reuse, Germany.
3. **Karakurt, S.**; Sanz-Prat, A.; Greskowiak, J.; Ergh, M.; Gerdes, H.; Massmann, G.; Rien, C.; Selinka, H.C.; Hübner, U.; Drewes, J.E., 2019. Kopplung der modifizierten Sickerschlitzen Technologie mit einem Plug-Flow-Bioreaktor Konzept (SMART $plus$) zur indirekten Wasserwiederverwendung durch Grundwasseranreicherung. Jahrestagung der Wasserchemischen Gesellschaft, Germany.
4. **Karakurt, S.**; Hellauer, K.; Hübner, U.; Jekel, M.; Drewes, J.E., 2017. Großtechnische Validierung der sequentiellen Grundwasseranreicherung. Jahrestagung der Wasserchemischen Gesellschaft, Germany.

9.3.2. Poster

Karakurt, S.; Schmid, L.; Timmermann, R.; McCurdy, S.; Hübner, U.; Helmecke, M.; Drewes, J.E., 2018. Abschätzung der Relevanz einer ungeplanten Wasserwiederverwendung und deren

Einfluss auf die Trinkwasserversorgung in Deutschland. Jahrestagung der Wasserchemischen Gesellschaft, Germany.

9.4. Supplementary information for Chapter 4

Dynamics of wastewater effluent contributions in streams and impacts on drinking water supply via riverbank filtration in Germany – A national reconnaissance

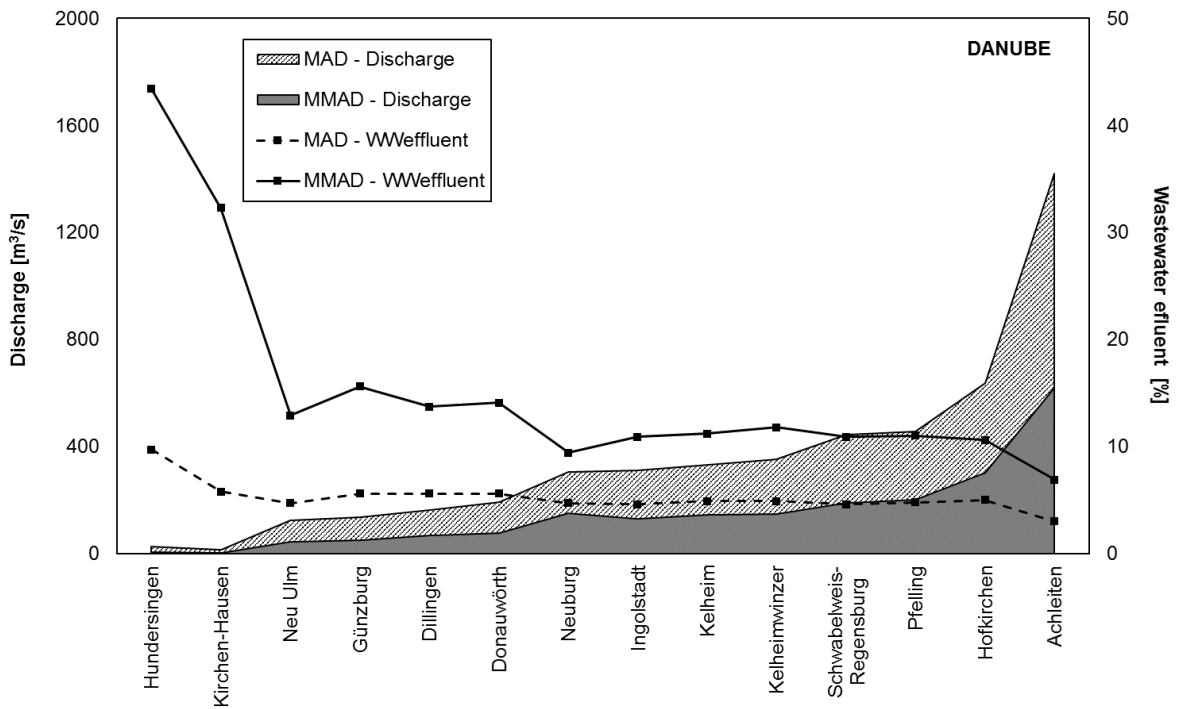
Sema Karakurt, Ludwig Schmid, Uwe Hübner, Jörg E. Drewes*

The Chair of Urban Water Systems Engineering, Technical University of Munich, Am Coulombwall 3, 85748 Garching, Germany

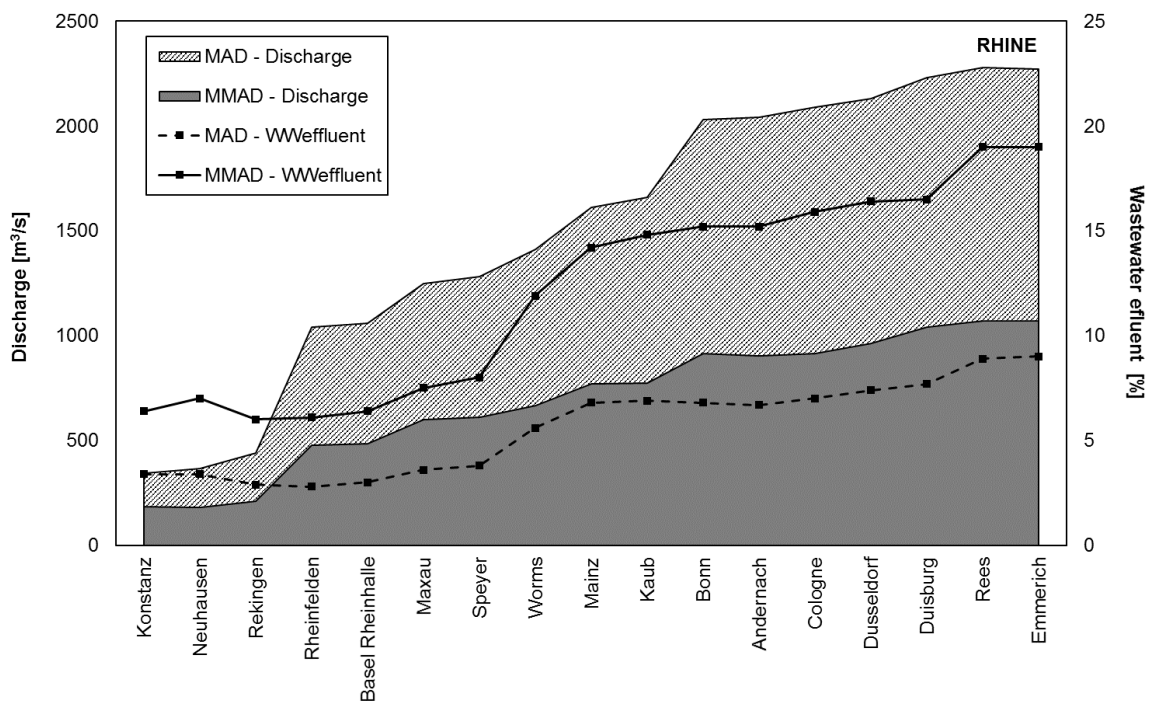
Jörg E. Drewes (jdrewes@tum.de, corresponding author)

SI-Table 9.4-1: Description and source of WWTP data for each federal states.

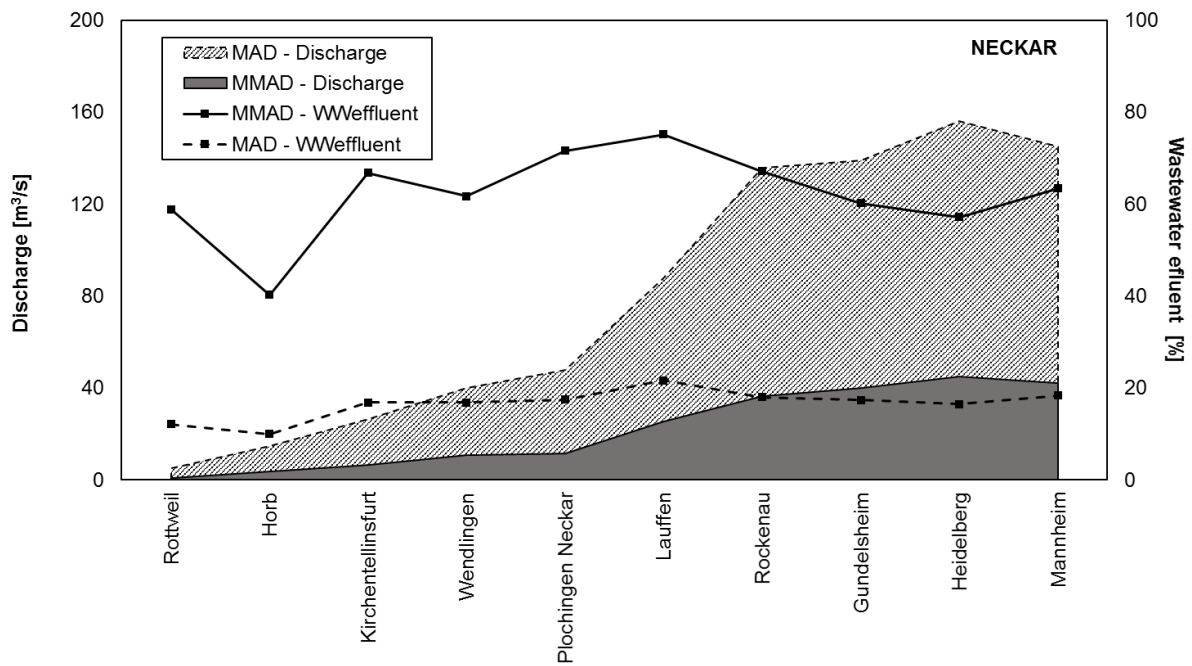
Federal States	Description	Source
Baden-Württemberg	WWTPs with a PE>50, mean WWTP effluent discharge value from 2010-2014.	Data provided by the federal state.
Bavaria	WWTPs with a PE>2000, WWTP effluent discharge value from 2016.	Thru.de
	WWTPs with a 50<PE<2000, WWTP effluent calculated from design size of the plants (2014).	Data provided by the federal state.
Berlin	WWTPs with a PE>50, mean WWTP effluent discharge value from 2007-2012.	Data provided by the Berlin water company.
Brandenburg	WWTPs with a PE>50, mean WWTP effluent discharge value from 2015.	Data provided by the federal state.
Hesse	WWTPs with a PE>50, mean WWTP effluent discharge value from 2007-2015.	Data provided by the federal state.
North Rhine-Westphalia	WWTPs with a PE>50, mean WWTP effluent discharge value from 2007-2015.	Data provided by the federal state.
Rhineland-Palatinate	WWTPs with a PE>50, mean WWTP effluent discharge value from 2007-2015.	Data provided by the federal state.
Saxony	WWTPs with a PE>50, mean WWTP effluent discharge value from 2012-2016.	Data provided by the federal state.
Bremen	WWTPs with a PE>2000, WWTP effluent discharge value from 2016.	Thru.de
Hamburg	WWTPs with a PE>2000, WWTP effluent discharge value from 2016.	Thru.de
Mecklenburg-Vorpommern	WWTPs with a PE>2000, WWTP effluent discharge value from 2016.	Thru.de
Lower Saxony	WWTPs with a PE>2000, WWTP effluent discharge value from 2016.	Thru.de
Saarland	WWTPs with a PE>2000, WWTP effluent discharge value from 2016.	Thru.de
Saxony-Anhalt	WWTPs with a PE>2000, WWTP effluent discharge value from 2016.	Thru.de
Schleswig-Holstein	WWTPs with a PE>2000, WWTP effluent discharge value from 2016.	Thru.de
Thuringia	WWTPs with a PE>2000, WWTP effluent discharge value from 2016.	Thru.de



SI-Figure 9-1: Discharge values and wastewater effluent contributions at the gauging stations along the river Danube under MMAD and MAD conditions.



SI-Figure 9-2: Discharge values and wastewater effluent contributions at the gauging stations along the river Rhine under MMAD and MAD conditions.



SI-Figure 9-3: Discharge values and wastewater effluent contributions at the gauging stations along the river Neckar under MMAD and MAD conditions.

Contributions of direct industrial discharges: An assessment of the relevance of direct industrial discharges was performed using data from North Rhine Westphalia, Germany's largest industrial region, based on the data and information provided by [MKULNV \(2014\)](#). In 2014, 458 out of 1,305 industrial direct dischargers discharged wastewater or process water, whereas the remaining 847 industrial complexes discharged unpolluted cooling water or storm water into a water body. In comparison, 22,440 industrial indirect dischargers were registered, for which wastewater was collected via a public sewer and released to a water body after treatment in a municipal WWTP. Based on these findings, the majority of industrial discharges is being considered in our study.

9.5. Supplementary information for Chapter 5

Developing a novel biofiltration treatment system by coupling high-rate infiltration trench technology with a plug-flow porous-media bioreactor

Sema Karakurt-Fischer^a, Alicia Sanz-Prat^b, Janek Greskowiak^b, Martin Ergh^c, Heiko Gerdes^c, Gudrun Massmann^b, Jürgen Ederer^a, Julia Regnery^a, Uwe Hübner^{a*}, Jörg E. Drewes^a

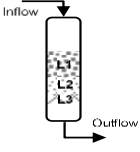
^aThe Chair of Urban Water Systems Engineering, Technical University of Munich, Garching, Germany.

^bCarl von Ossietzky University of Oldenburg, Institute for Biology and Environmental Sciences, Working Group Hydrogeology and Landscape Hydrology, Oldenburg, Germany.

^cBGS Umwelt GmbH, Darmstadt, Germany.

Uwe Hübner (u.huebner@tum.de, corresponding author)

SI-Table 9.5-1: Specifications of the dual-media filter ($d=44$ cm). Effective flow velocity (v_e) and hydraulic retention time (HRT) were characterized based on an influent flowrate of 300 L/h.



Layer	Depth [cm]	Media	Porosity [%]	v_e [m^3/m^2h]	HRT [min]
L1	45	Anthracite	0.50	4.53	6.03
L2	25	Sand	0.43	5.27	2.93
L3	10	Gravel	0.40	5.67	1.09

SI-Table 9.5-2: Feed water concentrations of all quantified TORCs during the baseline operation. Mean values are given with standard deviation; TORCs concentrations $< 4*LOQ$ were excluded.

TORCs (n=8-9)	LOQ [ng/L]	Mean [ng/L]	Median [ng/L]
Trimethoprim	5	48 ± 24	45
4-FAA	10	479 ± 176	420
Gabapentin	2.5	1397 ± 414	1342
Climbazole	5	166 ± 70	142
Sulfamethoxazole	5	260 ± 190	210
Citalopram	5	175 ± 39	199
Metoprolol	5	286 ± 35	292
Diclofenac	5	1052 ± 97	1037
Benzotriazole	50	5921 ± 1485	5746
Venlafaxine	2.5	409 ± 36	423
Carbamazepine	5	459 ± 60	450
Tramadol	5	198 ± 19	201

SI-Table 9.5-3: Empirically estimated and calibrated hydraulic conductivities in the SMARTplus bioreactor.

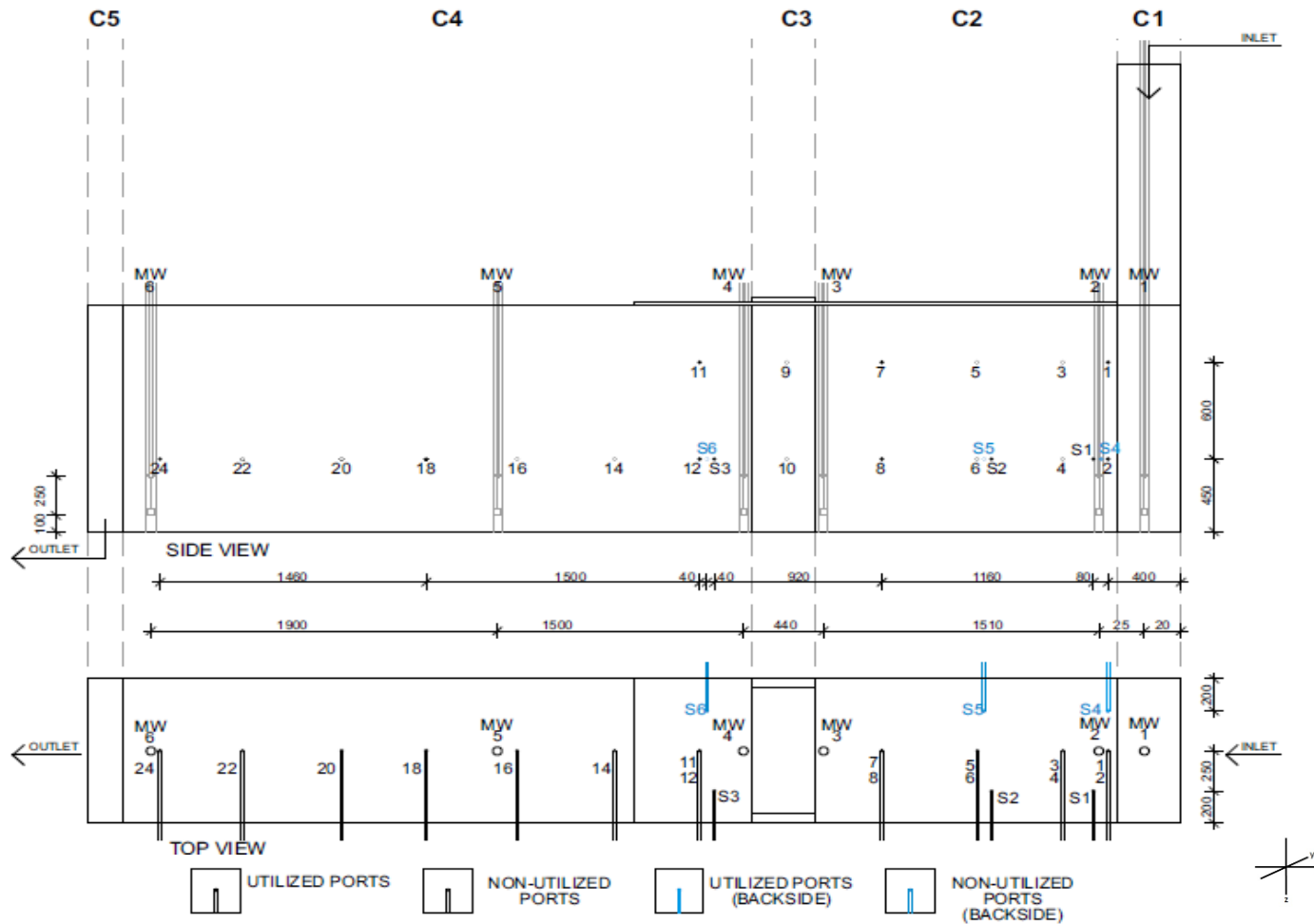
Compartment	Empirical hyd. Conductivity [m/s]	Calibrated hyd. conductivity [m/s]
C1 – Infiltr. Trench (Sand)	6.50E-03	5.00E-03
C1 – Infiltr. Trench (Gravel)	1.30E-01	3.11E-01
C2 – Prior to EA Compartment	6.50E-03	4.38E-03
C3 – EA Compartment	5.60E-02	6.40E-02
C4 – After EA Compartment	6.50E-03	5.50E-03
C5 – Outlet Compartment	1.30E-01	1.88E-01

SI-Table 9.5-4: Principal hydraulic, transport and numerical model parameters.

Name	Symbol	Value	units
Longitudinal dispersivity	α_l	0.02	m
Horizontal transverse dispersivity	α_{ht}	0.002	m
Vertical transverse dispersivity	α_{vt}	0.0002	m
Effective porosity flow (for the whole domain)	ε	0.5	-
Initial Time Step (SPRING)	Δt	0.5	min
Final simulation time (SPRING)	T_{end}	1720	min
Thickness of strictly parallel layers (SPRING)	L	0.02	m
Number of triangular volume element layers (SPRING)	$N_{elem-layer}$	72	-
Total number of triangular volume elements (SPRING)	N_{elem}	1.5818.480	
Number of node layers (SPRING)	$N_{node-layer}$	73	-
Total Number of nodes (SPRING)	N_{nodes}	795.408	-

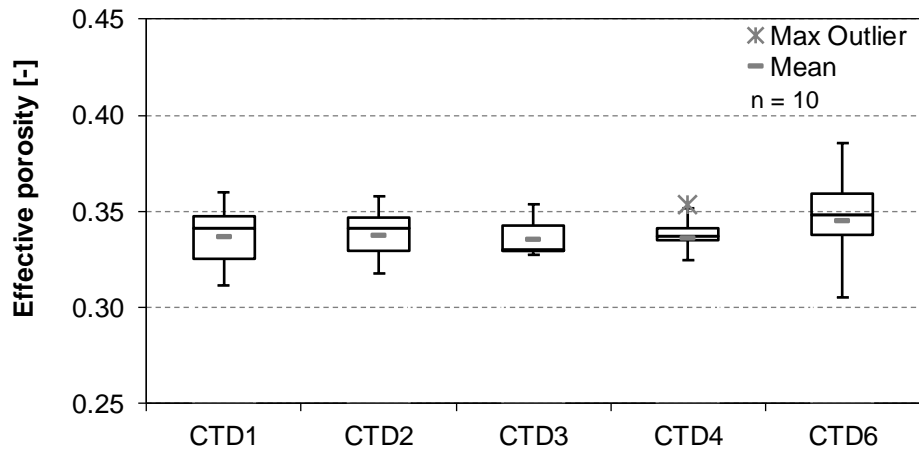
SI-Table 9.5-5: Estimation of the hydraulic residence times (HRT) at each observation point derived from truncated temporal moment of the simulated breakthrough curves based on a steady input concentration in the SMARTplus bioreactor (Luo et al., 2006).

Observation Point	Simulated HRT [hr.]
CTD1	2.87
CTD2	3.19
CTD3	7.09
CTD4	7.52
CTD5	10.29
CTD6	13.34
Port 1	0.44
Port 2	1.17
Port S1	1.47
Port S4	1.46
Port 7	3.22
Port 8	3.91
Port 11	8.98
Port 12	7.01
Port S3	7.20
Port 18	9.87
Port 24	12.32
Effluent	12.63

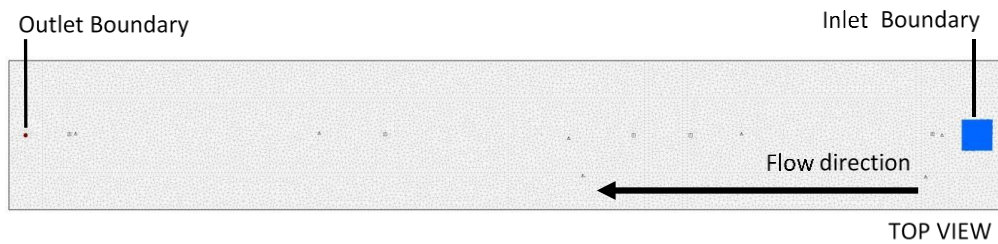


Port / MW	CTD-1	1	2	S4	CTD2	S1	3	4	S2	S5	5	6	7	8	CTD3	9	10	CTD4	S3	S6	11	12	14	16	CTD5	18	20	22	24	CTD6	Outflow	
Compartment	C1	C2	C2	C2	C2	C2	C2	C2	C2	C2	C2	C2	C2	C2	C2	C3	C3	C4	C4	C4	C4	C4	C4	C4	C4	C4	C4	C4	C4	C4	C4	C5
x [mm]	200	400	400	440	450	480	640	640	1060	1100	1140	1140	1640	1640	1900	2140	2140	2250	2560	2600	2640	2640	3140	3640	3750	4140	4640	5140	5600	5650	5850	
y [mm]	450	450	450	700	450	200	450	450	200	700	450	450	450	450	450	450	450	450	200	700	450	450	450	450	450	450	450	450	450	450	450	
z [mm]	100	1050	450	450	100	450	1050	450	450	450	1050	450	1050	450	100	1050	450	100	450	450	1050	450	450	450	100	450	450	450	450	100	0	

SI-Figure 9-4: Side and top view of the SMARTplus bioreactor together with the locations of the respective compartments, sampling ports and monitoring wells (MWs i.e. CTDs) at x, y and z coordinates in mm. Utilized sampling ports for the tracer tests and system monitoring are indicated in bold.



SI-Figure 9-5: Effective porosities in the bioreactor, derived by monitoring the partial changes in the fluid volume within the bioreactor at different times during the unsteady flow tests. Mean porosity of 0.35 was used as initial value in the numerical model.



SI-Figure 9-6: Numerical scheme of the true three-dimensional finite-element grid: top view of the volume elements and nodes at each layer, inflow (blue area) and outflow (red dot) boundaries.

9.6. Supplementary information for Chapter 6

Fate and transport of viruses within a high rate plug-flow biofilter designed for non-membrane based indirect potable reuse applications

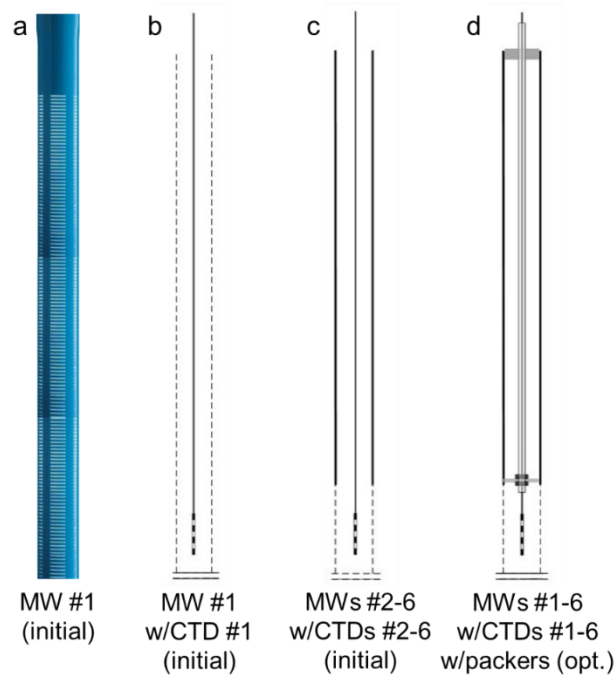
Sema Karakurt-Fischer^a, Christian Rien^b, Alicia Sanz-Prat^c, Regina Szewzyk^b, Uwe Hübner^a, Jörg E. Drewes^a, Hans-Christoph Selinka^{b*}

^aThe Chair of Urban Water Systems Engineering, Technical University of Munich, Germany

^bGerman Environment Agency, Environmental Hygiene, Microbiological Risks, Germany

^cBiology and Environmental Sciences, Carl von Ossietzky University of Oldenburg, Germany

Hans-Christoph Selinka (hans-christoph.selinka@uba.de, corresponding author)



SI-Figure 9-7: Initial (a, b and c) and optimized (opt.) configuration of MWs #1-6 with the packers and CTDs #1-6 (d).

SI-Table 9.6-1: Attenuation of naturally occurring surrogate (*F+* phages and somatic coliphages, $n=3$) and indicator viruses (*HuAdV* and *HuNV*, $n=2$) in the WWTP, RDMF and SMARTplus pilot bioreactor. While the LRVs for the indicator viruses are mean values, the LRVs for surrogate viruses were given as two individual values.

	F⁺ Phages	Som. coliphages	HuAdV	HuNV
Raw sewage conc.	$5.5 \pm 4.9 \cdot 10^5$ (pfu/L)	$9.7 \pm 7.2 \cdot 10^6$ (pfu/L)	$1.6-3.3 \cdot 10^5$ (gc/L)	$0.8-2.9 \cdot 10^6$ (gc/L)
LRVs	WWTP	1.6 ± 1.7	1.9 ± 0.5	1.0 / 1.0
	RDMF	0.4 ± 0.3	0.6 ± 0.4	1.3 / 0.4
	SMARTplus	$\geq 2.2 \pm 1.3$	$\geq 3.0 \pm 1.4$	$\geq 3.1 / 4.2$
	Total	$\geq 4.2 \pm 2.2$	$\geq 5.5 \pm 2.0$	$\geq 5.3 / 5.7$

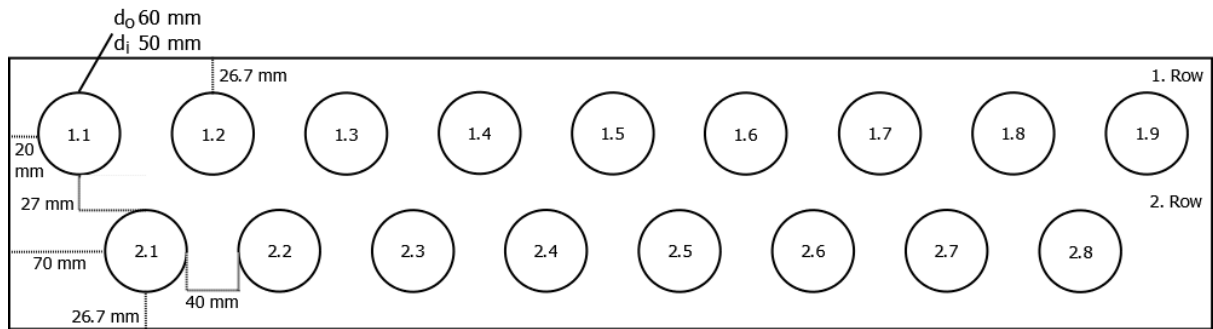
9.7. Supplementary information for Chapter 7

Characterizing a novel *in-situ* oxygen delivery device for establishing controlled redox zonation within a high infiltration rate sequential biofilter

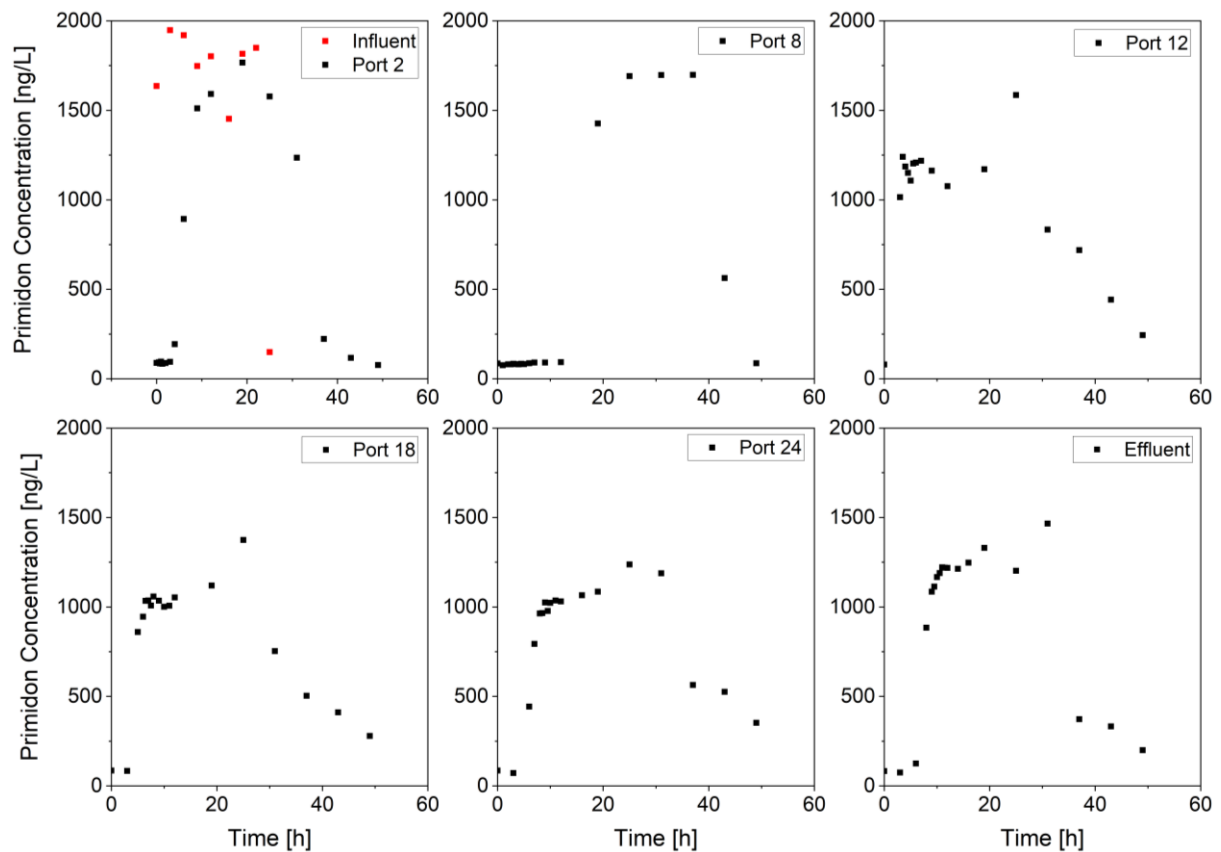
Sema Karakurt-Fischer, Emil Bein, Jörg E. Drewes, Uwe Hübner*

*The Chair of Urban Water Systems Engineering, Technical University of Munich, Garching, Germany.

Uwe Hübner (u.huebner@tum.de, corresponding author)



SI-Figure 9-8: The configuration of the contactor assembly with location of the infiltration wells (top view). The length of the infiltration wells are 1.1: 1190 mm; 1.2: 1288 mm; 1.3: 1386 mm; 1.4: 1390 mm; 1.5: 1390 mm; 1.6: 1390 mm; 1.7: 1386 mm; 1.8: 1288 mm; 1.9: 1190 mm; 2.1: 1239 mm; 2.2: 1337 mm; 2.3: 1390 mm; 2.4: 1390 mm; 2.5: 1390 mm; 2.6: 1390 mm; 2.7: 1337 mm; 2.8: 1239 mm.



SI-Figure 9-9: Breakthrough curves of conservative tracer primidone along the SMARTplus bioreactor following a pulse tracer test. The influent concentrations indicate the tracer concentrations in the feed water. The effluent BTC is the ensemble response at the bottom of the bioreactor. The coordinates of the sampling ports of the SMARTplus bioreactor are given at x (length), y (penetration depth) and z (height) coordinates in mm as follows: Port 2 (400, 450, 450); Port 8 (1640, 450, 450); Port 12 (2640, 450, 450); Port 18 (4140, 450, 450); Port 24 (5600, 450, 450); Effluent (5850, 450, 0).

9.8. Conference paper related to Objective #1

The following manuscript was published in the conference proceedings of the “12th IWA International Conference on Water Reclamation and Reuse”, held from 17.–20.06.2019 in Berlin, Germany.

The status of de facto potable reuse – A national reconnaissance of Germany

S. Karakurt, L. Schmid, U. Hübner, J.E. Drewes

The Chair of Urban Water Systems Engineering, Technical University of Munich,

Am Coulombwall 3, 85748 Garching, Germany; sema.karakurt@tum.de

Abstract

The contributions of wastewater treatment plant (WWTP) effluent discharges in surface water can become relevant for downstream drinking water supply via bank filtration, if health-based monitoring trigger levels (MTL) of wastewater-derived chemicals are exceeded in bank-filtered water. This study represents the first national reconnaissance quantifying WWTP effluent contributions under low and average discharge conditions in German rivers based on an automated assessment using ArcGIS as well as its consequences on indirect usage as drinking water source. In urban areas with sparse natural discharge, WWTP effluent contributions of more than 30-50% were determined under low flow conditions. By applying a conceptual model, critical bank filtrate shares were estimated resulting in MTL exceedances for health-relevant chemicals.

Keywords: bank filtration; *de facto* reuse; drinking water supply; health relevant trace organic chemicals; potable water reuse; surface water augmentation

Introduction

In many countries worldwide, drinking water supply heavily relies on indirect use of surface water via induced bank filtration (IBF) and aquifer recharge (AR). Especially in highly populated areas and where substantial natural base discharge is lacking, microbiological and chemical quality of surface water can be substantially affected by contributions from various point and non-point sources (e.g., WWTP effluents, agricultural drainages) (Bradley et al., 2016; Glassmeyer et al., 2005; Hass et al., 2012; Reemtsma et al., 2016). Considering more frequent or extended low-flow conditions in streams due to climate change impacts, this situation will likely become more prevalent in the future in many regions worldwide.

Occurrence of WWTP effluent in a stream that is subsequently used for drinking water abstraction has been previously referred to as *de facto* potable water reuse (NRC, 2012; Rice and Westerhoff, 2015). High WWTP effluent contributions in streams, which are used as a source of drinking water supply, have been documented nationwide in the USA and in a few regional scale studies by simple flow balances (Mujeriego et al., 2017; Rice and Westerhoff, 2015; Wang et al., 2017). So far, these studies did not consider the removal efficacy of drinking water treatment or naturally occurring attenuation processes during IBF and AR, both reducing the consumer exposure to contaminants. Assessing the degree of impact of WWTP effluents on drinking water quality is not trivial since it requires an understanding of stream flow dynamics, attenuation processes in the subsurface, and contributions of augmented groundwater in a drinking water production well. This comprehensive study is the first to quantify nationwide the relative contribution of WWTP effluents to streams under varying discharge conditions and to provide a conceptual impact assessment of *de facto* reuse for downstream drinking water abstraction via bank filtration or aquifer recharge.

Material and Methods

Long-term mean annual discharge (MAD) and mean minimum annual discharge (MMAD) from gauging stations at rivers in Germany and relevant streams in neighboring countries were gathered. The spatial and operational data for more than 7,700 WWTPs (i.e., location of the WWTP, point and amount of discharge, capacity and level of treatment) and stream gauging station runoff data of the German national river network were incorporated into an ArcGIS data model in collaboration with DHI WASY.

The WWTP effluents upstream of a river segment were cumulated and assigned to the following gauging station. The percentage of WWTP effluent contribution at each individual gauging station ($WW_{effluent} [\%]$) was then determined for MAD and MMAD conditions by calculating the ratio of the total discharge rate of upstream WWTPs ($\sum Q_{WW\ effluent}$) and the discharge data at the respective gauging station ($Q_{gauging\ station}$) using equation 9.1, which was coded into GIS using Python scripts. For rivers with more than two gauging stations, the MAD or MMAD along a river were first determined by linear interpolation, and the relative WWTP effluent contributions were subsequently calculated for these fictitious gauging stations with varying discharge conditions by the automated assessment as described. Due to lack of data, direct discharge of industrial WWTPs, agricultural drainage, and combined sewer and stormwater overflows were not included into this assessment. In addition, complete mixing at the point of discharge of WWTP effluent into the receiving river was assumed.

$$WW_{effluent} [\%] = \frac{\sum Q_{WW\ effluent}}{Q_{gauging\ station}} \cdot 100\% \quad [9.1]$$

There are no uniform databases of the origin and quality of raw water of individual waterworks available in Germany. For this reason, instead of a nationwide impact assessment, a conceptual approach estimating the relevance of elevated WWTP effluent contributions in rivers, coupled with the percent bank filtrate in raw water was developed. Conservative health relevant wastewater-derived chemicals, present at elevated concentrations in wastewater effluents and exhibiting persistent behavior under aerobic-anoxic conditions, were considered as indicator chemicals (Dickenson et al., 2011; Funke et al., 2015). Pathogenic risks were not considered in this study since German waterworks commonly apply IBF or AR with hydraulic retention times > 50 days, which can be considered an effective barrier for pathogens. For WWTP effluent contribution scenarios ranging from 0-100%, critical bank filtrate contributions (% $BF_{critical}$) in drinking water wells (i.e. raw water) were determined where monitoring trigger levels (MTLs) of indicator chemicals ($MTL_{indicator\ chemical}$) in raw water could be exceeded applying equation 9.2. If advanced treatment processes are employed subsequent to the conventional treatment processes (i.e., ozonation, activated carbon filtration), these processes might provide additional barriers to health-relevant chemicals and therefore additional margins of safety.

$$\text{Min. \% } BF_{critical} = \frac{MTL_{indicator\ chemical}}{\% WW_{effluent} * C_{WW\ effluent\ indicator}} * 100\% \quad [9.2]$$

Results and Discussion

Based on the results of this study, the contributions from WWTP effluents during MAD conditions vary only between 0-5% for more than 50% of the gauging stations of individual river basins nationwide except for the Neckar river basin, where more than 90% of the gauging stations exceeded 5% wastewater contributions also at MAD conditions (SI-Table 9.8-1). However, contributions from more than 20% are still dominating in river basins up- and downstream of urban centers, as well as river stretches characterized by generally low-discharge conditions, e.g. Rhine, Neckar, Main and Havel. During MMAD conditions, WWTP effluent contributions of more than 20% are dominating nationwide in a large number of river basins, e.g. Neckar, Rhine, Ems, Weser and Main. 60% of gauging stations in Neckar and more than 20% of gauging stations in Rhine and Ems exhibit WWTP effluent contributions of even more than 50% under MMAD conditions, which often prevail for longer periods between May and September.

Critical bank filtrate shares in wells, in which the MTL values for each of the three indicator chemicals (i.e., oxypurinol, OXY; carbamazepine, CBZ; valsartanic acid, VSA) are exceeded, were calculated for different WWTP effluent contributions ranging from 0-100%. Based on this conceptual approach, the MTL of oxypurinol exhibiting high average WWTP effluent concentrations would be exceeded in a scenario with only 5% bank filtrate and 60% WWTP effluent contribution in the stream. For carbamazepine, which exhibited lower WWTP effluent concentrations, MTL

exceedances would occur when both the WWTP effluent contribution to the stream and the bank filtrate share were about 60%. Where elevated WWTP effluent contributions dominate, elevated concentration of conservative health relevant chemicals can be expected in abstraction wells. For sites where the determined bank filtrate shares and relative effluent contributions would suggest potential exceedances of health advisory values, *de facto* reuse conditions were confirmed and additional mitigation measures should be taken.

SI-Table 9.8-1: Distribution of the WWTP effluent contributions for the selected river basins under MMAD and MAD discharge for all gauging stations (data shown as % gauging stations exceeding specific contributions).

River basins	MMAD Conditions			MAD Conditions		
	>5%	>20%	>50%	>5%	>20%	>50%
Neckar	98	96	60	91	23	0
Rhine	73	51	25	45	8	2
Ems	68	49	22	46	4	0
Weser	72	34	12	35	4	0
Main	72	44	7	41	1	0
Havel	38	17	9	15	4	3
Elbe-Saale	44	19	2	19	2	1
Danube	43	8	2	12	1	0
Eastern coastal area	27	7	2	2	1	1

Conclusions

The findings of this study reveal a high degree of WWTP effluent impact on streams, which also serve as an important source for drinking water abstraction, industrial usage or irrigation purposes, particularly in urbanized areas across Germany. The developed conceptual approach provides a universal qualitative assessment for any location worldwide to qualify possible *de facto* reuse conditions. With the assistance of this conceptual approach, possible hot spots of *de facto* reuse can be identified, if the site-specific data on indicator chemical concentrations in WWTP effluent and the degree of bank filtration are known. The proposed workflow can guide water utilities and regulators to assess the impact of wastewater-derived contaminations and to identify sites where comprehensive monitoring and additional mitigation strategies are needed to assure proper risk management.

9.9. Conference paper related to Objective #2

The following manuscript was published in the conference proceedings of the “12th IWA International Conference on Water Reclamation and Reuse”, held from 17.–20.06.2019 in Berlin, Germany.

Coupling high-rate infiltration trench technology with a plug-flow bioreactor (SMARTplus) for indirect potable reuse via groundwater recharge

S. Karakurt^a, A. Sanz-Prat^b, M. Ergh^c, U. Hübner^a, J.E. Drewes^a

^aThe Chair of Urban Water Systems Engineering, Technical University of Munich, Garching, Germany; sema.karakurt@tum.de;

^bInstitute for Biology and Environmental Sciences, Carl von Ossietzky University of Oldenburg, Oldenburg, Germany;

^cBGS Umwelt GmbH, Darmstadt, Germany

Abstract

Biotransformation of TOxCs during managed aquifer recharge (MAR) can be enhanced through provision of oxic and oligotrophic conditions by the sequential MAR technology (SMART), combining two infiltration steps with an intermediate aeration. Major bottlenecks impeding the widespread application of MAR and SMART in indirect potable reuse are their performance heterogeneity due to site-specific factors and large physical footprint. The aim of this study was to design and test the performance of a novel technology, SMART^{plus}, based on SMART that can be deployed independent of local hydrogeological conditions with a significantly reduced physical footprint, controlled redox zonation, and *in-situ* oxygen delivery for enhanced pathogen and TOxC removal.

Keywords: SMART, plug-flow bioreactor, indirect potable reuse, infiltration trench technology, trace organic chemicals, groundwater recharge

Introduction

Augmentation of drinking water supplies with reclaimed water via an environmental buffer, known as indirect potable reuse (IPR), reduces the dependency and burden on seasonally and climatically changing conventional water sources by shortening the natural hydrological replenishment cycle (Drewes and Khan, 2011). Given the origin of the source water used in IPR schemes, contaminants of concern (e.g., pathogenic microorganisms, trace organic chemicals, etc.) must be removed by reliable and redundant treatment processes to their threshold values and the water quality should be

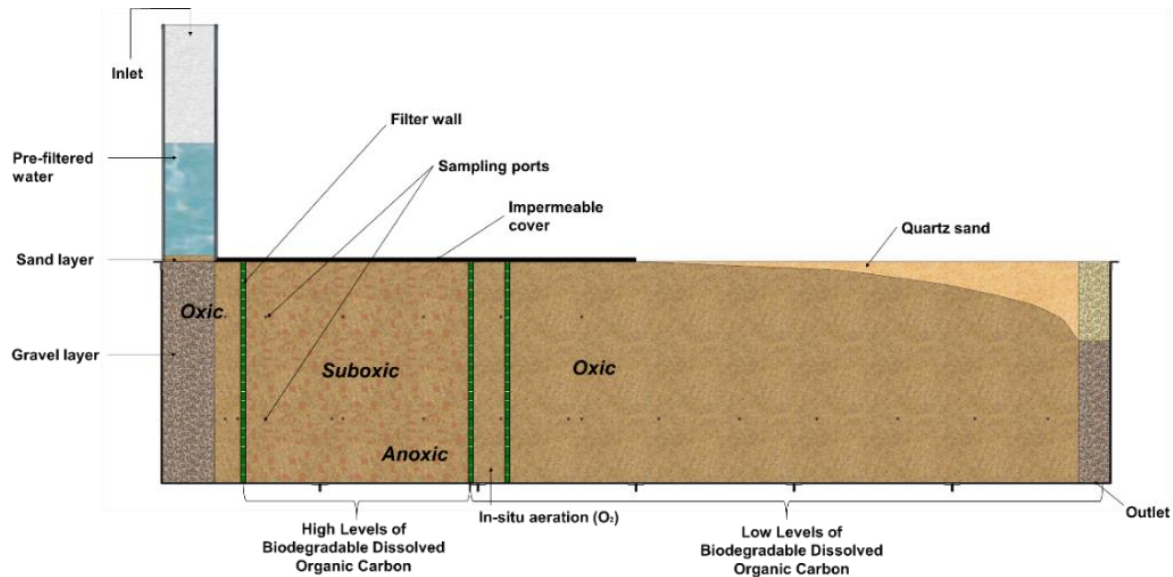
monitored closely. For this reason IPR design is characterized by multi-barrier approaches by applying combinations of advanced water treatment processes (e.g., membrane filtration, activated carbon adsorption, advanced chemical oxidation and biological treatment) and an environmental buffer providing additional retention and storage function prior to use (National Research Council, 2012). Low-energy managed aquifer recharge (MAR) systems such as soil-aquifer treatment take advantage of natural attenuation processes for chemical and microbial contaminants without any residual generation and chemical addition, while damping varying concentrations, and in many cases resulting in dilution with other water sources (Dillon, 2005; Drewes and Khan, 2011; Sharma and Amy, 2011). The interaction of different removal mechanisms (such as biotransformation, filtration, adsorption and ion exchange) in managed aquifer recharge (MAR) systems provides effective removal of many trace organic chemicals (TOrcs) and offers efficient inactivation of pathogens, especially viruses or protozoa. Previous studies demonstrated that carbon-limited and oxic conditions are favorable for enhanced trace organic chemical transformation (Hoppe-Jones et al., 2012; Rauch-Williams et al., 2010). To take advantage of these favorable conditions, sequential MAR technology (SMART) combining two infiltration steps with an intermediate aeration was developed and validated at pilot- and full-scale in the USA and Germany for the production of drinking water from surface waters impaired by wastewater effluents (Hellauer et al., 2018a; Regnery et al., 2015a).

Conventional MAR systems and the SMART concept commonly employ open recharge basins to facilitate infiltration of water through the vadose zone, which requires large physical areas and suitable subsurface conditions. In order to establish a sequence of controlled redox conditions during subsequent travel through the saturated zone, homogeneous flow conditions are required. Whereas native subsurface environments are usually characterized by a high degree of site specific heterogeneity, which makes the technology and performance transfer of both MAR systems difficult. Building upon this previous research, the aim of this study was to modify the overall design and improve performance of the SMART concept by an engineered approach that can be deployed independent of local hydrogeological conditions with a significantly reduced physical footprint. This novel SMART_{plus} concept is utilizing high-rate infiltration trench technology followed by a biofiltration system with plug-flow conditions characterized by highly controlled redox zonation and an *in-situ* introduction of electron acceptors as well as online monitoring and control systems. To provide plug-flow conditions and homogenous flow patterns, granular filter media with a high uniformity coefficient is employed in SMART_{plus} bioreactor. Since uncontrolled flow and mixing with native groundwater is not desired, the SMART_{plus} concept is designed to be hydraulically decoupled from the native groundwater.

Material and Methods

The SMART_{plus} bioreactor consists of a stainless steel tank (6.0 m length x 0.85 m width x 1.4 m height) with five compartments (C1-5), divided by steel mesh sheets (SI-Figure 9-10). A shaft

(0.35 x 0.85 x 1.5 m) is placed on top of the bioreactor at the influent side (C1) mimicking the infiltration trench. Water is distributed at the top of the shaft through a screened PVC pipe, which allows uniform distribution of feed water. A cover plate is used to seal the first 300 cm of the bioreactor. Along the entire length of the bioreactor, 24 sampling ports are installed at different heights and penetration depths.



SI-Figure 9-10: Schematic of the SMARTplus bioreactor tested at pilot-scale.

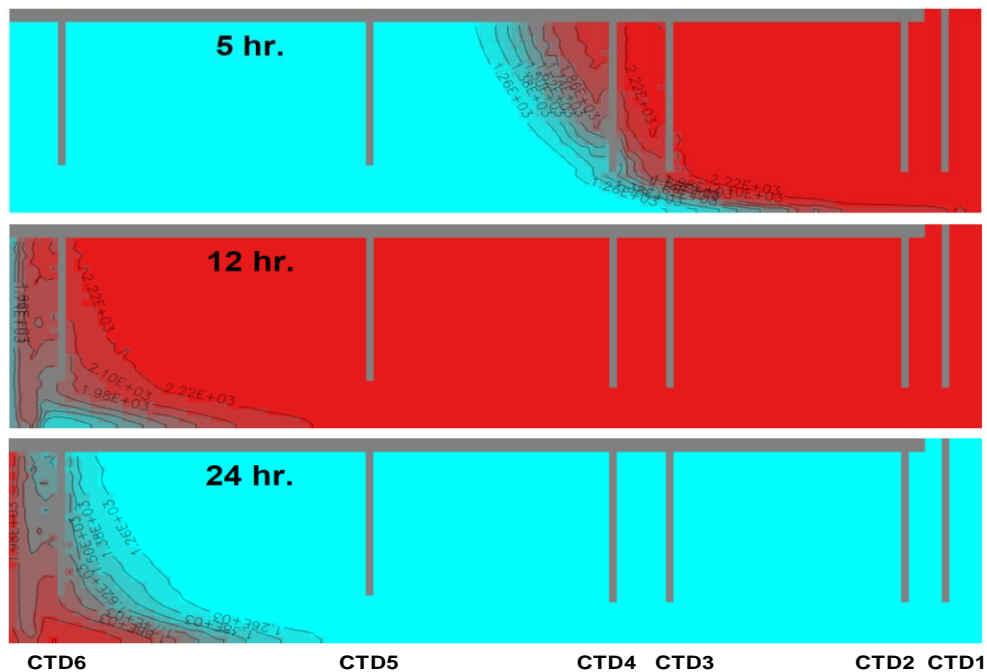
The bioreactor was continuously fed with tertiary effluent ($Q_{SMART}=300$ L/h) from a WWTP for more than 24 months in baseline operation. Sequential operation with *in-situ* introduction of oxygen has been initiated recently. To allow rapid vertical infiltration rates and establish plug flow among the SMARTplus bioreactor, the first compartment (C1, infiltration trench) is filled with gravel ($d_{10}=3.40$ mm) and with a thin sand layer ($d_{10}=0.75$ mm) on the top for the retention of any residual suspended solids. C2 and C4 (1st and 2nd infiltration step) are filled with technical sand ($d_{10}=0.75$ mm). C3 (electron acceptor compartment) is filled with gravel ($d_{10}=2.1$ mm) and the perforated infiltration wells, in which the oxygen permeable membrane conductors are submerged. The last compartment C5 is filled with gravel ($d_{10}=3.4$ mm) to allow high drainage rates. In addition, temperature, conductivity, water level and dissolved oxygen are continuously monitored in 6 PVC monitoring wells along the bioreactor and UV absorbance can be monitored at the influent and effluent of the system.

A 3-D hydraulic flow model was developed to determine the hydraulic retention time (HRT) and characterize the flow field and velocity distribution in the bioreactor. In order to improve the hydraulic parameters taken from the literature by numerical calibration and to validate 3D-Model an impulse tracer test with potassium bromide (Merck, Global) solution was conducted at a constant flow rate of 300 L/h for 12 hours. The tracer dosing was followed by conductivity monitoring every 10 minutes at 6 CTD sensors and effluent for 24 hours.

Water samples were collected weekly to bi-weekly based on estimated HRT in the SMART $plus$ at the inlet and outlet of the bioreactor, as well as at the end of the infiltration trench (distance from inlet: 40 cm; depth: 45 cm) and 1st infiltration step (164 cm; 45 cm) for ammonia, nitrate, bulk organic parameters and TOrCs. The DOC samples were analyzed by a vario TOC cube analyzer (Elementar, Germany). The UVA₂₅₄ was measured on a DR 6000™ UV-VIS spectrophotometer (Hach Lange, Germany). Nitrate and ammonia concentrations were determined by cuvette tests LCK 339 and 304 (Hach Lange, Germany) with a DR 6000™ UV-VIS spectrophotometer. TOrCs were quantified using HPLC-MS/MS (Sciex QTRAP5500 & Triple Quad6500) following the method described by Müller et al. (2017).

Results and Discussion

3D-model results represent a good fitting of the breakthrough curves with experimental data and revealed an average HRT of 11.5 hours. The snapshots at three different times during the simulation of the 12 hours pulse tracer test along the longitudinal cross section in the middle of the SMART $plus$ bioreactor are depicted in SI-Figure 9-11, indicating that the hydraulic conditions are closely approximating plug flow conditions.



SI-Figure 9-11: Spatial distribution of the tracer plume at three different times after pulse injection started. The red area corresponds with the high concentration of bromide, and the blue area with the background concentration.

The concentrations of DO, nitrate, DOC and TOrC in the feed water and along the bioreactor measured between a six months period are summarized in SI-Table 9.9-1. The feed water quality parameters strongly fluctuate due to the continuous feeding of the SMART $plus$ bioreactor with tertiary effluent. Within the first year of operation, microbial activity indicated by dissolved oxygen

measurements, significantly increased resulting in complete depletion of oxygen within the first compartment prior to sequential operation. No nitrate reduction (<0.5 mg N/L) and absence of dissolved oxygen (<1 mg/L DO) underlined the presence of suboxic conditions along the rest of the bioreactor. Different indicator trace organic chemicals, representing different degrees of biodegradability (trimethoprim and gabapentin: efficient removal, diclofenac: poor removal, carbamazepine: persistent), showed clear and consistent removal during the baseline operation prior to introduction of dissolved oxygen.

SI-Table 9.9-1: Average DO (n=15,512), DOC, and NO₃⁻-N (n=10-12) concentrations in feed water, at the end of the infiltration trench, 1st infiltration step and in the effluent between April-September 2018 during baseline operation of the SMARTplus bioreactor. The percent removals of TOrCs (n=10-12) are calculated by the TOrC concentrations at the infiltration trench, 1st infiltration step and bioreactor effluent normalized to corresponding feed water concentrations.

	Feed water concentrations	Infiltration trench	1st infiltration step	Effluent / Entire bioreactor
DO	5.1 ± 1.8 mg/L	1.0 ± 0.9 mg/L	0.0 ± 0.0 mg/L	0.0 ± 0.0 mg/L
NO₃⁻-N	12.6 ± 2.3 mg/L	12.7 ± 2.3 mg/L	12.8 ± 2.4 mg/L	12.7 ± 2.4 mg/L
DOC	10.2 ± 2.4 mg/L	8.1 ± 2.0 mg/L	7.8 ± 1.8 mg/L	7.5 ± 2.0 mg/L
Trimethoprim	45 ± 24 ng/L	85 ± 13 %	82 ± 11 %	85 ± 6 %
Gabapentin	1380 ± 477 ng/L	67 ± 16 %	69 ± 15 %	69 ± 17 %
Diclofenac	1027±113 ng/L	20 ± 8 %	17 ± 12 %	22 ± 16 %
Carbamazepine	453 ± 66 ng/L	< 5 %	< 5 %	< 5 %

Conclusions

The performance of the tracer experiments and their modeling results confirmed the establishment of quasi plug flow conditions under moderate flowrates in the SMARTplus bioreactor while applying infiltration trench technology and homogenous porous media. Plug flow conditions enables to control well defined redox zonation along the bioreactor to provide a homogenous water quality with enhanced TOrC removal. Establishment of SMARTplus bioreactor at pilot scale provided sound and reliable proof of concept regarding realization of plug flow conditions under high infiltration rates and *in-situ* redox zonation. Further investigations are planned to prove long-term removal of pathogen and chemical contaminants under sequential operation as well as different infiltration rates.

References

- Abegglen, C., Siegrist, H., 2012. Mikroverunreinigungen aus kommunalem Abwasser: Verfahren zur weitergehenden Elimination auf Kläranlagen. Bundesamt für Umwelt BAFU. Umwelt-Wissen 1214, Bern, 210 pp. www.bafu.admin.ch/uw-1214-d.
- Ahmed, T., Semmens, M.J., 1992. Use of sealed end hollow fibers for bubbleless membrane aeration: experimental studies. *Journal of Membrane Science* 69 (1-2), 1–10.
- Ahmed, T., Semmens, M.J., Voss, M.A., 2004. Oxygen transfer characteristics of hollow-fiber, composite membranes. *Advances in Environmental Research* 8 (3-4), 637–646.
- Alcalde-Sanz, L., Gawlik, B.M., 2014. Water Reuse in Europe: Relevant guidelines, needs for and barriers to innovation. A synoptic overview. Joint Research Centre, Luxembourg, 51 pp.
- Alcalde-Sanz, L., Gawlik, B.M., 2017. Minimum quality requirements for water reuse in agricultural irrigation and aquifer recharge: Towards a legal instrument on water reuse at EU level. Joint Research Centre, Luxembourg, 63 pp.
- Alidina, M., Li, D., Ouf, M., Drewes, J.E., 2014. Role of primary substrate composition and concentration on attenuation of trace organic chemicals in managed aquifer recharge systems. *Journal of Environmental Management* 144, 58–66.
- Al-saffar, H.B., Ozturk, B., Hughes, R., 1997. A Comparison of Porous and Non-Porous Gas-Liquid Membrane Contactors for Gas Separation. *Chemical Engineering Research and Design* 75 (7), 685–692.
- Altmann, J., Ruhl, A.S., Zietzschmann, F., Jekel, M., 2014. Direct comparison of ozonation and adsorption onto powdered activated carbon for micropollutant removal in advanced wastewater treatment. *Water Research* 55, 185–193.
- Anderson, W.B., DeLoyde, J.L., van Dyke, M.I., Huck, P.M., 2009. Influence of design and operating conditions on the removal of MS2 bacteriophage by pilot-scale multistage slow sand filtration. *Journal of Water Supply: Research and Technology-Aqua* 58 (7), 450–462.
- ARW, 2016. 73. Jahresbericht.
- Asano, T., Burton, F.L., Leverenz, H., Tsuchihashi, R., Tchobanoglous, G., 2007. *Water Reuse : Issues, Technologies, and Applications: Issues, Technologies, and Applications*. McGraw Hill professional. McGraw-Hill.

- Bae, J., Schwab, K.J., 2008. Evaluation of murine norovirus, feline calicivirus, poliovirus, and MS2 as surrogates for human norovirus in a model of viral persistence in surface water and groundwater. *Applied and Environmental Microbiology* 74 (2), 477–484.
- Barbieri, M., Carrera, J., Ayora, C., Sanchez-Vila, X., Licha, T., Nödler, K., Osorio, V., Pérez, S., Köck-Schulmeyer, M., López de Alda, M., Barceló, D., 2012. Formation of diclofenac and sulfamethoxazole reversible transformation products in aquifer material under denitrifying conditions: batch experiments. *Science of the Total Environment* 426, 256–263.
- Barcelona, M.J., Xie, G., 2001. In situ lifetimes and kinetics of a reductive whey barrier and an oxidative ORC barrier in the subsurface. *Environmental Science & Technology* 35 (16), 3378–3385.
- Bauer, R., Dizer, H., Graeber, I., Rosenwinkel, K.-H., López-Pila, J.M., 2011. Removal of bacterial fecal indicators, coliphages and enteric adenoviruses from waters with high fecal pollution by slow sand filtration. *Water Research* 45 (2), 439–452.
- Bazhenov, S.D., Bildyukevich, A.V., Volkov, A.V., 2018. Gas-Liquid Hollow Fiber Membrane Contactors for Different Applications. *Fibers* 6 (4), 76.
- Benstoem, F., Nahrstedt, A., Boehler, M., Knopp, G., Montag, D., Siegrist, H., Pinnekamp, J., 2017. Performance of granular activated carbon to remove micropollutants from municipal wastewater- A meta-analysis of pilot- and large-scale studies. *Chemosphere* 185, 105–118.
- Bernot, M.J., Becker, J.C., Doll, J., Lauer, T.E., 2016. A national reconnaissance of trace organic compounds (TOCs) in United States lotic ecosystems. *Science of the Total Environment* 572, 422–433.
- Berry, M., Taylor, C., King, W., Chew, Y., Wenk, J., 2017. Modelling of Ozone Mass-Transfer through Non-Porous Membranes for Water Treatment. *Water* 9 (7), 452.
- Bertelkamp, C., Reungoat, J., Cornelissen, E.R., Singhal, N., Reynisson, J., Cabo, A.J., van der Hoek, J.P., Verliefe, A., 2014. Sorption and biodegradation of organic micropollutants during river bank filtration: A laboratory column study. *Water Research* 52, 231–241.
- Bertelkamp, C., Verliefe, A.R.D., Schoutteten, K., Vanhaecke, L., Vanden Bussche, J., Singhal, N., van der Hoek, J.P., 2016. The effect of redox conditions and adaptation time on organic micropollutant removal during river bank filtration: A laboratory-scale column study. *Science of the Total Environment* 544, 309–318.

- Betancourt, W.Q., Schijven, J., Regnery, J., Wing, A., Morrison, C.M., Drewes, J.E., Gerba, C.P., 2019. Variable non-linear removal of viruses during transport through a saturated soil column. *Journal of Contaminant Hydrology* 223, 103479.
- Beyer, S., Szewzyk, R., Gnirss, R., Johne, R., Selinka, H.-C., 2020. Detection and Characterization of Hepatitis E Virus Genotype 3 in Wastewater and Urban Surface Waters in Germany. *Food and Environmental Virology* 12 (2), 137–147.
- Bieber, S., Snyder, S.A., Dagnino, S., Rauch-Williams, T., Drewes, J.E., 2018. Management strategies for trace organic chemicals in water - A review of international approaches. *Chemosphere* 195, 410–426.
- Bonadonna, L., Briancesco, R., Cataldo, C., Divizia, M., Donia, D., Panà, A., 2002. Fate of bacterial indicators, viruses and protozoan parasites in a wastewater multi-component treatment system. *The New Microbiologica* 25 (4), 413–420.
- Bourgin, M., Beck, B., Boehler, M., Borowska, E., Fleiner, J., Salhi, E., Teichler, R., Gunten, U.v., Siegrist, H., McArdell, C.S., 2018. Evaluation of a full-scale wastewater treatment plant upgraded with ozonation and biological post-treatments: Abatement of micropollutants, formation of transformation products and oxidation by-products. *Water Research* 129, 486–498.
- Bradley, P.M., Barber, L.B., Clark, J.M., Duris, J.W., Foreman, W.T., Furlong, E.T., Givens, C.E., Hubbard, L.E., Hutchinson, K.J., Journey, C.A., Keefe, S.H., Kolpin, D.W., 2016. Pre/post-closure assessment of groundwater pharmaceutical fate in a wastewater-facility-impacted stream reach. *Science of the Total Environment* 568, 916–925.
- Brookes, J.D., Hipsey, M.R., Burch, M.D., Regel, R.H., Linden, L.G., Ferguson, C.M., Antenucci, J.P., 2005. Relative Value of Surrogate Indicators for Detecting Pathogens in Lakes and Reservoirs. *Environmental Science & Technology* 39 (22), 8614–8621.
- Burke, V., Schneider, L., Greskowiak, J., Baar, P., Sperlich, A., Dünnebier, U., Massmann, G., 2018. Trace Organic Removal during River Bank Filtration for Two Types of Sediment. *Water* 10 (12), 1736.
- Casey, E., Glennon, B., Hammer, G., 1999. Oxygen mass transfer characteristics in a membrane-aerated biofilm reactor. *Biotechnology & Bioengineering Journal* 62 (2), 183–192.
- Charati, S.G., Stern, S.A., 1998. Diffusion of Gases in Silicone Polymers: Molecular Dynamics Simulations. *Macromolecules* 31 (16), 5529–2235.

- Clara, M., Strenn, B., Kreuzinger, N., 2004. Carbamazepine as a possible anthropogenic marker in the aquatic environment: investigations on the behaviour of Carbamazepine in wastewater treatment and during groundwater infiltration. *Water Research* 38 (4), 947–954.
- Côté, P., Bersillon, J.-L., Huyard, A., Faup, G., 1988. Bubble-free aeration using membranes: process analysis. *Water Pollution Control Federation* 60 (11), 1986–1992.
- Côté, P., Bersillon Jean-Luc, Huyard Alain, 1989. Bubble-free aeration using membranes: mass transfer analysis. *Journal of Membrane Science* 47 (1-2), 91–106.
- Dickenson, E.R.V., Snyder, S.A., Sedlak, D.L., Drewes, J.E., 2011. Indicator compounds for assessment of wastewater effluent contributions to flow and water quality. *Water Research* 45 (3), 1199–1212.
- Dika, C., Duval, J.F., Francius, G., Perrin, A., Gantzer, C., 2015. Isoelectric point is an inadequate descriptor of MS2, Phi X 174 and PRD1 phages adhesion on abiotic surfaces. *Journal of Colloid and Interface Science* 446, 327–334.
- Dillon, P., 2005. Future management of aquifer recharge. *Hydrogeology Journal* 13 (1), 313–316.
- DIN ISO 10705-1, 1995. Water quality-Detection and enumeration of bacteriophages-Part 1: Enumeration of F-specific RNA bacteriophages.
- DIN ISO 10705-2, 2000. Water quality-Detection and enumeration of bacteriophages-Part 2: Enumeration of somatic coliphages.
- DLZ, 2017. GeoBasis-DE / BKG (accessed 20.11.2017). http://www.geodatenzentrum.de/geodaten/gdz_rahmen.gdz_div?gdz_spr=deu&gdz_akt_zeile=5&gdz_anz_zeile=1&gdz_unt_zeile=1&gdz_user_id=0.
- Drewes, J.E., Anderson, P., Denslow, N., Jakubowski, W., Olivieri, A., Schlenk, D., Snyder, S.A., 2018. Monitoring strategies for constituents of emerging concern (CECs) in recycled water: Recommendations of a science advisory panel. SCCWRP Technical Report 1032 (accessed 3.05.2018). https://www.waterboards.ca.gov/water_issues/programs/water_recycling_policy/docs/2018/final_report_monitoring_strategies_for_cecs_in_recycled_water_april2018.pdf.
- Drewes, J.E., Hübner, U., Zhiteneva, V., Karakurt, S., 2017. Characterization of unplanned water reuse in the EU. European Commission DG Environment, 64 pp.
- Drewes, J.E., Khan, S.J., 2011. Water reuse for drinking water augmentation, in: Edzwald, J.K. (Ed.), *Water Quality & Treatment*, 6th ed. McGraw-Hill, New York, 16.1-16.48.

- Dullemont, Y.J., Schijven, J.F., Hijnen, W., Colin, M., Magic-Knezev, A., Oorthuizen, W.A., 2006. Removal of microorganisms by slow sand filtration: Part 1: General overview, in: Gimbel, R., Graham, N., Colins, M.R. (Eds.), *Recent Progress in Slow Sand and Alternative Biofiltration Processes*. IWA Publishing, pp. 12–20.
- Ebele, A.J., Abou-Elwafa Abdallah, M., Harrad, S., 2017. Pharmaceuticals and personal care products (PPCPs) in the freshwater aquatic environment. *Emerging Contaminants* 3 (1), 1–16.
- Eggen, R.I.L., Hollender, J., Joss, A., Schärer, M., Stamm, C., 2014. Reducing the discharge of micropollutants in the aquatic environment: The benefits of upgrading wastewater treatment plants. *Environmental Science & Technology* 48 (14), 7683–7689.
- Eggimann, S., Mutzner, L., Wani, O., Schneider, M.Y., Spuhler, D., Moy de Vitry, M., Beutler, P., Maurer, M., 2017. The Potential of Knowing More: A Review of Data-Driven Urban Water Management. *Environmental Science & Technology* 51 (5), 2538–2553.
- Escher, B.I., Stapleton, H.M., Schymanski, E.L., 2020. Tracking complex mixtures of chemicals in our changing environment. *Science* 367 (6476), 388–392.
- Esseili, M.A., Saif, L.J., Farkas, T., Wang, Q., 2015. Feline Calicivirus, Murine Norovirus, Porcine Sapovirus, and Tulane Virus Survival on Postharvest Lettuce. *Applied and Environmental Microbiology* 81 (15), 5085–5092.
- Essila, N., Semmens, M., Voller, V., 2000. Modeling Biofilms on Gas-Permeable Supports: Concentration and Activity Profiles. *Journal of Environmental Engineering* 126 (3), 250–257.
- EU, 2020. Regulation (EU) 2020/741 of the European Parliament and of the Council of 25 May 2020 on minimum requirements for water reuse.
- EU Commission, 2015. Communication from the Commission to the European Parliament, the Council, the European Economic and Social Committee and the Committee of the Regions: Closing the loop - An EU action plan for the Circular Economy, Brussels, 21 pp.
- European Environment Agency, 2015. Waterbase: UWWTD: Urban waste water treatment directive - reported data (accessed 24.09.2017). https://www.eea.europa.eu/ds_resolveuid/94eff864373b47efa866128df909ac48.
- Falås, P., Wick, A., Castronovo, S., Habermacher, J., Ternes, T.A., Joss, A., 2016. Tracing the limits of organic micropollutant removal in biological wastewater treatment. *Water Research* 95, 240–249.

- Fang, Y., Hozalski, R.M., Clapp, L.W., Novak, P.J., Semmens M. J., 2002. Passive dissolution of hydrogen gas into groundwater using hollow-fiber membranes. *Water Research* 36 (14), 3533–3542.
- Ferrari, B., Paxéus, N., Lo Giudice, R., Pollio, A., Garric, J., 2003. Ecotoxicological impact of pharmaceuticals found in treated wastewaters: study of carbamazepine, clofibrac acid, and diclofenac. *Ecotoxicology and Environmental Safety* 55 (3), 359–370.
- Fleig, M., Brauch, H.-J., Fink, A., Post, B., 2016. Sonderuntersuchungen zum Vorkommen organischer Spurenstoffe im Unterlauf des Mains, in: Geschäftsstelle der Arbeitsgemeinschaft Rheinwasserwerke e.V. (ARW) (Ed.), 73. Jahresbericht.
- Frohnert, A., Apelt, S., Klitzke, S., Chorus, I., Szewzyk, R., Selinka, H.-C., 2014. Transport and removal of viruses in saturated sand columns under oxic and anoxic conditions--Potential implications for groundwater protection. *International Journal of Hygiene and Environmental Health* 217 (8), 861–870.
- Frohnert, A., Kreißel, K., Lipp, P., Dizer, H., Hamsch, B., Szewzyk, R., Selinka, H.-C., 2015. Removal of Surrogate Bacteriophages and Enteric Viruses from Seeded Environmental Waters Using a Semi-technical Ultrafiltration Unit. *Food and Environmental Virology* 7 (2), 173–182.
- Fry, V.A., Selker, J.S., Gorelick, S.M., 1997. Experimental investigations for trapping oxygen gas in saturated porous media for in situ bioremediation. *Water Resources Research* 33 (12), 2687–2696.
- Funke, J., Prasse, C., Lütke Eversloh, C., Ternes, T.A., 2015. Oxypurinol - A novel marker for wastewater contamination of the aquatic environment. *Water Research* 74, 257–265.
- Gabelman, A., Hwang, S.-T., 1999. Hollow fiber membrane contactors. *Journal of Membrane Science* 159 (1-2), 61–106.
- Gerba, C.P., 2007. Chapter 5 Virus Occurrence and Survival in the Environmental Waters, in: , *Human Viruses in Water*, vol. 17. Perspectives in Medical Virology. Elsevier, pp. 91–108.
- Gerba, C.P., Betancourt, W.Q., Kitajima, M., 2017. How much reduction of virus is needed for recycled water: A continuous changing need for assessment? *Water Research* 108, 25–31.
- Gerba, C.P., Yates, M.Y., Yates, S.R., 1991. Quantitation of factors controlling viral and microbial transport in the subsurface, in: Hurst, C.J. (Ed.), *Modeling the environmental fate of microorganisms*. American Society for Microbiology, Washington, DC, pp. 77–88.

- German Environment Agency, 2017. Data - Urban waste water (accessed 20.02.2018).
<https://www.thru.de/3/urban-waster-water/>.
- German Environment Agency, 2018a. Bericht des Bundesministeriums für Gesundheit und des Umweltbundesamtes an die Verbraucherinnen und Verbraucher über die Qualität von Wasser für den menschlichen Gebrauch (Trinkwasser)* in Deutschland (2014 - 2016). German Federal Ministry of Health; German Environment Agency, Dessau-Roßlau, 75 pp.
- German Environment Agency, 2018b. List of substances evaluated according to GOW (accessed 16.12.18).
https://www.umweltbundesamt.de/sites/default/files/medien/374/dokumente/liste_der_nach_gow_bewerteten_stoffe_201802.pdf.
- Ghattas, A.-K., Fischer, F., Wick, A., Ternes, T.A., 2017. Anaerobic biodegradation of (emerging) organic contaminants in the aquatic environment. *Water Research* 116, 268–295.
- Girones, R., Ferrús, M.A., Alonso, J.L., Rodriguez-Manzano, J., Calgua, B., Corrêa, A.d.A., Hundesa, A., Carratala, A., Bofill-Mas, S., 2010. Molecular detection of pathogens in water--the pros and cons of molecular techniques. *Water Research* 44 (15), 4325–4339.
- Glassmeyer, S.T., Furlong, E.T., Kolpin, D.W., Cahill, J.D., Zaugg, S.D., Werner, S.L., Meyer, M.T., Kryak, D.D., 2005. Transport of chemical and microbial compounds from known wastewater discharges: Potential for use as indicators of human fecal contamination. *Environmental Science & Technology* 39 (14), 5157–5169.
- Goyal, S.M., Gerba, C.P., 1979. Comparative adsorption of human enteroviruses, simian rotavirus, and selected bacteriophages to soils. *Applied and Environmental Microbiology* 38 (2), 241–247.
- Grassi, M.E., Patterson, B.M., Davis, G.B., Robertson, B.S., McKinley, A.J., 2007. Estimation of ethanol mass delivery to groundwater from silicone polymer mats. *Environmental Science & Technology* 41 (15), 5453–5459.
- GRDC, 2017. River Discharge Data. GRDC (accessed 3.10.2017).
http://www.bafg.de/GRDC/EN/Home/homepage_node.html.
- Greskowiak, J., Prommer, H., Massmann, G., Johnston, C.D., Nützmann, G., Pekdeger, A., 2005. The impact of variably saturated conditions on hydrogeochemical changes during artificial recharge of groundwater. *Applied Geochemistry* 20 (7), 1409–1426.
- Greskowiak, J., Prommer, H., Massmann, G., Nützmann, G., 2006. Modeling seasonal redox dynamics and the corresponding fate of the pharmaceutical residue phenazone during artificial recharge of groundwater. *Environmental Science & Technology* 40 (21), 6615–6621.

- Grünheid, S., Amy, G., Jekel, M., 2005. Removal of bulk dissolved organic carbon (DOC) and trace organic compounds by bank filtration and artificial recharge. *Water Research* 39 (14), 3219–3228.
- Hamann, E., Stuyfzand, P.J., Greskowiak, J., Timmer, H., Massmann, G., 2016. The fate of organic micropollutants during long-term/long-distance river bank filtration. *Science of the Total Environment* 545-546, 629–640.
- Hannapel, S., Scheibler, F., Huber, A., Sprenger, C., 2014. Characterization of European managed aquifer recharge (MAR) sites: Analysis. HYDOR, KWB, 141 pp. http://demeau-fp7.eu/sites/files/M11_1%20catalogue%20of%20european%20MAR%20applications_plus_appendix.pdf (accessed 13.10.2017).
- Hartmann, N.M., Dartscht, M., Szewzyk, R., Selinka, H.-C., 2013. Monitoring of adenovirus serotypes in environmental samples by combined PCR and melting point analyses. *Virology Journal* 10.
- Hass, U., Duennbier, U., Massmann, G., 2012. Occurrence and distribution of psychoactive compounds and their metabolites in the urban water cycle of Berlin (Germany). *Water Research* 46 (18), 6013–6022.
- Hassa, J., Maus, I., Off, S., Pühler, A., Scherer, P., Klocke, M., Schlüter, A., 2018. Metagenome, metatranscriptome, and metaproteome approaches unraveled compositions and functional relationships of microbial communities residing in biogas plants. *Applied Microbiology and Biotechnology* 102 (12), 5045–5063.
- Haugen, K.S., Semmens, M.J., Novak P. J., 2002. A novel in situ technology for the treatment of nitrate contaminated groundwater. *Water Research* 36 (14), 3497–3506.
- Hazen, A., 1911. Discussion of Dams on Sand Foundations: Some Principles Involved in Their Design, and the Law Governing the Depth of Penetration Required for Sheet-Piling by König, Arnold C. *Transactions of the American Society of Civil Engineers* LXXIII (3), 175-189.
- Hellauer, K., Karakurt, S., Sperlich, A., Burke, V., Massmann, G., Hübner, U., Drewes, J.E., 2018a. Establishing sequential managed aquifer recharge technology (SMART) for enhanced removal of trace organic chemicals: Experiences from field studies in Berlin, Germany. *Journal of Hydrology* 563, 1161–1168.
- Hellauer, K., Mergel, D., Ruhl, A., Filter, J., Hübner, U., Jekel, M., Drewes, J., 2017. Advancing Sequential Managed Aquifer Recharge Technology (SMART) Using Different Intermediate Oxidation Processes. *Water* 9 (3), 221.

- Hellauer, K., Uhl, J., Lucio, M., Schmitt-Kopplin, P., Wibberg, D., Hübner, U., Drewes, J.E., 2018b. Microbiome-Triggered Transformations of Trace Organic Chemicals in the Presence of Effluent Organic Matter in Managed Aquifer Recharge (MAR) Systems. *Environmental Science & Technology* 52 (24), 14342–14351.
- Hermes, N., Jewell, K.S., Schulz, M., Müller, J., Hübner, U., Wick, A., Drewes, J.E., Ternes, T.A., 2019. Elucidation of removal processes in sequential biofiltration (SBF) and soil aquifer treatment (SAT) by analysis of a broad range of trace organic chemicals (TOrcs) and their transformation products (TPs). *Water Research* 163, 114857.
- Hernroth, B.E., Conden-Hansson, A.-C., Rehnstam-Holm, A.-S., Girones, R., Allard, A.K., 2002. Environmental factors influencing human viral pathogens and their potential indicator organisms in the blue mussel, *Mytilus edulis*: the first Scandinavian report. *Applied and Environmental Microbiology* 68 (9), 4523–4533.
- Hewitt, J., Leonard, M., Greening, G.E., Lewis, G.D., 2011. Influence of wastewater treatment process and the population size on human virus profiles in wastewater. *Water Research* 45 (18), 6267–6276.
- Hijnen, W., Schijven, J.F., Bonné, P., Visser, A., Medema G.J., 2004. Elimination of viruses, bacteria and protozoan oocysts by slow sand filtration. *Water Science and Technology*, 147–154.
- Hillenbrand, T., Tettenborn, F., Menger-Krug, E., Marscheider-Weidemann, F., Fuchs, S., Toshovski, S., Kittlaus, S., Wermter, P., Kersting, M., Abegglen, C., 2014. Maßnahmen zur Verminderung des Eintrages von Mikroschadstoffen in die Gewässer. German Environment Agency, Dessau-Roßlau, 254 pp.
- Hiller, C.X., Hübner, U., Fajnorova, S., Schwartz, T., Drewes, J.E., 2019. Antibiotic microbial resistance (AMR) removal efficiencies by conventional and advanced wastewater treatment processes: A review. *Science of the Total Environment* 685, 596–608.
- Ho, J., Seidel, M., Niessner, R., Eggers, J., Tiehm, A., 2016. Long amplicon (LA)-qPCR for the discrimination of infectious and noninfectious phix174 bacteriophages after UV inactivation. *Water Research* 103, 141–148.
- Höhne, M., Schreier, E., 2004. Detection and characterization of norovirus outbreaks in Germany: application of a one-tube RT-PCR using a fluorogenic real-time detection system. *Journal of Medical Virology* 72 (2), 312–319.
- Hooper, J., Funk, D., Bell, K., Noibi, M., Vickstrom, K., Schulz, C., Machek, E., Huang, C.-H., 2020. Pilot testing of direct and indirect potable water reuse using multi-stage ozone-biofiltration without reverse osmosis. *Water Research* 169, 115178.

- Hoppe-Jones, C., Dickenson, E.R.V., Drewes, J.E., 2012. The role of microbial adaptation and biodegradable dissolved organic carbon on the attenuation of trace organic chemicals during groundwater recharge. *Science of the Total Environment* 437, 137–144.
- Hoppe-Jones, C., Oldham, G., Drewes, J.E., 2010. Attenuation of total organic carbon and unregulated trace organic chemicals in U.S. riverbank filtration systems. *Water Research* 44 (15), 4643–4659.
- Jekel, M., Dott, W., Bergmann, A., Dünnebier, U., Gnirß, R., Haist-Gulde, B., Hamscher, G., Letzel, M., Licha, T., Lyko, S., Miehe, U., Sacher, F., Scheurer, M., Schmidt, C.K., Reemtsma, T., Ruhl, A.S., 2015. Selection of organic process and source indicator substances for the anthropogenically influenced water cycle. *Chemosphere* 125, 155–167.
- Karakurt, S., Schmid, L., Hübner, U., Drewes, J.E., 2019. Dynamics of Wastewater Effluent Contributions in Streams and Impacts on Drinking Water Supply via Riverbank Filtration in Germany-A National Reconnaissance. *Environmental Science & Technology* 53 (11), 6154–6161.
- Karakurt-Fischer, S., Bein, E., Drewes, J.E., Hübner, U., 2020a. Characterizing a novel in-situ oxygen delivery device for establishing controlled redox zonation within a high infiltration rate sequential biofilter. *Water Research* 182.
- Karakurt-Fischer, S., Sanz-Prat, A., Greskowiak, J., Ergh, M., Gerdes, H., Massmann, G., Ederer, J., Regnery, J., Hübner, U., Drewes, J.E., 2020b. Developing a novel biofiltration treatment system by coupling high-rate infiltration trench technology with a plug-flow porous-media bioreactor. *Science of the Total Environment* 722.
- Katsoyiannis, A., Samara, C., 2007. The fate of dissolved organic carbon (DOC) in the wastewater treatment process and its importance in the removal of wastewater contaminants. *Environmental Science and Pollution Research International* 14 (5), 284–292.
- Kavousi, F., Syron, E., Semmens, M., Casey, E., 2016. Hydrodynamics and gas transfer performance of confined hollow fibre membrane modules with the aid of computational fluid dynamics. *Journal of Membrane Science* 513, 117–128.
- Kebinger, B., Karakurt-Fischer, S., Zhiteneva, V., Steger, M., Hübner, U., Drewes, J.E., in review. Novel concepts for potable water reuse based on sequential managed aquifer recharge technology – An economic benchmark assessment. *Journal of Water Reuse and Desalination*.
- Klasmeier, J., Kehrein, N., Berlekamp, J., Matthies, M., 2011. Mikroverunreinigungen in oberirdischen Gewässern: Ermittlung des Handlungsbedarfs bei kommunalen Kläranlagen - Abschlussbericht. Institut für Umweltsystemforschung - Universität Osnabrück (accessed

10.01.2017).

https://www.lfu.bayern.de/wasser/abwasser_anthropogene_spurenstoffe/stoffflussmodell/doc/endlbericht.pdf.

- Klitzke, S., Schroeder, J., Selinka, H.-C., Szewzyk, R., Chorus, I., 2015. Attenuation and colloidal mobilization of bacteriophages in natural sediments under anoxic as compared to oxic conditions. *Science of the Total Environment* 518-519, 130–138.
- Kolpin, D.W., Furlong, E.T., Meyer, M.T., Thurman, E.M., Zaugg, S.D., Barber, L.B., Buxton, H.T., 2002. Pharmaceuticals, hormones, and other organic wastewater contaminants in U.S. streams, 1999-2000: a national reconnaissance. *Environmental Science & Technology* 36 (6), 1202–1211.
- König, A., Weidauer, C., Seiwert, B., Reemtsma, T., Unger, T., Jekel, M., 2016. Reductive transformation of carbamazepine by abiotic and biotic processes. *Water Research* 101, 272–280.
- König, C.M., Becker, M., Diehl, A., Seidel, T., Rosen, B., Rüber, O., Werth, B., Zimmermann, C., 2015. SPRING: Professional Water Systems Modelling Software.
- Kuehn, W., Mueller, U., 2000. Riverbank Filtration: An Overview. *Journal - American Water Works Association* 92 (12), 60–69.
- Li, D., Alidina, M., Drewes, J.E., 2014. Role of primary substrate composition on microbial community structure and function and trace organic chemical attenuation in managed aquifer recharge systems. *Applied Microbiology and Biotechnology* 98 (12), 5747–5756.
- Li, D., Alidina, M., Ouf, M., Sharp, J.O., Saikaly, P., Drewes, J.E., 2013. Microbial community evolution during simulated managed aquifer recharge in response to different biodegradable dissolved organic carbon (BDOC) concentrations. *Water Research* 47 (7), 2421–2430.
- Li, D., Sharp, J.O., Saikaly, P.E., Ali, S., Alidina, M., Alarawi, M.S., Keller, S., Hoppe-Jones, C., Drewes, J.E., 2012. Dissolved organic carbon influences microbial community composition and diversity in managed aquifer recharge systems. *Applied and Environmental Microbiology* 78 (19), 6819–6828.
- Li, J., Zhu, L.-P., Xu, Y.-Y., Zhu, B.-K., 2010. Oxygen transfer characteristics of hydrophilic treated polypropylene hollow fiber membranes for bubbleless aeration. *Journal of Membrane Science* 362 (1-2), 47–57.
- Loos, R., Carvalho, R., António, D.C., Comero, S., Locoro, G., Tavazzi, S., Paracchini, B., Ghiani, M., Lettieri, T., Blaha, L., Jarosova, B., Voorspoels, S., Servaes, K., Haglund, P., Fick, J., Lindberg, R.H., Schwesig, D., Gawlik, B.M., 2013. EU-wide monitoring survey on emerging

- polar organic contaminants in wastewater treatment plant effluents. *Water Research* 47 (17), 6475–6487.
- Loos, R., Gawlik, B.M., Locoro, G., Rimaviciute, E., Contini, S., Bidoglio, G., 2009. EU-wide survey of polar organic persistent pollutants in European river waters. *Environmental Pollution* 157 (2), 561–568.
- LUBW, 2018. Deutsches Gewässerkundliches Jahrbuch (accessed 23.01.2018). <http://www.dgj.de/>.
- Luo, J., Cirpka, O.A., Kitanidis, P.K., 2006. Temporal-moment matching for truncated breakthrough curves for step or step-pulse injection. *Advances in Water Resources* 29 (9), 1306–1313.
- Maeng, S.K., Sharma, S.K., Lekkerkerker-Teunissen, K., Amy, G.L., 2011. Occurrence and fate of bulk organic matter and pharmaceutically active compounds in managed aquifer recharge: a review. *Water Research* 45 (10), 3015–3033.
- Mansfeldt, C., Deiner, K., Mächler, E., Fenner, K., Eggen, R.I.L., Stamm, C., Schönenberger, U., Walser, J.-C., Altermatt, F., 2020. Microbial community shifts in streams receiving treated wastewater effluent. *Science of the Total Environment* 709, 135727.
- Marron, E.L., Mitch, W.A., Gunten, U.v., Sedlak, D.L., 2019. A Tale of Two Treatments: The Multiple Barrier Approach to Removing Chemical Contaminants During Potable Water Reuse. *Accounts of Chemical Research* 52 (3), 615–622.
- Massmann, G., Dünnebier, U., Heberer, T., Taute, T., 2008. Behaviour and redox sensitivity of pharmaceutical residues during bank filtration - Investigation of residues of phenazone-type analgesics. *Chemosphere* 71 (8), 1476–1485.
- Massmann, G., Greskowiak, J., Dünnebier, U., Zuehlke, S., Knappe, A., Pekdeger, A., 2006. The impact of variable temperatures on the redox conditions and the behaviour of pharmaceutical residues during artificial recharge. *Journal of Hydrology* 328 (1-2), 141–156.
- Medema, G., 2013. Microbial Risk Assessment of Pathogens in Water, in: Laws, E. (Ed.), *Environmental Toxicology*. Springer, New York.
- Merle, T., Pronk, W., Gunten, U.v., 2017. MEMBRO 3 X, a Novel Combination of a Membrane Contactor with Advanced Oxidation (O_3/H_2O_2) for Simultaneous Micropollutant Abatement and Bromate Minimization. *Environmental Science & Technology Letters* 4 (5), 180–185.
- Messner, M.J., Berger, P., 2016. Cryptosporidium Infection Risk: Results of New Dose-Response Modeling. *Risk Analysis* 36 (10), 1969–1982.

- Michen, B., Graule, T., 2010. Isoelectric points of viruses. *Journal of Applied Microbiology* 109 (2), 388–397.
- Mikat, H., 2009. Managed aquifer recharge today and tomorrow: Influencing factors and solution approaches (in German). *bbr – Fachmagazin für Brunnen- und Leitungsbau* 59 (7-8), 38–43.
- Moser, A., Wemyss, D., Scheidegger, R., Fenicia, F., Honti, M., Stamm, C., 2018. Modelling biocide and herbicide concentrations in catchments of the Rhine basin. *Hydrology and Earth System Sciences* 22 (8), 4229–4249.
- Mujeriego, R., Gullón, M., Lobato, S., 2017. Incidental potable water reuse in a Catalanian basin: Living downstream. *Journal of Water Reuse and Desalination* 7 (3), 253–263.
- Müller, B., Klemm, U., Mas Marques, A., Schreier, E., 2007. Genetic diversity and recombination of murine noroviruses in immunocompromised mice. *Archives of Virology* 152 (9), 1709–1719.
- Müller, J., Drewes, J.E., Hübner, U., 2017. Sequential biofiltration - A novel approach for enhanced biological removal of trace organic chemicals from wastewater treatment plant effluent. *Water Research* 127, 127–138.
- Müller, J., Jewell, K.S., Schulz, M., Hermes, N., Ternes, T.A., Drewes, J.E., Hübner, U., 2019. Capturing the oxic transformation of iopromide - A useful tool for an improved characterization of predominant redox conditions and the removal of trace organic compounds in biofiltration systems? *Water Research* 152, 274–284.
- Muntau, M., Schulz, M., Jewell, K.S., Hermes, N., Hübner, U., Ternes, T., Drewes, J.E., 2017. Evaluation of the short-term fate and transport of chemicals of emerging concern during soil-aquifer treatment using select transformation products as intrinsic redox-sensitive tracers. *Science of the Total Environment* 583, 10–18.
- National Research Council, 2012. *Water reuse: Potential for expanding the nations water supply through reuse of municipal wastewater*. The National Academies Press, Washington, DC.
- Nieminski, E., Bellamy, W.D., Moss, L.R., 2000. Using surrogates to improve plant performance. *Journal AWWA* 92 (3), 67–78.
- Nimmer, M.A., Wayner, B.D., Morr, A.A., 2000. In-situ ozonation of contaminated groundwater. *Environmental Progress* 19 (3), 183–196.
- Nödler, K., Hillebrand, O., Idzik, K., Strathmann, M., Schiperski, F., Zirlewagen, J., Licha, T., 2013. Occurrence and fate of the angiotensin II receptor antagonist transformation product valsartan acid in the water cycle-a comparative study with selected β -blockers and the persistent

- anthropogenic wastewater indicators carbamazepine and acesulfame. *Water Research* 47 (17), 6650–6659.
- NRC, 2012. *Water reuse: Potential for expanding the nation's water supply through reuse of municipal wastewater*, Washington D.C., xiii, 262.
- NRMMC-EPHC-NHMRC, 2008. *Australian Guidelines for Water Recycling: Augmentation of Drinking Water Supplies (Phase 2)*.
- Obiri-Nyarko, F., Grajales-Mesa, S.J., Malina, G., 2014. An overview of permeable reactive barriers for in situ sustainable groundwater remediation. *Chemosphere* 111, 243–259.
- O'Neill, J., 2016. *The Review on Antimicrobial Resistance: Tackling Drug-Resistant Infections Globally: Final Report and Recommendations*, 84 pp.
- Onesios, K.M., Bouwer, E.J., 2012. Biological removal of pharmaceuticals and personal care products during laboratory soil aquifer treatment simulation with different primary substrate concentrations. *Water Research* 46 (7), 2365–2375.
- Onesios, K.M., Yu, J.T., Bouwer, E.J., 2009. Biodegradation and removal of pharmaceuticals and personal care products in treatment systems: a review. *Biodegradation* 20 (4), 441–466.
- Orgill, J.J., Abboud, M.C., Atiyeh, H.K., Devarapalli, M., Sun, X., Lewis, R.S., 2019. Measurement and prediction of mass transfer coefficients for syngas constituents in a hollow fiber reactor. *Bioresource Technology* 276, 1–7.
- Pal, A., He, Y., Jekel, M., Reinhard, M., Gin, K.Y.-H., 2014. Emerging contaminants of public health significance as water quality indicator compounds in the urban water cycle. *Environment International* 71, 46–62.
- Pang, L., 2009. Microbial removal rates in subsurface media estimated from published studies of field experiments and large intact soil cores. *Journal of Environmental Quality* 38 (4), 1531–1559.
- Pérez-González, A., Urriaga, A.M., Ibáñez, R., Ortiz, I., 2012. State of the art and review on the treatment technologies of water reverse osmosis concentrates. *Water Research* 46 (2), 267–283.
- Petrie, B., Barden, R., Kasprzyk-Hordern, B., 2015. A review on emerging contaminants in wastewaters and the environment: current knowledge, understudied areas and recommendations for future monitoring. *Water Research* 72, 3–27.

- Rauch-Williams, T., Hoppe-Jones, C., Drewes, J.E., 2010. The role of organic matter in the removal of emerging trace organic chemicals during managed aquifer recharge. *Water Research* 44 (2), 449–460.
- Reemtsma, T., Berger, U., Arp, H.P.H., Gallard, H., Knepper, T.P., Neumann, M., Quintana, J.B., Voogt, P.d., 2016. Mind the gap: Persistent and mobile organic compounds-Water contaminants that slip through. *Environmental Science & Technology* 50 (19), 10308–10315.
- Reemtsma, T., Miehe, U., Duennbier, U., Jekel, M., 2010. Polar pollutants in municipal wastewater and the water cycle: occurrence and removal of benzotriazoles. *Water Research* 44 (2), 596–604.
- Reemtsma, T., Weiss, S., Mueller, J., Petrovic, M., González, S., Barcelo, D., Ventura, F., Knepper, T.P., 2006. Polar pollutants entry into the water cycle by municipal wastewater: a European perspective. *Environmental Science & Technology* 40 (17), 5451–5458.
- Regnery, J., Barringer, J., Wing, A.D., Hoppe-Jones, C., Teerlink, J., Drewes, J.E., 2015a. Start-up performance of a full-scale riverbank filtration site regarding removal of DOC, nutrients, and trace organic chemicals. *Chemosphere* 127, 136–142.
- Regnery, J., Gerba, C.P., Dickenson, E.R.V., Drewes, J.E., 2017. The importance of key attenuation factors for microbial and chemical contaminants during managed aquifer recharge: A review. *Critical Reviews in Environmental Science and Technology* 47 (15), 1409–1452.
- Regnery, J., Lee, J., Kitanidis, P., Illangasekare, T., Sharp, J.O., Drewes, J.E., 2013. Integration of Artificial Recharge and Recovery Systems for Impaired Water Sources in Urban Settings: Overcoming Current Limitations and Engineering Challenges. *Environmental Engineering Science* 30 (8), 409–420.
- Regnery, J., Wing, A.D., Alidina, M., Drewes, J.E., 2015b. Biotransformation of trace organic chemicals during groundwater recharge: How useful are first-order rate constants? *Journal of Contaminant Hydrology* 179, 65–75.
- Regnery, J., Wing, A.D., Kautz, J., Drewes, J.E., 2016. Introducing sequential managed aquifer recharge technology (SMART) - From laboratory to full-scale application. *Chemosphere* 154, 8–16.
- Rehfeld-Klein, M., 2017. Spurenstoffe in Oberflächengewässern und Rohwässern der Trinkwassergewinnung Berlins: Rahmenbedingungen, Probenahme, Maßnahmenplanung. Senatsverwaltung für Umwelt, Verkehr und Klimaschutz (accessed 15.05.2017). https://www.hlnug.de/fileadmin/dokumente/wasser/Archiv_Veranstaltungen/2017/Symposium_Spurenstoffe/Vortrag_Rehfeld-Klein.pdf.

- Rice, J., Via, S.H., Westerhoff, P., 2015. Extent and impacts of unplanned wastewater reuse in US rivers. *American Water Works Association* 107 (11), E571-E581.
- Rice, J., Westerhoff, P., 2015. Spatial and temporal variation in de facto wastewater reuse in drinking water systems across the U.S.A. *Environmental Science & Technology* 49 (2), 982–989.
- Rivett, M.O., Buss, S.R., Morgan, P., Smith, J.W.N., Bemment, C.D., 2008. Nitrate attenuation in groundwater: a review of biogeochemical controlling processes. *Water Research* 42 (16), 4215–4232.
- Rizzo, L., Gernjak, W., Krzeminski, P., Malato, S., McArdell, C.S., Perez, J.A.S., Schaar, H., Fattakassinou, D., 2020. Best available technologies and treatment trains to address current challenges in urban wastewater reuse for irrigation of crops in EU countries. *Science of the Total Environment* 710, 136312.
- Rose, J.B., Darbin, H., Gerba, C.P., 1988. Correlations of the Protozoa, *Cryptosporidium* and *Giardia*, with Water Quality Variables in a Watershed. *Water Science and Technology* 20 (11-12), 271–276.
- Safford, H.R., Bischel, H.N., 2019. Flow cytometry applications in water treatment, distribution, and reuse: A review. *Water Research* 151, 110–133.
- Sander, R., 2015. Compilation of Henry's law constants (version 4.0) for water as solvent. *Atmospheric Chemistry and Physics* 15 (8), 4399–4981.
- Scheurer, M., Storck, F.R., Graf, C., Brauch, H.-J., Ruck, W., Lev, O., Lange, F.T., 2011. Correlation of six anthropogenic markers in wastewater, surface water, bank filtrate, and soil aquifer treatment. *Journal of Environmental Monitoring* 13 (4), 966–973.
- Schijven, J., Pang, L., Ying, G.G., 2017. Evaluation of subsurface microbial transport using microbial indicators, surrogates and tracers, in: Farnleitner, A., Blanch, A., Rose, J., Jiménez-Cisneros, B. (Eds.), *Global Water Pathogen Project*. Michigan State University.
- Schijven, J.F., Hassanizadeh, S.M., 2000. Removal of Viruses by Soil Passage: Overview of Modeling, Processes, and Parameters. *Critical Reviews in Environmental Science and Technology* 30 (1), 49–127.
- Schijven, J.F., Hassanizadeh, S.M., 2002. Virus removal by soil passage at field scale and groundwater protection of sandy aquifers. *Water Science and Technology* 46 (3), 123–129.

- Schimmelpfennig, S., Kirillin, G., Engelhardt, C., Dünnbier, U., Nützmann, G., 2016. Fate of pharmaceutical micro-pollutants in Lake Tegel (Berlin, Germany): The impact of lake-specific mechanisms. *Environmental Earth Sciences* 75 (10).
- Schimmelpfennig, S., Kirillin, G., Engelhardt, C., Nützmann, G., Dünnbier, U., 2012. Seeking a compromise between pharmaceutical pollution and phosphorus load: Management strategies for Lake Tegel, Berlin. *Water Research* 46 (13), 4153–4163.
- Schmidt, N., Page, D., Tiehm, A., 2017. Biodegradation of pharmaceuticals and endocrine disruptors with oxygen, nitrate, manganese (IV), iron (III) and sulfate as electron acceptors. *Journal of Contaminant Hydrology* 203, 62–69.
- Seeger, E.M., Braeckevelt, M., Reiche, N., Müller, J.A., Kästner, M., 2016. Removal of pathogen indicators from secondary effluent using slow sand filtration: Optimization approaches. *Ecological Engineering* 95, 635–644.
- Senate Department for Urban Development and Housing Berlin, 2017. Berlin environmental atlas: 02.12 Groundwater levels of the main aquifer and Panke valley aquifer, Berlin, 17 pp. https://www.stadtentwicklung.berlin.de/umwelt/umweltatlas/e_text/eks212.pdf (accessed 6.09.2018).
- Sharma, S.K., Amy, G., 2011. Natural treatment systems, in: Edzwald, J.K. (Ed.), *Water Quality & Treatment*, 6th ed. McGraw-Hill, New York, 15.1–15.32.
- Simon, C., Daniel, R., 2011. Metagenomic analyses: past and future trends. *Applied and Environmental Microbiology* 77 (4), 1153–1161.
- Soller, J.A., Eftim, S.E., Nappier, S.P., 2018. Direct potable reuse microbial risk assessment methodology: Sensitivity analysis and application to State log credit allocations. *Water Research* 128, 286–292.
- Sprenger, C., Lorenzen, G., Hülshoff, I., Grützmacher, G., Ronghang, M., Pekdeger, A., 2011. Vulnerability of bank filtration systems to climate change. *Science of the Total Environment* 409 (4), 655–663.
- Storck, F.R., Schmidt, C.K., Lange, F.T., Henson, J.W., Hahn, K., 2012. Factors controlling micropollutant removal during riverbank filtration. *American Water Works Association* 104 (12), E643-E652.
- Suarez, S., Lema, J.M., Omil, F., 2010. Removal of pharmaceutical and personal care products (PPCPs) under nitrifying and denitrifying conditions. *Water Research* 44 (10), 3214–3224.

- Symonds, E.M., Griffin, D.W., Breitbart, M., 2009. Eukaryotic viruses in wastewater samples from the United States. *Applied and Environmental Microbiology* 75 (5), 1402–1409.
- Syngouna, V.I., Chrysikopoulos, C.V., 2013. Cotransport of clay colloids and viruses in water saturated porous media. *Colloids and Surfaces A: Physicochemical and Engineering Aspects* 416, 56–65.
- Syron, E., Casey, E., 2008. Membrane-aerated biofilms for high rate biotreatment: performance appraisal, engineering principles, scale-up, and development requirements. *Environmental Science & Technology* 42 (6), 1833–1844.
- Ternes, T.A., 1998. Occurrence of drugs in German sewage treatment plants and rivers. *Water Research* 32 (11), 3245–3260.
- Uehlinger, U.F., Wantzen, K.M., Leuven, R.S., Arndt, H., 2009. The Rhine River Basin, in: Tockner, K. (Ed.), *Rivers of Europe*. Academy Press, London, pp. 199–245.
- USEPA, 2012. Guidelines for Water Reuse. EPA/600/R-12/618, Washington, DC. <http://nepis.epa.gov/Adobe/PDF/P100FS7K.pdf>.
- USEPA, 2017. Potable Reuse Compendium, 203 pp. https://www.epa.gov/sites/production/files/2018-01/documents/potablereusecompendium_3.pdf.
- van Abel, N., Schoen, M.E., Kissel, J.C., Meschke, J.S., 2017. Comparison of Risk Predicted by Multiple Norovirus Dose-Response Models and Implications for Quantitative Microbial Risk Assessment. *Risk Analysis* 37 (2), 245–264.
- van der Wielen, P.W.J.J., Senden, W.J.M.K., Medema, G., 2008. Removal of bacteriophages MS2 and phiX174 during transport in a sandy anoxic aquifer. *Environmental Science & Technology* 42 (12), 4589–4594.
- van Houtte, E., Verbauwhe, i.J., 2008. Torreele's water re-use facility enabled sustainable groundwater management in de Flemish dunes (Belgium). *Water Practice and Technology* 3 (2).
- Vandenberg, J.A., Ryan, M.C., Nuell, D.D., Chu, A., 2005. Field evaluation of mixing length and attenuation of nutrients and fecal coliform in a wastewater effluent plume. *Environmental Monitoring and Assessment* 107 (1-3), 45–57.
- Vikesland, P.J., Pruden, A., Alvarez, P.J.J., Aga, D., Bürgmann, H., Li, X.-D., Manaiá, C.M., Nambi, I., Wigginton, K., Zhang, T., Zhu, Y.-G., 2017. Toward a Comprehensive Strategy to Mitigate Dissemination of Environmental Sources of Antibiotic Resistance. *Environmental Science & Technology* 51 (22), 13061–13069.

- Völker, J., Stapf, M., Miehe, U., Wagner, M., 2019. Systematic Review of Toxicity Removal by Advanced Wastewater Treatment Technologies via Ozonation and Activated Carbon. *Environmental Science & Technology* 53 (13), 7215–7233.
- Wang, Z., Shao, D., Westerhoff, P., 2017. Wastewater discharge impact on drinking water sources along the Yangtze River (China). *Science of the Total Environment* 599-600, 1399–1407.
- Weast, R.C., Lide, D.R., 1989. *CRC Handbook of chemistry and physics*, 70th ed. Boca Raton : CRC Press.
- WHO, 2006. *Guidelines for the safe use of wastewater, excreta and greywater: Policy and regulatory aspects (Volume 1)*. World Health Organization, Switzerland, 114 pp.
- WHO, 2011. *Guidelines for drinking water quality: Fourth edition incorporating the first addendum*, 631 pp. https://www.who.int/water_sanitation_health/publications/dwq-guidelines-4/en/.
- WHO, 2017. *Potable reuse: guidance for producing safe drinking-water*. World Health Organization, Geneva.
- Wickramasinghe, S.R., Semmens, M.J., Cussler, E.L., 1992. Mass transfer in various hollow fiber geometries. *Journal of Membrane Science* 69 (3), 235–250.
- Wiener, M.J., Jafvert, C.T., Nies, L.F., 2016. The assessment of water use and reuse through reported data: A US case study. *Science of the Total Environment* 539, 70–77.
- Wiese, B., Massmann, G., Jekel, M., Heberer, T., Dünnbier, U., Orlikowski, D., Grützmacher, G., 2011. Removal kinetics of organic compounds and sum parameters under field conditions for managed aquifer recharge. *Water Research* 45 (16), 4939–4950.
- Wilson, R.D., Mackay, D.M., 2002. Diffusive Oxygen Emitters for Enhancement of Aerobic In Situ Treatment. *Groundwater Monitoring & Remediation* 22 (2), 88–98.
- Wilson, R.D., Mackay, D.M., Cherry, J.A., 1997. Arrays of unpumped wells for plume migration control by semi-passive in-situ remediation. *Groundwater Monitoring & Remediation* 17 (3), 185–193.
- Wolf, A.V., 1966. *Aqueous Solutions and Body Fluids. Their Concentrative Properties and Conversion Tables*, 12th ed. Harper and Row Publishers, New York.
- WSV, 2017. PEGELONLINE (accessed 3.10.2017). <https://www.pegelonline.wsv.de/gast/start>.
- Yang, M.-C., Cussler, E.L., 1986. Designing hollow-fiber contactors. *Journal AIChE* 32 (11), 1910–1916.

- Zhang, L., Carvalho, P.N., Bollmann, U.E., Ei-Taliawy, H., Brix, H., Bester, K., 2019. Enhanced removal of pharmaceuticals in a biofilter: Effects of manipulating co-degradation by carbon feeding. *Chemosphere* 236, 124303.
- Zhuang, J., Jin, Y., 2003. Virus Retention and Transport as Influenced by Different Forms of Soil Organic Matter. *Journal of Environmental Quality* 32 (3), 816–823.
- Zietzschmann, F., Worch, E., Altmann, J., Ruhl, A.S., Sperlich, A., Meinel, F., Jekel, M., 2014. Impact of EfOM size on competition in activated carbon adsorption of organic micro-pollutants from treated wastewater. *Water Research* 65, 297–306.
- Zimmerman, J.B., Mihelcic, J.R., Smith, a.J., 2008. Global Stressors on Water Quality and Quantity. *Environmental Science & Technology* 42 (12), 4247–4254.